# 91
# Structure and Bonding

Springer
*Berlin*
*Heidelberg*
*New York*
*Barcelona*
*Budapest*
*Hong Kong*
*London*
*Milan*
*Paris*
*Santa Clara*
*Singapore*
*Tokyo*

# Bioinorganic Chemistry

## Trace Element Evolution from Anaerobes to Aerobes

Volume Editor: R. J. P. Williams

With contributions by
B. Abolmaali, J. C. Fontecilla-Camps,
I. A. C. Pereira, H. V. Taylor, M. Teixeira,
J. Telser, U. Weser, A. V. Xavier

Springer

In references Structure and Bonding is abbreviated
Struct. Bond. and is cited as a journal.

Springer WWW home page: http://www.springer.de

ISSN 0081-5993
ISBN 3-540-63548-3
Springer-Verlag Berlin Heidelberg New York

CIP Data applied for


Printed in Germany



Typesetting: Fotosatz-Service Köhler OHG, Würzburg
Cover: Medio V. Leins, Berlin
SPIN: 10552986 66/3020 - 5 4 3 2 1 0 - Printed on acid-free paper

## Volume Editor

Prof. R. J. P. Williams
University of Oxford
Inorganic Chemistry Laboratory
South Park Road
Oxford OX1 3QR, Great Britain
*E-mail: susie.compton@icl.ox.ac.uk*

## Editorial Board

# Preface

Knowledge of anaerobic biochemistry is essential to our understanding of the origin of life. It is of very considerable interest that while nickel is essential in many if not all anaerobes there is no known functional nickel protein encoded in the human genome. In fact nickel is generally stated to be toxic rather than essential for man and is deemed to be carcinogenic. Note that nickel in aerobes is confined to urease and is often kept away from the cytoplasm in vacuoles or vesicles of aerobic organisms. The first two articles in this volume present detailed views of the functional significance of nickel in largely present day anaerobes which we believe are not too distant from the only living cells some $3-4 \times 10^9$ years ago.

One of the articles describes F-430, a nickel complex with a cyclic ligand related to porphyrins. In strict anaerobes and in anaerobes able to withstand a low level of dioxygen, e.g. sulphur bacteria, both vitamin $B_{12}$, a cobalt complex, and heme, an iron complex, are present. They too are related to porphyrins. It is then of interest to compare and contrast their functions. Vitamin $B_{12}$ has been described in volume 20 (Hogenkamp HPC, Sando GN (1974) Struct Bond 20:23). In this volume the value of heme to anaerobes is stressed. Putting these three articles together we begin to see that early life had a requirement for trace elements in highly specified forms.

Copper is apparently absent from strict anaerobes and its value is associated very largely with oxidation or protection from oxidation in which highly oxidising agents such as dioxygen and superoxide are ligands. The contrast with the presumably primitive chemistry of heme and nickel in anaerobes could not be greater. However I believe that this switch from the use of nickel especially in anaerobic early evolution to the use of copper in today's aerobes is a major part of the evolution of all organisms. Thus this volume brings together in one place the remarkable development of the uses of three trace elements in an historical evolutionary context.

R. J. P. Williams

# Contents

# Contents of Volume 92

## Less Common Metals in Proteins and Nucleic Acid Probes

Volume Editor: Michael J. Clarke

# Biological Nickel

Juan C. Fontecilla-Camps

Laboratoire de Cristallographie et de Cristallogenèse des Protéines, Institut de Biologie Structurale Jean-Pierre Ebel, CEA-CNRS, 41, Avenue des Martyrs, 38027 Grenoble Cedex 1 France. E-mail: juan@lccp.ibs.fr

Nickel has so far been implicated as a cofactor in only a handful of biological reactions. These reactions are, however, central to many archae and bacteria as they provide reducing power from molecular hydrogen oxidation, readily available nitrogen from urease (also in plants and fungi) and acetyl-coenzyme A from CO and $CO_2$. As new microbial proteins are studied, the role of nickel is likely to extent to several other metabolic processeses. One of the major issues concerning catalytic Ni is whether it can be redox active in the biological context. Recent results concerning hydrogenases and CODHs indicate that their catalyses are carried out by NiFe centers; thus the role of Ni in these enzymes may be essentially catalytic without necessarily involving redox chemistry.

**Keywords:** Ni, hydrogenase, CO, dehydrogenase, urease, protein structure.



Structure and Bonding, Vol. 91

## 1 Introduction

Until relatively recently, Ni was not considered to be a biologically important oligoelement and only attracted attention because of its toxicity. The observation by Bartha and Ordal [1] in 1965 that chemotrophic $H_2$-utilizing anaerobic bacteria required Ni to grow and the subsequent identification of Ni as a component of hydrogenases [2, 3] provided definitive proof of the role of Ni in hydrogen-metabolism. Urease, the first enzyme to be crystallized [4] was also determined to be a Ni-protein [5]. In addition, CO oxidation and anaerobic acetyl-CoA synthesis, as well as $CH_4$ production from $CO_2$, have also been shown to be mediated by Ni-containing centers [6–8]. Very recently, a Ni-containing superoxide dismutase (SOD) has been identified [9], potentially expanding the catalytic role of Ni to many additional biological processes.

With the exception of urease, which is found in bacteria, fungi, algae and higher plants, the other Ni-mediated processes, such as hydrogen uptake and production, reduction of $CO_2$ to $CH_4$ and CO metabolism are restricted to bacteria and archae. In this chapter we will focus on these various metabolic reactions emphasizing the role played by nickel.

## 2 Nickel. The Element and Its Chemistry

Nickel has the atomic number 28 and its weight is 58.7. Among the five stable isotopes, $^{61}$Ni, (1.1% natural abundance) which has a nuclear spin of 3/2, is of special interest in biological spectroscopy [10, 11]. The abundance of Ni in Earth's crust at present is only about 0.02% (twice that of Co but 500 times less than that of Fe) ([10] and Refs. therein). On contemporary Earth, Ni is normally combined with sulfur, arsenic, silicium and antimony. In iron meteorites, however, Ni is associated with Fe constituting 5–20% of the alloy. Such relatively high Ni/Fe proportion reflects primordial planetary events and may be related to some fundamental Ni-based biological processes which were probably generated at the onset of life [12]. Metallic Ni is quite resistent to oxidation by air and water at normal temperature and it is used industrially, for instance, in the manufacture of coins. On the other hand, metallic Ni, when associated with a hydrogen species, is very reactive and it is used in the hydrogenation of vegetable oils and as a methanation catalyst for the production of methane from CO and $H_2$ [13, 14].

Commonly observed Ni oxidation states are 0, +1, +2, +3 and +4. The only stable valent state in simple salts is Ni(II). Other oxidation states require complex formation. The Ni(0) state is found, for instance, in complexes with strong ligands such as carbonyl and cyanide, Ni(I) in cyanide salts and the less common Ni(III) and Ni(IV) in complexes with hard ligands containing oxygen or nitrogen [10]. Modern biomimetic chemistry has generated many novel potentially relevant Ni(I), Ni(II) and Ni(III) compounds [15]. These will be cited here within the context of the various enzymatic activities.

The geometry of Ni complexes has been reviewed by Coyle [10]. Ni(II), $d^8$, four-coordinated complexes are usually square planar and diamagnetic whereas the less common tetrahedral Ni(II) complexes are paramagnetic (S = 1). The two coordination geometries can be exchangeable and may be determined by factors such as crystal packing ([10] and Refs. therein). When five-coordinated, Ni(II) species can have either trigonal-bipyramidal (TBP), square pyramidal or distorted geometries and be either high or low spin. Six-coordinated Ni(II) complexes are octahedral and have two unpaired electrons. Ni(0) and Ni(I) complexes are commonly tetrahedral whereas Ni(III) and Ni(IV) complexes are either octahedral, distorted octahedral or, less commonly, planar or TBP. As a conclusion, because Ni coordination complexes are known to have a wide variety of structures and oxidation states, it is expected that the properties of biological Ni will be largely dictated by the protein environment.

# 3 Nickel in Biology

## 3.1 The Proteins

Ni-containing enzymes are, in general, rather large multimeric proteins. Traditionally [15], catalytic Ni-enzymes have been divided into four classes: ureases, CO dehydrogenases/acetyl-CoA synthetases (CODH/ACS), *S*-methyl-coenzyme M reductases and hydrogenases. A recent report on a Ni-containing SOD [9] suggests that there may still be many additional Ni-enzymes to be discovered. If this is the case, the role of biological catalytic Ni will be considerably expanded. In addition, many Ni-binding proteins are being found involved in transport and assembly of the Ni-enzymes' active sites.

**Table 1.** General characteristics of representative urease, hydrogenase, and $CODH_S$

| Protein | Subunit compostition | Molecular weight | Cluster composition | Cluster location |
|---|---|---|---|---|
| Urease (K. aerogenes) | $(\alpha\beta\gamma)_3$ | $\alpha$ = 60.3 kDa<br>$\beta$ = 11.6 kDa<br>$\gamma$ = 11.0 kDa | 2 Ni ions | $\alpha$-subunit |
| Hydrogenase (D. gigas) | 1 Large subunit<br>1 Small subunit | L = 58 kDa<br>S = 32 kDa | NiFe<br>2 $[Fe_4S_4]$<br>1 $[Fe_3S_4]$ | Large subunit<br>Small subunit |
| CODH (R. rubrum) | – | 61.8 kDa | C-cluster (NiFe?)<br>B-cluster $[Fe_4S_4]$ | – |
| (C. thermoaceticum) | $\alpha_2\beta_2$ | $\alpha$ = 81.7 kDa<br>$\beta$ = 72.3 kDa | A-cluster (NiFe?)<br>C-cluster (NiFe?)<br>B-cluster $[Fe_4S_4]$ | $\alpha$-subunit<br>$\beta$-subunit<br>$\beta$-subuni |

**Fig. 1.** Ribbon representation of an $\alpha\beta\gamma$ unit of the crystallographic trimer of *K. aerogenes* urease. The Ni ions are located at the top of the $\alpha$ subunit (*light gray*) and are accessible from the solvent medium. The $\beta$ and $\gamma$ subunits are depicted in *dark* and *medium grey* respectively. This drawing was prepared with Molscript [126] by A. Volbeda. Coordinates were obtained from entry 1KAU [16] from the Protein Data Bank [127]

Table 1 summarizes the general characteristics of representative urease, hydrogenase and CODHs. As it will be further discussed below, the X-ray structures of only two Ni-containing proteins, urease and hydrogenase, are known [16, 17]. The former has the well known triose phosphate isomerase (TIM) barrel topology (Fig. 1) whereas the latter displays a so far unique folding (Fig. 2). The next challenge will be the elucidation of the crystal structures of the CODH/ACS enzyme of *Clostridium thermoaceticum* and of the simpler CODH from *Rhodospirillum rubrum*.

**Fig. 2.** Ribbon representation of the heterodimer hydrogenase from *D. gigas*. The large subunit is depicted in *white* whereas the small subunit flavodoxin-like domain [17] is shown in *dark gray* and the rest of the subunit in *medium gray*. Note that the active site NiFe cluster is buried in the large subunit. The [FeS] clusters coordinated by the small subunit are shown as *white* (Fe) and *dark* (S) *spheres*. This drawing was prepared by A. Volbeda with Molscript [126]

Significant medical interest has been elicited by the *Helicobacter pylori* urease, a possible component of the ulcer-inducing mechanism of the bacterium in humans [18, 19]. Hydrogen production from bacterial systems attracted a great deal of attention during the oil embargo of the 1970s. Recently, that interest has diminished but it can be anticipated that a renewal will take place as fossil fuel sources become depleted in the next thirty to fourty years and improved hydrogen-based engines are designed [20]. Although it is too early to tell, the elucidation of the acetyl-CoA mechanism of CODH/ACS may improve current industrial processes for acetate synthesis such as the one developed by Monsanto [21].

## 3.2 The Metal

Nickel is generally toxic for living organisms [11]. The toxicity is apparently related, at least partially, to the binding of Ni to DNA and its subsequent

mutagenic effect [22, 23]. It is therefore somewhat surprising to find that Ni is an essential trace element in several bacteria and archae and even in fungi, algae and higher plants [11]. It has been suggested that many of the Ni-related enzymatic reactions correspond to extremely ancient processes which arose at the onset of life and originated in the vicinity of volcanic vents where Fe, Ni, $H_2$, $CO_2$ and CO were abundant [12].

The possible role of Ni in biology, the related biomimetic chemistry and the Ni-containing enzymes have been frequently reviewed in the last few years [15, 18, 24–28]. Here, we will concentrate on urase and hydrogenase, for which three-dimensional structures have recently become available [16, 17], and on CODH, for which a significant amount of spectroscopic data has been reported lately (see below). The various aspects of *S*-methylcoenzyme M reductase genetics, chemistry and biology have been very recently reviewed in this series [29] and will not be further addressed here.

We will first briefly discuss the role of many accessory proteins in Ni transport into the cell and Ni enzyme active site assembly and the probable role of Ni-proteins as part of substrate sensors. Next, we will address the coordination of biological Ni and its possible catalytic properties.

## 4 Nickel Transport and Enzyme Active Site Assembly

Synthesis of Ni-containing enzymes requires specific protein factors that are responsible for the transport and incorporation of this ion. In plants, where Ni transport concerns mostly the synthesis of ureases, it has been shown that cultivation in nickel-deficient medium leads to leaflet tip necrosis due to urea accumulation ([30] and references therein). It has been suggested that the optimal coordination for protein Ni transport would be octahedral with two N and at least one O [31]. Interestingly, some plants are hyperaccumulators of Ni and can have as much as 1.2% dry weight Ni in the leaves [30]. In some hyperaccumulators, Ni extracted from vacuoles was found to be complexed by citrate, malate and malonate, the concentrations of the latter two compounds being significantly higher than in nonhyperaccumulators [32].

In bacteria and archae, the best studied systems are those of ureases and hydrogenases and to a lesser extent that of CODH. Some of the coding sequences are part of the operons coding for structural genes and their corresponding transcribed proteins have been described as either regulatory or accessory. Although the roles of the latter remain, for the most part, undefined, they seem to be Ni-binding proteins involved in active center assembly and/or enzyme activation [25]. Other proteins, such as those involved in high-affinity Ni transport for hydrogenase synthesis, may be coded by genes in a different operon; as in the case of the *E. coli nikABCDE* gene cluster [33], or its expression can be under the control of the same operon, as in *A. eutrophus* (*hoxN*) [34]. In the latter, the HoxN protein seems to be, at least partially, also responsible for providing Ni to urease, because inactivation of *hoxN* led to an increase in Ni requirement for the synthesis of both active hydrogenases and urease [35].

Similarly, *E. coli* cells containing a plasmid with the *Klebsiella aerogenes* urease gene cluster display enhanced activity in the presence of a second plasmid carrying hoxN [34]. The most remarkable feature of HoxN is its extremely high specifity and affinity for Ni ions, allowing *A. eutrophus* to express active Ni-dependent hydrogenase and ureases even when only traces of this ion are present [35]. A similar observation has been made when growing the sulfate-reducing bacterium *Desulfovibrio gigas* in the absence of Ni and in the presence of an excess of $Co^{2+}$ (C. Hatchikian, personal communication). A topological model of HoxN has been obtained by combining hydropathic profile amino acid sequence analyses [35, 36] with genetically engineered insertion of specific markers for periplasmic and cytoplasmic activities. The modelled HoxN is a membrane protein with seven putative transmembrane helices. Although this study made a tentative assignment of the amino acid regions that could correspond to periplasmic loops involved in Ni transport, no obvious Ni-binding motifs were found in these sequences [35]. In the urease gene cluster of *Bacillus* sp. strain TB-90, UreH, a protein that has 23% identity with HoxN is likely to be responsible for Ni high-affinity transport since deletion of a segment of this gene results in higher than usual Ni requirements for normal urease activity [35]. Similar Ni transport proteins are likely to exist in other microorganisms [37]. A Ni-binding accessory protein UreE with a naturally-occurring histidine tail has been also described [38].

In addition to transport proteins that bring Ni ions to the cytoplasm, the correct assembly of Ni-enzymes active sites requires at least two other classes of gene products: examples of these are the Ni-binding HypB (hydrogenase) and UreG (urease) which have GTPase activity [39] and chaperonins such as GroES (for hydrogenase of *E. coli*) and HspA (a GroES-like chaperonine for urease of *H. pylori*), respectively [40, 41]. It is worth noting that HspA contains a 27 amino acid domain that binds Ni with high affinity [41]. The requirement for nucleotide hydrolyzing enzymes and chaperonines *suggests an energy-driven, chaperon-mediated*, Ni incorporation in both hydrogenases and ureases. Since the partial amino acid sequence of an open reading frame found in the proximity of the CODH structural gene of *R. rubrum* also contains a nucleotide-binding domain [42], these enzymes may be generally required for Ni center assembly. Although in vitro Ni incorporation is possible in apoureases [43] and in Ni-defficient CODH A-clusters [44], provided both high Ni concentrations and (in ureases) $CO_2$ are supplied, hydrogenases cannot be reconstituted in this fashion. This may be related to the fact that hydrogenase maturation (implying Ni incorporation) generally requires the proteolysis of a C-terminal peptide from the large subunit [39], a process likely to be irreversible because it buries the active site in the structure [17] (Fig. 2). In the absence of Ni, the inmature form of the large subunit accumulates [40, 45]; subsequent addition of Ni in vitro using cell extracts results in the processing of the subunit, indicating the presence of a Ni-dependent protease activity [45]. This has been confirmed and extended by Maier & Böck [46] who have studied the effect of the various accessory proteins in *E. coli* hydrogenase 3 maturation. By using cell extracts of a *nik*$^-$ (Ni transport deficient) mutant, these authors have determined the need of the accessory proteins HypB, HypC, HypD, HypE, HypF and the protease

NycI in the development of hydrogenase activity from a Ni-free HycE (large subunit) precursor. The role of each of the accessory proteins was tested by using *nik⁻/accessory protein gene⁻* double mutants. The maturation of the hydrogenase subunit was specifically dependent on the addition of Ni. Neither $Fe^{2+}$, $Co^{2+}$, $Cu^{2+}$, nor $Zn^{2+}$ were able to substitute for it. From their study, Maier & Böck [46] conclude that 1) HycE precursor accumulated in mutants affected in *HypA, HypC, HypD, HypE* or *HypF* is incompetent for processing, 2) HycE precursor present in a *HypB* deletion mutant can be partially processed in vivo, but not in vitro, by addition of Ni; 3) HycE precursor from a *nik⁻* mutant shows processing both in vivo and in vitro; with added Ni; 4) HycE precursor detected in a HycI deletion mutant is already loaded with Ni in vivo and can be processed by purified HycI protease in vitro. Although many of the specific roles of the accessory proteins are unknown, they are generally essential for hydrogenase maturation. Only HypA appears to be dispensable, although this may be related to the presence of a homologous gene product (HybF) in the related hydrogenase 2 operon of *E. coli*, that was not mutated in that study [46]. Surprisingly, addition of GTP to cell extracts did not stimulate in vitro HypB-mediated processing, in conflict with results reported for *A. vinelandii* [45].

Very recently, a CO-dependent, CO-tolerant hydrogenase (CooH) lacking the gene sequence for the C-terminal peptide normally cleaved off upon maturation has been described [47]. The *cooH* gene is found upstream from *cooF*, a gene closely associated to the *cooS* CODH structural gene [42]. Although the presence of Ni in CooH has not been demonstrated, all the conserved Ni cysteine active site ligands (see below) are present. If this is indeed a Ni-protein, then its active site assembly must be significantly different from the equivalent process in CO-independent [NiFe] hydrogenases.

Another group of proteins displaying significant homology with hydrogenases, but also lacking the C-terminal maturation peptide, has been recently described [48, 49]. These putative Ni-binding proteins are postulated to be part of two-component regulatory systems involved in the control of hydrogenase expression. In both *B. japonicum* and *R. capsulatus*, the respective hydrogenase-like sequences *hupU* and *hupV*, are associated with genes coding for soluble kinases which are autophosphorylatable sensor proteins [49]. HupU shares amino acid similarities with both the large and small subunits of hydrogenase and can be regarded as an in-frame fusion of the *hupL* and *hupS R. capsulatus* structural genes. The *hupU* and *hupV* gene sequences also lack the C-terminal "maturation" region and if their protein products contain a Ni center, then its assembly may be similar to the one of the CO-dependent hydrogenase described above. The idea of a Ni-center playing the role of a substrate sensor by binding $H_2$ [50] is seductive since the homologous hydrogenase Ni-containing active site is known to bind $H_2$ (see below).

## 5
## The Coordination of Biological Nickel

Detailed natural Ni coordinations are only known from the crystallographic structures of urease from *K. aerogenes* [16] and hydrogenase from *D. gigas* [17].

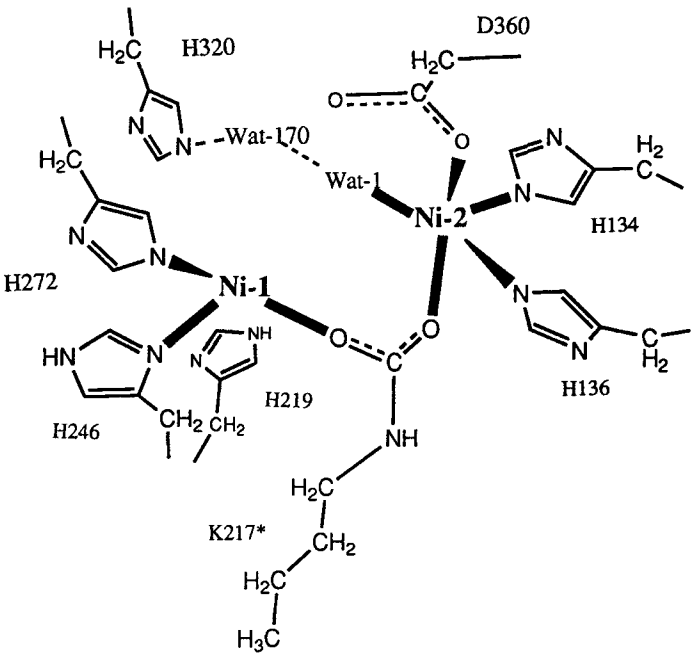


**Fig. 3.** The active site of *K. aerogenes* urease. The two Ni ion have different coordinations. Ni1 has an open ligand site that may be instrumental in catalysis (see Fig. 9). This figure was adapted from [16]

## 5.1 Urease

In urease, the two Ni centers are not equivalent [16]. The geometry of Ni1 can be approximately described as pseudotetrahedral with a weakly occupied fourth ligand. The geometry for Ni2 can, in turn, be defined as either distorted trigonal bipyramidal or distorted square pyramidal. As in ribulose-1,5-biphosphate carboxylase oxygenase (Rubisco) [51] and phosphotriesterase [52] the metal binuclear center is bridged by a carbamylated lysine residue (Fig. 3). In the case of Ni1, the rest of the coordination sphere is composed of two histidine residues and a weakly bound water molecule and for Ni2, of two histidine and one aspartic side chains and a tightly bound water molecule [16]. The Ni centers are in the stable diamagnetic 2+ state. Since Ni(II) model compounds with O,N ligands have a tendency to form octahedral complexes, it is clear that the protein environment in urease exerts a considerable influence on the Ni coordination geometry. This is also strongly suggested by the conservation of the active site geometry in the apoenzyme, excepting the carbamylated lysine residue which is not present [53] (Fig. 4). This conservation, along with solvent exposure of the active site (Fig. 1) may also explain why Ni can be readily incorporated to apourease in vitro in the sole presence of $CO_2$, which is required to form the modified lysine residue [54].

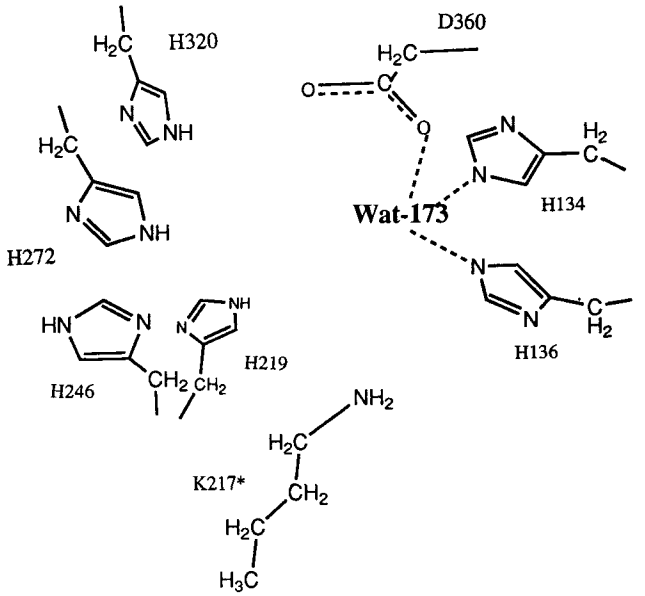


**Fig. 4.** The active site of apourease. Although the Ni ions are absent, the conformation of the active site residues remains essentially unchanged except for the decarbamylation of Lys 217. This may explain why Ni can bind to the apoenzyme restoring its catalytic activity provided $CO_2$ is added [54]. This figure was adapted from [53]

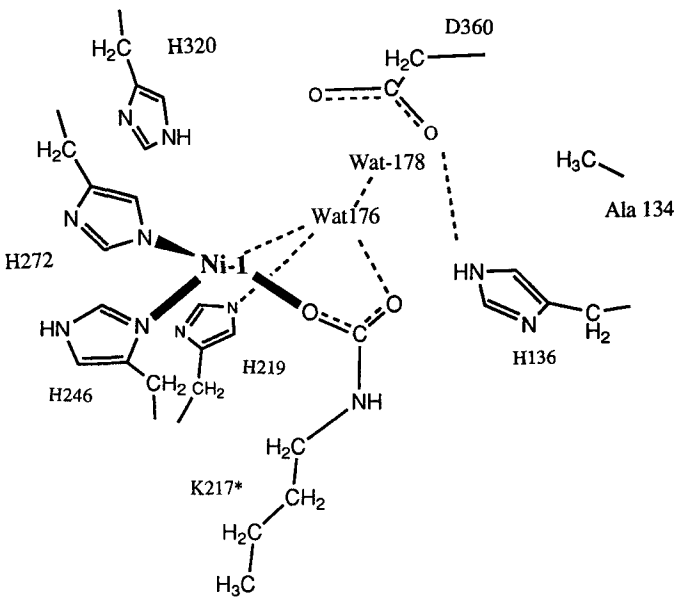


**Fig. 5.** The H134A mutant with a mononickel metallocenter. Although Lys 217 is carbamylated, the absence of Ni2 results in a completly inactive enzyme. Water molecules compensate for the missing ion. This figure was adapted from [55]

Very recently, a mononickel center has been characterized in a mutant of *K. aerogenes*urease [55] (Fig. 5). Replacement of one of the histidine ligands by Ala led to the loss of Ni2. The remaining Ni1 center has now octahedral geometry and binds three water molecules in addition to the original two histidines and one carbamylated lysine residues. Otherwise, the active site amino acid residues conformations are almost unchanged relative to the wild-type protein. Although the resulting protein is completely inactive (see below), the authors consider this to be a new biological Ni-binding site [55].

## 5.2 Hydrogenases

The crystal structure of *D. gigas* hydrogenase has shown that the active site, that was originally considered to be a mononuclear center [24] is actually heterobinuclear containing both Ni and Fe [16, 56, 57] (Fig. 6). Recent X-ray absorption (XAS) experiments [58, 59] have indicated a 2 $S^-$ ($Cl^-$) 3 N(O) Ni first sphere coordination in the hydrogenase from *Thiocapsa roseopersicina*. However, in agreement with earlier reports for the *D. gigas* enzyme [60] and the conservation of cysteine residues in the large subunit, only four cysteine thiolates coordinate the Ni ion (from motifs L2 and L5 in [24]). Of these, two are terminal and two bridge the Ni and Fe centers (Fig. 6). Based only on protein ligation, the coordination of the Ni ion appears to be square pyramidal with an in-plane vacant ligand site. However, in the crystal structure of the oxidized enzyme, the vacant site is occupied by a putative oxygen, probably oxo, species thus completing the square pyramidal coordination [56] (Fig. 6). The inability

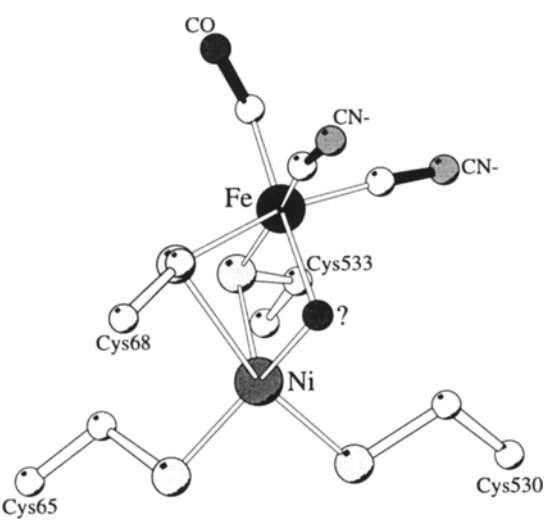


**Fig. 6.** The active site of hydrogenase. "?" represents a putative oxo ligand tightly bound to the Ni center. The assignment of CO und $CN^-$s is based on the protein environment (not shown) [56]

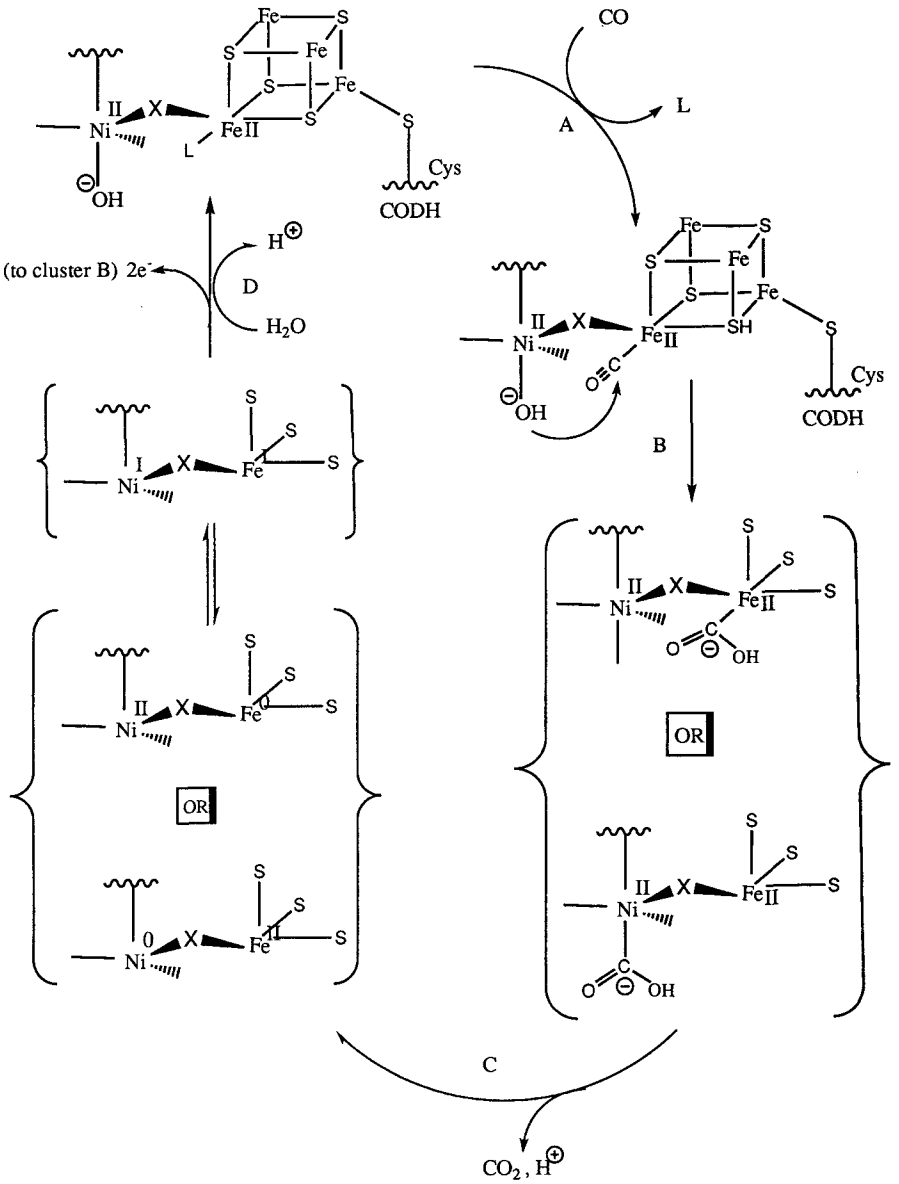


**Fig. 7.** A schema depicting the reaction shown in Eq. (4) and catalyzed by the C-center of CODHs. The active site in the resting state is depicted on the upper left corner. In this cycle the Ni ion is postulated to be redox active. This figure was adapted from [107]

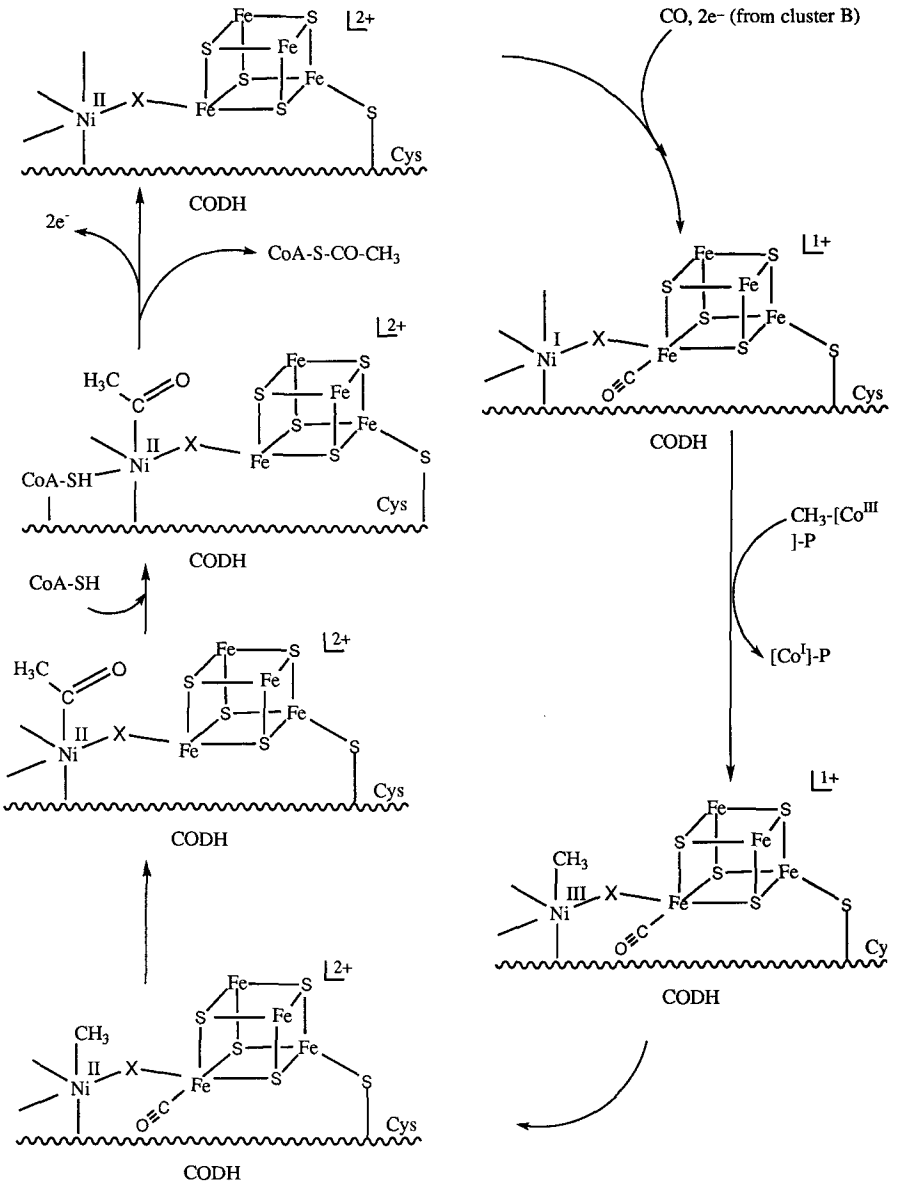


**Fig. 8.** Ragsdale's model for the reaction depicted in Eq. (5) and catalyzed by the A-cluster of CODH/ACS. This model proposes the insertion of CO (coming from the FeS cluster) into the Ni-$CH_3$ complex. This figure was adapted from [120]

of XAS to detect the actual Ni coordination, as well as the presence of the active center Fe ion, has been recently explained [61]. Similarly, neither EPR ([24] and Refs. therein) nor Mössbauer [62, 63] spectroscopy could detect the Fe center suggesting that it is in a low spin diamagnetic state, at least in those states that have been studied. The studies may have been further complicated by the presence of three additional [FeS] clusters in the enzyme (Table 1 and Fig. 2). A series of IR spectroscopic studies of *Chromatium vinosum* and *D. gigas* hydrogenases [56, 64, 65] along with the crystallographic evidence from the latter [56] have led to the conclusion that the active site Fe center is further coordinated by two cyanides and one carbon monoxide molecules (Fig. 6). The implications of this unique [NiFe] center for hydrogen catalysis will be discussed below.

### 5.3
### CODHs

The term carbon monoxide dehydrogenase (CODH) describes in fact two different classes of enzymes: the CODHs proper, represented by the *Rhodospirillum rubrum* enzyme, and the CODHs such as the one from *Clostridium thermoaceticum* which possesses both the CO oxidation (CODH) and acetyl coenzyme synthetase (ACS) activities. The enzyme from *R. rubrum* has an active center (the C-cluster) recently postulated to be a $[Fe_4S_4]$ cluster bridged by an unidentified redox active ligand to a Ni ion [66–68] (Fig. 7). The C-cluster Ni ion may be the substrate binding site for $CO/CO_2$ [67]. The *C. thermoaceticum* enzyme has an additional Ni containing center (the A-cluster) involved in acetyl coenzyme synthesis. This center is also postulated to be a $[Fe_4S_4]$ cluster bridged by an unidentified ligand (maybe inorganic sulfur or a cysteine thiolate) to a Ni ion (Fig. 8). The Ni center is thought to bind a $-CH_3$ group transferred from a methylated correnoid-iron-sulfur protein [69] whereas one of the Fe ions from the $[Fe_4S_4]$ cluster binds the substrate CO (but see [70]). Nothing is known concerning the rest of the Ni coordination sphere in either CODH A or C clusters although EXAFS experiments have indicated a mixed 2S, 2–3 N/O coordination in a distorted pentacoordinated or tetrahedral geometry for the C-cluster of *R. rubrum* [71].

## 6
## Catalytic Nickel

Biological catalysis by Ni can be divided in two broad classes: the hydrolase activity represented by urease and the redox-associated mechanisms typical of hydrogenase, S-methyl coenzyme M reductases and CODHs.

### 6.1
### Ureases

Ureases catalyse the hydrolysis of urea to ammonia and carbamate according to the reaction:

$$H_2NCONH_2 + H_2O \rightarrow NH_3 + H_2NCOOH \quad (1)$$

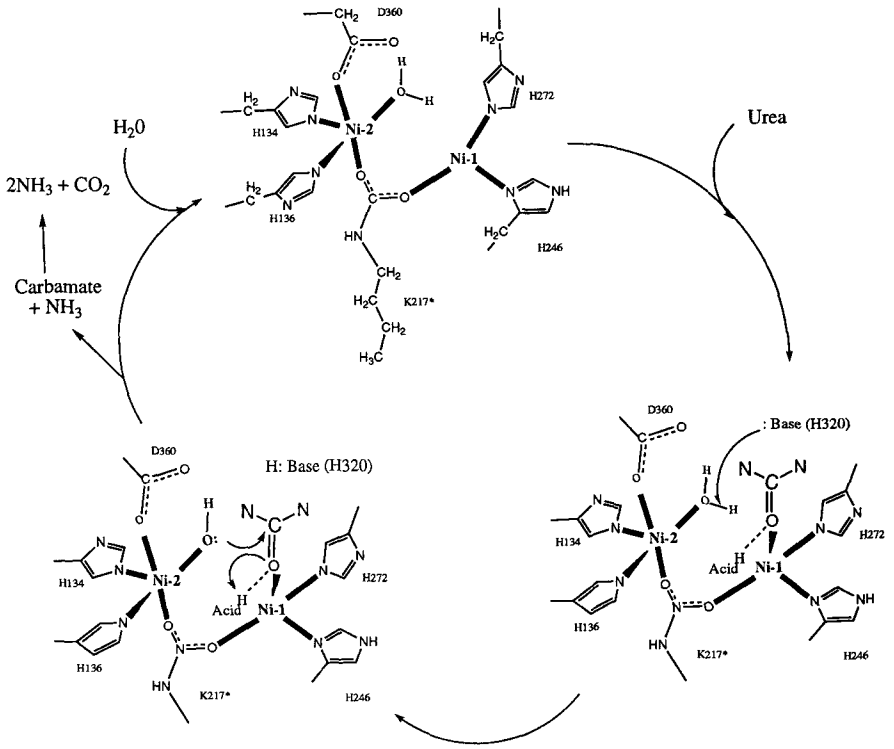


**Fig. 9.** The proposed catalytic cycle of urease [16, 74]. Note that the Ni1's empty coordination site (Fig. 3) may be the urea binding site. His 320 serves as the activator of the water molecule bound to Ni2. This figure was adapted from [74]

The binuclear Ni center seems to play a role similar to equivalent active sites in phosphotriesterase and methane monooxidase which have binuclear Zn and nonheme Fe centers, respectively [52, 72]. A generalized scheme postulates the polarization of the substrate through oxygen binding to one of the Ni centers, followed by nucleophilic attack by a Ni-bound hydroxyl (water dissociated) group (Fig. 9). The choice of Ni for this reaction is intriguing although it may be related to the high affinity of the urea-Ni ion binding [53] and/or the stability of the urease Ni-containing active site when compared to similarly coordinated catalytic Zn binuclear centers [73]. In these catalytic reactions the Ni ions, as $Ni^{2+}$, seem to play the role of Lewis acid catalysts [74].

Site-directed mutagenesis has been used to probe the role of residues close to the active site. The His219Ala (H219A) mutant has a Km of 1100 mM compared to 2.3 mM for wild type and a 3% Kcat relative to the latter [75]. The His320Ala (H320A) mutant, in turn, has a Km equivalent to the one of the wild type but a corresponding Kcat of only 0.003%. These results, along with other lines of evidence [75, 76], potentially implicate His219 in substrate binding and His320 as the catalytic base. The crystal structures of these two mutants have been solved and the following observations have been made: 1) H219A: besides

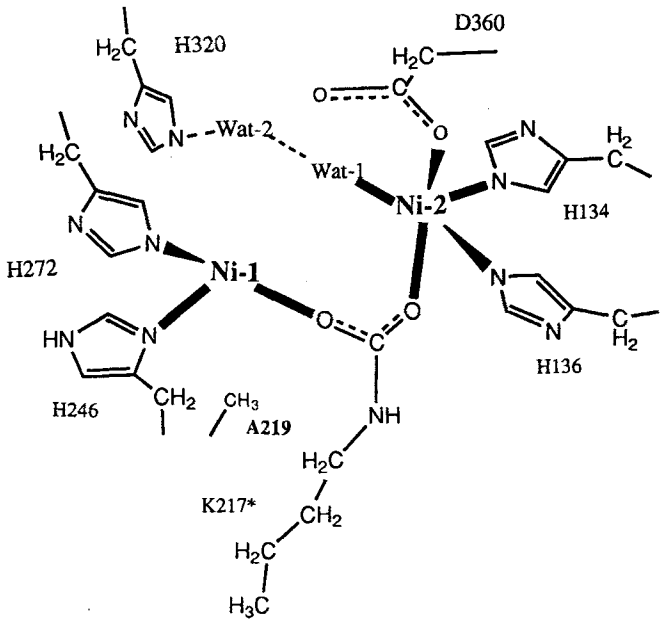


**Fig. 10.** The H219A urease mutant. The rearrangement of the active site geometry is mediated by an extra water molecule. This figure was adapted from [53]

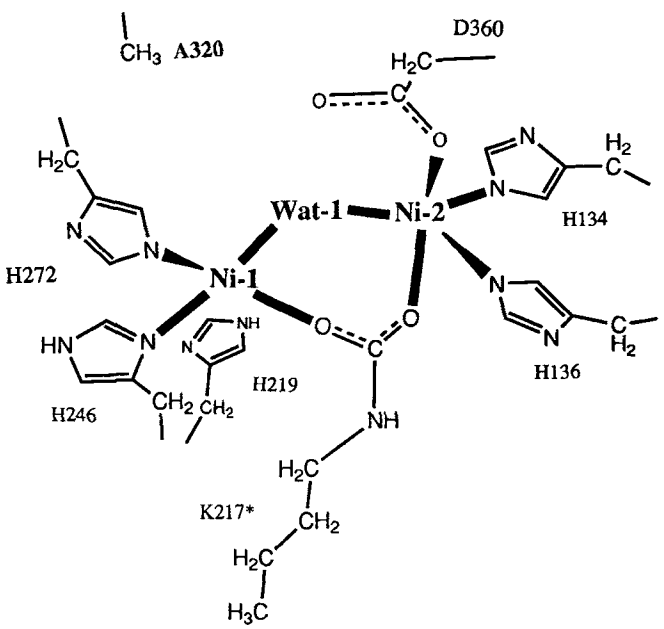


**Fig. 11.** The H320A urease mutant. The water molecule that originally was only bound to Ni2 has now moved into a bridging position. This figure was adapted from [53]

the absence of the histidine side chain only minor changes are observed. Both Wat-1 and W-170 maintain their positions and the Ni center and active site residues shift by less than 0.3 Å [53] (Fig. 10). The lower Kcat of this mutant is attributed to small shifts in the orientation of His320, provoked by a rotation of Asp 221 side chain in the absence of His219; 2) H320A: the only major structural changes are the loss of Wat-170 and a shift of Wat-1 which changes from a Ni2 ligand in the wild type enzyme (Fig. 3) to a bridging ligand between the two Ni centers (Fig. 11). This coordination change may be important since, if urea does bind at the normally empty fourth coordination site on Ni1, the filling of this site by Wat-1 could have a profound effect on catalysis. Thus, in addition to a role as a catalytic base, His 320 may also help maintaining an active site geometry that allows productive urea binding [53]. The mononickel mutant His134Ala (H134A) [55] (Fig. 5) displays no activity in spite of the presence of carbamylated Lys 217, emphasizing the importance of the binuclear center for catalysis.

## 6.2 Hydrogenases

Hydrogenases catalyse the splitting or synthesis of the hydrogen molecule according to the reaction:

$$H_2 \leftrightarrow 2H^+ + 2e^- \quad (2)$$

The reaction is heterolytic [77] producing $H^-$ and $H^+$ in the first step. There is no consensus regarding the role of Ni in hydrogenases. At least three potential redox-active species are found at the active site: the thiolate ligands [78] and the Fe [56] and Ni [24] ions. Several, as prepared, oxidized hydrogenases display various ratios of two electron paramagnetic resonance (EPR) signals known as Ni-A and Ni-B (Table 2). These are generally considered to arise from Ni(III) $d^7$ species although the two states show fundamental differences both chemically and spectroscopically [24, 79]. Activation of the enzyme in the Ni-A state is slow and temperature-dependent whereas enzyme displaying the Ni-B signal can be

**Table 2.** Biological nickel natural EPR signals

| Protein | Center | g-Values | Comments |
|---|---|---|---|
| Hydrogenase | | | |
| (D. gigas) | NiFe | Ni-A: 2.32 2.23 2.01 | "unready form" |
| | (Large sub-unit) | Ni-B: 2.34 2.16 2.01 | "ready form" |
| | | Ni-C: 2.19 2.16 2.01 | "active form" |
| | | Ni-C*: 2.35 2.13 2.04 | "photolyzed form" |
| CODH | | | |
| (R. rubrum) | NiFe (C-center) | 2.04 1.90 1.71 | "signal A" |
| (C. thermoaceticum) | NiFe (C-center) | 1.970 1.87 1.75 | "the $g_{av}$ = 1.86 signal" |
| | | 2.01 1.81 1.65 | "the $g_{av}$ = 1.82 signal" |
| | NiFe (A-center) | 2.080 2.074 2.028 | "NiFeC signal" |

readily activated [79]. EPR experiments using $^{17}O_2$ have indicated that both Ni-A and Ni-B states have bound oxygen at, or near, the Ni ion [80]. This has been confirmed by the crystallographic analysis of the as-prepared *D. gigas* hydrogenase that shows that the active site contains a tightly Ni-bound putative oxo species (Fig. 6). The crystalline enzyme displays mostly the Ni-A signal although, as commonly observed for this enzyme ([81] and Bertrand P, personnal communication), the signal amounts to significantly less than one spin/mole. Since the putative oxo species appears to be fully occupied [56] and IR spectroscopy poised at mid-point potentials of well EPR characterized species show mostly single states [56, 65], it is not possible to explain the nature of the EPR silent material in either IR spectroscopic or structural terms.

The EPR-monitored titration of hydrogenases [82, 83] shows what has been interpreted as alternated paramagnetic and diamagnetic Ni signals generated upon one-electron reductions. The one-electron reduction of the Ni-B form (the equivalent titration of the Ni-A species has not been reported) generates the EPR-silent Ni-SI state [81]. A new EPR-active species is obtained by an additional one-electron reduction. This species, called Ni-C, has attracted considerable attention perhaps because it is the only catalytically relevant form detectable by EPR. The Ni-C state can be photolyzed generating new EPR detectable species [24, 84] and this effect is modified by the use of $^2H$. Such isotopic effect indicates the presence of a hydrogen species that dissociates from Ni upon photolysis [24, 84]. Both Ni(III) $d^7$ and Ni(I) $d^9$ states have been postulated for the Ni-C form, with $H^-$, $H^+$ and $H_2$ possibly bound [24, 81]. Arguments against hydride binding to Ni stem from the very small hyperfine splitting due to exchangeable $^1H$ [85]. However, it has been suggested that the observed values are consistent with an equatorially-bound hydride [86]. Alternatively, it has been postulated that the photolyzed hydrogen species of Ni-C actually arises from the deprotonation of a thiol group bound to the Ni ion [82]. According to Barondeau et al. [81] the Ni-C form is stable in the absence of molecular hydrogen and cannot spontaneously reduce protons to $H_2$. These authors conclude that Ni-C is not the "active" species but corresponds to one of three relevant Ni states during the catalytic cycle.

Finally, the one-electron reduction of the Ni-C form results in a new diamagnetic species called Ni-R. A plausible catalytic cycle can be postulated where the enzyme in the Ni-SI state binds $H_2$ [81] yielding the two-electron more reduced Ni-R. Subsequent one-electron oxidations Ni-R $\rightarrow$ Ni-C $\rightarrow$ Ni-SI close the cycle. In addition to the redox changes, the various states differ in their degree of protonation, as indicated by the pH dependence of their redox potentials [87] (Fig. 12).

Maroney and co-workers have argued that Ni is unlikely to be redox active under physiological conditions and that the redox process is most likely ligand-based [78]. Consequently, these authors have provided an alternative description of the paramagnetic Ni-C state as being generated by the interaction of a thyil radical with a Ni(II) ion. This species is isoelectronic with a Ni(III)-$H^-$ bound to a thiolate according to the reaction:

$$\ddot{S}\text{-Ni(III)-H}^- \rightarrow \dot{S}\text{-Ni(II)-H}^- \qquad (3)$$

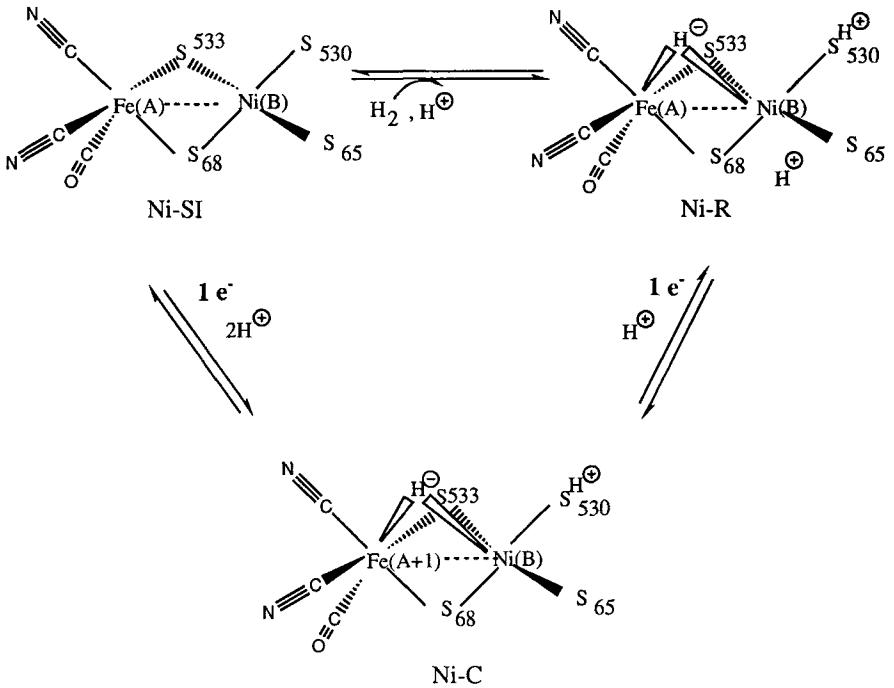


**Fig. 12.** Hydrogenase catalytic cycle. The hydride is postulated to bridge the two metal centers. Proton balance is based on the pH dependence of the redox potentials [87]. A + B = 2n

Relevant sulfur binding to Ni(III) has been modeled by Choudhury et al. [88]. Although similarly ligand-based reactions have been put forward concerning the oxidation of hydrogenase to the Ni-A state [78, 89, 90] the crystal structure of the as-prepared *D. gigas* hydrogenase rules out active site thiolate oxidation to either sulfinate or sulfenate in the Ni-A form. On the contrary, as indicated above (Fig. 6) the putative bridging oxo species is tightly bound to the Ni ion. *This implies that only the reductive redox processes could be ligand-based.*

One important reason for excluding redox processes that are purely Ni-based is that these would imply four different Ni redox states: Ni-B (Ni(III)) → Ni-SI (Ni(II)) → Ni-C (Ni(I)) → Ni-R (Ni(0)). Such changes, comprising potentials confined to those observed in hydrogenase (−100 to −400 mV), would be totally unprecedented [57, 91, 92]. Even one-electron changes at the Ni center during catalysis are unlikely judging from XAS experiments where only the Ni-A/B → Ni-SI transition displays a significative edge change, amounting to about 1 to 2 eV [61].

Based on our discovery of an active site NiFe center we have proposed mechanisms where both Ni and Fe play important roles during catalysis [56, 57, 93]. In these propositions, the Ni ion serves as the catalytic site proper, heterolytically splitting the $H_2$ molecule into $H^-$ and $H^+$ with the thiolate of Cys530 playing the role of a base; whereas the Fe ion intervenes in the one-electron oxidations. We have recently reviewed the most relevant model chemistry con-

sidering the structure of hydrogenase active site and favored a Ni(I) formal state for the molecular hydrogen binding species [57]. The main conclusions of that study were the following: 1) sulfur (or selenium) ligands in the first coordination sphere of the Ni seem to be required for hydride and/or CO binding and these species bind preferencially to Ni(I) [94, 95]; 2) thioethers and $\mu^2$-metalated thiolates (such as the ones found in hydrogenase active site) are good Ni(I) stabilizing ligands [96], 3) several unrelated species give Ni-C-like signals indicating that based on EPR alone Ni(III) and Ni(I) cannot be distinguished; and 4) in model compounds, the heterolytic cleavage of molecular hydrogen is assisted by a base [97]. The models we have proposed take these observations into account [56, 57, 93].

The fundamental role of the chalcogenide function corresponding to position 530 in *D. gigas* hydrogenase as a putative base during catalysis is illustrated by the presence of a selenocysteine in a equivalent position in several other hydrogenases [98, 99]. For instance, in the *Desulfomicrobium baculatum* enzyme, the $H_2$/HD exchange reaction is $>1.0$ whereas the contrary is true in the case of the *D. gigas* hydrogenase. The substitution of sulfur by selenium, that requires a special synthetic strategy [99], very likely represents a "fine-tuned" modification of the catalytic properties.

The discovery of triple-bonded species [100, 101], their crystallographic assignment as active site Fe ligands [56, 57] and their isotope-based identification [64] as being two CN-s and one CO has resulted in a a very powerful tool to probe redox changes at the hydrogenase active site by Fourier transform infrared (FTIR) spectroscopy [65, 101]. It is remarkable that both EPR (that monitor the magnetic changes of the Ni ion) and IR titrations (which detect electron density or coordination changes at the Fe center) follow almost identical patterns [65]. This suggests that at the active site, electron and proton additions are being sensed by both centers. One puzzling observation, however, is that the enzyme poised at selected potentials displays rather homogenous IR states [56, 65] whereas, as mentioned above, in the exactly equivalent experiment monitored by EPR, Ni normally titrates to significantly less than one spin/mole indicating that the sample is heterogeneous with respect to it [102]. A similar situation in CODH (see below) has been explained as arising from concomitant one-electron redox reactions which have very similar mid-point potentials [103]. Further experiments dealing with the crystallographic study of both reduced and CO-complexed forms of NiFe hydrogenases and with directed mutagenesis of selected residues potentially involved in electron and proton transfer, as well as those lining the active site cavity, are likely to shed more light on the Ni-mediated mechanism of hydrogen metabolism by micro-organisms.

## 6.3 CODHs

A general feature of CODHs is the presence of the CO-oxidation Ni-containing site called the C-center [103, 104] that catalyzes the reaction:

$$CO + H_2O = CO_2 + 2H^+ + 2e^- \quad (4)$$

An extended X-ray absorption fine structure (EXAFS) study carried out at the Ni K-edge has suggested that Ni in the C-center of *R. rubrum* CODH has a distorted tetrahedral or five-coordinate environment with 2S and 2–3 N/O ligands [71]. Although previous studies had indicated that the Ni ion could be part of the core of a $[NiFe_3S_4]$ cubane cluster [105], the EXAFS study has ruled out that possibility. Instead, a model consisting of a mononuclear Ni(II) site bridged by a cysteine thiolate or sulfide to a $[Fe_4S_4]$ cluster was proposed [71] (Fig. 7). Further studies have been carried out on the more complex CODH/ACS enzyme from *C. thermoaceticum* where the C-center is known to be located in the $\beta$-subunit [104]. These authors have proposed a mechanism for $CO/CO_2$ oxidation where the C-center can be stabilized in three states: an oxidized state (EPR silent, $S = 0$), a one-electron reduced state (EPR $g_{ave} = 1.82$) and a three-electron reduced state (EPR $g_{ave} = 1.86$) (Table 2). The cluster generating the $g_{ave} = 1.82$ EPR signal contains a distinct subsite called ferrous component II (FCII) that is possibly pentacoordinated (Fig. 7). The Ni site may be electronically linked to this subsite [66]. When the enzyme is in the $C_{1.82}$ form, it can oxidize CO catalytically. CO binds $C_{1.82}$, reacts with $OH^-$, becomes $CO_2$ while it tranfers two electrons to $C_{1.82}$ and dissociates from $C_{1.86}$ (Fig. 7). The respective redox potentials are for $CO/CO_2 = -520$ mV at pH 7.0 and for $C_{1.82}/C_{1.86} = -530$ mV, indicating that the free energy change for the reaction is small [104]. Inhibitor binding has been instrumental in defining the properties of the C-center [105]. Azide, thiocyanate and cyanate have been shown to bind to the C-center and inhibit CO oxidation [106]. A Mössbauer study has shown that all the irons in the Ni-deficient CODH from *R. rubrum* belong to cubane-type $[F_4S_4]$ clusters [66] indicating that the assignment of a Ni-X-$[F_4S_4]$ cluster for the C-center is probably correct [71]. A model for CO oxidation has been proposed by Qiu et al. (Fig. 7) [107]. The other center, called B, is a classic $[F_4S_4]$ cluster which spectroscopic features are independent of the presence of Ni in both *C. thermoaceticum and R. rubru*enzymes. The B-center mediates electron flow from the C-center to the external electron acceptors in *R. rubrum* CODH and to the A-cluster in *C. thermoaceticum* CODH [108].

In addition to reaction (4), the *C. thermoaceticum* enzyme is also capable of catalyzing the synthesis of acetyl-coenzyme A at the A-center located in the $\alpha$-subunit:

$$CH_3\text{-THF} + \text{CoASH} + \text{CO} \rightarrow \text{CoASCOCH}_3 + \text{THF} \qquad (5)$$

This reaction is part of the reductive acetyl-CoA (or Wood/Ljungdahl) pathway [6], the major mechanism of $CO_2$ fixation in anaerobic environments. Thus sulfate-reducers, methanogens and acetogens can convert CO (or $CO_2$) to cell carbon. Upon CO binding to the A-center a EPR signal ($g = 2.08, 2.074, 2.028$, see table II) appears. Because the signal shows hyperfine broadening upon $^{57}Fe$, $^{61}Ni$ and $^{13}C$ isotopic enrichment, indicating magnetic coupling between the two metals, it has been called the NiFeC signal [109]. The NiFeC signal is not only present in *C. thermoaceticum*, an acetogen, but also in *Methanosarcina thermophila*, a methanogenic bacterium [110] and may be a general feature of CO binding to the A-cluster in CODHs. Q-band electron nuclear double resonance (ENDOR) experiments using $^{57}Fe$, $^{61}Ni$ and $^{13}C$ [111] indicate that the most likely

stoichiometry for the novel NiFeC center is one nickel, three to four irons, four or more sulfurs, and one carbon atom. These experiments did not determine whether CO was bound to Ni or Fe. XAS experiments [112] indicate that the two metals are separated by 3.25 Å and consequently could be bridged by an (unidentified) ligand. Besides CO, the A-cluster binds a -$CH_3$ group from a methylated correnoid-iron-sulfur protein (CoFeSP). The methyl group originates from $CO_2$ which is first converted to methyl tetrahydrofolic acid (THF-$CH_3$ in reaction (5)). It was postulated that the binding of CO and -$CH_3$ can occur in any order. What was not determined, however, is whether the two substrates bind to the same or different metal centers. Ragsdale and coll. [113] concluded that one-electron reductive activation of the same metal site was necessary for methyl, CO and acetyl binding and that this site gives rise to the NiFeC EPR signal upon CO binding. Binding of CoA to CODH, on the other hand, is not sensitive to the redox potential. The insertion of CO to a Ni-$CH_3$ complex has been demonstrated for a model compound having (3S,1N) Ni coordination by Stavropoulos et al. [114]. These authors found that Ni(II)-$CH_3$, Ni(II)-$COCH_3$, and Ni(I)-CO are stable adducts. MacGregor et al. [115] have shown that even Ni(II)-CO complexes can be formed provided there is significant back-donation from the ligands to the Ni(II) center. If, as reported [112], the Ni center of *C. thermoaceticum* CODH A-cluster has a predominant sulfur coordination, a Ni(II)-CO complex may be a relevant catalytic intermediate. These results suggested that the same metal center (presumably Ni) could be the binding site of both CO and methyl, as well as the site where CO insertion to the metal-carbon bond occurs. FTIR studies have indicated that CO binds terminally to a metal center of the A-cluster giving rise to an IR band with $\nu_{CO} = 1995$ $cm^{-1}$ [116]. Replacement of CO by $^{13}CO$ shifts the $\nu_{CO}$ band to 1951 $cm^{-1}$. Isotopic exchange shows that the M-CO intermediate is a catalytically relevant precursor of acetyl-CoA:

$$\text{CODH} \xrightarrow[\text{CH}_3\text{-}^{12}\text{CO-CoA}]{^{13}\text{CO}} \underset{(\nu_{CO}=1951\ cm^{-1})}{\text{CODH-}^{13}\text{CO}} + \underset{(\nu_{CO}=1995\ cm^{-1})}{\text{CODH-}^{12}\text{CO}} \qquad (6)$$

The authors also showed that the 1995 $cm^{-1}$ band and the g = 2.074/2.028 EPR signal are signatures of the same (NiFeC) complex.

A major conclusion concerning the identity of the CO-binding metal center has been reached by Qiu et al. [117] using resonance Raman (RR) spectroscopy. This technique is complementary to FTIR spectroscopy in that it allows the study of metal-carbon vibrations. Firstly, the authors identified a M-C band at 360 $cm^{-1}$ that shifted when $^{12}CO$ was replaced by either $^{13}CO$ (356 $cm^{-1}$) or $^{18}CO$ (353 $cm^{-1}$). The shifts were also observed in an isotopic exchange experiment (as the one described above) leading Qiu et al. [117] to conclude that the RR 360 $cm^{-1}$ and IR 1995 $cm^{-1}$ bands arise from the same M-CO complex. In order to identify the nature of M, bacteria were grown using medium supplemented with either $^{54}Fe$ or $^{64}Ni$. Upon CO binding, the 360 $cm^{-1}$ band shifted to 362 $cm^{-1}$ in the $^{54}Fe$-enzyme but was not modified in the $^{64}Ni$-enzyme. This shows that in these experiments CO binds to Fe and *not* to Ni in the A-cluster of CODH. The authors conclude that "the Fe-S cluster of the A-cluster is directly involved in the mechanism of CODH catalysis, and is not simply an electron transfer agent" [117].

A similar approach has led Kumar et al. [118] to determine which center of the A-cluster binds the methyl group transfered from the CoFeSP. These authors first identified a Co-$CH_3$ stretching frequency at 429 $cm^{-1}$ (from CoFeSP) that disappeared upon addition of CODH, to be replaced by a new band at 422 $cm^{-1}$. The 422 $cm^{-1}$ band shifted frequencies when either $^{13}CH_3$ (410 $cm^{-1}$) or $C^2H_3$ (392 $cm^{-1}$) was used for methylation; it also shifted to 417 $cm^{-1}$ with samples enriched in $^{64}Ni$. The band did not shift, however, when samples were enriched in $^{54}Fe$ or $^{58}Fe$. These experiments show that the Ni center is the one to be methylated by CoFeSP.

From their results Ragsdale and coll. [118] have proposed a bimetallic catalytic mechanism for acetyl synthesis implying either CO migration from the Fe to the Ni-$CH_3$ complex or (probably less likely) migration of methyl from the Ni ion to the Fe center [119, 120] (Fig. 8). The proposed mechanism is reminiscent of the reaction devised by Monsanto for the industrial production of acetic acid from CO and $CH_3I$, with one important difference: the Mosanto process takes place at a mononuclear center. Kovacs [21] has pointed out the exceptional nature of the mechanism proposed by Ragsdale and coll.: not only does CO insertion to M-C bonds in model compounds occur generally at mononuclear sites; it also requires metal ligands with electron-acceptor properties that are not biologically available. Tucci and Holm [120] have obtained Ni(II)-$CH_3$-thiolate complexes that can react with CO and form Ni(II)-acyl-thiolate adducts. These are postulated to be reasonable analogs for the reaction of CoA · SH with a Ni(II)-$COCH_3$, a step in the reaction scheme advanced by Ragsdale and coll [118]. An alternative pathway is suggested by their work: the reaction of *bound* thiolate (CoA · SH) and acyl groups to form a thioether. This model chemistry is all mononuclear and, consequently, the authors strongly favor a similar intramolecular mechanism for CODH A-cluster acetyl-CoA synthesis (although similar principles could apply to a binuclear-based reaction).

A less well explored aspect of the postulated mechanism, namely the tranfer of a methyl group from CoFeSP to the Ni-center in the A-cluster of CODH, has been recently modelled by Ram et al. [121]. Alkyl transfer from an organocobalt(III) to Ni(I) has been shown to occur in high yields by a mechanism involving free methyl radicals with rates that are similar to those of the reaction of methylated CoFeSP with reduced CODH [118]. In the case of CODH, however, it is possible that the mechanism proceeds by a two-electron event such as a nucleophilic displacement, because radical pathways could be too agressive for the enzyme [121].

A study using the competitive inhibitor $C_2S$ [122] has shown that although this compound mimics CO binding, the $C_2S$-bound species is different from the CO-bound adduct (NiFeC) in one fundamental way: in $C_2S$-CODH the Ni and Fe centers from the A-cluster are magnetically isolated, as $^{61}Ni$, but not $^{57}Fe$ or $^{13}C_2S$, induces a (small) broadening of the EPR signal. No explanation was given for this observation although because the reaction with $C_2S$ is fully reversible, a disruption of the bridging NiFe ligation was considered unlikely [122]. $C_2S$ is postulated to bind, by analogy with CO, to an Fe center in the A-cluster.

The heterobimetallic mechanism proposed by Ragsdale et al. has been very recently seriously questioned by Barondeau and Lindahl [70]. Firstly, these

authors argue that although it seems reasonable to suppose that, as detected by RR spectroscopy, the Ni center binding the methyl group is located at the A-cluster, no evidence to this effect was actually provided by Kumar et al. [118]. According to Lindahl and coll., this is of some concern because only a small fraction of the Ni in CODH is in the A-cluster [44]. Using the chelating agent 1,10-phenanthroline (phen) only about 30% Ni(II) per $\alpha\beta$-dimer could be removed leading, nevertheless, to complete disappearance of the NiFeC signal and CO/acetyl-CoA exchange activity. This observation is consistent with the fact that the NiFeC EPR signal quantifies only to 0.3 spin/$\alpha\beta$-dimer and implies that 70% of the $\alpha$-subunits contain structurally similar but nonfunctional clusters [44]. These authors also wonder whether the Ni-$CH_3$ groups detected by Kumar et al. [118], using RR spectroscopy, were functional in a manner that would yield acetyl-CoA if CO and CoA were added ([44] and references therein). They also object to Holm and coll. model compounds [114, 120] as being relevant for CODH A-cluster catalysis because the CODH mimics react with methyl *anions* to yield Ni(0)-$CH_3$ whereas CODH would react with methyl *cations*, yielding a catalytic Ni(II)-$CH_3$ adduct that can return to its original electronic state as product forms. The Ni(II)-$CH_3$ state is described as being supported by model chemistry [123]. Lindahl and coll. reach the following general conclusions: 1) the 30% CODH labile Ni is the methyl binding site, the conclusion being based on two observations: first, none of the phen-treated enzyme was methylated, and second, bound methyl prevents phen from removing labile Ni. The lability of the Ni center is presented as evidence that it plays a catalytic role because, if acetyl-CoA synthesis proceeds by a migratory insertion step, then the binding site for the methyl group and CO should have two cis open coordination sites.

Lindahl and coll. also argue that the methyl group binds to the $A_{ox}$, and not the $A_{red}$, state [70]. Their argument goes as follows: if, as previously assumed, for methylation to occur the diamagnetic $A_{ox}$ has to be reduced to the paramagnetic $A_{red}$ $S = 1/2$ state (in CO-mediated reduction this would be the species giving rise to the NiFeC EPR signal), the resulting methylated adduct should also be paramagnetic since the reaction involves a diamagnetic methyl cation. However, the methylated A-cluster is EPR silent. As an alternative to the reduction of the A-cluster, these authors postulate that a different redox center has to be reduced prior to methylation. This center, called the D-center, is supposed to be a special pair of cysteines that can be oxidized to cystine (disulfide bond) at an unusually low potential ($E^{\circ\prime} < -350$ mV) and thereby maintain the labile Ni of the A-cluster in the Ni(II) state throughout during catalysis. According to the authors, the Ni(II) assignment is supported by the in vitro incorporation of this ion to CODH [70]. The following mechanism is proposed (see also Fig. 13):

$$[A_{ox}D_{ox}]^{n+} + 2\,e^- \overset{CH_3\text{-}Co_3+FeSP}{\longleftrightarrow} [A_{ox}D_{red}]^{(n-2)+} \leftrightarrow [CH_3\text{-}A_{ox}D_{ox}]^{(n-1)+} + Co^{1+}FeSP \tag{7}$$

$$[CH_3\text{-}A_{ox}D_{ox}]^{(n-1)+} + CO \leftrightarrow [CH_3\text{-}(CO)\text{-}A_{ox}D_{ox}]^{(n-1)+} \overset{CoAS^-}{\longleftrightarrow} CH_3\text{-}C(O)\text{-}SCoA + [A_{ox}D_{red}]^{(n-2)+}$$

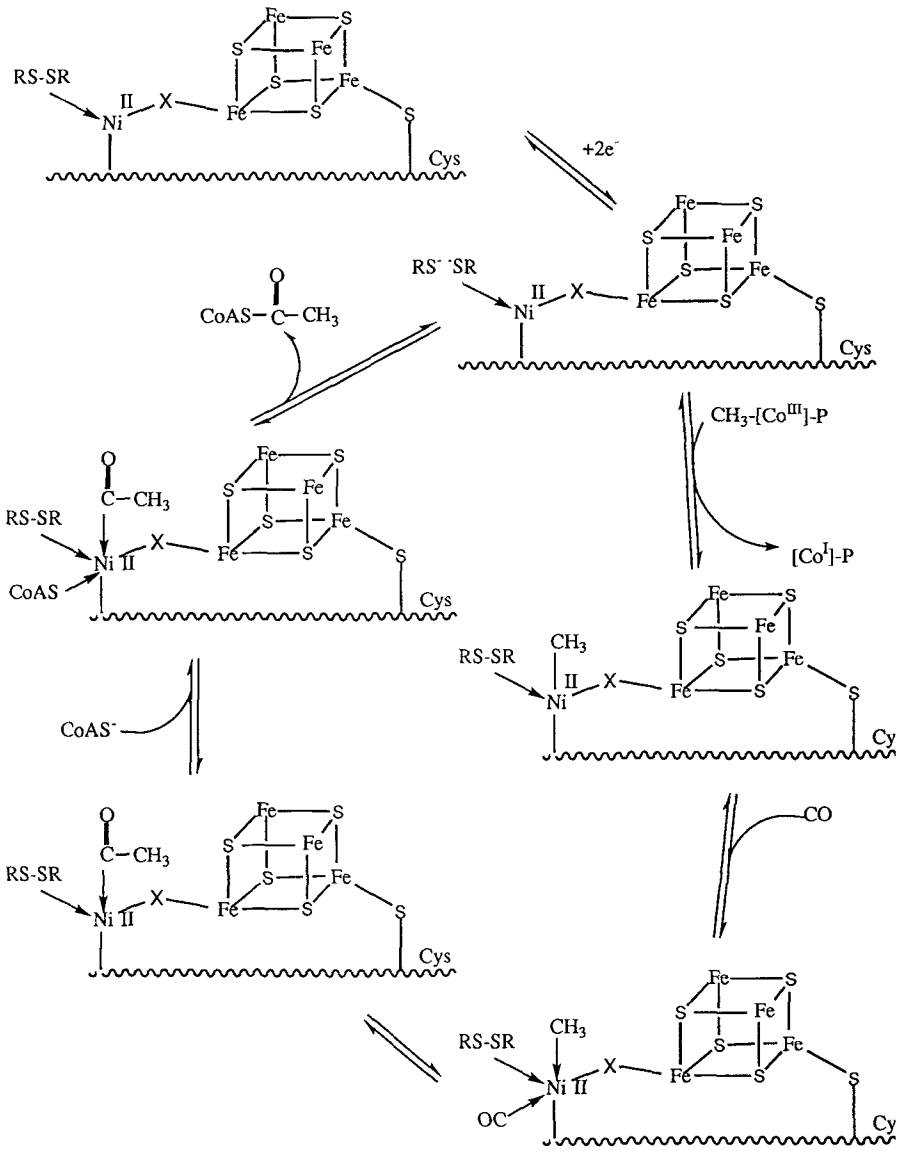


**Fig. 13.** Lindahl's model for the reaction depicted in Eq. (5) and catalyzed by the A-cluster of CODH/ACS. This model proposes the insertion of Ni-bound CO into the Ni-$CH_3$ complex. The special pair of cysteines (the D-center) is shown. *Arrows* are meant to indicate that the actual coordination position (axial or equatorial) is not known. This figure is based on [70]

One of the key points of the proposed mechanism is that the A-cluster remains in the $A_{ox}$ state throughout catalysis. This proposition is in conflict with previous hypotheses that have postulated that $A_{red}$-CO is a catalytic intermediate of acetyl-CoA synthesis [117, 124, 125]. Barondeau and Lindahl [70] argue that the Mössbauer evidence does not favor reduction of the $Fe_4S_4$ portion of the A-cluster which they suggest stays in the +2 state. If this is the case, then binding of CO to an $[Fe_4S_4]$ cluster, as postulated by Qiu et al. [117], would become problematic because there is no model chemistry to support CO binding to $[Fe_4S_4]^{2+}$. The same argument, against reduction of the putative $[Fe_4S_4]$ cluster, would apply to the scheme suggested by Tucci and Holm [120] (Fig. 8). Furthermore, these authors have suggested that a two-electron reduction process takes place in going from $A_{ox}$ to $A_{red}$ with the second electron reducing Ni(II) to Ni(I). Again, Barondeau and Lindahl [70] consider this proposition inadequate because of the lack of relevant model methylations of Ni(I) compounds to form Ni(III)-$CH_3$ adducts, as opposed to Ni(II)-$CH_3$ complexes, for which there are several examples in the literature. Finally, as stated above, these authors point out that most of the studied migratory insertion reactions involving metal-bound CO and methyl groups occur with these species coordinated to adjacent positions on a *single* metal ion.

Clearly, many of the aspects of the Ni-mediated catalytic mechanism of acetyl-CoA synthesis by CODH remain to be elucidated. Significant progress is being made however, and it may be expected that the current controversy concerning this process will soon be clarified as more relevant data becomes available.

## 7
## The Roles of Biological Nickel. A Conclusion

Four distinctive roles of biological Ni have been reviewed here: the Lewis acid-base chemistry in ureases, the heterolytic cleavage of hydrogen in hydrogenases, and the oxidation of CO and acetyl-CoA synthesis in CODH. Maybe the simplest one to analyze is the case of urease because there is no redox chemistry associated with catalysis and Ni is always in the stable Ni(II) state. The catalytic mechanism of this enzyme is not significantly different from that of phosphodiesterase which, however, uses other metal centers. The choice of Ni in urease, although somewhat enigmatic, can be rationalized by either an increased stability of the metal coordination or a high affinity of the metal for the carbonyl group of the substrate. Alternatively, the choice could be mostly historical, and be related to the fact that urea is a very simple organic substrate that probably constituted a major usable nitrogen source at a geological time when also the $H_2$ and CO Ni-associated metabolisms arose.

The elucidation of the role of Ni in hydrogenases and CODHs is complicated by the presence of extensive redox chemistry. The issue as to whether Ni is redox active in these enzymes has been subjected to considerable controversy. Prior to the discovery of a Fe ion in the active site of *D. gigas* hydrogenase, some authors assigned all the redox activity to Ni. This view has been challenged, however, by Ni model chemistry and XAS experiments which indicated both the

inability of the Ni(III)/Ni(II) and Ni(II)/Ni(I) couples to be restricted to the narrow redox potential range observed in hydrogenases and the absence of electron density changes in the Ni X-ray absorption edges for the various redox states studied. We have suggested that the redox active center at the hydrogenase active site could be the novel Fe center. A long-standing alternative to this proposition has been advanced by Maroney and co-workers, who have postulated that the redox activity is ligand(sulfur)-based (Eq. 3). In the catalytic mechanism very recently proposed by Barondeau and Lindahl for CODH A-cluster, the Ni center is also postulated to be redox-inactive, the two electrons being taken up by a disulfide bridge (Fig. 13). The C-center of CODH may, however, have a Ni(I) intermediate state (Fig. 7).

Sulfur-based oxidative inactivation of hydrogenase is ruled out by the crystal structure of the as-prepared enzyme because no extra electron density is associated with the cysteine ligands in the active site. On the contrary, a putative oxo ligand tightly binds the Ni ion. X-ray protein crystallography will not be able to distinguish between ligand and metal-based redox processes involving hydrogen because the changes in bond lengths are too subtle to be detected by this technique. Finally, the confirmation of the presence of a D-center in *C. thermoaceticum* CODH (and related enzymes) will have to await the solution of its crystal structure.

## 8 References


1. Bartha R and Ordal EJ (1965) J Bacteriol 89:1015
2. Lancaster JR (1980) FEBS Lett 115:285
3. Graf E-G, Thauer RK (1981) FEBS Lett 136:165
4. Sumner, JB (1926) J Biol Chem 69:435
5. Nixon NE, Gazzola C, Blakeley RL, Zerner B (1975) J Am Chem Soc 97:4131
6. Wood HG (1985) Annu Rev Biochem 54:1
7. Kumar M, Ragsdale SW (1992) J Am Chem Soc 114:8713
8. Gunsalus RP, Romesser JA, Wolfe RS (1978) Biochemistry 17:2374
9. Youn HD, Kim EJ, Roe JH, Hah YC, Kang SA (1996) Biochem J 318:889
10. Coyle CL, Stiefel EI (1988) The coordination chemistry of nickel: an introductory survey. In: Lancaster JR Jr (ed) The bioinorganic chemistry of nickel. VCH, New York, p 1
11. Hausinger RP (1987) Microbiological Reviews 51:22
12. Nisbet EG, Fowler CMR (1996) Geol Soc Spec Publ 118:239
13. Vannice MA (1976) Catal. Rev 14:153
14. Mills GA, Steffgen FW (1973) Catal Rev 8:159
15. Halcrow MA, Christou G (1994) Chem Rev 94:2421
16. Jabri E, Carr MB, Hausinger RP, Karplus PA (1995) Science 268:998
17. Volbeda A, Charon MH, Piras C, Hatchikian EC, Frey M, Fontecilla-Camps JC (1995) Nature 373:580
18. Mobley HLT, Island MD, Hausinger RP (1995) Biological Reviews 59:451
19. Cover TL, Blase MJ (1995) ASM News 60:21
20. Daimler-Benz HighTech Report (1994) 3:11
21. Kovacs JA, Shoner, Ellison JJ (1995) Science 270:587
22. Andronikashvili EL, Bregadze VG, Monaselidze YR (1988) Met Ions Biol Syst 23:331
23. Ciccarelli RB, Hapton RH, Jennette DW (1981) Cancer Lett 12:349
24. Albracht SPJ (1994) Biochim Biophys Acta 1188:167
25. Friedrich B, Schwartz E (1993) Annu Rev Microbiol 47:351

26. Przybyla AE, Robbins J, Menon N, Peck HD Jr, (1992) FEMS Microbiol Rev 88:109
27. Lancaster JR Jr (ed) (1988) The bioinorganic chemistry of nickel. VCH, New York
28. Maroney MJ (1994) Nickel: models of protein active sites. In: King RB (ed) Encyclopedia of Inorganic Chemistry. Wiley, Chichester, p 2412
29. Telser J (this series) to be completed
30. Drake H (1988) The coordination chemistry of nickel: an introductory survey. In: Lancaster JR Jr (ed) The bioinorganic chemistry of nickel. VCH, New York, p 111
31. Still ER, Williams RJP (1980) Inorgan Biochem 13:35
32. Brooks RR, Shaw S, Marfil AA (1981) Physiol Plant 51:167
33. Navarro C, Wu L-F, Mandrand-Berthelot MA (1993) Mol Microbiol 9:1181
34. Wolfram L, Friedrich B, Eitinger T (1995) J Bacteriol 177:1840
35. Eitinger T, Friedrich B (1991) J Biol Chem 266:3222
36. Kyte J, Dolittle RF (1982) J Mol Biol 157:105–132
37. Fu C, Javedan F, Moshiri F, Maier RJ (1994) Proc Natl Acad Sci USA 91:5099
38. Sriwanthana B, Island MD, Maneval D, Mobley HLT (1994) J Bacteriol 176:6836
39. Maier T, Böck A (1996) Adv Inorg Biochem, vol 11 Mechanisms of metallocenter assembly. Hauseinger RP, Eichhorn GL, Marzilli LG (eds) VCH, New York, p 173
40. Rodrigue A, Boxer DH, Mandrand-Berthelot MA, Wu L-F (1996) FEBS Lett 392:81
41. Kansau I, Guillain F, Thiberge JM, Labigne A (1996) Molecular Microbiology 22:1013
42. Kerby RL, Hong SS, Ensign SA, Coppoc LJ, Ludden PW, Roberts GP (1992) J Bacteriol 174:5284
43. Park I-S, Hausinger RP (1995) Proc Natl Acad Sci USA 91:3233
44. Shin W, Lindahl PA (1992) J Am Chem Soc 114:9718
45. Menon AL, Robson RL (1994) J Bacteriol 176:219
46. Maier T, Böck A (1996) Biochemistry 35:10089
47. Fox JD, Kerby RL, Roberts GP, Ludden PW (1996) J Bacteriol 178:1515
48. Elsen S, Richaud P, Colbeau A, Vignais PM, (1993) J Bacteriol 175:7404
49. Black LK, Fu C, Maier RJ (1994) J Bacteriol 176:7102
50. Vignais PM, Dimon B, Zorin A, Colbeau A, Elsen S (1997) J Bacteriol 179:290
51. Lorimer GH, Badger MR, Andrews TJ (1976) Biochemistry 15:529
52. Benning MM, Kuo JM, Raushel FM, Holden HM (1995) Biochemistry 34:7973
53. Jabri E, Karplus PA (1996) Biochemistry 35:10616
54. Park I-S, Hausinger RP (1996) Science 267:1156
55. Park IS, Michel LO, Pearson MA, Jabri E, Karplus PA, Wang S, Dong J, Scott RA, Koehler BP, Johnson MK, Hausinger R (1996) J Biol Chem 271:18632
56. Volbeda A, Garcin E, Piras C, de Lacey AL, Fernandez VM, Hatchikian EC, Frey M, Fontecilla-Camps JC (1996) J Am Chem Soc 118:12898
57. Fontecilla-Camps JC (1996) JBIC 1:91
58. Maroney MJ, Colpas GJ, Bagyinka C, Baidya N, Mascharak PK (1991) J Am Chem Soc 113:3692
59. Bagynka C, Whitehead JP, Maroney MJ (1994) J Am Chem Soc 115:3576
60. Scott RA, Wallin SA, Csechowski M, DerVartanian DV, Legall J, Peck Jr HD, Huynh BH (1984) J Am Chem Soc 106:6864
61. Gu Z, Dong J, Allan CB, Choudhury SB, Franco R, Moura JJG, Moura I, Legall J, Przybyla AE, Roseboom W, Albracht SPJ, Axley MJ, Scott RA, Maroney MJ (1996) J Am Chem Soc 118:11155
62. Huynh BH, Patil DS, Moura I, Teixeira M, Moura JJG, Dervartanian DV, Czechowski MH, Prickrill BC, Peck Jr. HD, Le Gall J (1987) J Biol Chem 262:795
63. Teixeira M, Moura I, Xavier AV, Moura JJG, Legall J, Dervartanian DV, Peck HD Jr, Huynh BH (1989) J Biol Chem 264:16435
64. Happe RP, Roseboom W, Pierik AJ, Albracht SPJ (1997) Nature 385:126
65. de Lacey AL, Volbeda A, Hatchikian EC, Frey M, Fontecilla-Camps JC, Fernandez VM J Am Chem Soc (in press)
66. Hu Z, Spangler NJ, Anderson ME, Xia J, Ludden PW, Lindahl PA, Münck E (1996) J Am Chem Soc 118:830

67. Anderson ME, Lindahl PA (1996) Biochemistry 35:8371
68. Lindahl PA, Münck E, Ragsdale SW (1990) J Biol Chem 265:3873
69. Kumar M, Qiu D, Spiro TG, Ragsdale SW (1995) Science 270:628
70. Barondeau DP, Lindahl PA, (1997) J Am Chem Soc 119:3959
71. Tan GO, Ensign SA, Ciurli S, Scott MJ, Hedman B, Holm RH, Ludden PW, Korszum ZR, Stephens, PJ, Hodgson, KO (1992) Proc Natl Acad Sci 89:4427
72. Green J, Dalton H (1989) J Biol Chem 264:17698
73. Omburo GA, Kuo JM, Mullins LS, Raushel FM (1992) J Biol Chem 276:13278
74. Lippard SJ, (1995) Science 268:996
75. Park I-S, Hausinger RP (1993a) Protein Sci 2:1034
76. Park I-S, Hausinger RP (1993b) J Prot Chem 12:51
77. Krasna AI (1979) Enzyme Microb Technol 1:165
78. Kumar M, Day RO, Colpas GJ, Maroney MJ (1989) J Am Chem Soc 111:5974
79. Fernandez VM, Hatchikian EC, Cammack R (1985) Biochem Biophys Acta 832:69
80. van der Zwaan JW, Coremans JMCC, Bouwens ECM, Albracht SPJ (1990) Biochem Biophys Acta 1041:101
81. Barondeau DP, Roberts LM, Lindahl PA (1994) J Am Chem Soc 116:3442
82. Roberts LM, Lindahl PA (1994) Biochemistry 33:14339
83. Roberts LM, Lindahl PA (1995) J Am Chem Soc 117:2565
84. Medina M, Hatchikian EC, Cammack R (1996) Biochem Biophys Acta 1275:227
85. van der Zwaan JW, Albracht SPJ, Fontjin RD, Slater SC (1985) FEBS Lett 179:271
86. Marganian Goldman C, Mascharak PK (1995) Comments Inorg Chem 18:1
87. Cammack R, Patil DS, Hatchikian EC, Fernandez VM (1987) Biochem Biophys Acta 912:98
88. Choudhury BC, Ray D, Chakrvorty A (1990) Inorg Chem 29:4603
89. Choudhury SB, Pressler MA, Mirza SA, Day RO, Maroney MJ (1994) Inorg Chem 33:4831
90. Farmer PJ, Verpeaux JN, Amatore C (1994) J Am Chem Soc 116:9355
91. Kruger HJ, Peng G, Holm RH (1991) Inorg Chem 30:734
92. Kruger HJ, Holm RH (1990) J Am Chem Soc 112:2955
93. Fontecilla-Camps JC, Volbeda A, Frey M (1996) TIBTECH 14:417
94. Baidya N, Olmstead MM, Mascharak PK (1991) Inorg Chem 30:929
95. Baidya N, Olmstead MM, Mascharak PK (1992) J Am Chem Soc 114:9666
96. Farmer PJ, Reibenspies JH, Lindahl PA, Darensbourg M (1993) J Am Chem Soc 115:4665
97. Shoner SC, Olmstead MM, Kovacs JA (1994) Inorg Chem 33:7
98. Teixeira M, Fauque G, Moura I, Lespinat PA, Berlier Y, Prickril B, Peck Jr. HD, Xavier AV, Legall J, Moura JJG (1987) Eur J Biochem 167:47
99. He SH, Teixeira M, LeGall J, Patil DS, Moura I, Moura JJG, DerVartanian DV, Huynh BH, Peck jr. HD (1989) J Bio Chem 264:2678
100. Bagley KA, Van Garderen CJ, Chen M, Duin EC, Albracht SPJ, Woodruff WH (1994) Biochemistry 33:9229
101. Bagley KA, Duin EC, Roseboom W, Albracht SPJ, Woodruff WH (1995) Biochemistry 34:5527
102. Shin W, Anderson ME, Lindahl PA (1993) J Am Chem Soc 115:5522
103. Kumar M, Lu W-P, Liu L, Ragsdale SW (1993) J Am Chem Soc 115:11646
104. Anderson ME, Lindahl PA (1994) Biochemistry 33:8702
105. Stephens PJ, McKenna M-C, Ensign SA, Bonam D, Ludden PW (1989) J Biol Chem 264:16347
106. Kumar M, Lu WP, Smith A, Ragsdale SW, McCraken J (1995) J Am Chem Soc 117:2939
107. Qiu D, Kumar M, Ragsdale SW, Spiro T (1996) J Am Chem Soc 118:10429
108. Spangler NJ, Lindahl PA, Bandarian VA, Ludden PW (1996) J Biol Chem 271:7973
109. Lindahl PA, Münck E, Ragsdale SW (1989) J Biol Chem 265:3873
110. Lu W-P, Jablonski PE, Rasche M, Ferry JG, Ragsdale SW (1994) J Biol Chem 269:9736
111. Fan C, Gorst cm, Ragsdale SW, Hoffman BH (1991) Biochemistry 30:431
112. Bastian NR, Diekert G, Niederhoffer EG, Teo BK, Walsh CP, Orme-Johnson WH (1988) J Am Chem Soc 110:5581

113. Lu W-P, Ragsdale SW (1991) J Biol Chem 266:3554
114. Stravropoulos P, Carrié M, Muetterties MC, Holm RH (1990) J Am Chem Soc 112:5385
115. Macgregor SA, Lu Z, Eisenstein O, Crabtree RH (1994) Inorg Chem 33:3616
116. Kumar M, Ragsdale SW (1992) J Am Chem Soc 114:8713
117. Qiu D, Kumar M, Ragsdale SW, Spiro GS (1994) Science 264:817
118. Kumar M, Qiu D, Spiro TG,Ragsdale SW (1995) Science 270:628
119. Qiu D, Kumar M, Ragsdale SW, Spiro TG (1995) J Am Chem Soc 117:2653
120. Tucci GC, Holm RH (1995) J Am Chem Soc 117:6489
121. Ram MS, Riordan GC, A.Yap GP, Liable-Sands L, Rheingold AL, Marchaj A, Norton JR, (1997) J Am Chem Soc 119:1648
122. Kumar M, Lu WP, Ragsdale SW (1994) Biochemistry 33:9769
123. Ram MS, Riordan CG (1995) J Am Chem Soc 117:2365
124. Lu W-P, Ragsdale SW (1991) J Biol Chem 266:3554
125. Gorst, Ragsdale SW (1991) J Biol Chem 266:20687
126. Kraulis PJ (1991) J Appl Cryst 24:140
127. Berstein FC, Koetzle TF, Williams GJB, Meyer EF, Brice MD, rodgers JR, Kennard O, Shomanouchi T, Tasumi M (1977) J Mol Biol 112:535

# Nickel in $F_{430}$

Joshua Telser

Chemistry Program, Roosevelt University, 430 South Michigan Avenue, Chicago, IL 60605-1394, USA. *Internet: jtelser@acfsysv.roosevelt.edu*

The terminal step in methane generation by several methanogenic organisms, of which the best studied is the archaeon *Methanobacterium thermoautotrophicum*, is catalyzed by the enzyme *S*-methyl coenzyme M reductase (methylreductase, EC 1.8.-.-). This enzyme contains a macrocyclic tetrapyrrole-derived cofactor, $F_{430}$, at the active site coordinating Ni(II) in the resting state. A Ni(I) state ($Ni^{I}F_{430}$) has been proposed as the active form of the cofactor. Extensive mechanistic and spectroscopic studies have been performed on the holoenzyme, isolated cofactor, and various synthetic model compounds. These studies are summarized in the present review.



Structure and Bonding, Vol. 91

## List of Abbreviations:

| | |
|---|---|
| $\delta$-ALA | 5-aminolevulinic acid |
| Br-HTP | 7-(bromoheptanonyl)-L-Threonine-$O^3$-phosphate |
| $BrPrSO_3$ | 3-bromopropanesulfonic acid |
| CV | cyclic voltammetry |
| DMF | *N,N*-dimethylformamide |
| EG | ethylene glycol |
| ENDOR | electron nuclear double resonance |
| EPR | electron paramagnetic resonance |
| ESEEM | electron spin echo envelope modulation |
| EXAFS | extended X-ray absorption fine structure |
| Fc | ferrocene |
| $F_{420}$ | deazaflavin cofactor (*N*-(-*N*-L-lactyl-*g*-L-glutamyl)-L-glutamic acid phosphodiester of 7,8-didemethyl-8-hydroxy-5-deazariboflavin 5′-phosphate) |
| $F_{430}$ | nickel tetrapyrrole pentacarboxylic acid cofactor |
| $F_{430}Me_5$ | nickel tetrapyrrole pentamethyl ester cofactor |
| 4,11-dieneN$_4$ | 5,7,7,12,14,14-hexamethyl-1,4,8,11-tetraazacyclotetradeca-4,11-diene |
| HPLC | high pressure liquid chromatography |
| HS-CoM | 2-thioethanesulfonic acid |
| HS-HTP | 7-(mercaptoheptanoyl)-L-threonine-$O^3$-phosphate |
| MCD | magnetic circular dichroism |
| MCR | methyl-coenzyme M reductase |
| methyl coenzyme M | 2-(methylthio)ethanesulfonic acid |
| MFR | methanofuran (4-[*N*-(4, 5, 7-tricarboxyheptanoyl-*g*-L-glutamyl-*g*-L-glutamyl-)-*p*-($\beta$-aminoethyl)phenoxymethyl]-2-(aminomethyl)furan) |
| MO | molecular orbital |
| MPT | methanopterin (2-amino-4-hydroxy-7-methylpteridine), NHE, normal hydrogen electrode |
| NMR | nuclear magnetic resonance |
| NOE | nuclear Overhauser effect |
| OEiBC | octaethylisobacteriochlorin (*tct*-2,3,7,8-tetrahydro-2,3,7,8,12,13,17,18-octaethylporphyrin dianion) |
| RNA | ribonucleic acid |
| RR | resonance Raman effect spectroscopy |
| SCE | saturated calomel ($Hg_2Cl_2$) reference electrode |
| TBAP | tetra-*n*-butylammonium perchlorate |

| | |
|---|---|
| TEAP | tetraethylammonium perchlorate |
| TBAT | tetra-*n*-butylammonium tetrafluoroborate |
| TFE | 2,2,2-trifluoroethanol |
| THF | tetrahydrofuran |
| UV | ultraviolet. |

# 1 Introduction

## 1.2 Overview of Nickel Enzymes

Nickel occupies an important role in the biological chemistry of the metallic elements, although its occurrence is far less pervasive than iron, copper, or zinc. Nickel biochemistry is of interest because the small number of Ni-containing biomolecules is somewhat compensated by the variety of functions that these molecules can perform. There are four types of Ni-dependent enzymes, all of which are found in lower organisms (bacteria and archaea), although one (urease) is also found in plants [1–4]. The role of nickel in higher organisms is not yet known, although it is an essential trace element in animals. These enzymes comprise urease, carbon monoxide dehydrogenase (CODH), hydrogenase (Ni-$H_2$ase; there are also $H_2$ases that contain only iron[5]), and methyl coenzyme M reductase (MCR), the subject of this review. A recent book by Hausinger provides an excellent overview of nickel biochemistry [4]. Also useful in this context is a recent review by Hausinger [2] and an older, but still relevant review by Walsh and Orme-Johnson [3]. Additionally, of particular interest to inorganic chemists is the recent and exhaustive review of the biomimetic chemistry of nickel by Halcrow and Christou [1]. Finally, there are a number of recent reviews of MCR and/or the $F_{430}$ cofactor [6–16].

## 1.2 Methanogens

Among the many types of anaerobic microorganisms are the methanogens, a class of strictly anaerobic archaea. These archaea are distinguished from eucaryotes and eubacteria on the basis of sequence homology of their 16S ribosomal RNA [8]. These organisms are extremely oxygen sensitive, but are found in all anaerobic environments, ranging from marine sediments to animal intestinal tracts, with sewage digestors being a particularly rich source of methanogens. Lipids, carbohydrates, proteins, and nucleic acids are decomposed by anaerobic bacteria to hydrogen, carbon dioxide, formic acid, and acetic acid. Methane is then produced by the reduction by hydrogen of carbon dioxide to methane; methanogens are the only organisms known to have obligate biosynthesis of methane [7, 14]. For many methanogens, carbon dioxide is the sole energy source, while a few species (e.g., *Methanosarcina barkeri*) can also utilize methanol, methylamines, and acetic acid [12, 16]. This is shown in the following equations:

$$CO_{2(g)} + 4H_{2(g)} \rightarrow CH_{4(g)} + 2H_2O_{(l)},\ \Delta G'^0 = -131\ \text{kJ/mol},$$
all methanogens; (1a)

$$CH_3OH_{(aq)} + H_{2(g)} \rightarrow CH_{4(g)} + H_2O_{(l)},\ \Delta G'^0 = -113\ \text{kJ/mol},$$
*Methanosarcina*; (1b)

$$CH_3CO_2H_{(aq)} \rightarrow CH_{4(g)} + CO_{2(g)},\ \Delta G'^0 = -36\ \text{kJ/mol},$$
*Methanosarcina*; (1c)

where the free energies are estimated for pH = 7; at typical biological concentrations, $\Delta G$ for Eq. (1a) is estimated at −17 kJ/mol and $\Delta G$ for Eq. (1c) is estimated at −23 kJ/mol [9]. All together, these organisms are responsible for the annual production of one billion tons of methane [13]. Details on the microbiology of methanogens have been reviewed [14, 16, 17], and will not be discussed further here, except to note that *Mb. thermoautotrophicum* grows optimally on 80% $H_2$ and 20% $CO_2$ at 65 °C over pH = 6.8–7.2 [18].

## 1.3 Methanogenesis

The elucidation over the past 25 years of the complete methanogenic pathway represents a landmark of biochemistry. This process was carried out largely by the groups of R. S. Wolfe in Urbana, Illinois, USA [15, 19, 20] and of R. K. Thauer in Marburg, Germany [13, 21]. The pathway for the reduction of carbon dioxide is shown schematically in Fig. 1. This pathway involves six coenzymes that had been previously unknown: methanofuran (MFR), methanopterin (MPT), coenzyme M (HS-CoM), 7-mercaptoheptanoylthreonine phosphate (HS-HTP, Coenzyme B), factor 420 ($F_{420}$), and factor 430 ($F_{430}$). The first five of these are shown in Fig. 2; note that both the oxidized and reduced forms of the deazaflavin cofactor $F_{420}$ are shown. The review by DiMarco et al. describes in detail the properties, occurrence, and biosynthesis of each of these novel cofactors [15]. Methanofuran (MFR), methanopterin ($H_4$MPT), and $F_{420}$ are involved in the earlier steps of methanogenesis and will be discussed only very briefly here. Coenzyme M, HS-HTP, and $F_{430}$ are involved in the later steps of methanogenesis, which are of interest here.

As shown in Fig 1, in the first step of methanogenesis, carbon dioxide is reduced to a formyl group as part of a carbamate formed by reaction with the primary amine of MFR. The formyl group is then transferred to *N*-5 of $H_4$MPT. A condensation (Schiff base formation) reaction with *N*-10 yields an imine which is then stepwise reduced to a methyl group bound at *N*-5 in reactions that involve $F_{420}$ as an electron donor. The methyl group is then transferred to coenzyme M (HS-CoM), which is converted to the methyl thioether, S-methyl coenzyme M ($CH_3$S-CoM). Each of these reactions is catalyzed by enzymes that have been identified, but are not well understood; the recent reviews by DiMarco et al. [15] and Won et al. [8] provide further information and key references on these enzymes.

The final step of methanogenesis then occurs, which consists of a metathesis reaction wherein $CH_3$S-CoM reacts with HS-HTP to yield the unsymmetrical

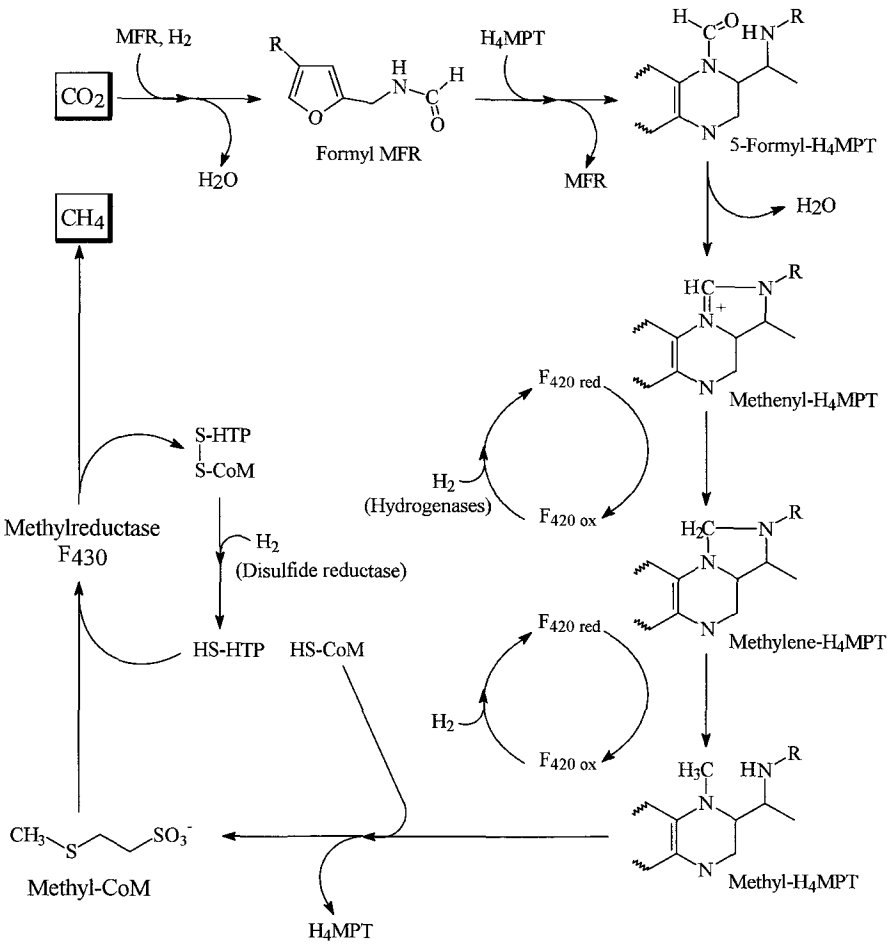


**Fig. 1.** The methanogenic pathway as adapted from the reviews by DiMarco et al. [15] and Jaun [9]. Partial structures for MFR and $H_4$MPT are included. Reproduced, with permission, from Reference [15], 1990, by Annual Reviews, Inc.

disulfide CoM-S-S-HTP and methane [22–24]. The reaction is catalyzed by methyl coenzyme M reductase, which is briefly described in Sect. 2. The concentration of CoM-S-S-HTP affects the first step of the methanogenic cycle, the formation of formyl-MFR [25]. The free thiol forms of CoM and HTP are then regenerated by a disulfide reductase [26].

## 2
## The Enzyme Containing $F_{430}$: Methyl-Coenzyme M Reductase

The metathesis reaction that generates methane and the disulfide CoM-S-S-HTP is catalyzed methyl coenzyme M reductase (MCR; methylreductase, EC 1.8.-.-). This enzyme has been isolated from several organisms (including

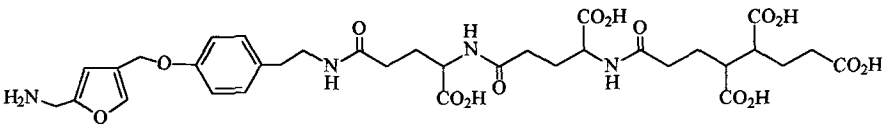

Methanofuran (MFR)

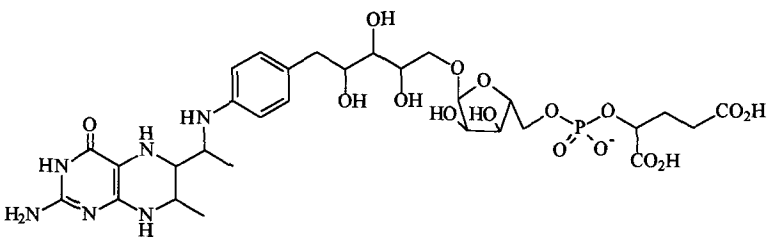

Tetrahydromethanopterin ($H_4$ MPT)

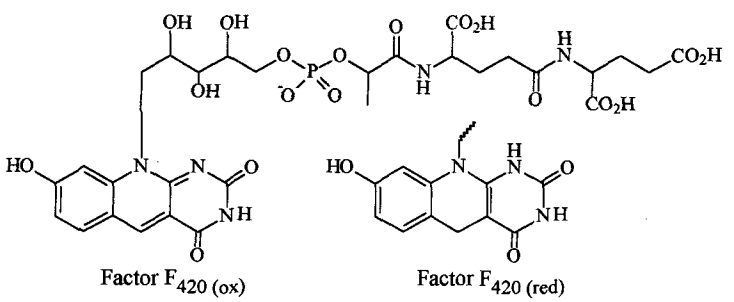

Factor $F_{420}$ (ox) Factor $F_{420}$ (red)

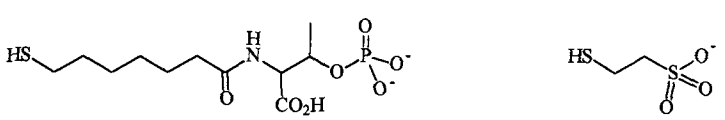

N-7-Mercaptoheptanoylthreonine-phosphate (HS-HTP) Coenzyme M

**Fig. 2.** Novel coenzymes found in methanogens that are employed in methanogensis

*Mb. thermoautotrophicum*, *Methanococcus voltae*, *Methanococcus jannaschii*, and *Methanosarcina barkeri* [19]) although by far the most studied is that which has been isolated from *Mb. thermoautotrophicum* (strains ΔH and Marburg) [27, 28]. Recently, MCR has also been isolated and purified from cell extracts of *Methanosarcina thermophila* [29] and *Methanopyrus kandleri* [30]. Two of these methanogenic archaea, *Mc. jannaschii* and *Mp. kandleri*, are of particular interest as they are extreme hyperthermophiles (optimal growth at 85 °C and 98 °C, respectively), thus representing organisms that appeared early in evolution. The ribosomal RNA of *Mp. kandleri* suggested that it was not closely relat-

ed to other methanogens [30]. Nevertheless, its MCR was quite similar to those of less thermophilic organisms. The complete genome of *Mc. jannaschii* has very recently been determined [31], which included identification of the genes coding for cofactor synthesis, MCR, and other methanogenic enzymes. This landmark event will help not only in understanding the evolution of life in general, but also in understanding methanogenesis and MCR in particular.

In *Mb. thermoautotrophicum* (strain ΔH), MCR has been found to be part of an enzymatic complex that includes the methylreductase and components A1, A2, A3a, and A3b [32]. These components may be involved in electron transfer reactions in the final steps of methanogenesis. However, MCR itself has been purified to homogeneity and is highly active without the A components, when properly activated [33–35]. For example, the presence of HS-HTP, $CH_3S$-CoM, and $Ti^{III}$(citrate) when combined with irradiation (> 400 nm) led to activation of MCR [33]. Incubation of cells with hydrogen prior to extraction also led to activity [34].

The enzyme complex has been proposed to be located in membrane associated particles within the cell (methanoreductosomes) [36]. MCR itself is a large, complex enzyme of $M_r \sim 300$ kDa with an $\alpha_2\beta_2\gamma_2$ subunit structure [27, 28]. Interestingly, MCR isolated from *Ms. thermophila*, in contrast to that from other organisms, has been reported to have an $\alpha_1\beta_1\gamma_1$ subunit structure, although this may be a consequence of the isolation procedure [29]. The genes coding for MCR have been identified: mcrA, mcrB, and mcrG, which code for the $\alpha$, $\beta$, and $\gamma$ subunits, respectively (there is also mcrC and mcrD, whose gene products have unknown function). The nucleotide sequence of these genes from *Ms. barkeri*, *Mc. vannieli*, *Mb. thermoautotrophicum* (strain Marburg, MCR I and II, see below), *Mc. voltae*, *Methanothermus fervidus*, and *Mp. kandleri* have been determined [11, 30, 37]. This gave the following molecular mass ranges for the encoded polypeptides of $60.5 < \alpha < 62.0$, $45.4 < \beta < 47.2$, $27.8 < \gamma < 30.1$, $\alpha_2\beta_2\gamma_2 \approx 270$ kDa. Note that the apparent molecular mass determined by electrophoretic mobility is higher, particularly for subunit $\gamma$, thus for *Mb. thermoautotrophicum*, $\alpha = 66$, $\beta = 48$, $\gamma = 37.5$, $\alpha_2\beta_2\gamma_2 \approx 303$ kDa. Extensive homology was found among the derived primary amino acid sequences for the MCR's from these organisms. However, no relation between the primary sequence and function or tertiary structure has yet been elucidated for MCR.

An important recent development was the discovery that *Mb. thermoautotrophicum* (Marburg) contained two isoenzymes of MCR: MCR I and MCR II, which have been purified and characterized [27, 38]. These differed in the size of the $\gamma$ subunit and in the primary sequence of all subunits, and in their catalytic properties. MCR II predominated when $H_2$ and $CO_2$ was not growth-rate limiting and was significantly more active than MCR I. Similar results were found for *Mb. thermoautotrophicum* (ΔH) [28]. Spectroscopic studies on these isoenzymes will be mentioned in Sects. 5.4 and 5.6.

MCR has associated with it three of the six novel methanogenic cofactors: HS-CoM, HS-HTP, and $F_{430}$. The enzyme has two tightly, but not covalently, bound molecules of HS-CoM and of $F_{430}$, and probably two of HS-HTP as well [8]. Only the location of the $F_{430}$ cofactor is known; each $\alpha$ subunit contains a molecule of $F_{430}$, so named because of its characteristic UV-visible absorption

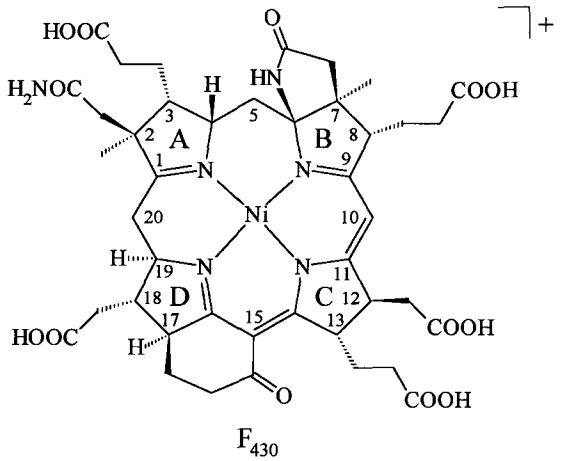


**Fig. 3.** Structure of the native form of $F_{430}$, as derived by crystallographic and spectroscopic analyses [39, 40]. The conventional ring labels and numbering scheme are indicated

spectrum. This cofactor is the primary focus of this review and has been shown to be a Ni(II) tetrapyrrole derivative, as depicted in Fig. 3 [39, 40].

## 3 Biosynthesis of $F_{430}$ and Its Relation to Other Naturally Occurring Tetrapyrroles

Gunsalus and Wolfe first reported the isolation of $F_{430}$ in 1978 [41], and it was soon shown to contain nickel. It seemed likely that $F_{430}$ was a nickel tetrapyrrole species, which was confirmed by Thauer and co-workers, as described in detail in the review by Thauer and Bonacker [6]. They showed that exactly eight moles of $^{14}$C-labelled 5-aminolevulinic acid ($\delta$-ALA), the biological building block of all naturally occurring porphyrins and corrins, were incorporated into one mole of $F_{430}$ [6, 42, 43]. Two moles of $\delta$-ALA (which is derived from glutamate) are converted to one mole of porphobilinogen and then four moles of porphobilinogen are cyclized to yield one mole of uroporphyrinogen III, the macrocyclic precursor to biological tetrapyrroles. The review by Warren and Scott [44], provides an excellent overview on these early steps of tetrapyrrole biosynthesis. Side chain modification and ring reduction reactions on uroporphyrinogen III yield the various naturally occurring tetrapyrrole macrocycles: hemes, sirohemes, chlorophylls, corrins (vitamin $B_{12}$), and $F_{430}$; each with its appropriate metal ion: iron, magnesium, cobalt, and nickel [45]. The elegant studies by Thauer and co-workers, in particular Pfaltz et al. [43] are summarized in Fig. 4, which shows the biosynthetic pathway of $F_{430}$, beginning with dihydrosirohydrochlorin, the common precursor to siroheme, corrinoids, and $F_{430}$.

Figure 5, based originally on a figure by Eschenmoser [13] and reproduced many times since then, shows the relationship between the macrocycle cores of these naturally occurring tetrapyrroles by indicating with heavy lines the de-

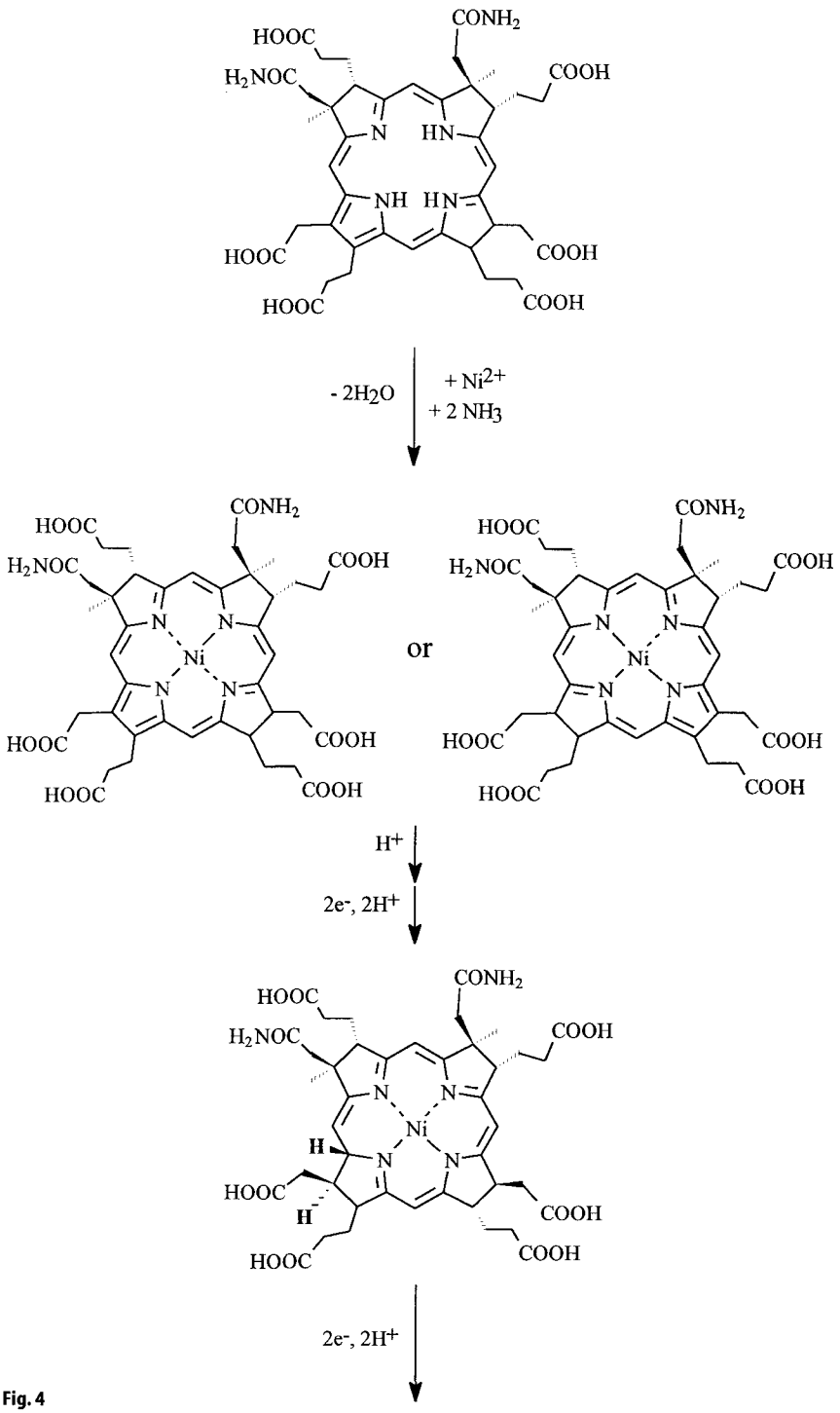
HOOC
CONH2
H2NOC
COOH
N
HN
NH
HN
HOOC
COOH
HOOC
COOH
- 2H2O
+ Ni2+
+ 2 NH3
HOOC
CONH2
H2NOC
COOH
N
N
Ni
N
N
HOOC
COOH
HOOC
COOH
or
HOOC
CONH2
H2NOC
COOH
N
N
Ni
N
N
HOOC
COOH
HOOC
COOH
H+
2e-, 2H+
HOOC
CONH2
H2NOC
COOH
N
N
Ni
H
N
N
HOOC
H
COOH
COOH
HOOC
2e-, 2H+

Fig. 4

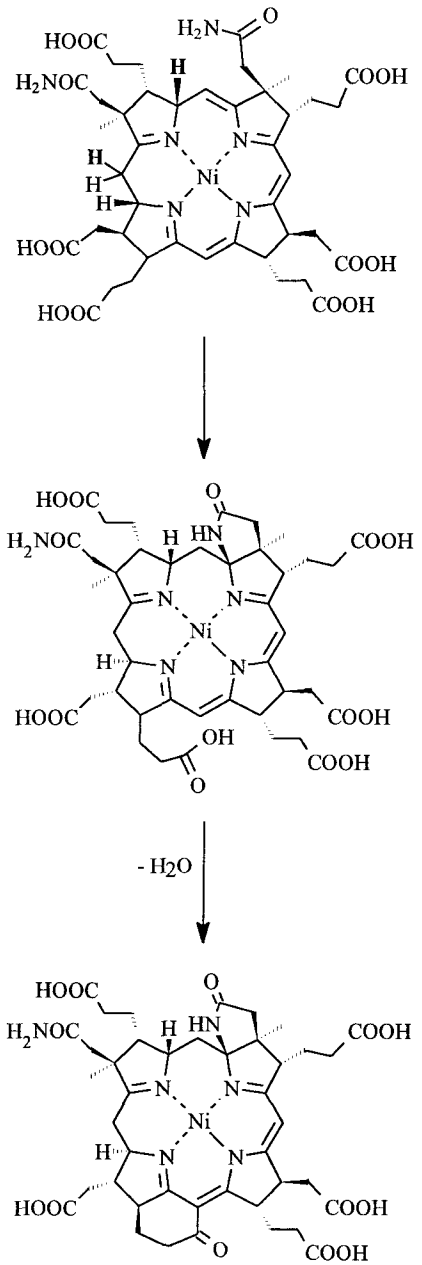


**Fig. 4.** Biosynthetic pathway of $F_{430}$ from dihydrosirohydrochlorin as deduced by Thauer and coworkers [6]. The precursor to dihydrosirohydrochlorin is urophorphyrinogen III (not shown), which is the starting point for all biological tetrapyrroles. Reproduced, with permission, from Reference [6], © 1990, by the Ciba Foundation, London, England

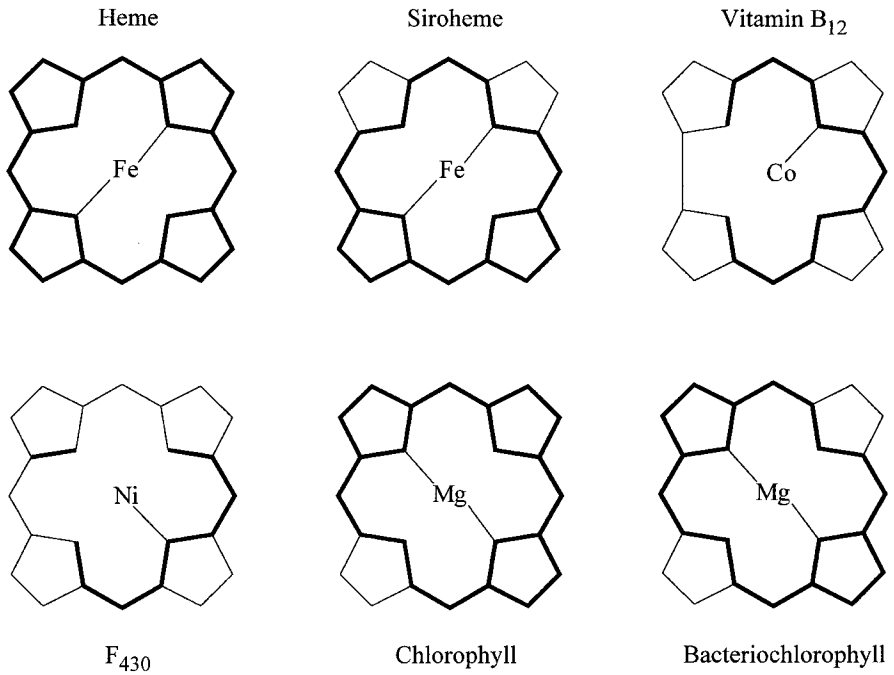


**Fig. 5.** Comparison of the $\pi$-system conjugation (delocalization) in various biological tetrapyrroles, as originally pointed out by Eschenmoser [90]. Heavy lines indicate the $\pi$-system in each tetrapyrrole. Reproduced, with kind permission, from Reference [10], © 1991, by Elsevier Science – NL, Sara Burgerhartstraat 25, 1055 KV Amsterdam, The Netherlands

gree of ring conjugation in each case. It is immediately evident that $F_{430}$ is the most highly reduced (saturated) of these tetrapyrrole species. None of the pyrroles of $F_{430}$ remains in its original fully conjugated form (and thus are actually 1-pyrrolines), as with the corrinoids, but in contrast to the corrinoids, all meso carbons are present and there is no conjugation pathway linking all four pyrrole-derived groups. This led to the term hydrocorphinoid: a hybrid of a porphyrinoid C-N skeleton with a corrinoid conjugation [8]. This minimal conjugation leads to the absence of both the characteristic visible absorption bands and fluorescence found in porphyrins. As will be discussed below, the high degree of saturation allows $F_{430}$ to be modeled by fully, or almost fully, saturated tetraaza macrocyclic nickel complexes.

As described by Friedmann et al. [10] the side chains of $F_{430}$ are also unusual. In contrast to the hemes, $F_{430}$ retains all eight carboxylate sidechains found in the biosynthetic precursor, uroporphyrinogen III, albeit with three in modified forms, so that $F_{430}$ is a pentaacid. The propionate sidechain on ring D is cyclized in a condensation (acylation) to give a fused cyclohexanone that is conjugated with the ring $\pi$-system; a unique feature of $F_{430}$ that has been reproduced in various synthetic models. Additionally, the acetate groups on rings A and B are amidated, with that on ring B cyclized to give a lactam. Finally, there are methyl

groups on rings A and B that are the identical to those in dihydrosirohydrochlorin, the precursor also to siroheme and $B_{12}$. The determination of the absolute stereochemistry of $F_{430}$ was a considerable achievement, and will be discussed in Sects. 5.1 and 5.2.

## 4 Isolation and Purification of $F_{430}$

In addition to enzyme-bound $F_{430}$, there is a large amount of free cofactor in the cytosol (>70% of the total amount of cofactor) [48] although under Ni-limiting growth medium, $F_{430}$ is bound mainly to MCR [49]. $F_{430}$ can be isolated from cell extracts relatively easily by extraction with ethanol [50–52]. Several groups have reported reversed-phase HPLC procedures for the purification of isolated $F_{430}$ [50, 51, 53, 54]. Of particular thoroughness was the study by Gorris et al., which included protocols for the purification and assaying of several cofactors from methanogen cell cultures and from a methanogenic fluidized bed reactor [51].

Isolated $F_{430}$ is thermally unstable and oxygen sensitive. As determined by Pfaltz et al. [55] and extensively studied by Keltjens et al. [50] native $F_{430}$ (C12, *S*; C13, *S*) can be thermally converted to 13-epimer-$F_{430}$ (C12, *S*; C13, *R*) and then to 12,13-diepimer-$F_{430}$ (C12, *R*; C13, *R*). An equilibrium mixture contains 4% native, 8% 13-epimer, and 88% 12,13-diepimer-$F_{430}$ [55]. Oxidation yields a red compound, $F_{560}$, which is 12,13-didehydro-$F_{430}$. Figure 6 shows these species, all of which result from reactions at ring C of $F_{430}$. These species can all be separated by reversed-phase HPLC so that spectroscopic and mechanistic studies can

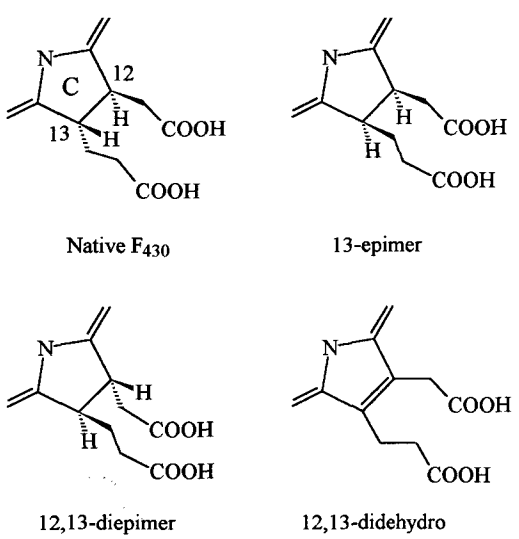


**Fig. 6.** Isomers of $F_{430}$. For clarity, only ring C is shown. Heat treatment of $F_{430}$ leads to the thermodynamically more stable 12,13-diepimer; oxidation leads to the 12,13-didehydro form ($F_{560}$)

be performed on a single compound; only native $F_{430}$ is considered to have biological relevance. Hydrogen and other reducing agents convert 12,13-didehydro-$F_{430}$ back to the native cofactor [55, 50].

# 5 Spectroscopic Investigation of $F_{430}$ and Model Compounds

## 5.1 NMR Studies

The isolation and purification of $F_{430}$ allowed the application of numerous spectroscopic methods. The most powerful among these, in terms of determining the novel ligand structure of $F_{430}$ was NMR. This technique, specifically 1D $^1$H-NOE difference spectroscopy, combined with the use of $^{13}$C-labeled biosynthetic precursors (i.e., isotopologs of $\delta$-ALA and of methionine) and the significant previous studies on related compounds, allowed the determination of the structure and relative configuration of $F_{430}$ [56]. However, in order for this study to have been successful, it was necessary to employ the pentamethyl ester of $F_{430}$, $F_{430}Me_5$, obtained by methanolysis of native $F_{430}$. As will be discussed in more detail below, native $F_{430}$ contains Ni(II) predominantly with axial bis-aquo coordination and a resulting $S=1$ electronic configuration (pseudo-octahedral $d^8$) [55]. Line-broadening by this paramagnetic center precluded NMR studies of the native cofactor. However, the use of the weakly-coordinating solvent 2,2,2-trifluoroethanol (TFE) favored a Ni(II) species absent axial coordination and a resulting $S=0$ electronic configuration (square-planar $d^8$). Under these conditions, a $^{13}$C 1D-NMR spectrum, although none for $^1$H (at 300 MHz), was obtained for comparison with that of $F_{430}Me_5$ [57]. Subsequently, Won et al. performed beautiful 500 MHz NMR studies of native $F_{430}$ in TFE-$d_3$ solution, using a variety of the latest 2D NMR techniques [53, 58]. These workers confirmed the earlier NMR studies, showing that the native and pentamethyl ester forms of $F_{430}$ had no major structural differences. However, ambiguity remained regarding the absolute configuration at C17-C18-C19 (on ring D); this could be either *R*, *R*, *S* (as originally proposed) or *S*, *S*, *R* (the reverse assignment). As described in Section 5b, the X-ray crystal structure of the bromide salt of 12,13-diepimer-$F_{430}Me_5$ was then reported, along with further 2D NMR studies [39]. The absolute configuration of this compound at C17-C18-C19 was found to be *S*, *S*, *R*. Won et al. then performed an exhaustive NMR study on 12,13-diepimer-$F_{430}$ in TFE-$d_3$ solution, combined with molecular modelling, which provided a complete structural picture of this form of the cofactor [40]. Therefore, it should be noted that the literature prior to 1992 depicted $F_{430}$ with absolute stereochemistry on ring D inverted from that which is currently accepted (Fig. 3).

## 5.2 X-Ray Diffraction (Crystallographic) Studies

The successful crystallization of the bromide salt of 12,13-diepimer-$F_{430}Me_5$ was a major breakthrough and was the culmination of an intensive effort [39]. No

suitable crystals had been obtained of native $F_{430}$ (the diepimer being thermodynamically more stable), and only bromide, as opposed to perchlorate, etc., was a suitable counter ion. The data refinement converged at an *R*-factor of 7.8% and the resulting structure showed disorder in the location of the bromide ion, and more importantly in the location of the propionate sidechain at C13 and of the ester group of the acetate sidechain at C18. Nevertheless, the assignment of absolute stereochemistry to all chiral centers in the molecule was possible. The structure of the macrocycle core was also of interest and was found to exhibit a highly $S_4$-ruffled, saddle-shaped conformation; the saddle deformation was the largest found to date for a metal hydroporphyrinoid complex. The Ni-N bonds were equivalent with bond length of 1.86 Å (see Table 1); the relevance of this will be discussed below.

The forementioned work by Färber et al. [39] represents the only structural characterization of a true $F_{430}$ species. However, there have been a number of

**Table 1.** Ni-N Distances in Complexes Relevant to $F_{430}$

| Complex | Spin state (*S*), axial ligands (solvent) | Ni-macrocycle N Distances, Å | Method, Reference |
|---|---|---|---|
| $F_{430}$ | 1, $H_2O$ | 2.10 | EXAFS [55] |
| $F_{430}Me_5$ | 0, none (THF) | 1.90 | EXAFS [72] |
| 12,13-diepimer-$F_{430}$ | 0, none ($H_2O$) | 1.89 | EXAFS [71] |
| 12,13-diepimer-$F_{430}$ | 1, *N*-Me-imidazole | 2.05 | EXAFS [71] |
| 12,13-diepimer-$F_{430}Me_5$ | 0, none, ($Br^-$ counterion) | 1.86 | X-ray [39] |
| $Ni^{II}$(OEiBC) | 0, none (THF) | 1.94 | EXAFS [65] |
| | | 1.942 | X-ray [59] |
| $Ni^{II}$(iBC 3) | 0, none (THF) | 1.93 | EXAFS [64] |
| | | 1.915 | X-ray [64] |
| $Ni^{II}$(4,11-dieneN$_4$) | 0, none ($CH_3CN$) | 1.93 | EXAFS [68] |
| *N-racemic* isomer[a] | ($ClO_4^-$ counterion) | 1.915 (Ni-$N_{amine}$), 1.884 (Ni-$N_{imine}$) | X-ray [69] |
| *N-meso* isomer[a] | | 1.938 (Ni-$N_{amine}$), 1.907 (Ni-$N_{imine}$) | |
| $Ni^{I}F_{430}$ | 1/2, none ($H_2O$) | 2.04, 1.90[b] | EXAFS [74] |
| $Ni^{I}F_{430}Me_5$ | 1/2, none (THF) | 2.03, 1.88[b] | EXAFS [72] |
| $Ni^{I}$(OEiBC) | 1/2, none (THF) | 2.07, 1.91[b] | EXAFS [65] |
| $Ni^{I}$(iBC 3) | 1/2, none (THF) | 2.00, 1.85[b] | EXAFS [64] |
| $Ni^{I}$(4,11-dieneN$_4$) | 1/2, none ($CH_3CN$) ($ClO_4^-$ counterion) | 2.06, 1.94[b] 2.066 (Ni-$N_{amine}$), 1.984 (Ni-$N_{imine}$) | EXAFS [68] X-ray [68] |

[a] This complex was crystallized into two different isomeric forms, *N-racemic* and *N-meso*, differentiated by the conformation at the amine nitrogens. Both of these were structurally characterized by Szalda and Fujita [69].

[b] EXAFS data-fitting required the use of two significantly different Ni-N bond distances, in equal proportion.

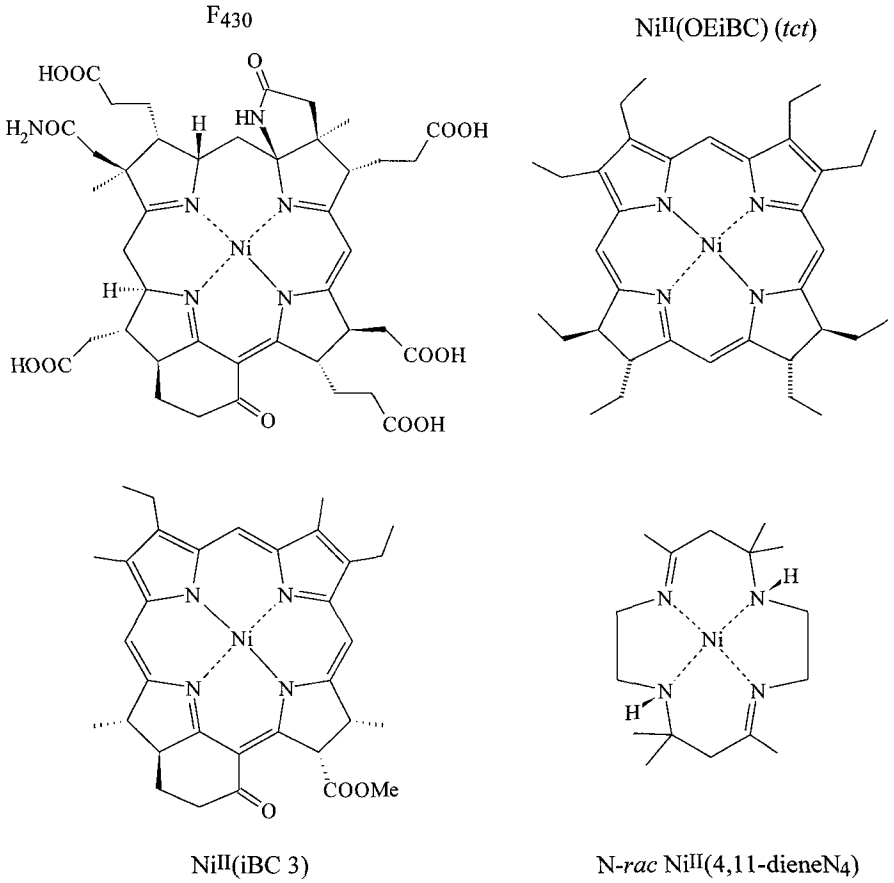


**Fig. 7.** $F_{430}$ and several synthetically accessible complexes that have been employed as model compounds for $F_{430}$ in its Ni(II) and Ni(I) forms [64, 65, 68]. The *trans-cis-trans* isomer of $Ni^{II}$(OEiBC) and the *N-racemic* isomer of $Ni^{II}$(4,11-dieneN$_4$) are shown

structural studies on model compounds for $F_{430}$. These comprised two classes of macrocyclic nickel complexes: those with ligands that are less highly saturated than $F_{430}$, chiefly hydroporphyrins such as isobacteriochlorins, and those with more highly reduced ligands, chiefly derivatives of 1,4,8,11-tetraazacyclotetradecane, such as 4,11-dieneN$_4$. Several representatives of these complexes are shown in Fig. 7. A detailed discussion of these studies is beyond the scope of this review, however we single out the crystallographic study of several isobacteriochlorins by Kratky et al. [59]. This work is relevant because $Ni^{II}$(OEiBC), in contrast to many other Ni(II) porphyrinoids, is easily reduced to the Ni(I) oxidation state, rather than to a ligand-centered $\pi$ radical [60–65] and thus this species has been proposed as a model for the putative active Ni(I) form of $F_{430}$ (see Sects. 5.4, 5.5, and 7). The *tct* isomer (see Fig. 7) of $Ni^{II}$(OEiBC) showed a single average Ni(II)-N bond length of 1.942 Å [59]. Also significant was the

study of a series of nickel hydroporphyrins containing the fused cyclohexanone ring found in $F_{430}$. The isobacteriochlorin, $Ni^{II}$(iBC3) (see Fig. 7), showed by X-ray crystallography an average Ni(II)-N bond length of 1.915(5) Å [64].

The Ni(I) forms of these hydroporphyrin model compounds have not been isolated, and thus have been studied in solution by EXAFS (see below). However, several Ni(I) complexes with tetraazamacrocyclic ligands have been isolated and structurally characterized by X-ray crystallography [66–70]. These studies showed that depending on the macrocyclic ligand's flexibility, reduction of Ni(II) to Ni(I) was associated with either expansion of the Ni-N distances, a distortion in the $NiN_4$ core (i.e., two sets of significantly different Ni(I)-N bond lengths) or both expansion and distortion.

### 5.3
### X-Ray Absorption (EXAFS) Studies

In contrast to the sole X-ray diffraction study described above, a number of X-ray absorption studies on various forms of $F_{430}$ have been performed. These studies have addressed several aspects of $F_{430}$ chemistry: axial ligand coordination to Ni [55, 71] conformational changes of the macrocycle nitrogen ligands to Ni as a function of Ni oxidation state [72] and comparison with model compounds [64, 65, 73]. The studies by Scott and co-workers showed that both enzyme-bound and isolated $F_{430}$ in aqueous solution at low temperature (< 250 K) contained 6-coordinate Ni(II) due to axial ligand coordination [55]. These axial ligands were water (bis-aquo) in isolated $F_{430}$, but were unknown in the holoenzyme. However, at higher temperatures a 4-coordinate, square-planar, form was in equilibrium with the psuedo-octahedral form. No evidence for any 5-coordinate form of $F_{430}$ was found [71]. The 4-coordinate form was favored in weakly coordinating solvents, such as TFE, which was used to advantage in the NMR studies. However, 13-monoepimer and 12,13-diepimer-$F_{430}$ did not form 6-coordinate complexes except with very strong ligands (e.g., cyanide, pyridine), in which case the resulting 6-coordinate epimeric forms were indistinguishable from the native form [71]. Thus a relatively subtle change in macrocyclic ligand conformation can have significant consequences on exogenous ligand affinity. Such tuning of axial ligand affinity can in turn have implications for enzyme action.

Perhaps the most important application of X-ray absorption techniques has been to compare native $F_{430}$ to the reduced form, $Ni^{I}F_{430}$. As will be discussed below, there is strong evidence that the active form of MCR contains $Ni^{I}F_{430}$. This Ni(I) form of the cofactor can be generated in solution, using chemical or electrochemical methods, but cannot be isolated, precluding X-ray crystallography. Thus, EXAFS studies of these Ni(I) solutions (as well as other solution spectroscopic techniques to be discussed below) have been very useful. Reduction of $F_{430}$ led to a dramatic change in the coordination to Ni, as seen in Table 1, which summarizes relevant Ni-N bond distances. As-isolated aqueous $F_{430}$ (i.e., $S = 1$, pseudo-octahedral with axially coordinated bis-aquo ligands) exhibited equivalent Ni(II)-N distances of 2.10 Å [55, 71] and $F_{430}Me_5$ in THF (i.e., $S = 0$, square-planar) also has equivalent Ni(II)-N distances of 1.90(2) Å

[72] in agreement with the average Ni(II)-distance determined from its crystal structure: 1.86(2) Å [39]. However, this contrasts with the EXAFS results for $Ni^{I}F_{430}Me_5$ generated by reduction using Na(Hg) amalgam in THF: *two* sets of Ni(I)-N distances were required: 1.88(3) and 2.03(3) Å [72]. Additionally, unpublished studies by Scott and co-workers show Ni(I)-N distances of 1.90(3) and 2.04(3) Å for $Ni^{I}F_{430}$ generated in aqueous solution by reduction with $Ti^{III}$(citrate) [74]. These results were explained in terms of the ability of the highly flexible $F_{430}$ skeleton to accommodate easily the "ideal" distances required by octahedral or square-planar Ni(II) [75] and by the relatively large Ni(I) ion (radius $r \geq 2.1$ Å) [62].

EXAFS studies on model compounds for $F_{430}$ have also been performed. These include hydroporphyrins such as the Ni(iBC 3) complex (Fig. 7), which in the reduced state showed two sets of Ni(I)-N bond lengths: 2.00(3) and 1.85(5) Å [64, 73] in striking contrast to the Ni(II) form, for which EXAFS showed equivalent Ni(II)-N bond lengths of 1.93(2) Å [64]. Similarly, EXAFS studies of Ni(II) and Ni(I) complexes with OEiBC showed the former having equivalent Ni(II)-N bonds, in agreement with the crystallographic data, while the latter required two sets of Ni(II)-N bond distances [65]. Similar distortions as a consequence of metal-centered reduction (i.e., Ni(II) to Ni(I)) have been found in EXAFS studies of tetraazacyclotetradecane complexes [68]. In contrast, ligand-centered reduction (i.e., formation of a $\pi$ anion radical) left the geometry around Ni(II) unchanged. This was the case for both the unsaturated (porphyrin and chlorin derivatives) [64, 73] and saturated (tetraazacyclotetradecane derivatives) complexes [68].

## 5.4 EPR Studies

EPR has proven to be of tremendous importance in the investigation of MCR and $F_{430}$ since this technique directly addresses the electronic structure of nickel. Aerobically purified MCR exhibits an EPR signal (known as $MCR_{ox1}$) that was not observable in isolated cofactor [9, 77, 78]. $MCR_{ox1}$ showed partly resolved hyperfine coupling to nitrogen ligands and when $^{61}$Ni-enriched medium was used, EPR line-broadening was observed due to unresolved hyperfine coupling to this magnetically active nucleus ($^{61}$Ni, $I = 3/2$), indicating that $MCR_{ox1}$ arose from a nickel-centered paramagnetic form of $F_{430}$. However, MCR in this state had low activity that did not correlate with $MCR_{ox1}$ EPR signal intensity, suggesting that $MCR_{ox1}$ represented an inactive species. Much more importantly, Albracht et al. identified two other EPR signals, $MCR_{red1}$ (axial) and $MCR_{red2}$ (rhombic), in *Mb. thermoautotrophicum* (Marburg) intact cells reduced by $H_2$ [78, 79]. Subsequently, Rospert et al. were able to maintain these signals in cell extracts as well [34]. Relevant EPR parameters are summarized in Table 2. In contrast to $MCR_{ox1}$, the intensity of the $MCR_{red1,2}$ signals correlated with enzyme activity [77, 79]. Similar results relating EPR signal intensity to methane formation from acetate in *Ms. barkeri* intact cells were found by Krzycki and Prince [80]. $MCR_{red2}$ was quantitatively converted to $MCR_{red1}$ by addition of the substrate $CH_3S$-CoM, and conversely, addition of HS-CoM in-

**Table 2.** EPR Parameters for Ni Complexes Relevant to $F_{430}$

| Complex | $g = [g_1, g_2, g_3]$ [a] | $A_{iso}(^{14}N)$ [b] (MHz) | Conditions,[c] [Reference] |
|---|---|---|---|
| $Ni^{I}F_{430}$ | 2.244, 2.063, 2.063 | 28 | $H_2O$/EG (55% v/v), pH ~10; Q-band; 2 K [88] |
| | 2.224, 2.061, 2.061 | 29 | $H_2O$, pH 10.4; X-band; 66 K [87] |
| $Ni^{I}$(12,13-diepimer-$F_{430}$) | 2.238, 2.057, 2.057 | 30 | $H_2O$, pH 10.4; X-band; 66 K [87] |
| $Ni^{I}F_{430}Me_5$ | 2.250, 2.074, 2.065 | 28 | THF; X-band; 88 K [81] |
| $Ni^{I}F_{430}$(NH-*n*-Bu)$_5$ | 2.244, 2.076, 2.060 | not obs. | THF; X-band; 113 K [82] |
| $Ni^{I}$(OEiBC) | 2.204, 2.080, 2.063 | 30 | 2-$CH_3$-THF; Q-band; 2 K [88] |
| | 2.2025, 2.083,2.061 | 30 | THF; X-band; 113 K [65] |
| $Ni^{I}$(iBC 3) | 2.199, 2.076, 2.064 | 30 | THF; X-band; 113 K [64] |
| $Ni^{I}$(4,11-dieneN$_4$) | 2.226, 2.055, 2.055 | not obs. | $CH_3CN$; X-band; 77 K [84] |
| $MCR_{red1}$ | 2.260, 2.088, 2.088 | not obs. | $H_2O$, pH 7.6; X-band; 77 K [77] |
| $MCR_{red2}$ | 2.285, 2.235, 2.184 | obs., not calc. | $H_2O$, pH 7.6; X-band; 77 K [77] |
| MCR-BrPrSO$_3$ | 2.223, 2.115, 2.115 | not obs.[d] | $H_2O$, pH 7.6; X-band; 77 K [77] |
| MCR-BrHTP | 2.210, 2.113, 2.113 | not obs.[d] | $H_2O$, pH 7.6; X-band; 77 K [77] |
| $MCR_{ox1}$ | 2.227, 2.159, 2.159 | not obs. | $H_2O$, pH 7.6; X-band; 77 K [77] |

[a] This assignment makes no assumption as to geometry, however, the value for $g_1$ is often reported as $g^z \equiv g_\parallel$ and $g_{2,3}$ is reported as $g_{x,y} \equiv g_\perp$.

[b] Isotropic hyperfine coupling constant from nitrogen ligands. Measured from resolved splitting in the EPR spectra, except for the study of Telser et al., which employed ENDOR [88].

[c] Solvent, microwave frequency (X-band ≈ 9.5 GHz; Q-band ≈ 35 GHz), and temperature are given.

[d] No evidence of hyperfine coupling to bromine ($^{79,81}Br$, $I = 3/2$) was observed.

creased $MCR_{red2}$ at the expense of $MCR_{red1}$ [34, 77]. In further contrast to $MCR_{ox1}$, both $MCR_{red}$ signals were quenched by oxygen and by chloroform. All of this evidence indicated that the $MCR_{red1,2}$ signals represented intermediates active in the catalytic cycle of MCR [77]. Their EPR parameters (see Table 2) indicated that these signals arose from a metal-centered paramagnetic species, for which $F_{430}$ was the only candidate in MCR. The $MCR_{red2}$ signal was observed in both isoenzymes of MCR (MCR I and MCR II) [38]. EPR studies of the interaction of MCR with substrate analogs have also been performed and are discussed in Sect. 7.

The origin of the $MCR_{red1,2}$ signals was facilitated by the very significant EPR work of Jaun on $F_{430}Me_5$. Jaun and Pfaltz reported the generation of $Ni^{I}F_{430}$ by

Na(Hg) amalgam in THF, which gave an EPR spectrum similar to that of $MCR_{red1}$ (see Table 2), which was characteristic of an approximately square-planar $S=1/2$ system with a $d^1_{x2-y2}$ electronic ground state [81]. Hamilton et al. obtained similar results using the penta-*n*-butylamide of $F_{430}$ [82]. Jaun was also able to generate electrochemically $Ni^{III}F_{430}$ (see Sect. 5.5), which gave an EPR spectrum characteristic for a tetragonally-distorted $S=1/2$ system with a $d^1_{z2}$ ground state ($g_{\|}=2.020$, $g_{\perp}=2.211$), which was unlike that seen in MCR itself (see Table 2) [83].

EPR studies on model compounds for $F_{430}$ have also been reported. It should be noted that the definitive work on the EPR and electrochemical behavior of tetraazamacrocyclic nickel complexes, analogous to $F_{430}$, was carried out by Busch and co-workers years before $F_{430}$ had been discovered [84]. In conjunction with their EXAFS studies, Renner et al. reported EPR results for a number of Ni porphyrinoid complexes [65, 64]. An extensive EPR and electrochemical study was reported earlier by Stolzenberg and Stershic [62]. EPR parameters for Ni(I) complexes are given in Table 2. EPR parameters for $\pi$ radicals are not given here; these species gave characteristic EPR spectra that were roughly isotropic with $g\approx 2.00$ [62, 64]. The reduction of Ni(II) tetrapyrroles is extremely sensitive to solvent, porphyrin ligand, temperature, and coordination of axial ligands in terms of whether a ligand or metal-centered reduction occurs [85, 86, 64]. Clearly, no obvious correlation can be made with degree of ligand saturation, as reduction of Ni(II) porphyrins, chlorins, and the more saturated hexahydroporphyrins and octahydroporphyrins all yielded $\pi$ anion radicals, while Ni(II) isobacteriochlorins and $F_{430}$ yielded Ni(I) species [62, 64]. Similarly, Ni(II) tetraazacyclotetradecatetraene complexes that differ only in whether or not two of the four double bonds are conjugated, yielded Ni(I) species when there was no conjugation and a ligand radical when there was [84]. Furthermore, among the complexes that are reduced at the metal, as seen by inspection of Table 2, there is no obvious correlation between ligand and whether an axial or a rhombic EPR spectrum is observed.

Recently, advanced EPR techniques have been applied to $F_{430}$. Holliger et al. performed EPR and ESEEM spectroscopy on isolated $Ni^{I}F_{430}$, generated by reduction using aqueous $Ti^{III}$(citrate) [87]. The EPR signal in this case closely resembled that for $MCR_{red1}$; much more so than that for $Ni^{I}F_{430}Me_5$ (see Table 2). Using $^2H$ ESEEM in $D_2O$ solution, they found no evidence for axial coordination of solvent to Ni(I). Thus $MCR_{red1}$ is either due to free cofactor, or if the cofactor is bound, then it lacks the axial coordination found in the resting state, Ni(II) form, thus rendering it able to bind substrate. Mechanistic aspects will be discussed further below. Very recently, the results of Holliger et al. were confirmed by Telser et al., who used $^{1,2}H$ pulsed ENDOR spectroscopy to demonstrate the absence of axial solvent ligation [88]. They also studied $^{14}N$ ENDOR signals arising from the pyrrole nitrogen ligands to Ni(I). The hyperfine coupling so determined agreed with earlier values based on EPR (four nitrogen ligands with $A_{iso}(^{14}N)\approx 30$ MHz; see Table 2), [81, 88] but also provided evidence for the existence of two types of nitrogen ligands, as seen by EXAFS.

## 5.5 Electrochemical Studies

Due to the redox activity of nickel complexes in general and the possible role of various oxidation states of $F_{430}$ in MCR activity, a number of electrochemical studies on $F_{430}$ and related species have been performed. Electrochemical data are summarized in Table 3 and are given relative to the normal hydrogen electrode (NHE). Jaun and Pfaltz first reported the reversible reduction of $F_{430}Me_5$ to $Ni^{I}F_{430}Me_5$ in THF and DMF at a potential of roughly −0.7 V [81]. Subsequently, Furenlid et al. reported reduction potentials in *n*-butyronitrile of −0.71 V for $F_{430}Me_5$ and −0.79 V for its 12,13-diepimeric form [72]. Similarly, several pentaalkylamides of 12,13-diepimer-$F_{430}$ were reversibly reduced at roughly −0.8 V [82]. As for studies on free acid cofactor, heat-extracted $F_{430}$ (i.e., 12,13-diepimer-$F_{430}$) exhibited a quasireversible reduction in DMF at roughly −0.6 V [89]. More recently, Holliger et al. performed a detailed spectroelectrochemical study of aqueous native and 12,13-diepimer-$F_{430}$ [87]. A Nernst plot using EPR quantitation yielded values for $E_{1/2}$ of −0.65 and −0.62 V for native and 12,13-diepimer-$F_{430}$, respectively. It had been proposed that native $F_{430}$ was more readily reduced (i.e., more positive $E_{1/2}$) than the 12,13-diepimeric form, because it could not as easily achieve the stable, $S_4$-ruffled conformation [55, 90]. This appeared to be the case in organic solvents, but not necessarily in aqueous solution. Furthermore, the reduction potential in the holoenzyme is not known, wherein protein conformational effects can contribute, although it should be similar to that measured for the isolated cofactor [87]. The $E_{1/2}$ values for several model compounds for $F_{430}$ are also given in Table 3. It is difficult to compare directly electrochemical data that have been determined in different solvents and supporting electrolytes and with various reference electrodes. Nevertheless, it is clear that although these complexes were used as models for $F_{430}$ due to their formation of Ni(I) species, the potentials required were much more negative. This means that the natural cofactor is remarkably easy to reduce to the Ni(I) form, compared both to less saturated [62, 64] and to more saturated [84] macrocyclic Ni complexes.

Furthermore, the relatively unsaturated Ni complexes, such as $Ni^{II}$(OEiBC) and $Ni^{II}$(iBC 3), were oxidized to ligand-centered $\pi$ cation radicals (at potentials generally $< +1$ V) [64]. In contrast, Jaun reported the reversible oxidation of $F_{430}Me_5$ in acetonitrile at +1.45 V (NHE; +0.825 vs ferricenium/ferrocene) [83]. Relatively saturated macrocyclic Ni complexes were also oxidizable to Ni(III) species [84]. The potentials required were generally lower (roughly +0.9 – 1.2 V, see Table 3), although a series of 16-membered tetraazamacrocycles exhibited roughly the same $E_{1/2}$ value as $F_{430}$ (~1.5 V) [84]. The formation of Ni(III) is relevant to the mechanism of MCR as will be discussed in Sect. 7.

## 5.6 Optical Spectroscopic Studies (UV-Vis, MCD)

$F_{430}$ exhibits a characteristic absorption band at 430 nm, which gives the cofactor its name. Optical absorption studies ($F_{430}$ is non-emissive) have been performed by several groups, generally in conjunction with other techniques such as EPR,

**Table 3.** Electrochemical Data for Ni Complexes Related to $F_{430}$

| Complex, Reduction | $E_{1/2}$ (V, NHE)[a] | Conditions,[b] Reference |
|---|---|---|
| $NiF_{430}$; Ni(II,I) | − 0.65 | $H_2O$, pH 10.4; $Ti^{III}$(citrate); EPR[c] [87] |
| Ni(12,13-diepimer-$F_{430}$); Ni(II,I) | − 0.62<br>− 0.58 | $H_2O$, pH 10.4; $Ti^{III}$(citrate); EPR[c] [87]<br>DMF; TEAP; AgCl\|Ag [89] |
| Ni($F_{430}Me_5$); Ni(II,I) | − 0.67,[d] − 0.70[d]<br>− 0.71 | THF, DMF; $LiClO_4$, TBAP; $Fc^+$\|Fc[d,e] [81]<br>$CH_3(CH_2)_2CN$; TBAP; SCE [72] |
| Ni(12,13-diepimer-$F_{430}Me_5$); Ni(II,I) | − 0.79 | $CH_3(CH_2)_2CN$; TBAP; SCE [72] |
| Ni($F_{430}$(*NH-n*-Bu)$_5$); Ni(II,I) | − 0.80 | DMF; TEAP; AgCl\|Ag [82] |
| Ni(OEiBC); Ni(II,I) | − 1.30, − 1.22 | $CH_3CN$, DMF; TBAP; SCE [62] |
| Ni(iBC 3); Ni(II,I) | − 1.09 | THF; TBAP; SCE [64] |
| Ni(4,11-dieneN$_4$); Ni(II,I) | − 1.29[f] | $CH_3CN$, TBAT; AgCl\|Ag[g] [84] |
| Ni($F_{430}Me_5$); Ni(III,II) | + 1.45[h] | $CH_3CN$; TBAT; $Fc^+$\|Fc[e] [83] |
| Ni(4,11-dieneN$_4$); Ni(III,II) | + 1.26[i] | $CH_3CN$; TBAT; AgCl\|Ag[g] [84] |

[a] Determinded by cyclic voltammogramms showing reversible electrochemical behavior, except for the study of Holliger et al., which employed EPR to monitor the extent of chemical reduction by $Ti^{III}$(citrate) and a Nernst plot to determine $E_{1/2}$ [87]. All values are vs NHE, unless otherwise noted.

[b] Solvent, supporting electrolyte, and original reference electrode are given. Herein are used the following standard potentials vs NHE: (AgCl, saturated KCl)|Ag, + 0.20 V; SCE, + 0.24 V; 0.1 *M* calomel, + 0.34 V [124].

[c] CV not used (see note (a)).

[d] Reported as − 1.29, − 1.32 V vs $Fc^+$|Fc [81].

[e] Due to variation in conditions, etc., various potentials have been reported for the $Fc^+$|Fc couple: the study by Furenlid et al. yielded a $Fc^+$|Fc potential of + 0.70 V [72], while the study by Jaun and Pfaltz yielded + 0.82 V (reported as + 0.48 V vs 0.1 *M* calomel) [81], and + 0.54 V is a commonly used standard potential for $Fc^+$|Fc [123]. Herein is used + 0.625 V, which was the value estimated by Jaun in a later study [83].

[f] Reported as − 1.57 V vs AgCl, 0.1 *M* $Cl^-$|Ag [84].

[g] Reference electrode was (AgCl, 0.1 *M* $Cl^-$)|Ag; herein this reference is considered to be + 0.28 V vs NHE.

[h] Reported as + 0.825 V vs $Fe^+$|Fc [83]. This potential was also quoted by Renner et al. as + 1.52 V (+ 1.28 V vs SCE) [64], due to differing values for $Fc^+$|Fc (see note (e)).

[i] Reported as + 0.98 V vs (AgCl, 0.1 *M* $Cl^-$)|Ag [84].

Raman, or electrochemistry. The studies of Shiemke et al. were particularly significant [55, 71]. These studies demonstrated the 4- and 6-coordinate forms of $F_{430}$, as described above in Sect. 5.3. In parallel work, the binding of axial ligands to $F_{430}Me_5$ has been studied [9]. In this case, 5- as well as 6-coordinate species were formed, which may be a consequence of the use of organic solvents that allowed the intermediate 5-coordinate species to be spectroscopically observed.

Optical absorption has also been used to monitor the reduction of various forms of $F_{430}$. Reduction in both aqueous solution (by $Ti^{III}$(citrate) of both native and 12,13-diepimer-$F_{430}$) [87] and in organic solvents (by Na amalgam of $F_{430}Me_5$ [81] and several pentaalkylamide forms [82]) led to characteristic changes in the UV-visible spectra: the band at ~430 nm decreased and new

bands at ~380 and ~755 nm (~715 in aqueous solution) grew in. In agreement with this work on isolated cofactor, active MCR preparations (i.e., by hydrogen incubation) exhibited a band at 386 nm that disappeared upon exposure to oxygen or chloroform [34].

The various model compounds also exhibited characteristic optical absorption changes upon reduction of Ni(II) to Ni(I) [62, 64, 65, 68, 73]. A detailed discussion is beyond the scope of this review, but it is worth noting that optical absorption spectra (as can EPR) can easily distinguish between metal- and ligand-centered reductions [64].

MCD has proven to be extremely valuable in studying $F_{430}$, because, in contrast to EPR, this technique is readily applicable to $S = 1$ systems, such as often exhibited by Ni(II). A detailed MCD study by Hamilton et al. showed that isolated native $F_{430}$ contained pseudo-octahedral Ni(II) ($S=1$) with axial zero-field splitting, $D = +9(1)$ $cm^{-1}$ and that holoenzyme MCR (*Mb. thermoautotrophicum* ΔH) also contained pseudo-octahedral Ni(II) with $D = +10(1)$ $cm^{-1}$ [91]. A parallel and simultaneous MCD study by Cheeseman et al. on isolated and enzyme-bound $F_{430}$ (from *Mb. thermoautotrophicum* Marburg) likewise found these to contain $S=1$ Ni(II) with $D=+9.0(3)$ $cm^{-1}$, $E/D=0$, and $D=+8.5(3)$ $cm^{-1}$, $|E/D|=0.20(5)$, respectively [92]. These studies were significant in that they demonstrated a strong similarity between isolated and enzyme-bound $F_{430}$, and furthermore, that in the holoenzyme Ni(II) was likely axially coordinated by water-like (i.e., oxygenic) ligands. Hamilton et al. also studied by MCD the 12,13-diepimeric and 12,13-didehydro forms of $F_{430}$ [91] and the two isoenzymes of MCR [28].

### 5.7
### Vibrational Spectroscopic Studies (Resonance Raman)

Resonance Raman (RR) spectroscopy has been very helpful in understanding chromophores in metalloproteins and their model compounds, especially heme proteins and porphyrins. MCR and $F_{430}$, while not truly in this category, have also been profitably studied by this technique. RR was used in conjunction with EXAFS and UV-visible spectroscopic studies to elucidate the nature of 4- and 6-coordination to Ni(II) in isolated and enzyme-bound $F_{430}$, as discussed above in Sects. 5.3 and 5.6 [93, 91, 55, 71]. Concurrent with the RR studies on $F_{430}$, there have been several beautiful RR studies by Shelnutt and co-workers on hydrocorphinoids structurally related to $F_{430}$ [94–96]. Recently, RR has also been used to study $Ni^{I}$(OEiBC) [97]. Reduction of $Ni^{II}$(OEiBC) led to structural distortions analogous to those seen by EXAFS.

## 6
## Theoretical Studies of $F_{430}$ and Model Compounds (Molecular Mechanics)

As alluded to above, there are two non-enzymatic aspects of $F_{430}$ that are of fundamental chemical interest: why is $F_{430}$ reduced at the metal, rather than at the ligand, and what are the conformational effects in this unusual macrocyclic li-

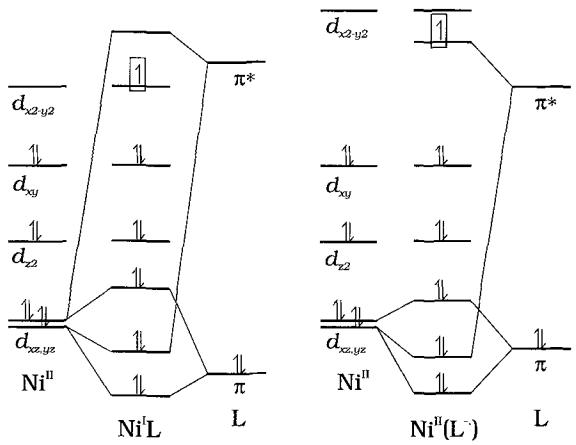


**Fig. 8.** Qualitative diagram showing the relative energy levels of the frontier MO's in macrocyclic Ni complexes, modified from a diagram by Jaun [7]. A reducing equivalent (boxed electron) can go into either a metal-centered MO, leading to a Ni(I) complex (left), or into a ligand-centered MO, leading to a $\pi$-system radical (right)

gand? The first aspect is best discussed in the reviews by Jaun [7, 9]. As discussed above in Sect. 5.5, the reduction potential of Ni(II) in $F_{430}$ is unusually positive. Furthermore, Ni(II) readily adds axial ligands so as to convert from square-planar $d^8$ ($S = 0$) to pseudo-octahedral ($S = 1$). These both indicate that the Ni $3d_{x2-y2}$ orbital is relatively low in energy, in the first case with respect both to this orbital in other Ni(II) complexes and to ligand $\pi^*$ orbitals, and in the second case with respect to the Ni $3d_{z2}$ orbital. These two possibilities are shown schematically in Fig. 8, noting that the MO diagrams are only qualitative and that they do not take into account mixing among metal $3d$ orbitals (e.g., $d_{z2}$ character in $d_{x2-y2}$, caused by rhombic ligand-field terms) or mixing between metal and ligand orbitals. As pointed out by Jaun [9] the most systematic analysis of these effects was done by Busch and co-workers (before $F_{430}$ was discovered) using relatively saturated tetraaza macrocyclic complexes [84]. More recently, other significant studies on these, and on relatively unsaturated porphyrinoid complexes, have been made [98, 68, 64, 65, 62]. These studies showed that the weaker ligand field, resulting in a lower energy $d_{x2-y2}$ orbital, was favored in a ligand with a relatively large coordination hole and that was relatively rigid. The core hole is controlled both by the ligand size and by its conformation, notably $S_4$-ruffling in tetrapyrroles. However, the ligand must not be too rigid, which is the case for porphyrins and chlorins, because upon reduction the ligand cannot well accommodate the larger Ni(I) ion. Apparently, $F_{430}$ perfectly balances these requirements. However this is not the complete story since the possibility of ligand-centered reduction must also be considered. Totally saturated tetraaza-macrocycles obviously cannot compete for the reductant electron, nor can those with two unconjugated double bonds (e.g., 4,11-dieneN$_4$, Fig. 7), however those with conjugated double bonds (e.g., 1,3-dieneN$_4$) yielded a ligand-centered radical [84]. Of course, $F_{430}$ has a significantly more extended conjugated system

than does a 1,3-diene, and OEiBC even more so, with the resulting smaller $\pi$–$\pi^*$ gap that would seem to favor ligand-centered reduction. Along with the ligand's monoanion charge, the conjugated carbonyl group in $F_{430}$ (ring C) has been implicated as facilitating metal-centered reduction [9]. However, this must be only part of the explanation since Ni(II) porphyrins, chlorins, hexa- and octahydroporphyrins with exactly this functional group are nevertheless reduced at the ligand, although the isobacteriochlorin (iBC 3, Fig. 7) gives Ni(I) [64] as does OEiBC itself, which lacks this carbonyl. The balance mentioned above apparently is also achieved in isobacteriochlorins, as well as in $F_{430}$. Despite significant theoretical work on porphyrins [64, and references therein] there is at present no theoretical explanation that provides a *comprehensive* picture of this delicate balance of electronic and geometrical effects the control ligand versus metal-centered reduction in the whole range of Ni(II) tetraazamacrocyclic complexes. It is clear that Nature has designed $F_{430}$, using the normal tetrapyrrole building blocks, so as to produce a ligand that optimally generates Ni(I).

The above discussion has dealt with reduction of $F_{430}$ to the putative active form. Unfortunately, there is little structural information on $Ni^IF_{430}$, except that regarding the direct coordination environment around Ni(I), as derived in solution by EXAFS, EPR, and related techniques (Sect. 5.4, 5.6, 5.7). In contrast, NMR and crystallographic studies have provided detailed information on the solution and solid-state conformation of isolated $F_{430}$ and derivatives, as well as of numerous model compounds (Sects. 5.1, 5.2). This information has provided the basis for several studies using conformational analysis, both of $F_{430}$ [99, 100, 40] and of model compounds [101, 102].

Zimmer and Crabtree performed a detailed conformational analysis of $F_{430}$ using molecular mechanics [100]. Their work found that the original stereochemical assignment at C17 was energetically more favorable, although this preference may be alleviated by protein conformational effects. Their chief conclusions were that $F_{430}$ is extremely flexible, and in particular that it may achieve trigonal bipyramidal, as well as square planar, geometry. Trigonal bipyramidal geometry was proposed as being mechanistically relevant, as will be discussed below. Zimmer continued this work and analyzed by molecular mechanics the epimerization and oxidation of $F_{430}$ [99]. Zimmer found that in the reduction of 12,13-dehydro-$F_{430}$ ($F_{560}$) native $F_{430}$ is produced, rather than the thermodynamically more stable 12,13-diepimer, because a smaller conformational change was required in the first case [99]. Kaplan et al. performed a related molecular mechanics study on a simplified analog of $F_{430}$ to understand axial ligand binding [102]. They found, in contrast to the above discussion of factors leading to Ni(I) formation, that the core hole in $F_{430}$ was not significantly larger than in more oxidized hydroporphyrin ligands, and thus did not contribute to the increased affinity of $F_{430}$ for axial ligands [102].

## 7 Mechanistic Studies of $F_{430}$ and Model Compounds

Mechanistic studies represent one of the most significant areas of research on MCR and $F_{430}$, and although it is generally accepted that $F_{430}$ is the active site of

MCR, there is still no definitive mechanism for the final step of methanogenesis. Furthermore, relatively little mechanistic work has been done using MCR, as opposed to model compounds, and more distressingly, this work is not that recent.

An early, and very thorough, mechanistic study using active MCR from *Mb. thermoautotrophicum* (ΔH) was performed by Wackett et al. [103]. These workers developed kinetic assays and investigated a variety of analogs to the native substrate, $CH_3S$-CoM. These substrate analogs were based on rational modifications of the various subunits of $CH_3S$-CoM (see Fig. 2): the terminal alkyl (that yields the alkane product), the heteroatom bound to the alkyl, and the terminal sulfonate. This process led to the discovery of three kinetically competent substrates and five inhibitors. MCR activity was very sensitive to the nature of the terminal alkyl group: $CH_3CH2S$-CoM was a substrate, while the propyl and cyclopropyl derivatives were non-substrates; $CF_2HS$-CoM was a substrate, while $CF_3S$-CoM was not; and $CH_2=CHCH_2S$-CoM was a potent inhibitor [103]. Presumably, the steric requirements of the active site are quite stringent, as well as inductive effects on the thioether bond to be cleaved. Substitution of thioether sulfur by oxygen and by selenium yielded, respectively, a weak inhibitor of MCR and a very active substrate for methane production. This dramatic effect was postulated as arising from the involvement of a Ni-E (E = S, Se) bond in enzyme action [103]. Another beautiful study was performed by Ahn et al. using a cell-free extract of *Ms. barkeri* [104]. These workers determined the stereochemical course of methanogenesis using the optically active substrate isotopologs (*R*)- and (*S*)-[1-$^2H_1$, $^3H$]ethyl-coenzyme M ($CH_3$-(*R*,*S*)$C_2H_3HS$-CoM). They found that replacement of the sulfur of alkyl-CoM by hydrogen to give alkane proceeded with net inversion of configuration [104]. This inversion could occur via displacement of sulfur by Ni(I) since the subsequent protonation of the bound alkyl would occur with retention of configuration [104]. Finally, but concurrent with the above two studies, was the work of Rospert et al. using substrate analogs of general type X-$(CH_2)_3$-$SO_3$, where X = F, Br, I (i.e., $CH_3S$-CoM wherein the methylthio group was replaced by halomethyl), which showed these compounds, especially the bromide analog, $BrPrSO_3$, to be effective competetive inhibitors of MCR [77]. Purified enzyme or cell extract with these inhibitors exhibited an axial EPR signal (MCR-$BrPrSO_3$, see Table 2) similar to other MCR signals and no hyperfine coupling to any of these magnetically active halogen nuclei ($^{19}F$, $I = 1/2$; $^{79,81}Br$, $I = 3/2$; $^{127}I$, $I = 5/2$) was observed [77]. A brominated derivative of HTP also led to a novel axial EPR signal (MCR-BrHTP, see Table 2) [77]. The exact nature of the species giving rise to these EPR signals was uncertain, however they likely resulted from an indirect inhibitor-Ni rather than a direct Ni-X interaction. Advanced EPR techniques (ESEEM, ENDOR) might prove helpful in this addressing this question.

Several mechanistic studies, chiefly by Jaun and co-workers, have been made using $F_{430}Me_5$ [9, 83, 105, 106]. Also relevant are a number of studies on model compounds for $F_{430}$ [61, 107, 101, 108–116]. Interestingly, $Ni^IF_{430}Me_5$ has not been shown to react with thioethers, including $CH_3S$-CoM [9]. However, $Ni^IF_{430}Me_5$ did react with more activated sources of the methyl group such as

sulfonium ions ($R_2S^+$-$CH_3$), methyl halides, and methyl tosylates ($CH_3$-$OSO_2$-$C_6H_5CH_3$) and triflates ($CH_3$-$OSO_2CF_3$) as shown below:

$$CH_3\text{-}X + 2Ni^{I}F_{430}Me_5 + BH \rightarrow CH_4 + 2Ni^{II}F_{430}Me_5 + B^- + X^-;$$

where BH was a source of acidic protons such as thiols, alcohols, and ammonium salts [107]. Lin and Jaun performed extensive kinetic studies on the reductive cleavage of methyl sulfonium ions catalyzed by $Ni^{I}F_{430}Me_5$ [105]. They showed that the final hydrogen in the product methane did derive from acid (BH as above) and that the reaction did not proceed via outer-sphere electron transfer to the sulfonium [105]. Rather, Jaun and co-workers had found evidence for an intermediate, which they proposed to be $CH_3$-$Ni^{II}F_{430}Me_5$ [107]. This species, analogous to that in vitamin $B_{12}$ chemistry, was independently prepared by reaction of $Ni^{II}F_{430}Me_5$ with $(C^2H_3)_2Mg$ and was identified by $^2H$ NMR, as the $^2H$ resonances were substantially shifted by interaction with the paramagnetic Ni(II) [106]. Addition of acid converted this methyl-Ni species to $F_{430}Me_5$. The observation of $CH_3$-$Ni^{II}F_{430}Me_5$ was consistent with the stereochemical observations for MCR described above.

Similar reactivity towards activated methyl compounds, especially methyl iodide, has been observed for $Ni^{I}$OEiBC [114, 115, 61, 116] and for $Ni^{I}$(tmtaa) (where tmtaa is the dianion of 6,8,15,17-tetramethyl-5,14-dihydrodibenzo [*b,i*] [1, 4, 8, 11]tetraazacyclotetradecine) [112, 113]. $Ni^{I}$(tmtaa), generated in situ by reduction of $Ni^{II}$(tmtaa) and observed by EPR, was proposed as the active catalyst in the reduction by $NaBH_4$ of alkyl halides to alkanes. Recently, a different Ni(I) tetraazamacrocyclic complex, produced by irradiation of the Ni(II) parent compound with 5 MeV electrons, produced small amounts of methane from subsequently added $CH_3S$-CoM [111]. The represented the first report of reactivity of any identifiably Ni(I) species with the natural substrate.

Another interesting approach was taken by Berkessel and co-workers, who synthesized Ni(II) complexes with salen-derivative ligands having a pendant thioether group [101, 108]. They found that intramolecular electron transfer from sulfur to nickel can easily occur. This, combined with other evidence, as described above, led to a proposed catalytic cycle for the final step of methanogenesis, as shown in Fig. 9. The same mechanism was simultaneously proposed by Jaun [83].

The above extensive discussion is based on $Ni^{I}F_{430}$ as being the active form. There is, however, also some evidence that Ni(III) could instead (or also) be involved. As mentioned in Sect. 5.5, $F_{430}Me_5$ can be reversibly oxidized to $Ni^{III}F_{430}Me_5$, which was characterized by EPR [83]. The very positive reduction potential of $Ni^{III}F_{430}Me_5$ (+1.45 V NHE) and the fact that although the EPR signal $MCR_{red1}$ corresponded to that of $Ni^{I}F_{430}$, there was no EPR signal observed in the enzyme that corresponded to that of $Ni^{III}F_{430}Me_5$, the sensitivity to oxidants of $MCR_{red1,2}$ and overall the reducing conditions used in enzyme assays all argue against the involvement of $Ni^{III}F_{430}$. However, a methyl-Ni(III) species could have quite different electronic/redox properties from the reported $Ni^{III}F_{430}$ [83]. Alkyl-$Ni^{III}$(OEiBC) species have also been proposed as intermediates in the reaction of $Ni^{I}$OEiBC with alkyl halides [114]. Thus, another

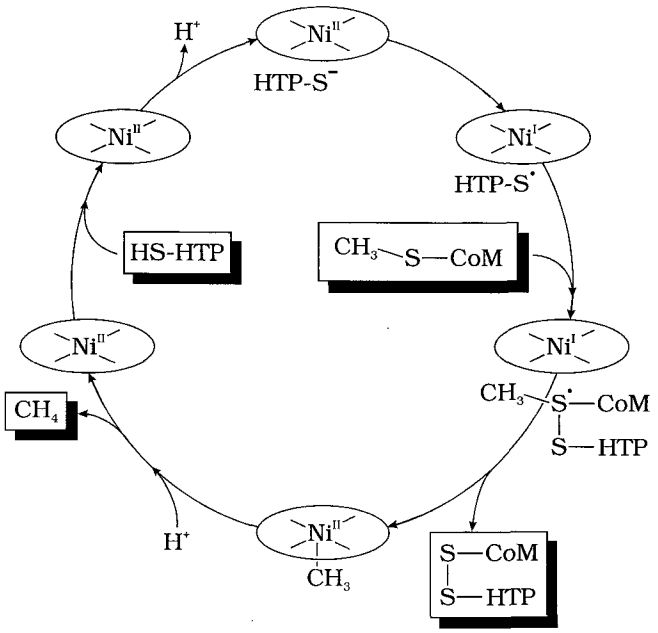


**Fig. 9.** Catalytic cycle proposed for the final step of methanogenesis, involving a $Ni^{I}F_{430}$ intermediate, adapted from a mechanism proposed by Berkessel [108] also proposed simultaneously by Jaun [9, 83]. The $F_{430}$ macrocyclic ligand is represented by a disk. Axial coordination to Ni by sulfur-containing species is likely, but not explicitly shown. The overall charge on the $F_{430}$ species is not known nor indicated. Reproduced, with permission, from Reference [108], © 1991, by Academic Press, Orlando, FL, USA

mechanism has been proposed by Jaun for MCR action [83] which is shown in somewhat modified form in Fig. 10.

There has been model compound evidence in support of the involvement of Ni(III), although quite differently from the catalytic cycle given in Fig. 10. Drain et al. studied the reactions in aqueous solution of what they believed to be a pentaazamacrocyclic complex of Ni(II) ([1,4,7,10,13-pentaazacyclohexadecane-14,16-dionato(2-)]nickel(II)) with several alkyl-CoM derivatives [109, 110]. The choice of derivatives was analogous to those used by Wackett et al. [103] and the results showed strong similarities, such as activity with $CF_2HS$-CoM and inhibition with $CF_3S$-CoM. The conversion of $CH_3S$-CoM to methane was stoichiometric in nickel complex, but catalytic if an oxidant such as $I_2$ or NaClO was added. Drain et al. proposed the following scheme to explain methanogenesis under oxidizing conditions (where $L^?$ = a ligand originally proposed by Drain et al. to be 1,4,7,10,13-pentaazahexadecane-14,16-dione; its identity is now unknown [117]) [109, 110]:

$$Ni^{II}L^? + CH_3S\text{-}CoM \leftrightarrow L^?Ni^{II}S(CH_3)CoM$$
$$L^?Ni^{II}S(CH_3)CoM + H_2O \rightarrow L^?Ni^{III}S\text{-}CoM + CH_4 + OH^-$$
$$L^?Ni^{III}S\text{-}CoM + OH^- \rightarrow {}^1/_2\, O_2 + Ni^{II}L^? + HS\text{-}CoM$$

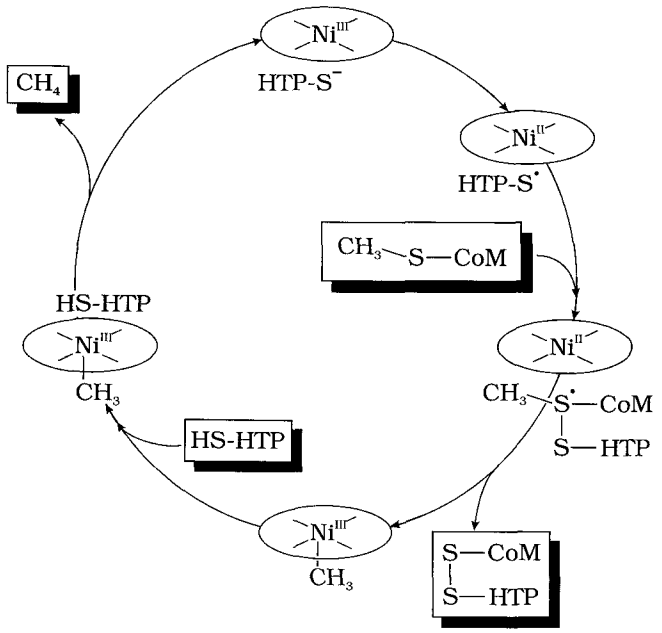


**Fig. 10.** Catalytic cycle proposed for the final step of methanogenesis, involving a $Ni^{III}F_{430}$ intermediate, modified for this review from a mechanism originally proposed by Jaun [83]. The $F_{430}$ macrocyclic ligand is represented by a disk. Axial coordination to Ni by sulfur-containing species is likely, but not explicitly shown. The overall charge on the $F_{430}$ species is not known nor indicated. Reproduced with modifications, with permission, from Reference [83], © 1990, by Verlag Helvetica Chimica Acta, Basel, Switzerland

$$Ni^{II}L^{?} + HS\text{-}CoM \leftrightarrow L^{?}Ni^{II}S(H)CoM$$
$$^{1}/_{4}\,O_2 + HS\text{-}CoM \rightarrow {}^{1}/_{2}\,H_2O + {}^{1}/_{2}\,(CoM\text{-}S\text{-}S\text{-}CoM)$$
$$\text{Net: } CH_3S\text{-}CoM + {}^{1}/_{2}\,H_2O \rightarrow CH_4 + {}^{1}/_{4}\,O_2 + {}^{1}/_{2}\,(CoM\text{-}S\text{-}S\text{-}CoM)$$

A reductant other than hydroxide could in principle have been used so that dioxygen was not produced. This work was performed before the role of HS-HTP had been uncovered, and in any case it would be difficult in model compound work to generate specifically a mixed disulfide. Although it is unlikely that the above scheme is that which occurs in MCR, the fact that in aqueous solution the natural substrate was catalytically converted to methane by a Ni complex represented an excellent example of using small molecules as *functional* models of enzyme action.

A futher difficulty, but also an opportunity, with the above work is that it has very recently been shown that the *active* species did not contain as a ligand 1,4,7,10,13-pentaazacyclohexadecane-14,16-dione (L). An extremely careful study by Zhang et al. showed that authentic NiL was inactive towards methane production [117]. However, these workers did reproduce the essential features of the work of Drain et al. by using "NiL" prepared from less highly purified starting materials [117]. Some as-yet unidentifed species, present in very low

concentration and presumably a Ni complex of a nitrogen donor ligand, was thus quite active at biomimetic MCR chemistry.

## 8 Applications of $F_{430}$ and Model Compounds in Environmental Chemistry

A recent application of methanogenic bacteria has been in the reductive dehalogenation of halogenated (chiefly chlorinated) organic compounds found as pollutants in wastewater and other environmental sources. This area is beyond the scope of this review, however several recent references are noted. The study by Gantzer and Wackett provides an excellent introduction to the challenges posed by the biostability of (poly)chlorinated organic compounds [118].

Isolated $F_{430}$ [118–120] MCR (*Mb. thermoautotrophicum*) [121] cell extracts (*Ms. barkeri* [120] and *Mb. thermoautotrophicum* [121]) and whole cells (*Mb. thermoautotrophicum*) [122] have all been investigated as catalysts for the reductive dehalogenation of a wide range of environmentally important chloroalkanes, chloroalkenes, chloroarenes, and other halogenated organic compounds. As part of this work, Holliger et al. proposed a mechanism for the conversion of 1,2-dichloroethane to ethene and/or chloroethane that involved the reaction of $Ni^{I}F_{430}$ (generated by $Ti^{III}$(citrate)) with 1,2-dichloroethane to yield $F_{430}$ and a chloroethyl radical [120].

The effectiveness of various forms of $F_{430}$ (isolated cofactor, cell extract, etc.) at accomplishing environmentally desirable chemical transformations has been found to vary greatly. Nevertheless, because of its societal importance this area is one that will likely see significant future interest, which may lead to a better understanding of MCR action.

## 9 Concluding Remarks

Less than thirty years ago, techniques for the mass culture of methanogens were developed [20]. Less than twenty years ago (1978), Gunsalus and Wolfe obtained a yellow, low-molecular weight extract from a methanogen [41]. Since that time, tremendous progress has been made in understanding the importance of that extract. The discovery of $F_{430}$, with its unusual tetrapyrrole-derived ligand and biologically uncommon metal, has inspired numerous biochemical, spectroscopic, and synthetic efforts that have pointed out the key role played by this cofactor within MCR in the final step of methanogenesis.

Nevertheless, there are still many questions that remain, in part due to the fact that $F_{430}$ has reawakened interest in the coordination chemistry of nickel with macrocyclic ligands. There are also many questions regarding enzyme assembly (the roles of the A components), and MCR structure and activity that need to be answered [123] but here we note only those related to $F_{430}$ itself. There exists a plausible mechanism for the generation of methane from $CH_3S$-CoM catalyzed by reduced $F_{430}$, but it is not definitive. For example, the proposed intermediates have not been conclusively related to EPR signals seen for MCR ($MCR_{red1,2}$). Furthermore, there is a need for mechanistic studies of MCR

that include the continued development of substrate analogs and inhibitors. This had a promising start 5–10 years ago [77, 103, 104] but has not recently been extended. Parallel work on model compounds is also needed, in particular studies in aqueous solution using biologically relevant substrates. Again, this was begun nearly a decade ago [109, 110] but has not been extended except now to show that a mystery species was the active catalyst [117]. The many studies of macrocyclic Ni(I) complexes in organic solvents have been very rewarding, but in terms of understanding MCR action, they can lead an objective observer to think of the analogy of the man looking for his keys under the lamppost because there the light is best.

Finally, the work on Ni(I) complexes has itself raised fundamental questions regarding coordination chemistry. As mentioned above, there is no comprehensive theoretical explanation (involving metal orbitals, core size, ligand saturation, ligand distortion, etc.) that can explain ligand versus metal-centered reduction in Ni(II) complexes of the type discussed here. Related to this, there is still not a clear picture as to the factors that control the Ni(II) reduction potential and the EPR properties (e.g., axial versus rhombic signals) of the resulting Ni(I) species. These needed theoretical efforts could be complemented by further synthetic work, such as to prepare more examples of five-coordinate macrocyclic Ni(I), Ni(II), and Ni(III) species of the types proposed in MCR mechanisms, especially with axial alkyl ligands, such as done by Lin and Jaun [106] and with available sulfur-containing ligands, as done by Berkessel et al. [101, 108]. Such efforts could also assist in the development of catalysts for the reductive dehalogenation of environmental contaminants.

In conclusion, $F_{430}$ will likely remain an inspiration and a challenge to chemists and biologists for years to come.

**Acknowledgements.** I thank Prof. R. A. Scott, University of Georgia (USA), for providing unpublished EXAFS results, Prof. R. K. Thauer, University of Marburg (Germany), for providing figures and helpful information about current crystallographic studies, and Prof. E. T. Smith, Florida Institute of Technology (USA) and Dr. M. W. Renner, Brookhaven National Laboratory (USA), for helpful comments about electrochemical data.

## 10 References and Notes

1. Halcrow MA, Christou G (1994) Chem Rev 94:2421
2. Hausinger RP (1994) Sci Total Environ 148:157
3. Walsh CT, Orme-Johnson WH (1987) Biochemistry 26:4901
4. Hausinger RP (1993) Biochemistry of nickel, Plenum, New York
5. Adams MWW (1990) Biochim Biophys Acta 1020:115
6. Thauer RK, Bonacker, LG (1994) In: Chadwick D, Ackrill K (eds) The biosynthesis of the tetrapyrrole pigments. John Wiley, Chichester, UK, p 210
7. Jaun B (1994) Chimia 48:50
8. Won H, Olson KD, Summers MF, Wolfe RS (1993) Comments Inorg Chem 15:1
9. Jaun B (1993) Met Ions Biol Syst 29:287
10. Friedmann HC, Klein A, Thauer RK (1991) Biosynthesis of tetrapyrroles. In: Jordan PM (ed) New Compr Biochem 19, Elsevier, Amsterdam, NL, p 139
11. Friedmann HC, Klein A, Thauer RK (1990) FEMS Microbiol Rev 87:339
12. Wolfe RS (1985) Trends Biol Sci 396

13. Thauer RK (1985) Biol Chem Hoppe-Seyler 366:103
14. Whitman WB (1985) The Bacteria 8:2–720
15. DiMarco AA, Bobik TA, Wolfe RS (1990) Annu Rev Biochem 59:355
16. Daniels L, Sparling R, Sprott GD (1984) Biochim Biophys Acta 113
17. Jones WJ, Nagle DP Jr, Whitman WB (1987) Microbiol Rev 51:135
18. Schönheit P, Moll J, Thauer RK (1980) Arch Microbiol 127:59
19. Hartzell PL, Wolfe RS (1986) Syst Appl Microbiol 7:376
20. Wolfe RS (1991) Ann Rev Microbiol 45:1
21. Ankel-Fuchs D, Hüster R, Mörschel E, Albracht SPJ, Thauer RK (1986) Syst Appl Microbiol 7:383
22. Rouviere PE, Wolfe RS (1988) J Biol Chem 263:7913
23. Wackett LP, Honek JF, Begley TP, Shames SL, Niederhoffer EC, Hausinger RP, Orme-Johnson WH, Walsh CT (1988) In: Lancaster JR Jr (ed) The bioinorganic chemistry of nickel. VCH Publishers, New York
24. Hartzell PL, Wolfe RS (1986) Proc Natl Acad Sci USA 83:6726
25. Bobik TA, Wolfe RS (1988) Proc Natl Acad Sci USA 85:60
26. Hedderich R, Thauer RK (1988) FEBS Lett 298:65
27. Rospert S, Linder D, Ellermann J, Thauer RK (1990) Eur J Biochem 194:871
28. Brenner MC, Ma L, Johnson MK, Scott RA (1992) Biochim Biophys Acta 1120:160
29. Jablonski PE, Ferry JG (1991) J Bacteriol 173:2481
30. Rospert S, Breitung J, Ma K, Schwörer B, Zirngibl C, Thauer RK, Linder D, Huber R, Stetter KO (1991) Arch Microbiol 156:49
31. Bult CJ, White O, Olsen GJ, Zhou L, Fleischmann RD, Sutton GG, Blake JA, FitzGerald LM, Clayton RA, Gocayne JD, Kerlavage AR, Dougherty BA, Tomb J-F, Adams MD, Reich CI, Overbeek R, Kirkness EF, Weinstock KG, Merrick JM, Glodek A, Scott JL, Geohagen NSM, Weidman JF, Fuhrmann JL, Nguyen D, Utterback TR, Kelley JM, Peterson JD, Sadow PW, Hanna MC, Cotton MD, Roberts KM, Hurst MA, Kaine BP, Borodovsky M, Klenk H-P, Fraser CM, Smith HO, Woese CR, Venter JC (1996) Science (Washington, DC) 273:1058
32. Rouvière PE, Wolfe RS (1989) J Bacteriol 171:4556
33. Olson KD, McMahon CW, Wolfe RS (1991) Proc Natl Acad Sci USA 88:4099
34. Rospert SR, Böcher R, Albracht SPJ, Thauer RK (1991) FEBS Lett 291:371
35. Ellermann J, Hedderich R, Böcher R, Thauer RK (1988) Eur J Biochem 172:669
36. Mayer F, Rohde M, Salzmann M, Jussofie A, Gottschalk G (1988) J Bacteriol 170:1438
37. Klein A, Allmansberger R, Bokranz M, Knaub S, Müller B, Muth E (1988) Mol Gen Genet 213:409
38. Bonacker LG, Baudner S, Mörschel E, Böcher R, Thauer RK (1993) Eur J Biochem 217: 587
39. Färber G, Keller W, Kratky C, Jaun B, Pfalz A, Spinner C, Kobelt A, Eschenmoser A (1991) Helv Chim Acta 74:697
40. Won H, Olson KD, Hare DR, Wolfe RS, Kratky C, Summers MF (1992) J Am Chem Soc 114:6880
41. Gunsalus RP, Wolfe RS (1978) FEMS Microbiol Lett 3:191
42. Diekert G, Gilles H-H, Jaenchen R, Thauer RK (1980) FEBS Lett 119:118
43. Pfaltz A, Kobelt A, Hüster R, Thauer RK (1987) Eur J Biochem 170:459
44. Warren MJ, Scott AI (1990) Trends Biochem Sci 15:486
45. In addition to these relatively well-known tetrapyrroles, there is a copper-containing tetrapyrrole, turacin (Cu-uroprophyrinogen III), the feather pigment of the turaco bird [46]. A second nickel-containing tetrapyrrole, of unknown function, has also been discovered in very low concentration in the tunicate, Tridemnum solidum, and has thus been called tunichlorin [47]. The degree of unsaturation and type of sidechains in tunichlorin relate it to chlorophyll, rather than to $F_{430}$
46. Blumberg WE, Peisach J (1965) J Biol Chem 240:870
47. Bible KC, Buytendorp M, Zierath PD, Rinehart KL (1988) Proc Natl Acad Sci USA 85: 4582
48. Hausinger RP, Orme-Johnson WH, Walsh C (1984) Biochemistry 23:801

49. Diekert G, Konheiser U, Piechulla K, Thauer RK (1981) J Bacteriol 148:459
50. Keltjens JT, Hermans JMH, Rijsdijk GJFA, Van der Drift C, Vogels GD (1988) Antonie van Leeuwenhoek 54:207
51. Gorris LGM, Van der Drift C, Vogels GD (1988) J Microbiol Methods 8:175
52. Shiemke AK, Hamilton CL, Scott RA (1988) J Biol Chem 263:5611
53. Won H, Summers MF, Olson KD, Wolfe RS (1990) J Am Chem Soc 112:2178
54. Shiemke AK, Shelnutt JA, Scott RA (1989) J Biol Chem 264:11236
55. Pfaltz A, Livinston DA, Jaun B, Diekert G, Thauer RK, Eschenmoser A (1985) Helv Chim Acta 68:1338
56. Pfaltz A, Jaun B, Fässler A, Eschenmoser A, Jaenchen R, Gilles H-H, Diekert G, Thauer RK (1982) Helv Chim Acta 65:828
57. Livingston DA, Pfaltz A, Schreiber J, Eschenmoser A, Ankel-Fuchs D, Moll J, Jaenchen R, Thauer RK (1984) Helv Chim Acta 67:334
58. Olson KD, Won H, Wolfe RS, Hare DR, Summers MF (1990) J Am Chem Soc 112:5884
59. Kratky C, Angst C, Johansen JE (1981) Angew Chem, Intl Ed Engl 20:211
60. Stolzenberg AM, Stershic MT (1987) Inorg Chem 26:3082
61. Stolzenberg AM, Stershic MT (1988) J Am Chem Soc 110:5397
62. Stolzenberg AM, Stershic MT (1988) J Am Chem Soc 110:6391
63. Renner MW, Forman A, Wu W, Chang CK, Fajer J (1989) J Am Chem Soc 111:8618
64. Renner MW, Furenlid LR, Barkigia KM, Forman A, Shim HK, Simpson DJ, Smith KM, Fajer J (1991) J Am Chem Soc 113:6891
65. Renner MW, Furenlid LR, Stolzenberg AM (1995) J Am Chem Soc 117:293
66. Suh MP, Kim HK, Kim MJ, Oh KY (1992) Inorg Chem 31:3620
67. Suh MP, Lee YJ, Jeong JW (1995) J Chem Soc, Dalton Trans 1577
68. Furenlid LR, Renner MW, Szalda DJ, Fujita E (1991) J Am Chem Soc 113:883
69. Szalda DJ, Fujita E, Sanzenbacher R, Paulus H, Elias H (1994) Inorg Chem 33:5855
70. Ram MS, Riordan CG, Ostrander R, Rheingold AL (1995) Inorg Chem 34:5884
71. Shiemke AK, Kaplan WA, Hamilton CL, Shelnutt JA, Scott RA (1989) J Biol Chem 264: 7276
72. Furenlid LR, Renner MW, Fajer J (1990) J Am Chem Soc 112:8987
73. Furenlid LR, Renner MW, Smith KM, Fajer J (1990) J Am Chem Soc 112:1634
74. Wang S, Scott RA. Unpublished observations
75. The strain-free Ni(II)-N distances calculated by molecular mechanics for octahedral S=1 and square-planar S=0 Ni(II) are 210 and 191 Å, respectively [76]
76. Hancock RD, Dobson SM, Evers A, Wade PW, Ngwenya MP, Boeyens JCA, Wainwright KP (1988) J Am Chem Soc 110:2788
77. Rospert S, Voges M, Berkessel A, Albracht SPJ, Thauer RK (1992) Eur J Biochem 210:101
78. Albracht SPJ, Ankel-Fuchs D, van der Zwaan JW, Fontijn RD, Thauer RK (1986) Biochim Biophys Acta 955:50
79. Albracht SPJ, Ankel-Fuchs D, Böcher R, Ellermann J, Moll J, van der Zwaan JW, Thauer RK (1986) Biochim Biophys Acta 955:86
80. Krzycki JA, Prince RC (1990) Biochim Biophys Acta 1015:53
81. Jaun B, Pfaltz A (1986) J Chem Soc, Chem Commun 1327
82. Hamilton CL, Ma L, Renner MW, Scott RA (1991) Biochim Biophys Acta 1074:312
83. Jaun B (1990) Helv Chim Acta 73:2209
84. Lovecchio FV, Gore ES, Busch DH (1974) J Am Chem Soc 96:3109
85. Lexa D, Momenteau M, Mispelter J, Savéant JM (1989) Inorg Chem 28:30
86. Kadish KM, Franzen MM, Han BC, Araullo-McAdams C, Sazou D (1991) J Am Chem Soc 113:512
87. Holliger C, Pierik AJ, Reijerse EJ, Hagen WR (1993) J Am Chem Soc 115:5651
88. Telser J, Fann Y-C, Renner MW, Fajer J, Wang S, Zhang H, Scott RA, Hoffman BM (1997) J Am Chem Soc 119:733
89. Crumbliss AL, McLachlan KL, Siedow JN, Walton SP (1990) Inorg Chim Acta 170:161
90. Eschenmoser A (1986) Ann NY Acad Sci 471:108
91. Hamilton CL, Scott RA, Johnson MK (1989) J Biol Chem 264:11605

92. Cheesman MR, Ankel-Fuchs D, Thauer RK, Thomson AJ (1989) Biochem J 260:613
93. Shiemke AK, Scott RA, Shelnutt JA (1988) J Am Chem Soc 110:1645
94. Shelnutt JA (1989) J Phys Chem 93:6283
95. Crawford BA, Findsen EW, Ondrias MR, Shelnutt JA (1988) Inorg Chem 27:1842
96. Shelnutt JA (1987) J Am Chem Soc 109:4169
97. Procyk AD, Stolzenberg AM, Bocian DF (1993) Inorg Chem 32:627
98. Kratky C, Waditschatka R, Angst C, Johansen JE, Plaquevent JC, Schreiber J, Eschenmoser A (1985) Helv Chim Acta 68:1312
99. Zimmer M (1993) J Biomol Struct Dyn 11:203
100. Zimmer M, Crabtree RH (1990) J Am Chem Soc 112:1062
101. Berkessel A, Bolte M, Griesinger C, Huttner G, Neumann T, Schiemenz B, Schwalbe H, Schwenkreis T (1993) Angew Chem, Int Ed Engl 32:1777
102. Kaplan WA, Suslick KS, Scott RA (1991) J Am Chem Soc 113:9824
103. Wackett LP, Honek JF, Begley TP, Wallace V, Orme-Johnson WH, Walsh CT (1987) Biochemistry 26:6012
104. Ahn Y, Krzycki JA, Floss HG (1991) J Am Chem Soc 113:4700
105. Lin SK, Jaun B (1992) Helv Chim Acta 75:1478
106. Lin SK, Jaun B (1991) Helv Chim Acta 74:1725
107. Jaun B, Pfaltz A (1988) J Chem Soc, Chem Commun 293
108. Berkessel A (1991) Bioorg Chem 19:101
109. Drain CM, Sable DB, Corden BB (1990) Inorg Chem 29:1428
110. Drain CM, Sable DB, Corden BB (1988) Inorg Chem 27:2396
111. Zilbermann I, Golub G, Cohen H, Meyerstein D (1994) Inorg Chim Acta 227:1
112. Arai T, Kashitani K, Kondo H, Sakaki S (1994) Bull Chem Soc Jpn 67:705
113. Arai T, Kondo H, Sakaki S (1992) J Chem Soc, Dalton Trans 2753
114. Lahiri GK, Stolzenberg AM (1993) Inorg Chem 32:4409
115. Lahiri GK, Schussel LJ, Stolzenberg AM (1992) Inorg Chem 31:4991
116. Helvenston MC, Castro CE (1992) J Am Chem Soc 114:8490
117. Zhang Z, Petersen JL, Stolzenberg AM (1996) Inorg Chem 35:4649
118. Gantzer CJ, Wackett LP (1991) Environ Sci Technol 25:715
119. Krone UE, Laufer K, Thauer RK, Hogenkamp HPC (1989) Biochemistry 28:10061
120. Holliger C, Schraa G, Stupperich E, Stams AJM, Zehnder AJB (1992) J Bacteriol 174:4427
121. Holliger C, Kengen SWM, Schraa G, Stams AJM, Zehnder AJB (1992) J Bacteriol 174:4435
122. Castro CE, Helvenston MC, Belser NO (1994) Environ Toxicol Chem 13:429
123. The x-ray crystal structure of MCR has just been determined at 1.45 Å resolution by RK Thauer and co-workers (Ermler U, Grabarse W, Shima S, Goubeaud M, Thauer RK Science, submitted for publication). Among its many important results, this study shows that the Ni(II) ion of $F_{430}$ is axially coordinated by the thiol group of CoM and by the side chain amide oxygen of $Gln^{\alpha 147}$. The structural information also allowed proposals on MCR mechanism.
124. Bard AJ, Faulkner LR (1980) Electrochemical methods: fundamentals and applications. Wiley, New York

# Hemeproteins in Anaerobes

Inês A. C. Pereira · Miguel Teixeira · António V. Xavier

Instituto de Tecnologia Química e Biológica, Universidade Nova de Lisboa, Rua da Quinta Grande, 6 – Apartado 127, 2780 Oeiras, Portugal.
*E-mail: Ipereira@ITQB.UNL.PT*

Hemeproteins are widespread in all groups of living organisms, both as components of key biological processes as well as in very specific metabolic pathways. By variation of either the heme porphyrin structure or the heme protein environment, the function and behavior of the hemeproteins may vary drastically, allowing its role in the most diverse processes. In this short review, selected examples of hemeproteins from anaerobes will be presented, aiming to show the basic, common features of these family of proteins, as well as their diversity in terms of function and composition.

**Keyword:** Protein, enzymes, heme, anaerobes, cytochromes



Structure and Bonding, Vol. 91

## 1 Introduction

Hemeproteins are widespread in all groups of living organisms, from archaea to eukaryotes, and from aerobes to anaerobes. Whichever its origin, the actual role of the hemeproteins is always related to the basic properties of the metal center, fine tuned by the protein environment. These basic properties will be first analyzed, constituting a framework to discuss several key examples of hemeproteins in anaerobic microorganisms. We will not attempt to present a comprehensive survey of all types of known hemeproteins in anaerobes. Instead, some cases will be presented, mainly from *Desulfovibrio* species, as case studies which will reveal the principal features of hemeproteins in anaerobes. A particular emphasis will be given to novel examples. The microbial diversity is immense, having as an obvious consequence that as more and more unrelated organisms are found and studied in detail, more and more proteins and/or unexpected properties will be discovered.

A first and key question arises with the definition of a strict anaerobe. While many microorganisms have in the past been considered as such, meaning that they could not sustain even minor amounts of dioxygen, recent advances at both the microbiological and molecular biological levels have raised major doubts [1]. For example, as will be discussed in the next sections, sulfate-reducing bacteria were shown to sustain life under microaerophilic conditions; in fact, it was already known for a long time that some of these bacteria contained superoxide dismutase and catalase. Are these enzymes present just as detoxifying mechanisms? Methanogenic archaea are also considered as strict anaerobes; however, based on the complete genome sequencing of *Methanococcus jannaschii* [2], it appears that this archaeon may contain several redox proteins with fairly high (positive) reduction potentials, as deduced from the comparison of the predicted aminoacid sequence of several coding units. Proteins with high homologies to hemerythrin, a dioxygen-binding protein found in tunicates [3] may be expressed in this "strict anaerobe". A similar protein, rubrerythrin, which contains rubredoxin- and hemerythrin-like centers is also found in sulfate reducing bacteria [4]. These proteins have very high reduction potentials (up to +280 mV in *D. vulgaris* rubrerythrin [4]). Whether such proteins reflect unexpected metabolic diversities of these organisms, or constitute an armament of defences against dioxygen, which may, even if transiently, "invade" their normal living habitats, is an open question. Hence, at this stage, it is clear that even at the microbiological level the degree of deep knowledge on bacterial/archaeal physiology is still very incomplete.

With these constraints in mind, we will refer in this review to examples of hemeproteins in organisms that have been considered as strict anaerobes, meaning that their ability to *grow* under aerobic conditions has not been shown so far.

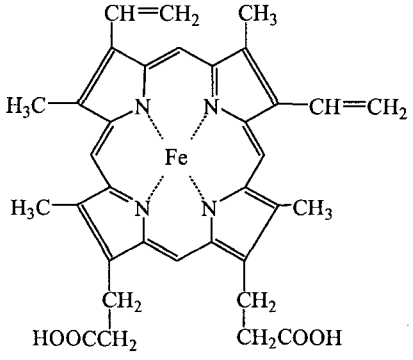


Heme *b*

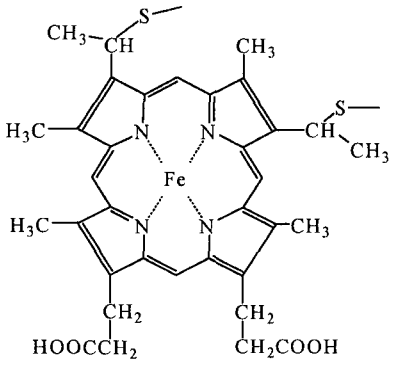


Heme *c*

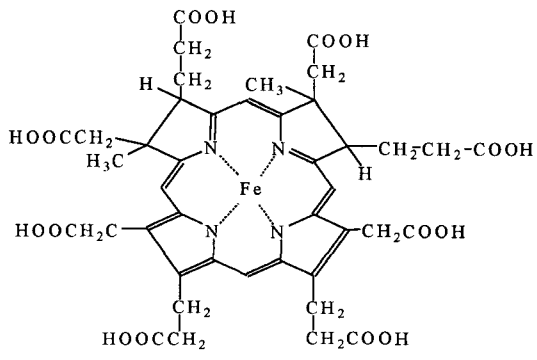


Siroheme

**Fig. 1.** Most common heme groups found in proteins from anaerobes

**Table 1.** Examples of hemeproteins from anaerobes, containing each type of porphyrin (*ET* = electron transfer; *EA* = enzymatic activity)

| Porphyrin | Heme type | Protein | Function |
|---|---|---|---|
| Protoporphyrin IX | *b* | Cytochrome *b* | ET |
| | *c* | Mono- and multiheme cytochromes | ET<br>EA |
| Siroporphyrin | Siroheme | sulfite reductase | EA |
| Uroporphyrin I | | Rubredoxin:oxygen oxidoreductase | $O_2$ reductase |

## 1.1 Porphyrin Types and Axial Ligands

The heme moiety is a porphyrin, which, through its four pyrrol nitrogens binds, in an almost square planar geometry, to one iron. The most common, naturally occurring porphyrins in anaerobes are depicted in Fig. 1. Only the *c*-type hemes are covalently bound to the polypeptide chain, through tioether linkages between the porphyrin vynil sidechains and cysteinyl residues, usually forming a common aminoacid sequence motif -Cys-X-Y-Cys-His- [5]. Hemes of the *a*- and *d*-types have not been found in anaerobes (Table 1). However, the presence of an open reading frame coding for an analogue of subunit I of mitochondrial cytochrome *c* oxidase in *Desulfovibrio vulgaris* has recently been reported [6], although it remains to be shown whether such a protein is indeed expressed and if it contains *a*-type hemes. A new and unexpected type of porphyrin (uroporphyrin I) was recently found in a novel protein from the sulfate reducer *Desulfovibrio gigas* (see Sect. 5.4).

In all hemeproteins, the iron is five- or six-coordinated, and the axial ligands are provided by aminoacid residues of the protein backbone. Although a large number of aminoacid sidechains could serve as ligands to the iron, only a very limited type of residues have so far been identified for this role in naturally occurring proteins. The fifth ligand is, in most cases, a histidine, bound through the nitrogen N3 of the imidazole ring; in cytochromes of the *c*-type the fifth ligand is a histidine residue immediately following the two cysteines in the above mentioned sequence motif. Five-coordinated hemes are high-spin in both oxidation states. In six-coordinated hemes, the other ligand is generally either a methionine or a histidine. Thiolates and phenolates or bis-methionine ligation [7] have also been found, but not in anaerobes. A possible exception is rubredoxin-oxygen oxido-reductase from *D. gigas*, whose heme irons may be bound to cysteines (see Sect. 5.4). Primary amines, probably due to their high pKa, have not been found as ligands under physiological pH conditions, with one known exception: in cytochrome *f* from turnip, the sixth ligand is the $\alpha$ amino-group of the tyrosil N-terminal residue [8] (Table 2). Six coordinated hemes are generally low-spin in both oxidation states. The ligand field at the heme iron is very close to the crossover point for the high- and low-spin states; subtle variations of the strength of one of the axial ligands may change the spin state.

**Table 2.** Axial ligands in cytochromes from anaerobes

| Fifth ligand | Sixth ligand | Found in anaerobes | Protein |
|---|---|---|---|
| Histidine | Histidine | + | Multiheme cytochromes |
| Histidine | Methionine | + | Monoheme cytochrome *c* |
| Histidine | - | + | Multiheme cytochromes |
| Histidine | Amine | - | cytochrome *f* |
| Methionine | Methionine | - | Bacterioferritin |

## 1.2 Redox Properties

The heme-iron is limited to two stable redox states: the ferric, Fe(III), and the ferrous, Fe(II), states. Higher formal oxidation states, as Fe(IV), have been shown to occur in catalytic intermediates of reactions involving dioxygen. In spite of this apparent limitation, the hemeproteins cover an extremely wide range of reduction potentials, with a parallel only in the iron-sulfur proteins, from ~ +400 mV to ~ -500 mV. This fact leads to the finding of hemeproteins in most electron transfer chains, from anaerobic to aerobic systems. The actual reduction potential of a heme group is a function of multiple, interplaying factors, which can be roughly divided into three major groups: i) the axial ligands, ii) the heme environment and iii) redox-linked chemical equilibria [5].

Roughly, the reduction potential decreases with increasing $\sigma$ donor capability of the axial ligand: methionine bound hemes have, in general, higher reduction potentials, while histidine-bound ones have the lowest. The most unambiguous evidence comes from site-directed mutagenesis experiments, in which one of the axial ligands is substituted, maintaining the overall heme environment. For example, substitution of a methionine by a lysine or a histidine leads to a decrease of ~ -200 mV of the reduction potential [9]. But, if naturally occurring cytochromes with any type of axial ligands are compared, it is immediately clear that the axial ligands are but one of the factors controling their reduction potentials (Fig. 2).

As would be expected from the reduction potential of the environment where anaerobes live, most cytochromes found in these organisms have low-reduction potentials, associated with a bis-histidinyl coordination. However, even with this type of heme ligation, cytochromes with fairly high reduction potentials have been found in anaerobes, as will be discussed below. Only a few His-Met cytochromes have so far been identified in anaerobes, which have a reduction potential of ~ 0 mV, lower than that of analogous cytochromes from aerobes.

The wide spread of reduction potentials, for hemes with the same type of axial ligation, is due to the second group of factors referred above and generally ascribed as the heme environment. As recently discussed in detail [10-13], the actual reduction potential of a heme is a result of several interplaying electrostatic factors, such as electric charges on neighbor or even distant residues, dipolar and hydrogen-bonding interactions, solvent exposure, and

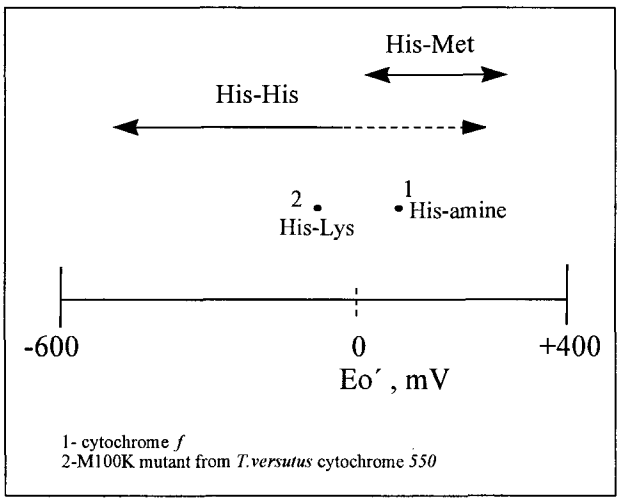


**Fig. 2.** Reduction potential range covered by heme proteins

heme-heme (homotropic) interactions. Redox-linked equilibria may also contribute to the fine control of the reduction potential. In small hemeproteins, for which high resolution three dimensional structures are available, conformational changes associated with redox equilibria are minor. In contrast, ligand-binding may cause drastic changes in the redox behavior. A particular case of heterotropic interactions will be analyzed in the next section.

### 1.3
### pH Equilibria

The most important and universal type of chemical equilibria to which a heme protein is subjected in natural environments is pH equilibria, involving the protein aminoacid residues and the ionizable groups of the porphyrin, the propionate side chains. Beside the effects on the overall protein structure, which are outside the scope of this review, the major consequences of proton equilibria may be the changes of the heme reduction potential (electron affinity), called the redox-Bohr effect (see Sect. 3.2), by analogy to the pH effect on the oxygen affinity of hemoglobin (Bohr effect).

### 1.4
### Function

The function of the heme proteins may be divided into the following groups: electron transfer, chemical catalysis, storage, and transport. A basic structural feature of the heme moiety distinguishes the first group. In order to be able to bind a molecule, either for transport purposes or for initiating a chemical

reaction, the heme group needs to have a vacant coordination position, and hence, either in its "native" or "resting" state or in a catalytic intermediate state, it is five coordinated, high-spin. On the contrary, the transfer of electrons does not imply the making or breaking of bonds at the heme iron. In fact, the electron transfer process is much more efficient if the heme retains its coordination sphere throughout the process since this leads to a minimal reorganization energy. As a consequence, for the hemes in proteins which function just in electron transfer, it has been clearly demonstrated that they are six-coordinated, low-spin in both oxidation states. However, even this electron transfer role may be coupled to other functions such as energy transduction (see Sect. 3.2).

Due to its redox properties, most hemes function as electron transfer components, transferring electrons either between other proteins in redox chains, or inside a multiredox center protein or enzyme. The wide range of reduction potentials available for a heme facilitates its function in most redox chains, from anaerobic respiratory chains to oxygen respiration.

Besides the strict electron transfer function, hemeproteins may display intrinsic catalytic activities, generally in redox reactions. The simplest reactions, which are those usually found in anaerobes, involve the reduction or oxidation of small molecules, such as nitrogen oxides (NO and $NO_2$ [14]), sulfur oxides ($SO_3^{2-}$), elemental sulfur and sulfide, dioxygen and hydrogen peroxide. More complex reactions may also be performed by heme proteins, namely those involving the oxidation of organic molecules, although this type of reaction has not yet been found in anaerobes.

## 2 Monoheme Cytochromes

Very few monoheme proteins have been detected in anaerobes. A monoheme cytochrome, known as cytochrome $c_{553}$, is present in some strains of sulfate-reducing bacteria. It has only been isolated from *Desulfovibrio vulgaris* Hildenborough [14] and Miyazaki [15], *Desulfomicrobium baculatum* [16, 17] and *Desulfovibrio desulfuricans* [17, 18], although it is present in other *Desulfovibrio* strains [19]. This small protein (9 kDa) contains a single heme coordinated by a histidine and a methionine, and has a reduction potential in the range of 0 to 50 mV [16–20].

Structural studies by 1D-NMR on cytochrome $c_{553}$ have suggested that there is a change in conformation between the two oxidation states [22], involving an inversion of the chirality of the methionine ligand [21]. However, in more recent studies by 2D-NMR only small structure variations were observed between the two oxidation states [22], as commonly found in monoheme *c*-type cytochromes.

The tertiary structure of ferrocytochrome $c_{553}$ from *D. vulgaris* Hildenborough has recently been obtained by NMR [23, 24]. Despite the low sequence homology, striking structural similarities between this protein and representatives of both eukaryotic (cytochrome *c* from tuna) and prokaryotic (*Pseudomonas aeruginosa* $c_{551}$) cytochromes *c* have been recognised [25].

Preliminary crystallographic results have also been reported for ferricytochrome $c_{553}$ from *D. vulgaris* Miyazaki [26]. The amino acid sequences of cytochrome $c_{553}$ from the two strains of *D.vulgaris* present strong homology to each other and to cytochrome $c_{551}$ from *Pseudomonas* [27–29], a cytochrome with a much higher reduction potential.

The finding of a signal peptide in cytochrome $c_{553}$ shows that the protein is located in the periplasm [27]. Cytochrome $c_{553}$ from *D. vulgaris* Miyazaki is reduced by the periplasmic hydrogenase only at a slow rate [30], whereas, in *D.vulgaris* Hildenborough, it is efficiently reduced [31]. Its physiological function is still uncertain. It has been reported to act as an electron acceptor for formate and lactate dehydrogenases [15, 32, 33]. Cloning of the cytochrome $c_{553}$ gene in *D. vulgaris* Miyazaki showed that it is part of an operon which encodes another protein with strong similarities with the cytochrome *c* oxidase subunit I from various organisms [6]. This finding raises major questions regarding the function of cytochrome $c_{553}$. Several *Desulfovibrio* species have been found to sustain microaerophilic conditions. Although generally considered as *strict anaerobes*, when exposed to oxygen, sulfate-reducing bacteria are capable of surviving as well as of taking advantage of its presence in terms of energy conservation [1, 34, 35]. In the presence of oxygen, *Desulfovibrio gigas* uses internal reserves of polyglucose, which are metabolized by the Embden-Meyerhof-Parnas pathway thus generating NADH and ATP [36, 37]. In this particular bacterium the reduction of oxygen occurs through a soluble redox chain (see Sect. 5.4). Although no cytochrome *c* oxidase activity has yet been found in *Desulfovibrio*, cytochrome $c_{553}$ could be the electron donor to this terminal oxidase in the presence of oxygen.

A monoheme protein has also been isolated from the denitrifier *Wolinella succinogenes* [38]. This soluble *c*-type cytochrome of 8.2 kDa has a reduction potential of 105 mV at pH 7.6, and displays a spin equilibrium in the ferric form between a five-coordinate high-spin form and a low-spin one, where methionine occupies the sixth coordination position.

## 3 Multiheme *c*-Type Cytochromes

Several anaerobes, mainly sulfate-reducing bacteria, contain a range of multiheme *c*-type cytochromes, ranging from two to sixteen hemes in a single polypeptide chain or monomer (Table 3). The actual function, as well as the evolutionary pressure for the development of such unique proteins is, in most cases, unknown. Most of these proteins are called cytochromes $c_3$, which are characterized by having *c*-type hemes with two histidinyl residues as axial ligands, and approximately 25 aminoacid residues per heme. As early as 1974, the most well studied cytochrome $c_3$, the tetraheme cytochrome $c_3$, was described as a biological capacitor [39]. The redox behavior of these proteins is extremely complex, due to multiple homotropic (heme-heme redox potential interactions) and heterotropic (heme redox potential to $pK_a$ of ionizable groups interactions) cooperativities. Most surprisingly, and in contrast to what might have been expected on the basis of simple electrostatic interactions, significant

**Table 3.** Multiheme cytochromes *c* in proteins from anaerobes

| N° hemes | Protein | Organism |
|---|---|---|
| 2 | Split Soret<br>Diheme cyt. | *D. desulfuricans*<br>*Wollinella* |
| 3 | Cyt. $c_{551.5}$ | *D. acetoxidans* |
| 4 | Tetraheme cyt. $c_3$<br>monomers and dimers | *Desulfovibrio* |
| 6 | Nitrite reductase (?)<br>Hexaheme cyt. | *Desulfovibrio*<br>*D. acetoxidans* |
| 8 | Octaheme cyt. | *D. acetoxidans* |
| 12 | Dodecaheme cyt. | *D. desulfuricans* |
| 16 | Hexadecaheme cyt. | *Desulfovibrio* |

positive cooperativities are found in these proteins, as will be described in detail in Sect. 3.2. Although a detailed study has so far been performed only for the tetraheme cytochromes, similar behaviors may be anticipated for the cytochromes containing a larger number of hemes. Moreover, as the number of hemes in a single protein increases, it appears that the range of reduction potentials covered by these proteins increases: in some newly studied proteins, a span as large as ~ 500 mV was found (see Sect. 4). Do these proteins have an as yet unknown catalytic function? Or, as will be discussed for the tetraheme cytochromes, do they act as molecular transducers or capacitors, being capable of transferring a certain number of electrons very efficiently through a built-in electron transfer pathway, due to significant overlap of the wavefunctions of each heme redox center, from specific electron donors to specific acceptors? This could be a way of avoiding the release of toxic catalytic intermediates to the cell.

### 3.1
### Cytochrome $c_{551.5}$

So far only a triheme cytochrome $c_3$ has been found: the cytochrome $c_{551.5}$ from the sulfur-reducer *Desulfuromonas acetoxidans*, formerly known as cytochrome $c_7$ [40]. It is a 9 kDa cytochrome with several analogies to the tetraheme cytochromes $c_3$ from *Desulfovibrio* [41], including the low reduction potentials ($E_1^0 = -140$ mV, $E_2^0 = -210$ mV and $E_3^0 = -240$ mV at pH 7.6) [42]. Its solution structure was recently determined by NMR [41, 43, 44], showing that the relative orientation of the three hemes is similar to three of the four hemes in cytochromes $c_3$. Despite the fact that *D. acetoxidans* possesses no hydrogenase [45], cytochrome $c_{551.5}$ is readily reduced by hydrogenases from *Desulfovibrio*, which probably reflects its similarity to cytochrome $c_3$ [41]. Recently, it has been found that cytochrome $c_{551.5}$ has a high activity as polysulfide reductase, which indicates that it may be the terminal reductase in *D. acetoxidans* [46].

## 3.2 Tetraheme Cytochromes $c_3$

The tetraheme cytochromes $c_3$ ($M_r$ ~ 15,000) are the most widely characterized of the cytochrome $c_3$ family. Since a review article has recently been published on these cytochromes [47], we will concentrate on the analysis of the most recent literature, and in particular of the cytochrome $c_3$ from *Desulfovibrio vulgaris* Hildenborough on which more detailed studies have been carried out.

After they were first isolated from *D. vulgaris* in 1952 [48], tetraheme cytochromes $c_3$ have been detected in large quantities in the periplasm of the *Desulfovibrionacea* family as well as in other sulfate reducers, where they can function as a coupling protein to hydrogenase [49]. These small, very soluble and stable proteins, which are low-spin in both oxidation states, are specially well suited for physico-chemical and structural studies, being the best characterized multiheme cytochromes.

The primary [47] and tertiary structures of several tetraheme cytochromes $c_3$ are known [50–53]. Although having a small homology in terms of their amino acid sequences, the architecture of the four heme core is strictly conserved, as is the general folding of their polypeptide main chain. In fact, besides the heme attachment sites consisting of four residues per heme, ...H...C-X-X-(X)-(X)-C-H..., which are strictly conserved, only up to six other residues, depending on the sequence alignment chosen, are conserved. Thus, not surprisingly, the thermodynamic properties of the several tetraheme cytochromes $c_3$ are quite different. In particular, the comparatively low reduction potential of the individual hemes, typically between 0 and – 400 mV, as well as their relative value is widely variable. Also, their pIs range between 5 and 10.

As depicted in Table 4, for all those tetraheme cytochromes $c_3$ where the heme reduction potentials are unequivocally assigned to their position in the structure, the order of heme oxidation is different [54–57]. However, they have in common the fact that two of the hemes have identical, pH dependent reduction potentials.

The X-ray crystal structure of *D. vulgaris* (Hildenborough) ferricytochrome $c_3$ is known [51] and a preliminary solution structure for the ferrocytochrome has been obtained by NMR [58]. Also, the reduction potentials for each of its four hemes, as well as the specific assignment to their position in the structure

**Table 4.** Order of reduction of the four hemes in cytochrome $c_3$ from several organisms. The numbering of the hemes is done according to their position in the primary structure. Hemes I and II of *D. desulfuricans* (27774) have very similar reduction potentials, and the same is observed for hemes I and IV of *Dsm. baculatum*

| Order of Reduction | 1st | 2nd | 3rd | 4th |
|---|---|---|---|---|
| *D. vulgaris* | IV | I | II | III |
| *D. gigas* | IV | III | II | I |
| *D. desulfuricans* (27774) | III | IV | I | II |
| *Dsm. baculatum* | III | I | IV | II |

**Table 5.** Thermodynamic parameters for *D. vulgaris* cytochrome $c_3$. The diagonal (*bold face*) numbers represent the microscopic reduction potentials (mV) and the energy for deprotonating the ionizable redox-Bohr center [meV, ($pK_a$2.3RT)/F)] of the fully reduced molecule. The off-diagonal values give the redox interaction due to individual heme oxidation and protonation of the redox-Bohr center [54]

| Heme | I | II | III | IV | Ionizable group |
|---|---|---|---|---|---|
| I | **- 245** | - 43 | 20 | - 4 | - 70 |
| II | | **- 267** | - 8 | 8 | - 30 |
| III | | | **- 334** | 32 | - 18 |
| IV | | | | **- 284** | - 6 |
| Ionizable group | | | | | **439** |

was determined [59]. Their heme to heme redox interactions (redox cooperativities), as well as the pH dependence of their reduction potentials (redox-Bohr cooperativities), have been determined by NMR coupled to visible spectroscopy redox titrations [54] (Table 5).

The number of protons involved in the redox-Bohr cooperativity was titrated, showing that this effect involves two protons [60]. Furthermore, kinetic NMR studies have shown that the intramolecular electron exchange (heme to heme) is extremely fast [61], that these two redox-Bohr protons have diffusion controlled exchange rates and that they titrate with the same pKa [54].

Taking into consideration the above mentioned properties, the complex network of thermodynamic parameters presented in Table 5 can be rationalized as follows:

(i) Since the intramolecular electron exchange is fast, the system is thermodynamically controlled and the overall four one-electron reduction processes are governed by the following stepwise macroscopic reduction potentials: - 250, - 306, - 303, and - 345 mV, at pH 6.8.

(ii) Since the redox-Bohr effect cooperativities are all positive, as expected for an electrostatic based interaction, the macroscopic $pK_a$'s of the redox-Bohr protons increase along the reduction process (5.3, 5.6, 6.4, 7.1, and 7.4).

(iii) Since there is a strong positive redox cooperativity (- 43 mV) between the second and the third heme to be reduced (Hemes II and I) a two-electron step is achieved. In fact, the macroscopic reduction potential of the third step is similar to that of the second [cf. (i)].

(iv) Since the largest positive redox-Bohr cooperativities (see Table 5) are observed for Hemes I (second Heme to be reduced) and Heme II (third heme to be reduced), at physiological pHs [cf. (i)] the double protonation (reduction) step assists the double reduction (protonation). Thus, the relative architecture of these two hemes and the protonation center constitutes the necessary structural motif for a coupled $2e^-/2H^+$ step.

This coupling between the reduction and protonation sites is the thermodynamic basis for the transduction of electronic to protonic energy (Fig. 3). Again, at physiological pH, the deprotonated one-electron reduced cytochrome

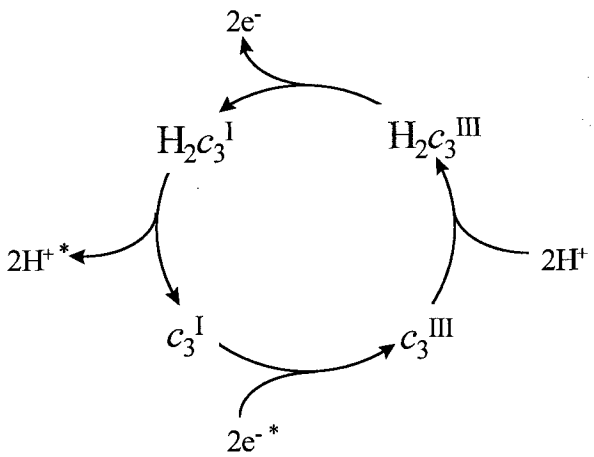


**Fig. 3.** Redox/protonation cycle of tetraheme cytochrome $c_3$. Two high energy electrons ($2e^{-*}$) plus two low energy protons ($2H^+$) convert the deprotonated one electron species ($c_3^I$) into the protonated three-electron species ($H_2c_3^{III}$). The cycle is completed by donating two low energy electrons ($2e^-$) and two high energy protons ($2H^{+*}$). The decrease in electronic energy is coupled to the increase in acidity of the ionisable redox-Bohr groups

($c_3^I$, pKa = 5.6) receiving two electrons with very negative redox potential (−315 and −324 mV) becomes protonated ($H_2c_3^{III}$, pKa = 7.1), and the redox centers loose redox energy. When this protonated species donates two electrons, with less negative reduction potential (−284 and −266 mV) the resulting species is acidified (energized).

This energy transduction is crucial for the bioenergetic metabolism of sulfate reducers. In fact, it has been proposed that ATP synthesis is driven by $H_2$ oxidation in the periplasm [62]: hydrogen formed in the cytoplasm, as a result of oxidation of metabolites coupled to the activity of a cytoplasmic hydrogenase, diffuses to the periplasm, where it is reoxidised. This "hydrogen cycle" [62] results in the activation of the ATP synthase. Furthermore, some sulfate reducing bacteria can generate ATP in the presence of $H_2$ as the sole energy source [63]. However, since the periplasmic hydrogenase (catalysing the reaction $H_2 \rightleftharpoons 2H^+ + 2e^-$) looses its efficiency as the pH lowers, the electronic to protonic energy step performed by cytochrome $c_3$ (the $2e^-$ to $2H^+$ energy transduction), becomes crucial so that the protons produced can be acidified at the expenses of electronic energy and subsequently used for ATP synthesis.

This energy transduction step [64], although functionally equivalent to those involving the redox-linked pumping of protons across the membrane [65], can be achieved in aqueous solution in the absence of a membrane confinement, and is in full agreement with the Williams localized theory for energy transduction [66].

Although the molecular basis for the $2e^-/2H^+$ concerted step performed by cytochrome $c_3$, as well as its implication in the energy generation mechanism, has not been unequivocally demonstrated, we can now propose a mechanism

for this functional activity, based on the information gathered so far. The center for the redox-Bohr effect, involving two protonation groups, must be close to Heme I, since it is this heme which has a stronger pH dependence of its reduction potential. Furthermore, pH NMR titrations show that propionate 6 in the oxidised state has a pKa identical to that of the redox-Bohr [54]. The X-ray structure shows that this propionate is H-bound to the peptide NH of residue C46 [53]. This residue is next to a Lys with a positive charge which stabilises the negative charge of the propionate 7 of the same heme. Thus, the protonation of propionate 6 destroying this H-bound, may result in a movement of the polypeptide chain, so that the positive charge of this Lys will no longer stabilise propionate 7. Thus, two protons would be coupled to the reduction of this heme. Furthermore, since C46 is one of the residues covalently bound to Heme II, a movement of the polypeptide chain and/or its rearrangement could be responsible for the positive cooperativity between Hemes I and II.

The extremely complex redox behavior of the tetraheme cytochrome $c_3$ is probably also operative in the other multiheme cytochromes. However, with an even higher number of hemes per subunit it becomes impossible to perform such detailed studies. Hence, the reduction potentials quoted for the cytochromes in the next sections must be considered as apparent macroscopic potentials which simply reproduce the overall redox profile.

### 3.3
### Tetraheme Cytochrome $c_3$ Dimers

A cytochrome containing eight hemes has been isolated from *D. gigas* [67], *Desulfomicrobium baculatum* Norway 4 [68] and *Desulfovibrio africanus* [69]. It has been named as the cytochrome $c_3$ ($M_r$ 26,000) because of its molecular mass of 26 kDa, but was previously known as cytochrome $cc_3$. It was shown to be composed of two identical 4-heme subunits of 13,500 Da, both in *Dsm. baculatum* Norway 4 [70], and in *D. gigas* [71]. In this last case the two subunits are linked by two disulfide bridges.

The reduction potentials of the *Dsm.baculatum* cytochrome $c_3$ ($M_r$ 26,000) hemes were determined by cyclic voltammetry, and found to be as low as those of cytochrome $c_3$ [72]. Based on the four values obtained (−210, −270, −325, −365 mV at pH 7.6) the authors proposed that the hemes are bis-histidinyl coordinated. The amino-acid sequence of the *Dsm.baculatum* cytochrome $c_3$ ($M_r$ 26,000) was compared to the sequences of several polyheme cytochromes, giving evidence that this cytochrome is distinct from cytochrome $c_3$ ($M_r$ 13,000) [73]. The sequence of the *D. gigas* cytochrome has also been determined [71]. The crystal structure of the *Dsm. baculatum* cytochrome $c_3$ ($M_r$ 26,000) was obtained at 2.16 Å resolution [74]. Preliminary X-ray studies have also been reported for the *D.gigas* cytochrome [75].

The physiological role of cytochrome $c_3$ ($M_r$ 26,000) has not been elucidated. It can be reduced by hydrogenase in a similar way to cytochrome $c_3$ (13,000) [49, 76]. *D. gigas* cytochrome $c_3$($M_r$ 26,000) was shown to stimulate the reduction of thiosulfate by a partially purified extract, using $H_2$/hydrogenase as electron donor [77], but this was not observed with purified thiosulfate reductase [78].

Also, in *D. gigas*, this cytochrome was shown to couple the electron transfer between aldehyde oxidoreductase and hydrogenase in the presence of flavodoxin [79]. It should be pointed out that it still remains to be proved that these cytochromes are not just degradation products of larger proteins.

### 3.4
### Hexadecaheme Cytochromes *c*

A high molecular mass cytochrome (Hmc) has been isolated from *D. vulgaris* strains Hildenborough [80, 81] and Miyazaki [82], and from *D. gigas* [83]. It is a monomer of 65 kDa containing 16 hemes. Cloning of the Hmc gene in *D. vulgaris* Hildenborough revealed that it is part of a large operon encoding what seems to be a transmembrane redox complex, which was proposed as constituting the missing link between periplasmic hydrogen oxidation and cytoplasmic sulfate reduction [84]. In agreement with this proposal, it has recently been reported that Hmc can be isolated in larger amounts from the membranes than from the soluble fraction [85]. The sequence of the Hmc gene shows that the protein is organized in three $c_3$-like domains, and an incomplete fourth one with only three hemes, with a remaining isolated heme outside these domains [84]. A Mössbauer study on *D. vulgaris* Hildenborough Hmc has showed that it contains two high-spin hemes and fourteen low-spin ones [85], and a similar situation seems to occur in the *D. gigas* Hmc [83]. The redox properties of Hmc have been studied in detail [82, 85, 86]. The heme reduction potentials cover a wide range of values, but seem to be roughly divided in three groups: 4 to 5 hemes have $E^0$s of – 30 mV to – 100 mV, 3 to 4 hemes have $E^0$s around –170 mV and 7 to 8 hemes have a lower $E^0$ of – 250 to – 280 mV [85]. These reduction potentials are pH dependent. The physiological function of Hmc has not yet been unequivocally elucidated. Although it may be involved in electron transport across the membrane, its redox partners are not known. Hmc can be reduced by hydrogenases, but only at a much slower rate than cytochrome $c_3$ [85]. As proposed by Rossi et al. [84], the multiple domains of Hmc may act as electron acceptor/donor sites for several, as yet unidentified, physiological partners. The presence of high-spin hemes in Hmc suggests that it may have an enzymatic function.

## 4
## Other Heme Proteins

Soluble proteins containing *b*-type hemes have not been detected in anaerobes, with the exception of catalase; all other examples of *b*-type cytochromes known so far are membrane-associated. A catalase was isolated from *D. vulgaris* [87], and its activity has also been detected in other strains of *Desulfovibrio* species. Superoxide dismutase activities have also been detected in these bacteria [87]. As mentioned in the introduction, the finding of catalase and superoxide dismutase in an anaerobe is puzzling. It is not known whether these enzymes are just used for detoxification or indicate the presence of adaptation capabilities to oxygenic environments.

A *b*-type cytochrome is present in the membranes of *D. gigas* [88] but has never been isolated. Cells grown in the presence of fumarate show increased amounts of this cytochrome, suggesting it is part of the fumarate reductase system. An open reading frame in the operon of the high molecular mass cytochrome from *D. vulgaris* Hildenborough also shows similarities to the cytochrome *b* subunit of the ubiquinol-cytochrome *c* reductase complex [84]. However, there is a similar degree of similarity between this open reading frame and some quinone-binding proteins and so it was proposed that it could code for a quinone-binding protein [85]. Another *b* cytochrome is found in the membranes of some methanogenic archaea [89–91]. In *Methanosarcina barkeri* this cytochrome was isolated as a complex with the heterodisulfide reductase, where it can act as the electron donor to this reductase [89].

A diheme cytochrome has been isolated from one species of sulfate-reducing bacteria, *Desulfovibrio desulfuricans* ATCC 27774 [92]. It has been named as the Split-Soret cytochrome as it displays a shoulder at 415 nm for the Soret band of the reduced form. It is a dimer of a 26 kDa subunit, each containing two hemes *c*. The function of this cytochrome has not been elucidated and it was observed that it is present in cells grown both on nitrate or sulfate. A diheme cytochrome of 11 kDa was isolated from *Wolinella succinogenes*, but the low yield of purified protein prevented detailed structural studies [38].

A new six heme-containing cytochrome was recently found in *Desulfuromonas acetoxidans* [46]. This cytochrome is isolated as a homopentamer of a 50 kDa subunit, with six hemes per subunit. The reduction potential of the hemes ranges from +100 to −375 mV, and one of the hemes displays unusual EPR characteristics. The function of this cytochrome was not yet elucidated. Another cytochrome containing eight hemes was also isolated from *Dsm. acetoxidans* [46]. This cytochrome has no similarities to cytochrome $c_3$ ($M_r$ 26,000). It is an oligomer of 170 kDa, with a single subunit of 65 kDa. It has both high and low-spin hemes, which are involved in strong magnetic interactions. The reduction potential of the hemes covers a very wide range from +180 to −250 mV at pH 7.6.

The purification of a 12-heme cytochrome from *Desulfovibrio desulfuricans* ATCC 27774, with a molecular mass of 41 kDa, was reported [92]. Not enough histidines were detected in the amino-acid composition for all the hemes to have bis-histidinyl coordination.

## 5 Complex Heme Proteins

Complex heme proteins which contain redox centers other than just electron transfer hemes are normally associated with enzymatic catalysis. In this section, we will refer to some of the best studied complex heme proteins: sulfite reductase, nitrite reductase, formate dehydrogenase, fumarate reductase and rubredoxin-oxygen oxidoreductase.

## 5.1 Sulfite Reductases

Sulfite reductases contain siroheme and iron-sulfur centers. Siroheme, also present in some nitrite reductases, is an iron tetrahydroporphyrin of the isobacteriochlorin type with eight carboxylic acid side-chains (Fig. 1). Siroheme isolated from *Desulfovibrio* species was found to be a monoamide, heptamethyl ester derivative, rather than the usual octamethyl ester derivative, which suggests that in these organisms an amidated form of the siroheme may be the physiologically active prosthetic group [93]. Sulfite reductases are divided into two classes, the assimilatory and the dissimilatory enzymes. The assimilatory sulfite reductases produce sulfide for use in the cell biosynthetic pathways. The dissimilatory enzymes are present in the sulfate-reducing organisms, and reduce sulfite as a respiratory substrate in a process coupled to ATP formation.

Assimilatory sulfite reductases have been isolated from some anaerobic bacteria like *D. vulgaris* Hildenborough [94], *Methanosarcina barkeri* [95] and *Desulfuromonas acetoxidans* [96]. They are characterised by having a low molecular mass of about 20 kDa, and a single subunit that contains one siroheme and one $[4Fe4S]^{2+/1+}$ cluster. The siroheme is fully metallated and its iron is low-spin, in contrast to the dissimilatory sulfite reductases. In vitro, they perform the six-electron reduction of sulfite to sulfide, which is also in contrast to the dissimilatory enzymes, which form trithionate, thiosulfate and sulfide in varying amounts. The primary sequence of the *D. vulgaris* enzyme has been determined by cloning of its gene [97]. Expression of this gene in a *Desulfovibrio* host led to the production of recombinant sulfite reductase which cannot be distinguished from the native one in terms of activity or spectroscopic characteristics [98].

The dissimilatory sulfite reductases from bacteria have been divided into four classes according to their visible absorption spectra: desulfoviridin (628 nm), desulforubidin (545 nm), desulfofuscidin (576 nm) and P-582 (582 nm) [99]. They are all heterooligomers of high molecular mass, and when assayed in vitro form a mixture of products containing trithionate, thiosulfate and sulfide. The product distribution varies with the assay conditions, and so it is still a matter of dispute whether the physiological product of these enzymes is sulfide or not [100] (Fig. 4). A similar dissimilatory sulfite reductase has also been purified from the thermophilic archaeon *Archaeoglobus fulgidus* [101].

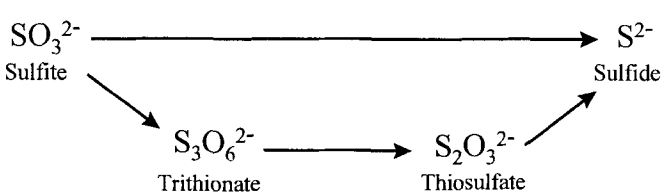


**Fig. 4.** The two possible mechanisms of sulfite reduction: a direct six-electron reduction to sulfide, or via the intermediates trithionate and thiosulfate

Desulfoviridin has been isolated from *D. gigas* [102], *D. vulgaris* [103], *D. salexigens* [104] and *D.desulfuricans* Essex 6 [105]. Its subunit composition, cellular localization, structure and arrangement of the catalytic centers are still a matter of debate. Desulfoviridin is a heterooligomer of about 200 kDa, which was considered to be composed by two subunits of 50 kDa ($\alpha$) and 40 kDa ($\beta$) in an $\alpha_2\beta_2$ arrangement. Recently, a third subunit of 11 kDa ($\gamma$) was discovered in *D.vulgaris* desulfoviridin, and an $\alpha_2\beta_2\gamma_2$ composition was proposed [106]. By immunological studies, this subunit was also found to be present in desulfoviridins from *D. vulgaris oxamicus* (Monticello), *D. gigas* and *D. desulfuricans* ATCC 27774 [106]. Cloning of the gene of the $\gamma$ subunit showed that it is not part of the same operon as the $\alpha$ and $\beta$ subunits, and that its expression varies with the growth phase [107]. When the genes for the $\alpha$ and $\beta$ subunits were cloned, it was discovered that a third gene was present, immediately downstream of the other two subunits [108]. This gene encodes a protein of only 78 amino-acids which was called DsvD. A gene with significant homology to this one was also found, immediately downstream of the genes of the $\alpha$ and $\beta$ subunits of the *A. fulgidus* sulfite reductase [108], which suggests that DsvD may have an important role in the reduction of sulfite.

Desulfoviridin is usually purified from the cytoplasmic fraction of the cells. However, since the enzyme must be involved in the electron transport-coupled energy conservation mechanism, one might expect that it should be membrane-associated. It has been observed with extracts of *D. vulgaris* that sulfide production from reduction of sulfite depends on the presence of membranes (with soluble extracts a mixture of products is observed, but when membranes are added the only product is sulfide) [109]. Immunocytochemical experiments have shown that the sulfite reductase from *D. gigas*, *D. vulgaris* Hildenborough and *Thermodesulfobacterium mobile* are all present in the cytoplasm [110]. In contrast, desulfoviridin from *D. desulfuricans* Essex 6 was purified both from the soluble and the membrane fractions [105, 111]. The two enzymes are identical, except that the membrane-bound desulfoviridin displays activity with cytochrome $c_3$, reduced by $H_2$/hydrogenase, as electron donor, whereas the soluble enzyme does not. The distribution of sulfite reductase activity between the soluble and membrane fractions depends very much on the method used for cell rupture [105], which suggests that desulfoviridin is only lightly associated with the membrane, and that cleavage of this sensitive association releases the enzyme to the cytoplasmic fraction.

Desulfoviridin was reported to contain a siroheme which was more than 70% demetallated [112–114], but it was described that a more careful purification of the *D. vulgaris* desulfoviridin yields a fully metallated enzyme [115]. However, a recent report where this purification procedure was repeated contradicts this observation [116].

Some controversy also surrounds the catalytic centers of desulfoviridin. A bridging cysteine thiolate ligand between the siroheme and the $[4Fe4S]^{2+/1+}$ cluster was proposed for the assimilatory sulfite reductase from *E. coli* [117], and recently confirmed by determination of the X-ray structure at 1.6 Å resolution [118]. A similar model was proposed for desulfoviridin [112, 113], but was questioned due to the detection by EPR of an unusually high spin system with

S = 9/2, proposed to originate from a complex FeS center, which is not involved in magnetic interaction with the siroheme [114, 119].

Desulforubidin was purified from *Desulfomicrobium baculatum* Norway 4 [120] and DSM 1743 [113], and recently from *Desulfosarcina variabilis* [119]. This type of sulfite reductase is characterized by an absorption peak at 545 nm. Their molecular mass and subunit structure are very similar to that of desulfoviridins, and a $\gamma$ subunit has also been observed [119, 121]. In contrast to desulfoviridin, the sirohemes are fully metallated.

Desulfofuscidin has only been isolated from extreme thermophilic sulfate reducers of the genus *Thermodesulfobacterium*, namely from *Thermodesulfobacterium commune* (DSM 2178, ATCC 33708) [122] and *Thermodesulfobacterium mobile* (DSM 1276), formerly called *Desulfovibrio thermophilus* [123]. It is characterised by an absorption peak at 576 nm and a molecular mass of around 170 kDa. It seems to be a tetramer of four very similar subunits with a mass of 48 kDa, and contains four molecules of fully metallated siroheme per molecule. Immunocytochemical experiments have shown that desulfofuscidin from *T.mobile* is located in the cytoplasm [110].

The sulfite reductase P-582 has only been isolated from the moderate thermophile *Desulfotomaculum nigrificans* [124]. It has a molecular mass of 194 kDa with an $\alpha_2\beta_2$ composition and exhibits an absorption peak at 582 nm.

## 5.2 Nitrite Reductases

There are two classes of nitrite reductases: those involved in denitrification, which reduce nitrite to gaseous nitrogen oxides and the assimilatory and dissimilatory enzymes, which reduce nitrite directly to ammonia [125, 126]. Two types of denitrifying enzymes have been described, those containing hemes *c* and $d_1$ and those which contain only copper. There are also two kinds of assimilatory/dissimilatory enzymes: the siroheme containing nitrite reductases like that of *E. coli*, which is used for detoxification of nitrite from the cytoplasm and is not coupled to energy conservation; and the heme *c* nitrite reductases, which are usually coupled to energy conservation [127]. This last type of nitrite reductase is that usually associated with strict anaerobes, so only this one will be discussed in more detail.

The heme *c* nitrite reductase was isolated from anaerobes or facultative anaerobes like *Desulfovibrio desulfuricans* (ATCC 27774) [128], *Wolinella succinogenes* [129], *Escherichia coli* [130], two *Vibrio* species [131,132] and *Sulfurospirillum deleyianum* [133]. In *D. desulfuricans* (ATCC 27774), *W. succinogenes* and *S.deleyianum* the enzyme is membrane-bound, and in the other cases it was isolated from the soluble fraction.

These nitrite reductases are described as monomers of about 60 kDa, containing six *c*-type hemes, five being low-spin and one high-spin in the as-isolated state [134]. However, recent evidence has indicated that the situation may be more complex. In *E. coli*, the gene for the nitrite reductase (*nrfA*) codes for a 50 kDa cytochrome containing four (or five), rather than six heme-binding sites [135]. The membrane-bound enzymes were shown not to be monomers,

but heterooligomers of two subunits of about 60 kDa and 20 kDa, forming complexes with large molecular masses [136, 137]. It is possible that the nitrite reductases isolated from the soluble fractions are dissociated subunits of the membrane-bound complex. Several spectroscopic [134, 138, 139] and kinetic studies [140, 141] have been carried out on the nitrite reductase. The nitrite reductase from *D.desulfuricans* (ATCC 27774) was recently shown to reduce sulfite with a high activity compared to the dissimilatory sulfite reductases [137]. This finding raises some questions regarding the sulfate metabolism in the sulfate reducing bacteria.

## 5.3 Formate Dehydrogenase and Fumarate Reductase

A formate dehydrogenase has been isolated from the anaerobes *Wolinella succinogenes* [142], *Methanobacterium formicicum* [143], *Clostridium pasteurianum* [144] and *Desulfovibrio vulgaris* Hildenborough [15, 32]. The enzyme has three subunits: the larger subunit contains a molybdenum cofactor, the second subunit contains iron-sulfur centers and the smaller subunit is a hydrophobic protein which anchors the enzyme to the membrane and contains a *b*-type cytochrome [145]. This *b*-type cytochrome is the menaquinone-reactive site of the enzyme [146]. In *D. vulgaris* the enzyme is periplasmic, and seems to contain a *c*-rather than a *b*-type cytochrome [32]. In *W. succinogenes*, it is membrane-bound facing the periplasmic side [147]. The formate dehydrogenase genes have been cloned in both *W. succinogenes* [145] and *M. formicicum* [143].

A cytochrome *b*-containing fumarate reductase was isolated from *W. succinogenes* [148]. It is also formed by three subunits: two are hydrophilic proteins, one containing FAD, and the other iron-sulfur centers, and the third is a hydrophobic protein containing two hemes *b* [149, 150]. The membrane-bound hydrogenase of *W. succinogenes* also has a heme *b*-containing subunit, which is the site of quinone reaction, and this cytochrome *b* has no homologies to that of the formate dehydrogenase or fumarate reductase [151]. Increased amounts of cytochrome *b* are found in the membranes of *Desulfovibrio gigas* grown in fumarate [88], suggesting that it may also be a part of the fumarate reductase. A membrane-bound fumarate reductase was purified from *Desulfovibrio multispirans* but was not reported to contain heme *b* [152].

## 5.4 Flavohemeproteins-ROO

A so far unique hemeprotein was recently identified in the sulfate-reducing bacterium *Desulfovibrio gigas*. In this micro-organism a three-component soluble electron transfer chain couples NADH oxidation to oxygen reduction to water, allowing $NAD^+$ regeneration by oxygen utilization. The proteins involved are a flavoprotein, NADH:Rubredoxin oxidoreductase (NRO) [153], a rubredoxin (Rd) and a Rubredoxin: oxygen oxidoreductase (ROO) [154] (Fig. 5). As $NAD^+$ can be recovered in this pathway, more ATP can be generated per glucose mole-

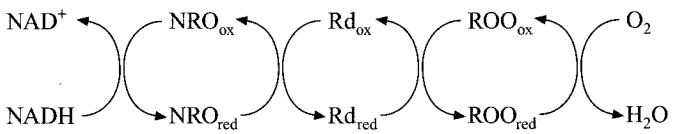


**Fig. 5.** The soluble electron-transfer chain from NADH to $O_2$ in *D. gigas*

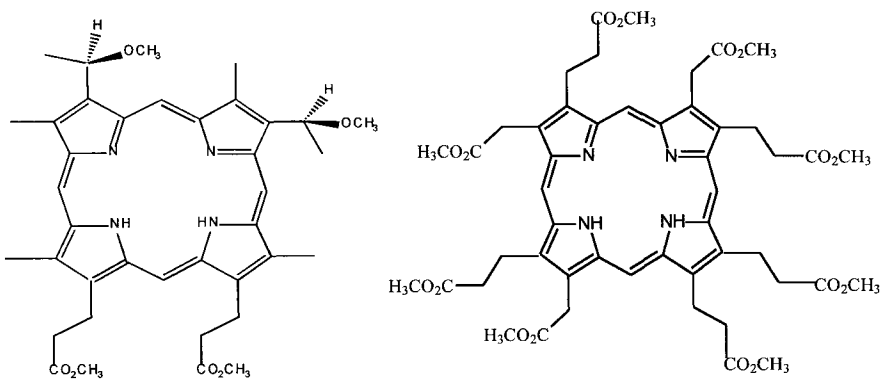


**Fig. 6.** Structure of the methylated porphyrins in ROO

cule (see Sect. 2). However, for *D. gigas*, it has not been unequivocally proven whether ATP can also be generated by oxidative phosphorilation.

ROO is an 86 kDa homodimeric flavohemeprotein containing two FAD molecules, and two unique hemes per monomer. The hemes were found to be a mesoheme IX derivative, possibly bound to the polypeptide chain through an as yet unknown compound and one Fe-uroporphyrin I (Fig. 6) [155]. The identification of a type I Fe-uroporphyrin, so far considered as a non-metabolite that accumulates in large amounts in some genetically-linked porphyrias, in a physiologically active enzyme is unprecedented and raises the possibility that Uroporphyrin I may play important roles in other organisms. The spectroscopic properties of ROO have been studied in detail [156]. The EPR characteristics of ROO hemes are unique and have strong similarities with the features of P-450 hemes, suggesting that ROO hemes may be bound to cysteines. By EPR and visible spectroscopy studies it was recently found that the flavins are the electron acceptor centers from reduced rubredoxin (Rd) and that its reduction proceeds through an anionic semiquinone radical; the reaction with oxygen occurs in the flavin moiety [156]. The function of the heme centers in ROO remains to be elucidated.

On the basis of its cofactors, ROO may be considered as a member of the large superfamily of flavoheme proteins [157–159], which based on their reactivity towards oxygen may be divided in two broad groups. One group com-

prises mainly the so-called flavohemoglobins, as the hemoglobin-like protein from *E. coli* [157]. These soluble proteins have protoheme IX and FAD as cofactors and share domains from the Globin and Ferredoxin-$NADP^+$ reductase families. Their function is still uncertain; it has been suggested that these proteins may play a role as oxygen sensors or transporters. Another member of this group is the cytochrome P-450 from *Bacillus megaterium* [160], which among the cytochromes P-450, presents the unique feature of having both the heme moiety and flavin domains in a single polypeptide chain. The other group aggregates the flavohemeproteins that have not been reported to react with oxygen and is somehow more heterogeneous in terms of size and cofactors, as well as catalytic activities.

## 6 Conclusions

This review shows how diverse the field of hemeproteins is, even in the restrict group of anaerobic microorganisms. With the same basic building unit, the heme core, such diverse functions as electron transfer, reduction of sulfite and nitrite, dismutation of hydrogen peroxide, are found.

Very detailed knowledge of some of the proteins in this group has been obtained, particularly regarding their structure and mode of action. Nevertheless, a lot of work remains to be done, specially on the physiological function of most of the known hemeproteins, and their interactions with soluble and membrane-bound enzymatic complexes.

**Note added in proof.** The number of hemes of the *c*-type nitrite reductases so far determined are probably incorrect: the analysis of the gene data from *Haemophilus influenzae* [161] as well as from *E. coli* show that the large subunit (60 kDa) contains four typical heme binding motifs C–X–Y–C–H, plus an unusual one in which the histidine adjacent to the cysteine is substituted by a lysine, and which may correspond to the catalytic site. The small subunit (25.6 kDa) contains five complete heme binding motifs. Hence, it may be antecipated that the subunits of the *c*-type nitrite reductases are the first examples of pentaheme cytochromes.

**Acknowledgements.** Part of the work reported in this review is a result of research projects financed by the European Community and by JNICT and PRAXIS XXI Program (Portugal). We gratefully acknowledge our collaborators, mentioned in the references. The continuous close collaboration of Prof. Jean LeGall for over 20 years is especially acknowledged.

## 7 References

1. LeGall J, Xavier AV (1996) Anaerobe 2:1
2. Bult CJ et al. (1996) Science 273:1058
3. Holmes MA, Letrong I, Turley S, Sieker LC, Stenkamp RE (1991) J Mol Biol 218:583
4. LeGall J, Prickril BC, Moura I, Xavier AV, Moura JJG, Huynh B-H (1988) Biochemistry 27:1636
5. Moore GR, Pettigrew GH (1990) In: Cytochromes c: evolutionary, structural and physicochemical aspects. Springer, Berlin, Heidelberg, New York, p 241

6. Kitamura M, Mizugai K, Taniguchi M, Akutsu H, Kumagai I, Nakaya T (1995) Microbiol Immunol 39: 75
7. Cheesman MR, Kadir FHA, Al-Basseet J, Al-Massad F, Farrar J, Greenwood C, Thomson AJ, Moore GR (1992) Biochem J 286:361
8. Martinez SE, Huang D, Szczepaniak A, Cramer WA, Smith WA (1994) Structure 2:95
9. Ubbink M, Campos AP, Teixeira M, Hunt NI, Hill HAO, Canters G (1994) Biochemistry 33:10051
10. Zhou H-X (1997) J Biol Inorg Chem 2:109
11. Bertini I, Gori-Savellini G, Luchinat C (1997) J Biol Inorg Chem 2:114
12. Mauke AG, Moore GR (1997) J Biol Inorg Chem 2:119
13. Gunner MR, Alexov E, Torres E, Lipovaca S (1997) J Biol Inorg Chem 2:126
14. LeGall J, Bruschi-Heriaud M (1968) In: Okunuki K, Kamen MD, Sezuko I (eds) Structure and function of cytochromes. University of Tokyo Press, University Park Press, p 467
15. Yagi T (1979) Biochim Biophys Acta 548:96
16. Fauque G, Bruschi M, LeGall J (1979) Biochem Biophys Res Comm 86:1020
17. Moura I, Fauque G, LeGall J, Xavier AV, Moura JJG (1987) Eur J Biochem 162:547
18. Eng LH, Neujahr HY (1989) Arch Microbiol 153:60
19. Our unpublished results
20. Koller KB, Hawkridge FM, Fauque G, LeGall J (1987) Biochem Biophys Res Comm 145:619
21. Senn H, Guerlesquin F, Bruschi M, Wüthrich K (1983) Biochim Biophys Acta 748:194
22. Blanchard L, Blackledge MJ, Marion D, Guerlesquin F (1996) FEBS Lett 389:203
23. Marion D, Guerlesquin F (1992) Biochemistry 31I:8171
24. Blackledge MJ, Medvedeva S, Poncin M, Guerlesquin F, Bruschi M, Marion D (1995) J Mol Biol 245:661
25. Blackledge MJ, Guerlesquin F, Marion D (1996) Proteins: Struct, Funct Genet 24:178
26. Nakagawa A, Higuchi Y, Yasuoka N, Katsube Y, Yagi T (1990) J Biochem 108:701
27. Van Rooijen GJH, Bruschi M, Voordouw G (1989) J Bacteriol 171:3575
28. Bruschi M, LeGall J (1972) Biochim Biophys Acta 271:48
29. Nakano K, Kikumoto Y, Yagi T (1983) J Biol Chem 258:12409
30. Yagi T (1994) Methods Enzymol 243:104
31. Verhagen MFJM, Wolbert RBG, Hagen WR (1994) Eur J Biochem 221:821
32. Sebban C, Blanchard L, Bruschi M, Guerlesquin F (1995) FEMS Microbiol Lett 133:143
33. Ogata M, Arihara K, Yagi T (1981) J Bichem (Tokyo) 89:1423
34. Diling W, Cypionka H (1990) FEMS Microbiol Lett 71:123
35. Marschall C, Frenzel P, Cypionka H (1993) Arch Microbiol 159:168
36. Santos H, Fareleira P, Xavier AV, Chen L, Liu M-Y, LeGall J (1995) Biochem Biophys Res Comm, 195:551
37. Fareleira P, LeGall J, Xavier AV, Santos H (1997) J Bacterid, 179:3972
38. Moura I, Ming LY, Costa C, Liu MC, Pai G, Xavier AV, LeGall J, Payne WJ, Moura JJG (1988) Eur J Biochem 177:673
39. LeGall J (1974) La Recherche 50 987
40. Probst I, Bruschi M, Pfennig N, LeGall J (1977) Biochem Biophys Acta 460:58
41. Coutinho IB, Turner DL, Liu MY, LeGall J, Xavier AV (1996) J Biol Inorg Chem 1:305
42. Bruschi M, Loufti M, Bianco P, Haladjian J (1984) Biochem Biophys Res Comm 120 : 384
43. Banci L, Bertini I, Bruschi M, Sompornpisut P, Turano P (1996) Proc Natl Acad Sci USA 93:14396
44. Turner DL, Costa HS, Coutinho IB, LeGall J, Xavier AV (1997) Eur J Biochem 243:474
45. Pfennig N, Biebl, H (1976) Arch Microbiol 110:3
46. Pereira IAC, Pacheco I, Liu MY, LeGall J, Xavier AV, Teixeira M (1997) Eur J Biochem, inpress
47. Coutinho IB, Xavier AX (1994) Methods Enzymol 243:119
48. Postgate JR (1952) Biochem J 56:xi
49. Bell JR, Lee JP Peck Jr HD, LeGall J (1978) Biochimie 60:315
50. Higuschi Y, Kusonoki M, Matsuura Y, Yasuoka N, Kakudo M (1984) J Biol Chem 172:109
51. Czjzek M, Payan F, Guerlesquin F, Bruschi M, Haser R (1994) J Mol Biol 243:653

52. Morais J, Palma N, Frazão C, Caldeira J, LeGall J, Moura I, Moura JJG, Carrondo MA (1995) Biochemistry 34:12830
53. Matias PM, Morais J, Coelho R, Carrondo MA, Wilson K, Dauter Z, Sieker L (1996) Prot Sci 5:1342
54. Turner DL, Salgueiro CA, Catarino T, LeGall J, Xavier AX (1996) Eur J Biochem 241:723
55. Coutinho IB, Turner DL, LeGall J, Xavier AX (1993) Biochem J 294:899
56. Piçarra-Pereira MA, Turner DL, LeGall J, Xavier AX (1993) Biochem J 294:909
57. Louro RO, Pacheco I, Turner DL, LeGall J, Xavier AX (1996) FEBS Lett 390:59
58 Messias AC, Kastrau DHW, Costa HS, LeGall J, Banci L, Turner DL, Santos H, Xavier AV (1996) Proceedings of XVIIth International Conference on Magnetic Resonance In: Biological Systems, 1996, Keystone, Colorado
59. Salgueiro CA, Turner DL, Santos H, LeGall J, Xavier AV (1992) FEBS Lett 314:155
60. Louro RO, Catarino T, Salgueiro CA, LeGall J, Xavier AV (1996) J Biol Inorg Chem 1:34
61. Santos H, Moura JJ, Moura I, LeGall J, Xavier AX (1984) Eur J Biochem 141:287
62. Odom JM, Peck Jr HD (1981) FEMS Microbiol Lett 12:47
63. Badziong W, Thauer RK, Zeikus, JG (1978) Arch Microbiol 116:41
64. Louro RO, Catarino T, LeGall J, Xavier AV (1997) J Biol Inorg Chem 2:488
65. Wikström M, Bogachev A, Finel M, Morgan JE, Punstinen A, Raitio M, Verkhovskaya M, Verkhovsky MI (1994) Biochim Biophys Acta 1187:106
66. Williams RJP (1978) FEBS Lett 85:9
67. Hatchikian EC, Bruschi M, LeGall J, Dubourdieu M (1969) Bull Soc Fr Physiol Vég 15:381
68. Guerlesquin F, Bovier-Lapierre G, Bruschi M (1982) Biochem Biophys Res Comm 105:530
69. Pieulle L, Haladjian J, Bonicel J, Hatchikian EC (1996) Biochem Biophys Acta 1273:51
70. Czjzek M, Payan F, Haser R (1994) Biochimie 76:546
71. Bruschi M, Leroy G, Bonicel J, Campese D, Dolla A (1996) Biochem J 320:933
72. Loufti M, Guerlesquin F, Bianco P, Haladjian J, Bruschi M (1989) Biochem Biophys Res Comm 159:670
73. Bruschi M, Leroy G, Guerlesquin F, Bonicel J (1994) Biochem Biophys Acta 1205:123
74. Czjzek M, Guerlesquin F, Bruschi M, Haser R (1996) Structure 4:395
75. Sieker LC, Jensen LH, LeGall J (1986) FEBS Lett 209:261
76. Haladjian J, Bianco P, Guerlesquin F, Bruschi M (1991) Biochem Biophys Res Comm 179:605
77. Hatchikian EC, LeGall J, Bruschi M, Dubourdieu M (1972) Biochem Biophys Acta 258:701
78. Hatchikian EC (1975) Arch Microbiol 105:249
79. Barata BAS, LeGall J, Moura JJG (1993) Biochemistry 32:11559
80. Higuchi Y, Inaka K, Yasuoka N, Yagi T (1987) Biochim Biophys Acta 911:341
81. Bruschi M, Bertrand P, More C, Leroy, G, Bonicel J, Haladjian J, Chottard G, Pollock WBR, Voordouw G (1992) Biochemistry 31:3281
82. Ogata M, Kiuchi N, Yagi T (1993) Biochimie 75:977
83. Chen L, Pereira MM, Teixeira M, Xavier AV, LeGall J (1994) FEBS Lett 347:295
84. Rossi M, Pollock WBR, Reij MW, Kevn RG, Fu R, Voordouw G (1993) J Bacteriol 175:4699
85. Pereira IAC, LeGall J, Xavier AX, Teixeira M (1997) J Biol Inorg Chem 2:23
86. Verhagen MFJM, Pierik AJ, Wolbert RBG, Mallée LF, Voorhorst WGB, Hagen WR (1994) European J Biochem 225:311
87. Hatchikian EC, LeGall J, Bell GR (1977) In: Michelson AM, McCord JM, Fridovich I (eds) Superoxide and superoxide dismutases. Academic Press, London, p 159
88. Odom JM, Peck HD (1981) J Bacteriol 147:161
89. Heiden S, Hedderich R, Setzke E, Thauer RK (1994) Eur J Biochem 221:855
90. Peer CW, Painter MH, Rasche ME, Ferry JG (1994) J Bacteriol 176:6974
91. Kühn W, Fiebig K, Hippe RA, Mah B, Huser A, Gottschalk G (1983) FEMS Microbiol Lett 20:407

92. Liu MC, Costa C, Coutinho IB, Moura JJG, Moura I, Xavier AV, LeGall J (1988) J Bacteriol 170:5545
93. Matthews JC, Timkovich R, Liu M-Y, LeGall J (1995) Biochemistry 34:5248
94. Huynh BH, Kang L, Der Vartanian DV, Peck HD, LeGall J (1984) J Biol Chem 259:15373
95. Moura JJG, Moura I, Santos H, Xavier AV, Scandellari M, LeGall J (1982) Biochem Biophys Res Comm 108:1002
96. Moura I, Lino AR, Moura JJG, Xavier AV, Fauque G, Peck HD, LeGall J (1986) Biochem Biophys Res Comm 141:1032
97. Tan J, Helms LR, Swenson RP, Cowan JA (1991) Biochemistry 30:9900
98. Tan J, Soriano A, Lui SM, Cowan JA (1994) Arch Biochem Biophys 312: 516
99. Hatchikian EC (1994) Methods Enzymol 243:276
100. Akagi JM (1995) In: Barton LL (ed) Sulfate-reducing bacteria. Plenum, New York, p 89
101. Dahl C, Kredich NM, Deutzmann R, Trüper HG (1993) J Gen Microbiol 139:1817
102. Lee JP, Peck HDJr (1971) Biochem Biophys Res Comm 45:583
103. Lee JP, LeGall J, Peck HD Jr (1973) J Bacteriol 115:529
104. Czechowski M, Xavier AV, Barata BAS, Lino AR, LeGall J (1986) J Ind Microbiol 1:139
105. Steuber J, Cypionka H, Kroneck PMH (1994) Arch Microbiol 162:255
106. Pierik AJ, Duyvis MG, Helvoort JMLM, Wolbert RBG, Hagen WR (1992) European J Biochem 205:111
107. Karkhoff-Schweizer RR, Bruschi M, Voordouw G (1993) Eur J Biochem 211:501
108. Karkhoff-Schweizer RR, Huber DP, Voordouw G (1995) Appl Environ Microbiol 61:290
109. Drake HL, Akagi JM (1978) J Bacteriol 136:916
110. Kremer DR, Veenhuis M, Fauque G, Peck HD, LeGall J, Lampreia J, Moura JJG, Hansen TA (1988) Arch Microbiol 150:296
111. Steuber J, Arendsen AF, Hagen WR, Kroneck PMH (1995) Eur J Biochem 233:873
112. Murphy MJ, Siegel LM (1973) J Biol Chem 248:6911
113. Moura I, LeGall J, Lino AR, Peck HD, Fauque G, Xavier AV, DerVartanian DV, Moura JJG,, Huynh BH (1988) J Am Chem Soc 110:1075
114. Pierik AJ, Hagen WR (1991) Eur J Biochem 195:505
115. Wolfe BM, Liu SM, Cowan JA (1994) Eur J Biochem 223:79
116. Marrit SJ, Hagen WR (1996) Eur J Biochem 238: 724
117. Christner LM, Münck E, Janick PA, Siegel LM (1981) J Biol Chem 256:2098
118. Crane BR, Siegel LM, Getzoff ED (1995) Science 270:59
119. Arendsen FA, Verhagen MFJM, Wolbert RBG, Pierik AJ, Stams AJM, Jetten MSM, Hagen WR (1993) Biochemistry 32:10323
120. Lee JP, Yi C-S LeGall J, Peck HD Jr (1973) J Bacteriol 115:453
121. Friedrich M, Schink B (1995) Arch Microbiol 164:271
122. Hatchikian EC, Zeikus JG (1983) J Bacteriol 153:1211
123. Fauque G, Lino AR, Czechowski M, Kang L, DerVartanian DV, Moura JJG, LeGall J, Moura I (1990) Biochem Biophys Acta 1040:112
124. Trudinger PA (1970) J Bacteriol 104: 158
125. Brittain T, Blackmore R, Greenwood C, Thomson AJ (1992) Eur J Biochem 209:793
126. Berks BC, Ferguson SJ, Moir JWB, Richardson DJ (1995) Biochim Biophys Acta 1232:97
127. Steenkamp DJ, Peck Jr HD (1981) J Biol Chem 256:5450
128. Liu M-C, Peck Jr HD (1981) J Biol Chem 256:13159
129. Liu M-C, Liu M-Y, Payne WJ, Peck Jr HD, LeGall J (1983) FEMS Microbiol Lett 19:201
130. Kajie S-I, Anraku Y (1986) Eur J Biochem 154:457
131. Rehr B, Klemme J-H (1986) FEMS Microbiol Lett 35:325
132. Liu M-C, Bakel BW, Liu M-Y, Dao TN (1988) Arch Biochem Biophys 262:259
133. Schumacher W, Kroneck PMH (1991) Arch Microbiol 156:70
134. Costa C, Moura JJG, Moura I, Liu MY, Peck Jr HD, LeGall J, Wang Y, Huynh, BH (1990) J Biol Chem 265:14382
135. Darwin A, Hussain H, Griffiths L, Grove J, Sambong, Y Bueby S, Cole J (1993) Mol Microbiol 9:1255
136. Schumacher W, Kroneck PMH (1994) Biochem Biophys Res Comm 205:911

137. Pereira IAC, Abreu IA, Xavier AX, LeGall J, Teixeira M (1996) Biochem Biophys Res Comm 224:611
138. Blackmore RS, Gadsby PMA, Greenwood C, Thomson AJ 1990) FEBS Lett 264:257
139. Blackmore RS, Gadsby PMA, Greenwood C, Thomson AJ (1990) Biochem J 271:253
140. Blackmore RS, Brittain T, Greenwood C (1990) Biochem J 271:457
141. Blackmore RS, Brittain T, Gadsby PMA, Greenwood C, Thomson AJ (1990) Biochem J 271:259
142. Kröger A, Winkler E, Innerhofer A, Hackenberg H, Schägger H (1979) Eur J Biochem 94:465
143. Shuber AP, Orr EC, Recny MA, Schendel PF, May HD, Schauer NL, Ferry JG (1986) J Biol Chem 261:12942
144. Liu C, Mortenson LE (1984) J Bacteriol 159:375
145. Bokranz M, Gutmann M, Körtner C, Kojro E, Fahrenholz F, Lauterbach F, Kröger A (1991) Arch Microbiol 156:119
146. Unden G, Kröger A (1983) Biochim Biophys Acta 725:325
147. Kröger A, Dorrer E, Winkler E (1980) Biochim Biophys Acta 589:118
148. Unden G, Hackenberg H, Kröger A (1980) Biochim Biophys Acta 591:275
149. Lauterbach F, Kortner C, Albracht SP, Unden G, Kröger A (1990) Arch Microbiol 154:386
150. Kortner C, Lauterbach F, Tripier D, Unden G, Kröger A (1990) Mol Microbiol 4:855
151. Dross F, Geisler V, Lenger R, Theis F, Krafft T, Fahrenholz F, Kojro E, Duchêne A, Tripier D, Juvenal K, Kröger A (1992) Eur J Biochem 206:93
152. He SH, DerVartanian DV, LeGall J (1986) Biochem Biophys Res Comm 135:1000
153. Chen L, Lui M-Y, LeGall J, Fareleira P, Santos H, Xavier AV (1993) Eur J Biochem 216:443
154. Chen L, Liu M-Y, LeGall J, Fareleira P, Santos H, Xavier AV (1993) Biochem Biophys Res Comm 193:100
155. Timkovich R, Burkhalter RS, Xavier AV, Chen L, LeGall J (1994) Bioorganic Chem 22:284
156. Gomes CM, Silva G, Oliveira S, LeGall J, Liu M-Y, Xavier AV, Rodrigues-Pousada C, Teixeira M (1997), J Biol Chem, in press
157. Ioannidis N, Cooper CE, Poole R K (1992) Biochem J 288:649
158. Probst I, Wolf G, Schlegel HG (1979) Biochim Biophys Acta 576:471
159. Chapman S K, White SA, Reid GA (1991) Adv Inorg Chem 36:257
160. Narhi LO, Fulco AJ (1986) J Biol Chem 261:7160
161. Fleischmann RD, Adams MD, White O, Clayton RA, Kirkness EF, Kerlavage AR, Bult CJ, Tomb J-F, Dougherty BA, Merrick JM, McKenney K, Sutton G, Fitzhigh W, Fields CA, Gocayne JD, Scott JD, Shirley R, Liu L-I, Glodeck A, Kelley JM, Weidmann JF, Phillips CA, Spriggs T, Hedblom E, Cotton MD, Utterback TR, Hanna MC, Nguyen DT, Saudek DM, Brandon RC, Fine LD, Fritchamnn JL, Geoghagen NSM, Gnehm CL, McDonald LA, Small KV, Fraser CM, Smith HO and Venter JC (1995) Science 269:496

# Evolutionary Aspects of Copper Binding Centers in Copper Proteins

B. Abolmaali · H.V. Taylor · U. Weser*

Anorganische Biochemie, Physiologisch-Chemisches Institut der Eberhard-Karls Universität Tübingen, Hoppe-Seyler-Strasse 4, D-72076 Tübingen, Germany.
*E-mail:ulrich.weser@uni-tuebingen.de*

A great number of active centers in proteins and enzymes contain transition metals. Each metal imposes specific catalytic properties on the protein which could not be achieved when employing a different metal. The special role and characteristic reactivity of coordinated copper is illustrated by looking at the evolutionary aspects of copper proteins. The evolution of copper-binding sites is closely linked to that of copper proteins. Copper centers have evolved according to various principles, similar to the evolutionary development of proteins and enzymes. Three basic principles may be observed: the copper-binding centers of metallothioneins and type 1 copper centers developed in non-metal proteins; the transformation of the metal-binding centers of iron or manganese proteins led to the development of the type 2 copper centers; and the trinuclear copper-binding centers of the blue oxidases were formed by alterations and recombinations of type 1 copper centers. Simple, although as yet unknown, mononuclear copper centers gave rise to the type 3 copper-binding sites of the hemocyanins and tyrosinases, as well as to the $Cu_A$- and $Cu_B$-centers of the cytochrome oxidases and $N_2O$-reductase. According to this assignment, copper proteins containing either type 1 copper, type 3 copper, $Cu_A$-centers, or $Cu_B$-centers share a common ancestor. They developed at least in part by divergent evolution. Type 2 copper proteins are the products of convergent evolution and, consequently, show little or no phylogenetic homology.



* for correspondence.

Structure and Bonding, Vol. 91

## List of Symbols and Abbreviations

| | |
|---|---|
| A-Hc | arthropod hemocyanin |
| acy | amicyanin |
| az | azurin |
| CD | circular dichroism |
| DOPA | 3,4-dihydroxyphenylalanine |
| ESR | electron spin resonance |
| HSAB | hard, soft acids, bases |

| | |
|---|---|
| M-Hc | mollusk hemocyanin |
| paz | pseudoazurin |
| pcy | plastocyanin |
| SOD | superoxide dismutase |
| TOPA | 2,4,5-trihydroxyphenylalanine |
| TPQ | 2,4,5-trihydroxyphenylalanine quinone |

# 1 Introduction

An attempt has been made to present and critically analyze the evolutionary and phylogenetic aspects of copper-binding centers in biological systems. Copper proteins and enzymes will be grouped according to their phylogenetic origins. The principles and mechanisms behind the evolution of individual enzymes will be educed. These principles will be applied to the evolution of copper-binding sites, which is closely linked to that of copper proteins. Three basic mechanisms will be presented whose application probably led to the generation of new copper-binding centers and, thus, to new catalytic properties of enzymes. An attempt will be made to uncover the connection between the occurrence of specific proteins and enzymes in the various phyla of life and the potential mechanisms behind the development of the respective copper-binding centers. The structural and functional properties of potential ozone-metabolizing enzymes are of special interest. It remains of interest which properties of copper-binding centers would be essential for the controlled reaction of ozone in living systems.

## 1.1 Biological Evolution and the Chemistry of Copper

Our Earth is approximately 4.6 billion years old, and its first primitive life-forms arose as early as half a billion to one billion years after its formation [1]. The young planet had yet to cool to its current temperature and violent volcanic eruptions repeatedly covered its surface with lava. The atmosphere was totally different from the one known today, consisting mainly of water vapor ($H_2O$), methane ($CH_4$), nitrogen ($N_2$) and ammonia ($NH_3$). Low concentrations of hydrogen ($H_2$) and carbon monoxide (CO) occurred, as well as, hydrogen cyanide (HCN) generated by the reaction of ammonia with methane [1]. The most striking difference between this primordial atmosphere and today's was the almost total lack of molecular oxygen ($O_2$) resulting in a reducing atmosphere. Due to the lack of molecular oxygen, there was no stratospheric ozone layer protecting the Earth from ultraviolet radiation [2] – this primitive atmosphere would have been fatal for most of today's life-forms. But only this harsh environment could give birth to life. The following is intended to show how the conditions mentioned above could lead to life and its evolution, as well as to illuminate the roles played by the elements copper and oxygen.

As shown in laboratory experiments [2a] small molecules such as water, ammonia and methane can, under suitable conditions, form simple amino acids.

On primordial Earth, electrical discharges or ultraviolet radiation may have served as energy sources for these reactions, although radioactivity or thermal energy were available as well. Upon treating a mixture of the compounds mentioned above with various types of energy, not only simple amino acids but other essential biochemical compounds are synthesized as well including carbohydrates, purines, pyrimidines, various nucleotides and fatty acids [2]. The type of organic molecules, which served as building blocks for the first life forms, are synthesized from inorganic compounds. In time, inanimate matter itself gave birth to life as defined by a cellular structure, metabolism, the ability to propagate, growth and movement.

Which events took place to create the first living organism from simple organic molecules? How could primitive organisms evolve into highly complex life-forms such as plants and animals? How did the chemical composition of the earth's crust and atmosphere affect the development of living beings, and in what manner did these living beings affect the chemical composition of their environment?

### 1.1.1
### *From Organic Compounds to Living Organisms*

The organic compounds created from the primordial atmosphere were quasi inert as long as there were no organisms utilizing them. Consequently, these amino acids, carbohydrates, purines, pyrimidines, nucleotides and fatty acids accumulated in the course of millions of years. Concurrently, the Earth cooled off, vapor condensed to water, and the oceans emerged. The reducing quality of the atmosphere and the still relatively high temperatures led to polymerization of the available monomers to polypeptides, polynucleotides, and possibly even polysaccharides [3]. These polymerization reactions occur by dehydration and, for this reason, cannot take place in an aqueous environment. They therefore may have taken place at structures offering an aqueous microenvironment such as clay, basaltic glasses, or pyrite ($FeS_2$). Both simple monomers and complex polymeric compounds are water soluble, with the exception of the fatty acids which spread as a thin layer on the water's surface, and accumulated in the oceans over millions of years [1].

According to the definition of living beings, the first life-forms must have been equipped with a cellular structure, metabolism and the ability to propagate. Possibly these features were acquired when micelles were formed from the lipid layer on the surface of the oceans. These micelles enclosed simple and polymeric compounds of varying concentrations. A process which repeated itself manifold in the course of millions of years without creating life. But at an opportune moment, all essential compounds and conditions were met: energy producing structures, a simple form of replication, the correct concentrations of low molecular mass compounds and the suitable micelle size. Although not spectacular, the first living micelle had been born.

The oldest known prokaryotic microfossils are approximately 3.5 billion years old. Consequently, life must have emerged between 3.5 and four billion years ago [2]. This was, in geological terms, only a short time after the Earth had

cooled off and the oceans had developed. But what life-form could live at temperatures near the boiling point of water?

### 1.1.2 *The First Forms of Life*

The earliest organisms on Earth were surrounded by an oxygen-free atmosphere. Therefore, energy production must have been based on chemoorganotrophic, chemolithotrophic or phototrophic reactions. It has been estimated that the concentration of $H_2S$ in the primordial oceans was about $10^{-3}$ mol/l. Both of the following reactions generate enough energy to synthesize ATP and may have been the energy producing steps in early organisms' metabolism [1]:

$$FeCO_3 + 2H_2S \rightarrow FeS_2 + H_2 + H_2O + CO_2 \qquad G^{\circ\prime} = 61.7 \text{ kJ/mol}$$
$$FeS + H_2S \rightarrow FeS_2 + H_2 \qquad G^{\circ\prime} = 41.9 \text{ kJ/mol}$$

The hydrogen produced by both reactions could react with elemental sulfur to regenerate $H_2S$. Or, alternatively, energy coupling could have occurred by splitting hydrogen into two protons and electrons thereby generating a proton gradient across a primitive membrane ultimately leading to the formation of ATP or another source of energy [1].

The primordial environment was not only anaerobic but hosted temperatures near the boiling point of water. Some organisms still live under similar conditions – the hyperthermophilic archaea found primarily in hot sulfurous springs. These organisms are able to reduce sulfur to $H_2S$ and, if grown on a medium containing $Fe^{2+}$, produce pyrite [1]. Other primordial organisms may have used chemoorganotrophic mechanisms to generate energy, e.g., fermentation. Energy production by photosynthesis must be considered improbable in these first organisms as photosynthesis requires more and more highly specialized enzymes than the previous two sources of energy. The main feature of the first life-forms would be a very simple metabolism utilizing few enzymes and, if any, only very simple cofactors [1].

The reactivity of ultraviolet irradiation which had been an indispensable factor for the origin of life soon became highly dangerous for primitive organisms. Consequently, these early life-forms could only occupy ecological niches which protected them from direct solar radiation. It is, therefore, very probable that the first ecological niches were narrow layers of water two to three meters under the surface of the oceans, a depth by which water has absorbed most of the harmful ultraviolet radiation [1]. The colonization of other habitats, especially land, was not yet possible.

### 1.1.3 *The Origin of Photosynthesis*

Iron-sulfur clusters were probably the first systematic structures of bacterial electron-transport chains. They are found in all classes of organisms from bacteria to man. The development of porphyrins, the basic material for the synthe-

sis of cytochromes and chlorophylls, was a second, key step in the development of electron-transport chains. Membrane-bound cytochromes were, and still are, essential components of electron-transport chains. The development of chlorophyll was fundamental for the utilization of solar energy. The first phototrophic organisms merely used this energy to produce ATP while reducing electron donors such as $H_2S$. This primordial phototrophic metabolism is similar to that of the green and red sulfur bacteria known today [1].

The next step towards colonizing land was the development of photosynthesis which took place approximately 2.5 billion years ago. Now both ATP and NADPH could be produced photosynthetically, leading to more efficient usage of solar energy. The by-product of this new energy source was molecular oxygen. And, although oxygen must have been toxic for the majority of organisms, the development of the first photosynthetic, oxygen producing organism was of crucial importance for further evolution on Earth.

Prior to the development of photosynthesis, interactions between living beings and their surroundings had been one-sided. Organisms had had to adapt to conditions predetermined by their environment and had not been able to influence them. Photosynthetic organisms revolutionized these interactions. Throughout its first million years, life had been confined to its narrow aqueous environment by the harsh solar radiation. Now photosynthesis enabled life to alter its environment, blocking the lethal solar radiation from the earth's surface and thereby making life possible anywhere in the world, even out of water.

### 1.1.4 *The Role of Oxygen*

A period of 1.5 billion years passed before the first oxygen-producing organisms evolved [1] – a period characterized by an anaerobic, reducing atmosphere, a high influx of ultraviolet radiation, and slow chemical and biological evolution. Then, over the next 1.5 billion years, oxygen-producing organisms increased the atmospheric concentration of molecular oxygen to current levels [1]. This increase in atmospheric oxygen was paralleled by a decrease in ultraviolet radiation reaching the earth's surface. The oxygen generated in the oceans rose to the upper atmospheric layers where it was converted into ozone by ultraviolet radiation. In the following millions of years, the equilibrium between the generation and the destruction of ozone led to a stratospheric ozone layer, protecting our planet's surface from ultraviolet radiation [4]:

$$3O_2 + h\nu_{(<242\,nm)} \rightarrow 2O_3$$
$$2O_3 + h\nu_{(220-320\,nm)} \rightarrow 3O_2$$

The stratospheric ozone layer created a filter for ultraviolet radiation up to a wavelength of 320 nm, thus removing the barrier that solar radiation had been to the colonization of new habitats. Millions of years after the development of the ozone layer the first organisms colonized land.

Another remarkable change in the atmosphere caused by the rising concentration of molecular oxygen was its inversion from a reducing to an oxidizing atmosphere. The initial atmospheric components were oxidized and removed [3]:

$$CH_4 + 2O_2 \rightarrow CO_2 + 2H_2O$$
$$4NH_3 + 3O_2 \rightarrow 2N_2 + 6H_2O$$
$$\text{metals/minerals} + O_2 \rightarrow \text{ores/rocks}$$

This "new" atmosphere contained totally different components compared to the primordial atmosphere and consisted mainly of nitrogen, oxygen, and small amounts of carbon dioxide.

Oxygenizing the atmosphere to its current level occurred over a period of 1.5 billion years – what were the direct biological and evolutionary consequences? Organisms were forced to adapt to the presence of oxygen and to an increasingly oxidizing atmosphere. For most early life-forms, oxygen was toxic. As a result, obligate anaerobic organisms such as the archaea and eukarya withdrew to regions which had remained more or less free of oxygen. Other organisms, i.e., bacteria, learned to utilize oxygen instead: they developed electron-transport phosphorylation based on iron-sulfur clusters and membrane-bound cytochromes. They invented oxidative phosphorylation, i.e., aerobic respiration, by using oxygen as the terminal electron acceptor [1]. This proved to be a selective advantage similar to that of the first oxygen producing organisms. Aerobic respiration is much more efficient in generating energy than lithotrophic processes or anaerobic fermentation. In addition to its high respiratory efficiency, oxygen soon became a practically inexhaustible resource accelerating the growth and distribution of these species.

When the atmospheric concentration of molecular oxygen had increased to approximately 10%, complex organisms containing various organelles began to develop from primitive eukaryotes which only contained a nucleus. Both outstanding features of bacteria, photosynthesis (chloroplasts) and respiration (mitochondria), were harnessed for the eukarya by endosymbiosis. Then, 900 million years ago – the concentration of atmospheric oxygen had increased to its current 20% – various eukaryotic species developed into multicellular organisms [1] bringing life one step closer to colonizing land.

Archaea, bacteria, and eukarya adapted to their surroundings in totally different manners. The archaea withdrew to hot sulfurous regions where conditions remained similar to those of the primordial world. They stayed anaerobic. The bacteria adapted to the new environment by learning to utilize water and oxygen. The eukarya had the advantage of a nucleus but only by harnessing photosynthesis and respiration through endosymbiosis were they able to become the most "progressive" life-forms [1]. They exchanged the advantages of single-celled organisms, e.g., a haploid genome and rapid adaptability for the benefits of multicellular life.

In summary, three applications of oxygen had decisive effects on the chemical and biological evolution: the oxidizing atmosphere, the stratospheric ozone layer and the development of aerobic respiration.

### 1.1.5
### *The Phylogenetic Tree*

Only a short time after life came into being, the phylogenetic tree branched into two distinctive lines (Fig. 1). The one led to bacteria and the other, millions of years later, divided into archaea and eukarya. Bacteria and archaea are prokaryotic, eukarya are eukaryotic organisms.

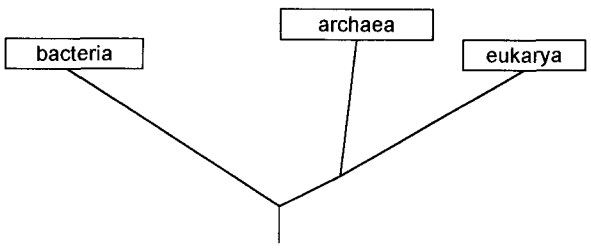


**Fig. 1.** Phylogenetic tree. Based on Brock et al. 1994 [1]

#### *1.1.5.1*
#### *Bacteria (Eubacteria)*

The phylogenetic tree of bacteria (Fig. 2) consists of twelve distinct groups (phyla) of which that of the purple bacteria is the largest. Although most are phototrophic, chemoorganotrophic and chemolithotrophic forms exist as well. It is likely that the ancestor of the purple bacteria was phototrophic although

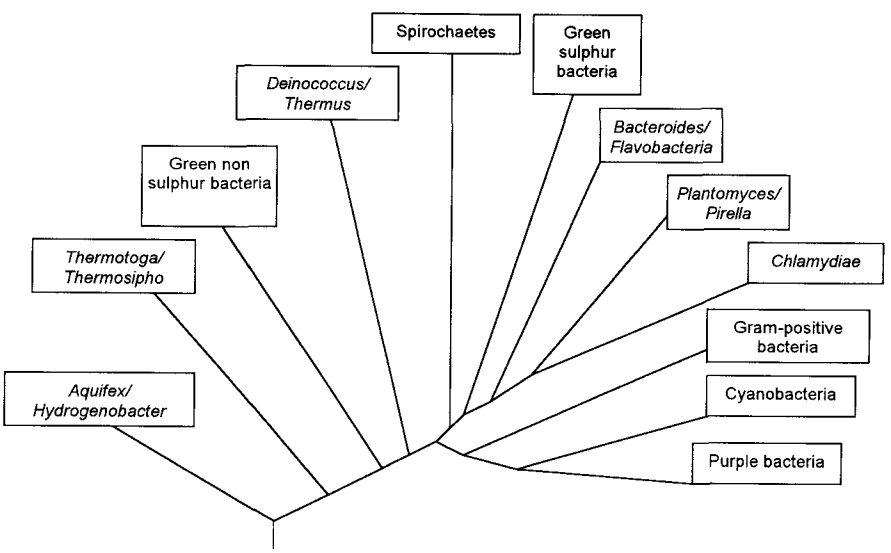


**Fig. 2.** Phylogenetic tree of bacteria. Based on Brock et al. 1994 [1]

this trait has been lost in various purple bacteria while adapting to an environment. Purple bacteria may be subdivided into five distinct groups [1]:

- alpha (*Pseudomonas* (some species), *Nitrobacter, Agrobacterium*)
- beta (*Pseudomonas, Alcaligenes, Bordetella*)
- gamma (*Escherichia, Azotobacter,* fluorescent *Pseudomonas* species)
- delta (*Bdellovibrio, Desulfovibrio*)
- epsilon (*Helicobacter*)

The green sulfur bacteria (*Chlorobium*) are only distantly related to other phyla of bacteria. The fact that they utilize photosynthesis shows, however, that photosynthesis must have developed at an early stage of bacterial evolution.

While green non-sulfur bacteria (*Chloroflexus*) are similar to the green sulfur bacteria in many physiological and structural features, these two phyla are not closely related. Most green non-sulfur bacteria are thermophilic.

One branch of the cyanobacteria is unique in that it leads to the plants' chloroplasts. According to the endosymbiont theory, chloroplasts evolved from prokaryotes which were similar to today's cyanobacteria.

Both free-living and parasitic forms of spirochetes (*Borrelia*) exist. Many of the parasitic forms are pathogenic.

Gram-positive bacteria can be divided into rods and cocci. This phyla includes endospore formers, lactic acid bacteria, most anaerobic and aerobic cocci, coryneform bacteria, actinomycetes, and the majority of mycoplasmas.

The other phyla contain but few genera which consist of facultative and obligate aerobic and anaerobic organisms [1].

#### *1.1.5.2*
#### *Archaea (Archaebacteria)*

The phylogenetic tree of the archaea includes four phyla: methanogens, halophiles, hyperthermophiles and thermoplasma (Fig. 3) [1]. The methanogens, halophiles and thermoplasma are phylogenetically closely related, slightly less

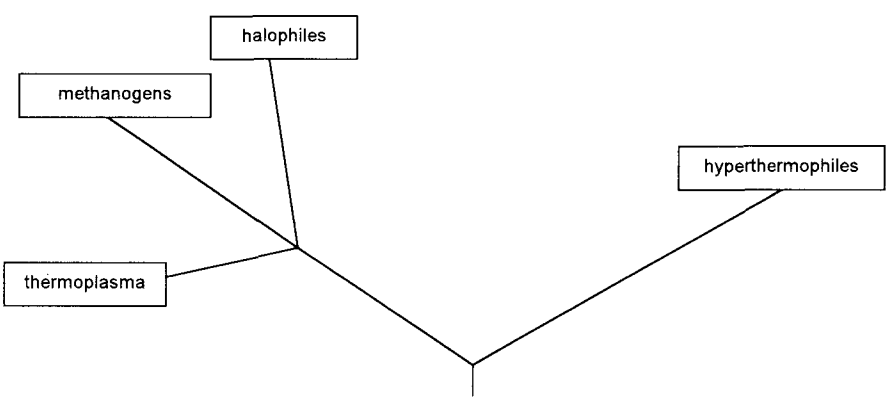


**Fig. 3.** Phylogenetic tree of archaea. Based on Brock et al. [1]

so the hyperthermophiles. The latter show some remarkable traits, for example, optimal growth at temperatures between 80 and 100 °C. Some species even favor temperatures of 105 °C. Most hyperthermophiles require sulfur for optimal growth. In most cases, sulfur acts as the electron-acceptor utilizing hydrogen as the electron-donor. Only one species uses sulfur as an electron-donor and here the electrons are transferred to oxygen [1]. Hyperthermophiles are adapted to conditions resembling those of primordial Earth. The genera of hyperthermophiles has evolved only slowly and, therefore, still shares many features with the earliest life-forms.

#### *1.1.5.3*
#### *Eukarya (Eukaryotes)*

A multitude of organisms may be found within the eukarya, ranging from highly complex multicellular organisms with distinctive cell-types to single-celled forms lacking special organelles. These single-celled forms include Diplomonadidae and Microsporae. Both genera are obligate parasites and lack not only organelles but 5.8S and 18S RNA as well. They do, however, share 16S RNA with bacteria. In this, Diplomonadidae and Microsporae resemble the first primitive eukaryotes to own a nucleus [1]. Endosymbiosis and a relatively high concentration of atmospheric oxygen favored the development of higher and

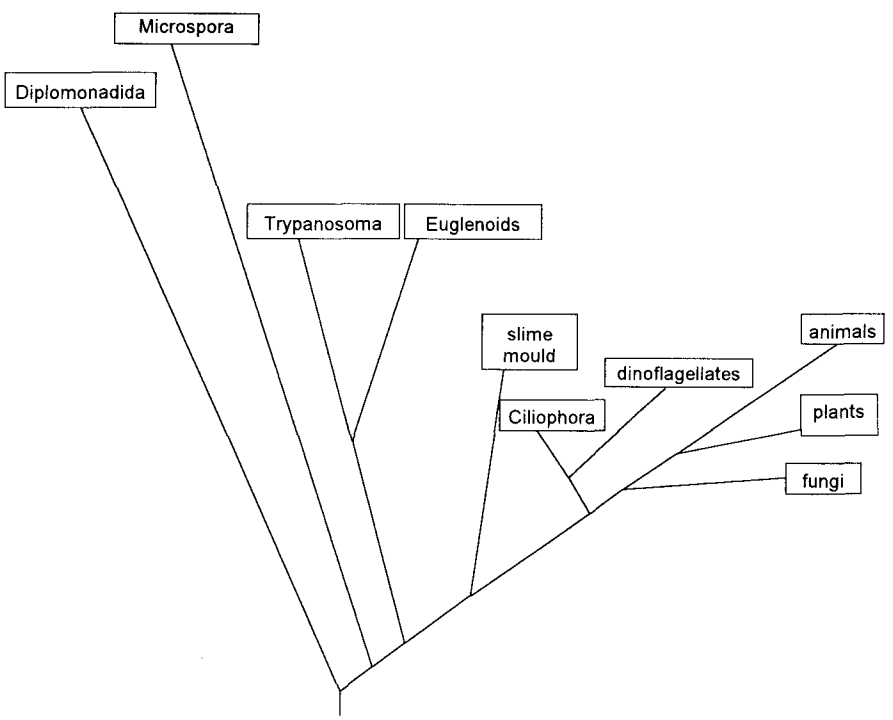


**Fig. 4.** Phylogenetic tree of eukarya. Based on Brock et al. 1994 [1]

more complex organisms. The phylogenetic tree of the eukarya has more species, genera, class and family diversity in phenotypes than any other kingdom of life (Fig. 4).

### 1.1.6
### *The Explosion of Species*

For the three billion years between the origin of life and the development of the first multicellular organisms, Earth had only hosted microbial life-forms. Then, 900 million years ago, the first multicellular organisms evolved from the domain of eukarya [1]. In contrast to many other evolutionary events, the development of multicellular organisms was not unique and occurred many times in several different variations. However, two basic principles can be distinguished. In the first case, various, isolated cells unite to form a cell-cluster, a process called aggregation (occurring, for example, with the slime mold *Dictyostelium*). In the other case, cells fail to separate after cell-division but remain connected within a gelatinous sheath (*Volvox*). In both cases, the cells diversify into vegetative and generative cell lines [5].

Single-celled evolution had been a slow process in which organisms which had been separated for millions of years differed only slightly. The development of multicellularity, however, paved the way for an explosive increase in biodiversity: organisms now not only differed in their basic metabolism, they changed their outer shape and architecture, they developed functional structures (such as specialized tissues and organs) as well as new modes of movement and reproduction. Life spread to more and more ecological niches, colonizing land and even the air. Life had come a long way from its origins.

Morphological development and the colonization of new biological niches mutually favored each other. As a result, all conceivable biological niches have now been settled by almost perfectly adapted organisms. This is not to say that evolution has come to an end, the ever changing environment demanding ever new adaptations from the world's inhabitants.

### 1.1.7
### *Copper Coordination and Chemistries in Biological Evolution*

Many of the active sites of today's proteins contain stably complexed transition metals (Mn, Fe, Co, Ni, Cu, Zn) thus providing these proteins and enzymes with catalytic properties which could not be achieved by other means. The choice of the metal depends on its ionic radius, on the reaction to be catalyzed, on the redox potential needed, on the type of ligands available and, last but not least, on the biological availability of the metal itself.

Copper was biologically unavailable for the first two billion years of life. The reducing atmosphere and the $10^{-3}$ molar oceanic concentrations of $H_2S$ locked copper in its $Cu^+$ form from which it precipitated as insoluble $Cu_2S$ [6, 7]. This extremely stable form of copper barred it from use in biological systems. However, iron, in contrast to copper, exists in a soluble form, $Fe^{2+}$, under these conditions. Consequently, it found application in a wide variety of proteins.

The oxygenation of the atmosphere increased the stability and hence the concentration of oxidized transition metal ions. Oxidation of $Cu^+$ led to soluble $Cu^{2+}$, whereas soluble $Fe^{2+}$ was converted into $Fe^{3+}$ which, in water, occurs mainly as $Fe(OH)_3$, a poorly soluble compound. To maintain the function of vital iron proteins and enzymes, special accumulation and storage mechanisms had to be developed for iron [7a, 7b].

The occurrence, functions, and reactions catalyzed by copper enzymes indicate that copper only became biologically relevant after oxygen began to accumulate in the atmosphere.

- No copper proteins have been discovered in anaerobic archaea.
- Copper proteins either transport oxygen or function as electron carriers with high redox potentials.
- In all reactions catalyzed by copper enzymes, oxygen either functions as a substrate or as an electron-acceptor.
- While the extracellular milieu is oxidizing, cytosol has reducing properties. With the exception of the cellular form of SOD, all known copper proteins and enzymes are found in the extracellular space or in organelles and vesicles (which may be considered extracellular, as well).
- The reactions catalyzed by copper enzymes are restricted to functions required by higher life forms:
  - extracellular oxidases;
  - hormone synthesis;
  - synthesis of connective tissues;
  - N/O-metabolism.
- The functions of copper proteins are restricted to:
  - electron transport in photosynthesis and nitrogen metabolism;
  - oxygen transport.

On first sight, it seems contradictory for copper proteins to catalyze photosynthetic reactions as photosynthesis was a prerequisite for copper to become biologically available. The explanation – several photosynthetic functions which, in early photosynthesis, had been fulfilled by cytochromes are now fulfilled by copper proteins. Plastocyanin has been found to be the electron donor in photosystem I of higher plants [8]. Eukaryotic algae use cytochrome *c 553* [9] while both plastocyanin and/or cytochrome *c* are found in green and blue-green algae (cyanobacteria) [8, 10–15]. When grown on copper-depleted media, cyanobacteria only produce cytochrome *c 533* [16]. As the copper concentration of the medium increases, cyanobacterium *Pseudoanabaena catenata* begins to produce plastocyanin as well. Under these conditions, *Nostoc muscorum*, another cyanobacterium, discontinues the production of cytochrome *c 533* totally in favor of plastocyanin. Some green algae will also replace plastocyanin by cytochrome *c 533* under conditions of copper deficiency [10, 11]. These organisms possibly reflect an intermediate stage of early evolution when cytochrome *c 533* was augmented and then replaced by plastocyanin.

Table 1 summarizes the connections between chemical and biological evolution as described above.

**Table 1.** Interactions between chemical and biological evolution

| years past (in billions) | chemical and biological situation | effects |
|---|---|---|
| 4.6 | development of our solar system | development of Earth |
| 4.0–3.5 | reducing atmosphere<br>lack of an ozone layer<br>composition of the primordial atmosphere | development of life |
| 3.5–2.0 | conditions hostile of life on Earth's surface | slow development of species in narrow ecological niches |
| 2.0–1.0 | development of photosynthesis | atmosphere is oxygenated |
| 1.5–1.0 | oxygenated atmosphere | development of an ozone shield<br>development of aerobic respiration<br>copper becomes bio-available |
| 1.0 | copper is employed as a biogenic metal | refinement of photosynthesis<br>utilization of oxygen as electron-acceptor<br>new oxygen-transport proteins<br>production of hormones<br>further development of connective tissue<br>protection from reaction oxygen species<br>→ the explosion of species |

## 1.2 Copper in Biological Systems

In biological systems, copper occurs as part of the active site of proteins or enzymes. The various ways in which copper is bound to these copper-binding centers are of special interest.

In most cases, copper participates directly in the catalytic cycle. However, in certain enzymes, copper only generates an internal cofactor without participating in catalysis itself. Irrespective of the exact mechanism and the exact number of copper ions involved in the reaction, the participating copper ions change their redox states during catalysis. Electrons are transferred either between copper ion and substrate or between copper ion and redox partner with the redox potentials of the participating compounds determining the electron flux. In biological systems copper has, until now, only been observed as Cu(I) or Cu(II) . Models suggesting the existence of Cu(III) have had to be dismissed in favor of other explanations. Why is Cu(III) only found in small peptides, whereas Cu(I) and Cu(II) are predominant in proteins and enzymes? The electron configuration of elementary copper is $3d^{10}4s^1$. Removing an electron from the 4*s*-shell creates the $3d^{10}$, diamagnetic $Cu^+$-ion. $Cu^{2+}$ and $Cu^{3+}$ are generated by removing one or two electrons from the 3*d*-shell. The unpaired *d*-orbital electron causes $Cu^{2+}$ to be paramagnetic (Table 2).

In aqueous solutions, the three types of copper ions form complexes with appropriate ligands differing in coordination number and stereochemistry.

**Table 2.** Electron configuration and magnetic properties of the three oxidation states of copper. $Cu^{2+}$ contains an unpaired electron and is therefore EPR-active. $Cu^{+}$ and $Cu^{3+}$ are EPR-inactive. These features are utilized in spectroscopic experiments studying copper oxidation states in electron-transfer reactions. When two $Cu^{2+}$-centers are in close proximity to each other, antiferromagnetic coupling of the two unpaired electrons renders both copper centers EPR-inactive

| oxidation state | electron configuration | magnetic properties |
|---|---|---|
| $Cu^{+}$ | $3d^{10}$ | diamagnetic |
| $Cu^{2+}$ | $3d^{9}$ | paramagnetic |
| $Cu^{3+}$ | $3d^{8}$ | diamagnetic |

According to Pearson's concept [16a], small compounds, which are not easily polarized, are classified as 'hard', while large and easily polarized compounds are classified as 'soft' (Table 3).

It is a general rule that hard acids form stable complexes with hard bases, while soft acids form stable complexes with soft bases. This rule applies to copper-complexes as well: an increase in oxidation number changes copper ions from soft to hard resulting in a change in preferred ligands. In the active site of proteins, copper can only be complexed by amino acids or small compounds such as $H_2O$, $OH^-$ or $PO_4^{3-}$. In agreement with the HSAB-concept, the 'soft' ion, $Cu^{+}$, is preferably complexed by amino acids such as Cys, $Cys^-$ and Met, while the 'harder' $Cu^{2+}$ may also be coordinated by the 'harder' compound $H_2O$ or amino acids Tyr, $Tyr^-$, Ser, Thr, or His. As the 'hardest' of copper's three oxidation states, $Cu^{3+}$ requires very 'hard' ligands. Soft ligands would be oxidized by $Cu^{3+}$ which in turn would be reduced to $Cu^{2+}$. Therefore, $Cu^{3+}$ is only stable in complexes consisting solely of 'hard' ligands such as Tyr, $OH^-$ and $Tyr^-$. A protein containing $Cu^{3+}$ in its active site would be able to participate in reactions requiring extremely high redox potentials. Although the required ligands are of course present in the natural repertoire of amino acids, $Cu^{3+}$ has yet to be found in a protein or enzyme. This may be because redox potentials of such a magnitude have not yet been needed and thereby become a selective advantage in evolution. Another reason could be the lack of a structure for placing $Cu^{2+}$ into the active site of a protein where it could be oxidized by either a ligand or substrate. Or, simply, while Tyr, $OH^-$ and $Tyr^-$ are 'hard' enough to stabilize $Cu^{3+}$, such a

**Table 3.** Hard and soft acids and bases. Based on Hughes 1990 [17]

| acids | | | | | | bases | | | | |
|---|---|---|---|---|---|---|---|---|---|---|
| hard | | intermediate | | soft | | hard | intermediate | | | soft |
| $H^+$ | $Mn^{2+}$ | $Zn^{2+}$ | $Sn^{2+}$ | $Cu^{+}$ | $Pd^{2+}$ | $H_2O$ | $NH_3$ | $Br^-$ | RSH | $R_3P$ |
| $Li^+$ | $Cr^{3+}$ | $Cu^{2+}$ | $Pb^{2+}$ | $Ag^{+}$ | $Pt^{2+}$ | ROH | $RNH_2$ | $N_3^-$ | $R_2S$ | $R_3As$ |
| $Na^+$ | $Fe^{3+}$ | $Ni^{2+}$ | | $Au^{+}$ | $Cd^{2+}$ | $R_2O$ | $Cl^-$ | $NO_2^-$ | $RS^-$ | $H^-$ |
| $K^+$ | $Co^{3+}$ | $Fe^{2+}$ | | $Tl^{+}$ | | $OH^-$ | $PO_4^{3-}$ | | | $S_2O_3^{2-}$ |
| | | | | | | $OR^-$ | $SO_4^{2-}$ | | | |

complex may not be stable enough in itself to be part of the active site of a protein or enzyme.

The different oxidation states of copper ions not only favor distinct ligands but distinct stereochemistries of the copper-complexes as well. The conformational geometry of a complex depends on the orbital geometry of the central ion [17]. Sterical hindrances excluded, $Cu^+$-ligands favor a tetrahedral conformation, while those of $Cu^{2+}$ favor a square planar conformation (Table 4) [17]. In the copper-binding sites of proteins, ligands and conformations may differ greatly from those normally preferred.

**Table 4.** Favored stereochemistries of two oxidation states of copper. Based on Hughes 1990 [17]

| oxidation state | coordination numbers | stereochemistry |
|---|---|---|
| $Cu^+$ | 2 | linear |
| | 3 | planar |
| | 4 | tetrahedral[a] |
| $Cu^{2+}$ | 4 | square planar[a] |
| | 4 | distorted tetrahedral |
| | 5 | square pyramidal |
| | 5 | trigonal bipyramidal |
| | 6 | distorted octaheral |

[a] Common conformation.

### 1.2.1 *Copper-Binding Centers*

Copper-complexes are most stable when the preferred ligands surround the central ion in its favored geometry. Disturbances of such an arrangement destabilize the respective oxidation-state. However, were the copper oxidation states of proteins and enzymes stable, the resulting copper-binding centers would be unsuited for the catalysis of redox reactions. A redox-active copper center must be able to switch between the oxidation states Cu(I) and Cu(II) with little energy involved. In the copper-binding centers of proteins and enzymes this is achieved in two different ways. In the first, copper is coordinated in part by ligands favoring Cu(I) and in part by others favoring Cu(II). In the second, ligand stereochemistries are created which lay between the common geometries for Cu(I) and Cu(II). In the latter case, the ligands are fixed in their positions by the stable protein scaffold. The choice of ligands and their stereochemistry determine the redox potential of the central copper ion [6]. A tetrahedral distortion of the planar geometry favored by $Cu^{2+}$ facilitates the reduction of $Cu^{2+}$ to $Cu^+$, i.e., the redox potential rises. The same effect is achieved by introducing soft ligands favoring $Cu^+$ [6].

In aqueous solution, the redox potential of the redox couple $Cu^{2+}/Cu^+$ is $E^\circ = +153$ mV [6]. In contrast to this, the range of redox potentials found in copper proteins and enzymes extend from +183 mV in halocyanin [18] to +785 mV in

the type 1 copper center of laccase [19]. This wide range of relatively high redox potentials was achieved by the evolution of various copper-binding centers. In these centers, the coordinating amino acid residues are fixed within a relatively stiff protein scaffold. They therefore force the central copper ion into a defined stereochemistry. In electron-transport proteins which function by switching between $Cu^{+}$ and $Cu^{2+}$, ligands and stereochemistries lay between the preferred of both oxidation states without favoring one of them. This minimizes local reorganization energy and is probably how redox potentials are optimized for respective reactions [6].

The high redox potentials of copper proteins make them highly suitable for reactions with oxygen. In the course of evolution, six different types of copper-binding centers have evolved for catalyzing the various reactions and will be described in the following.

#### *1.2.1.1*
#### *Type 1 Copper Centers*

A remarkable feature of some copper-proteins is an intensive blue color based on the spectroscopic properties of the type 1 copper center. Type 1 copper centers show a characteristic absorption band at approximately 600 nm and an extinction coefficient exceeding 3000 l $mol^{-1}$ $cm^{-1}$. In comparison, the extinction coefficient of the hexaquacopper(II) complex, $[Cu(OH_2)_6]^{2+}$, whose blue color is much less intensive, is only 5–10 l $mol^{-1}$ $cm^{-1}$ [6]. This difference in spectro-

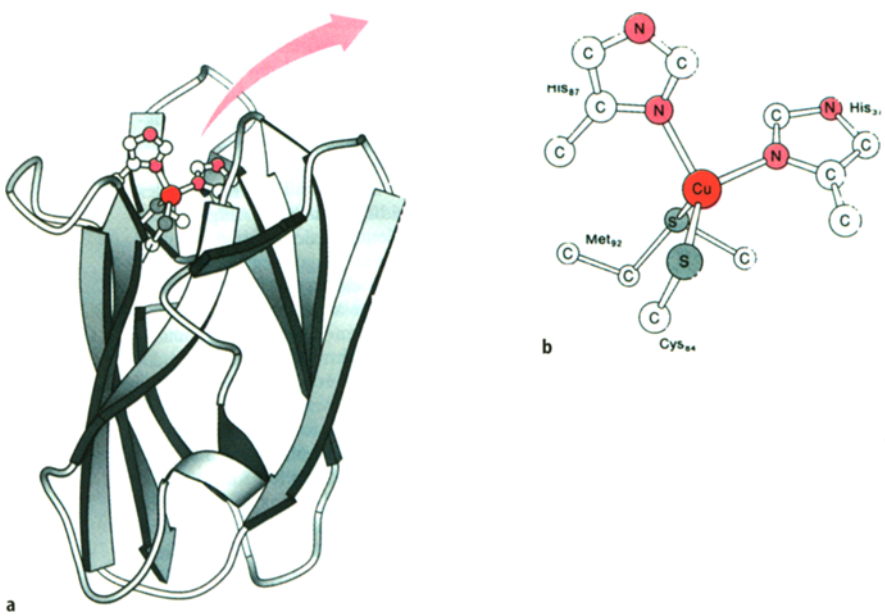


**Fig. 5.** **a** The structure of plastocyanin from poplar. **b** Stick-and-ball model of the plastocyanin type 1 copper center. From Lippard and Berg 1995 [6] with permission

scopic properties as compared to those of the hexaquacopper(II) complex is most pronounced in type 1 copper centers. These spectroscopic characteristics are, similar to the increase in redox potential, the result of the geometric arrangement of ligands within the copper-binding site [6].

Commonly, type 1 copper is coordinated by two histidine, one cysteine, and one methionine residue [6] (Fig. 5). Depending on the protein, the stereochemistries of the copper centers lay between distorted trigonal bipyramidal (e.g., in azurin [20, 21]) and distorted tetrahedral (e.g., in plastocyanin [20, 22]). In both cases, the methionine residue is the ligand most distant from the copper ion [20]. In addition to the ligands mentioned above, a fifth ligand has recently been discovered in some type 1 copper centers, a carbonyl O-atom opposing the methionine ligand [21, 23]. In azurin, the five ligands form a distorted trigonal bipyramidal geometry. In plastocyanin, however, the fifth ligand is more distant from the copper ion and the weak coordination results in a more tetrahedral geometry. The methionine residue is unnecessary for the spectroscopic or for the functional properties of type 1 copper centers: in phytocyanins, a group of small blue proteins, it has been replaced by a glutamine residue [24] and in ceruloplasmin one of the type 1 copper centers lacks this ligand completely [25] (Fig. 8).

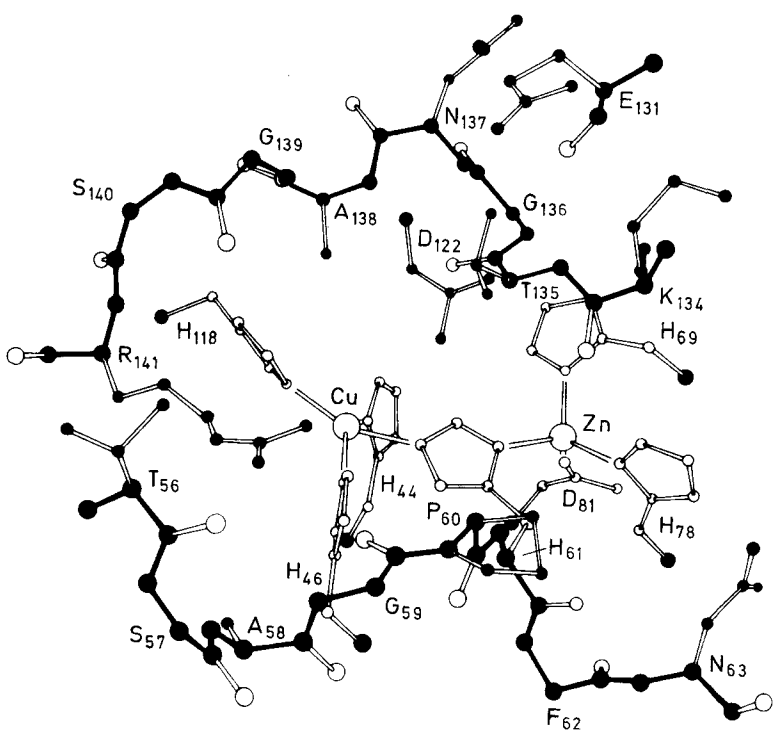


**Fig. 6.** The catalytic center of Cu,Zn-superoxide dismutase from bovine erythrocytes. From Tainer et al. 1983 [33] with permission

Type 1 copper centers are found in small blue proteins, in blue oxidases and in nitrite reductase. In the latter, the distorted ligand geometry causes a shift in the absorption band resulting in a green instead of a blue enzyme [26, 27].

#### *1.2.1.2*
#### *Type 2 Copper Centers*

The properties of the type 2 copper centers resemble those of copper(II) complexes [17]. This indicates that the geometric conditions are less critical than in type 1 copper centers.

Type 2 copper centers appear in oxidases, oxygenases, nitrite reductase, and in Cu,Zn-superoxide dismutase. While type 1 copper centers are restricted to electron transport [17], type 2 copper centers are directly involved in oxygen metabolism. In amine oxidase and galactose oxidase they are responsible for the production of an internal cofactor. Oxidases, oxygenases and nitrite reductase reduce oxygen to hydrogen peroxide ($H_2O_2$) by a two-electron-transfer. Cu,Zn-superoxide dismutase catalyses the disproportionation of two superoxide anion radicals ($\bullet O_2^-$) to hydrogen peroxide and oxygen.

Type 2 copper centers are not uniform in ligand or ligand stereochemistries. One common feature is, however, that in the active enzyme, one coordination site is always free to bind oxygen. The most common ligand in type 2 copper centers is histidine. Tyrosine (often modified), methionine, and cysteine occur as well. There are three histidines and a modified tyrosine in amine oxidase and lysyl oxidase [28]. In diamine oxidase, two of the histidine residues have probably been replaced by cysteines [29]. In galactose oxidase, the copper ion is coordinated by two tyrosines, two histidines and an acetate ion [30]. Dopamine-$\beta$-hydroxylase contains two differently coordinated copper ions per functional unit. One is coordinated by three histidines and a methionine and the other by two histidines and another, yet unknown, ligand [31]. Last but not least, the type 2 copper ion in Cu,Zn-superoxide dismutase is coordinated by four histidine residues, one of which connects the copper ion to the zinc ion, the second metal ion in the active site of the enzyme [32, 33] (Fig. 6).

#### *1.2.1.3*
#### *Type 3 Copper Centers*

Type 3 copper centers occur in hemocyanin (an oxygen-transport protein) and in tyrosinase (a monooxygenase) and are binuclear centers with antiferromagnetically coupled copper ions [6]. Although their functions differ, the copper centers of the two enzyme classes are very similar [34]. Each of the two copper ions is coordinated by three histidine residues in a trigonal planar stereochemistry (Fig. 7) and the ligands of the two copper ions themselves are arranged antiprismatically [35, 36]. While reduced, hemocyanines are colorless but turn blue upon oxidation [34]. Type 3 copper centers show a strong absorption at approximately 345 nm which is assumed to be caused by ligand-metal charge transfer [6].

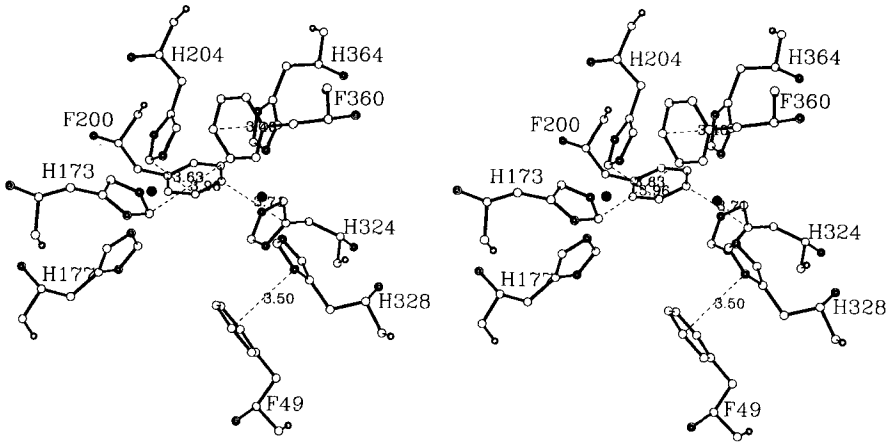


**Fig. 7.** The type 3 copper center of hemocyanin from *Limulus polyphemus*. From Hazes et al. 1993 [37] with permission. This figure and Fig. 30 were based on the Art Blot Program [38]

### *1.2.1.4*
### *Trinuclear Centers*

Blue oxidases contain trinuclear centers, formally constructed of a single type 2 and a single type 3 copper center, in which the three copper ions form a triangle [25] (Fig. 8). Both copper ions of the type 3 copper center are coordinated by three histidines, while two histidines coordinate the type 2 copper ion [36, 37]. In contrast to the type 3 copper centers of hemocyanin and tyrosinase, the ligands of the two copper ions are arranged prismatically [36, 39] as steric hindrance by the type 2 copper center prevents an antiprismatic arrangement. These trinuclear centers are one of the two known enzymatic structures able to reduce oxygen to water.

### *1.2.1.5*
### *$Cu_A$-Centers*

$Cu_A$-centers are found in cytochrome *c* oxidases and in $N_2O$-reductase [40, 41]. In both enzyme classes, $Cu_A$-centers subtract electrons from an external donor and transfer them either directly to the active site or indirectly via a further redox-active center [42–44]. Until recently, knowledge concerning the structure of $Cu_A$-centers was incomplete. This situation was alleviated by the publication of the crystal-structures of cytochrome *c* oxidase from *Paracoccus denitrificans* and bovine heart in 1995 [43, 44]. According to these data, $Cu_A$-centers contain [2Cu-2S] structures similar to those in [2Fe-2S]-type iron-sulfur clusters. Both sulfur ligands are donated by cysteine residues in the peptide chain and form a planar structure with the copper ions [43–45]. In both structures, an electron can be delocalized over both metal-ions. In the iron-sulfur center this effect is observed in the reduced form [$Fe^{2.5+}$–$Fe^{2.5+}$], while in the $Cu_A$-center the delo-

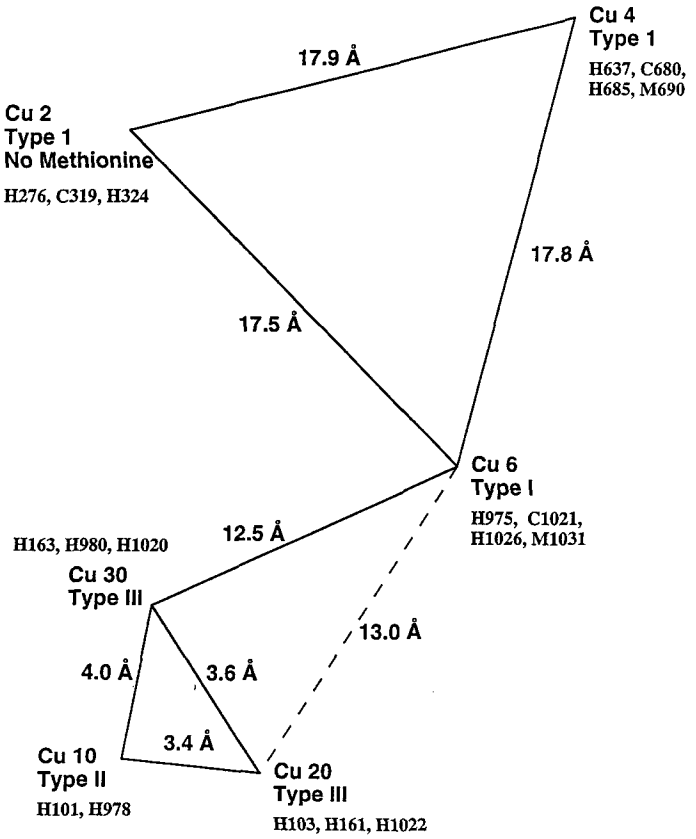


**Fig. 8.** The steric relationships between the copper centers of ceruloplasmin. From Zaitseva et al. 1996 [25] with permission

calized electron is found in the oxidized form: $[Cu^{1.5+}-Cu^{1.5+}]$ [43–49]. In the $Cu_A1$ site, the copper ion is liganded by a histidine and methionine residue in addition to the two cysteines. In the $Cu_A2$ site, the methionine residue is replaced by a glutamate. The ligand environments of the two copper ions resemble the type 1 copper centers of plastocyanin and stellacyanin. This resemblance also extends to the tertiary structure and amino acid sequence of the regions flanking the $Cu_A$-dimer [43, 50–52]. Both copper ions are coordinated in a distorted tetrahedron [44] (Fig. 9).

### *1.2.1.6*
### *$Cu_B$-Centers*

$Cu_B$-centers occur in cytochrome oxidases where they are always coordinated to a heme group forming a $Cu_B$-heme cluster. The metal ions of the two redox-active centers are coupled antiferromagnetically and lack bridging ligands [43,

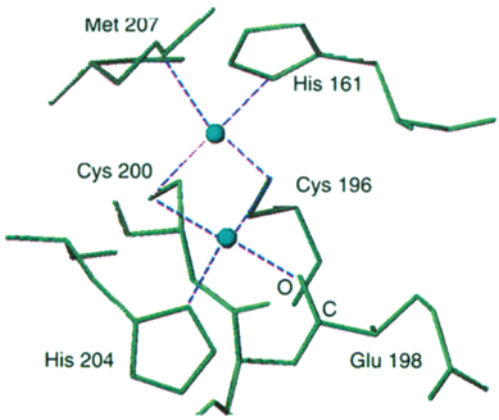


**Fig. 9.** Structure of the $Cu_A$-center of cytochrome *c* oxidase from bovine heart. The *gray circles* represent the copper ions, the *dotted lines* are the coordinate bonds between the copper ions and ligands. From Tsukihara et al. 1995 [44] with permission

44]. Histidine occupies three coordinations sites of $Cu_B$ as well as the fifth coordination site of the heme-iron, opposing the copper ion [43] (Fig. 10). The $Cu_B$-heme cluster is the binding site for oxygen [44, 53]. These $Cu_B$-heme clusters and the trinuclear centers of blue oxidases are the only known structures able to reduce oxygen to water by a four-electron reduction.

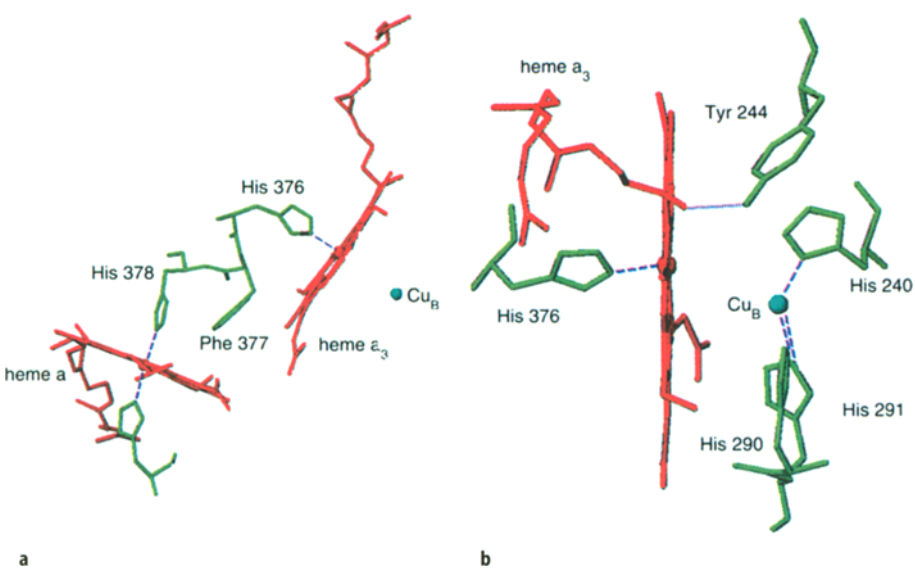


**Fig. 10a, b.** $Cu_B$-heme *a* cluster of cytochrome *c* oxidase from bovine heart: **a** its steric relation to the second heme *a*-center; **b** the three histidine ligands of $Cu_B$. From Tsukihara et al. 1995 [44] with permission

### *1.2.1.7*
### *Copper-Binding Sites in Metallothioneins*

Cadmium, zinc, and copper bind to metallothioneins in different oxidation states and stoichiometries. In class I metallothioneins, 20 cysteine residues occur all of which participate in metal-ion binding. In zinc-metallothionein, seven $Zn^{2+}$ ions are coordinated by three cysteine ligands each. A similar stoichiometry occurs in cadmium-metallothionein [54, 55]. Additionally, basic amino acids (lysine and arginine) are in the close neighborhood of the cysteine residues and it had been suggested that they participated in the metal-binding as well [56, 57]. Two cysteine residues occur in a Cys-x-Cys motive while the third cysteine residue is offset by some amino acids [58].

The tertiary structure of apo-metallothionein resembles a random coil. Metal-binding, however, effects a noticeable conformational change resulting in a defined tertiary structure [58]. This suggests that the structure of the metal-binding centers is only formed upon metal binding (Fig. 11).

In contrast to the metallothioneins mentioned above containing 7 divalent ions, copper-thioneins contain 12 Cu(I)-ions [59–61]. Copper-thioneins contain Cu(I) as the soft ligand, cysteine, favors this oxidation state [62–65]. Binding 12 copper(I) ions also requires a different geometry than that occurring in the other metallothioneins. The stoichiometries of the class I copper-metallothioneins was determined by CD-, UV- and luminescence-emission spectrometry [59]: copper-thioneins contain two oligonuclear copper-binding sites, a $Cu_6S_{11}$-cluster in the $\alpha$-domain and a $Cu_6S_9$-cluster in the $\beta$-domain.

Similar oligonuclear centers may occur in class II metallothioneins as well [66]. In this class, 8 copper ions are coordinated by 12 cysteine ligands (Fig. 12). Two of these eight copper ions do not contribute to the characteristic CD-spectrum and may easily be removed by copper chelators [67]. Consequently, the

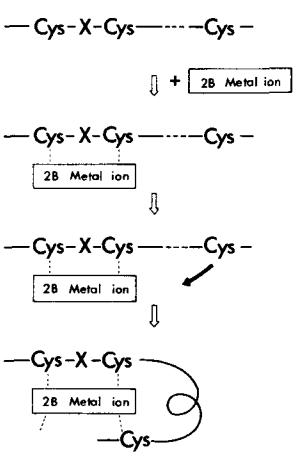


**Fig. 11.** Formation of the trithiolate complex of metallothionein with a transition metal (2B). From Kägi et al. 1979 [58] with permission

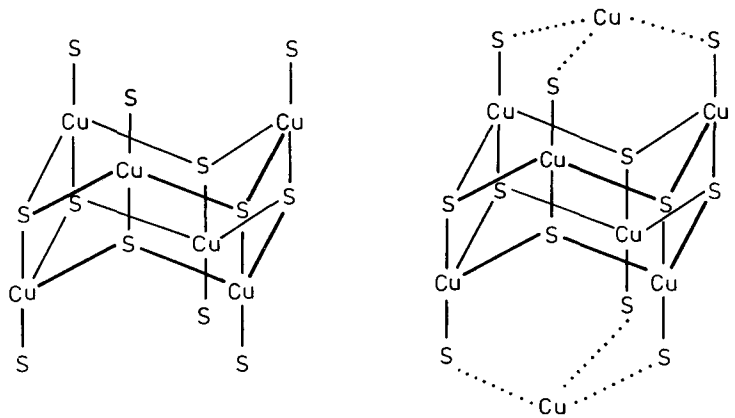


**Fig. 12.** Proposed structures of metal-thiolate clusters of $Cu_6$- and $Cu_8$-thioneins from yeast. From Hartmann et al. 1992 [66] with permission

manner of their binding probably differs from that of the other six copper ions [66].

According to this model, all of the copper ions in $Cu_6$-thionein are stably coordinated by four cysteine residues each. In $Cu_8$-thioneins, an additional copper ion is added to each end of the $Cu_6$-oligonuclear cluster. These two exposed positions are less stable, facilitating the extraction of the two copper ions.

## 1.3 Copper Proteins

Copper proteins occur in all three kingdoms of life: archaea, bacteria, and eukarya. They are either redox proteins or oxido-reductases, catalyzing reactions requiring high redox potentials. Non-catalytic copper proteins are electron- or oxygen-transport proteins. Copper enzymes may be divided into oxidases, mono- and di-oxygenases, and superoxide degrading enzymes. The type of copper center varies with its function and the function of a copper center varies with its surroundings. In this section, the properties, functions, and mechanisms of copper proteins and enzymes will be presented as known.

### 1.3.1 *Small Blue Proteins*

Small blue proteins are involved in various biochemical processes. Where their physiological function is known, it is that of single-electron transport proteins. The range of their redox potentials reaches from +183 mV (Halocyanin [18], +184 mV Stellacyanin [68] to 680 mV (Rusticyanin [68, 69]) as compared to $Cu^{2+}/Cu^{+}$, $E^{\circ} = +153$ mV. Very few redox proteins function in this range. This feature, and their characteristic blue color are the product of the type 1 copper center, the only redox-active group in these proteins. During electron

transport, the oxidation state of the central copper ion switches between Cu(I) and Cu(II). Four ligands, one cystein, one methionine, and two histidines, typically coordinate type 1 copper centers. In some small blue proteins, e.g., in azurin, a fifth, weakly interacting ligand has been discovered, an axial carbonyl oxygen [20, 23, 36, 70].

Under normal conditions, small blue proteins are monomeric. Their molecular masses range from 10 to 22 kD; the corresponding chain lengths vary from 97 to 139 amino acids. Sequence homologies allow small blue proteins to be divided into five group according to their phylogenetic relationship:

- the plastocyanin family (plastocyanin, amicyanin, pseudoazurin, halocyanin);
- azurin;
- the phytocyanins (stellacyanin, umecyanin, the basic blue protein, cusacyanin);
- auracyanin; and
- rusticyanin.

The phytocyanins differ from the other small blue proteins in that the "normal" methionine ligand of the copper ion is replaced by a glutamate residue [24]. The phytocyanins as well as auracyanin are also characterized by their high extent of glycosylation which, in some cases, doubles the weight of the protein [68, 71–73].

Most currently known small blue proteins are found either in bacteria or in eukarya. However, a small blue protein, halocyanin [74], was recently discovered in *Natronobacterium pharaonis* [75]. The fact that this bacterium belongs to the kingdom of the archaea will require new deliberations as to when and where the precursor of the small blue proteins originated.

#### *1.3.1.1*
#### *The Plastocyanin Family*

The sequence homologies of plastocyanin, pseudoazurin, amicyanin, and halocyanin are reflected in the similarities of their tertiary structures and in the crystal structures of plastocyanin [22], pseudoazurin [76, 77] and amicyanin [20, 78]. The peptide chains of plastocyanin and pseudoazurin consist of eight, and that of amicyanin nine, $\beta$-sheets which are connected by loops. The protein consists of two sandwiched planes, formed by strands 2, 8, 7, and 4 on the one side and strands 2, 1, 3, and 6 on the other. Strand 2 belongs to both planes, and strands 0 and 5 are not part of the sandwich [20, 71, 78]. Strand 0 is the N-terminal strand in amicyanin which is formally an elongation of the peptide chain as compared to plastocyanin and pseudoazurin (Fig. 13).

The amino acid residues coordinating the copper ion occupy corresponding positions in the $\beta$-sheets of plastocyanin, pseudoazurin, and amicyanin (Table 5).

The first histidine residue is in strand 4. The other ligands are situated in the loop connecting strands 7 and 8. The copper atom is bound in a depression near the surface of the protein formed by strands 2a, 4, 7, and 8. The distorted tetrahedral stereochemistries of the type 1 copper centers differ slightly from protein to protein [20]. Although small, these differences are ultimately responsible

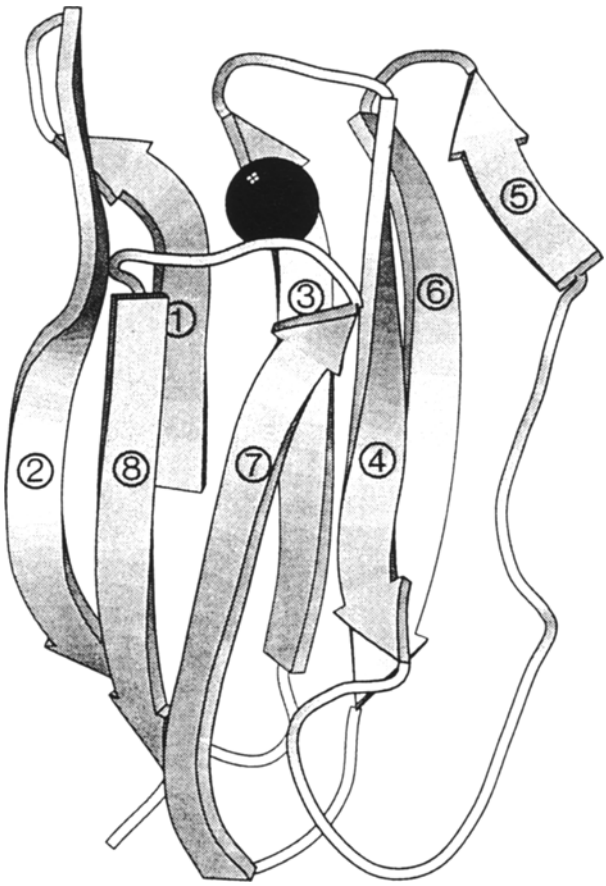


**Fig. 13.** Tertiary structure of plastocyanin from poplar. The two, four-stranded planes oppose each other and enclose the copper ion. From Rydén and Hunt 1993 [71] with permission. The coordinates for oxidized poplar pastocyanin originally determined by [22] were obtained from the Brookhaven Data Bank. The program MOLSCRIPT [79] was used for depiction

**Table 5.** Position of the copper ligands in plastocyanin, pseudoazurin, and amicyanin

| | His | Cys | His | Met |
|---|---|---|---|---|
| Pcy (poplar)[a] | 37 | 84 | 87 | 92 |
| Paz (*Alcaligenes*)[b] | 40 | 78 | 81 | 86 |
| Acy (methylobacterium)[c] | 54 | 93 | 96 | 99 |

[a] Chothia and Lesk 1982 [80].
[b] Vakoufari et al. 1994 [70].
[c] Romero et al. 1994 [20].

for the manifold redox potentials of the proteins of the plastocyanin family. An alignment of the amino acid sequences of plastocyanin (pcy) from poplar, pseudoazurin (paz) from *alcaligenes* and amicyanin (acy) from Pseudomonas reveals that, in comparison to plastocyanin, pseudoazurin has been elongated by about 30 amino acid residues at its C-terminus. Amicyanin, on the other hand, has been elongated by about 20 amino acid residues at its N-terminal end [22, 71, 78] (Fig. 14).

**Plastocyanin**

Plastocyanin, like all small blue proteins, is a monomeric protein which contains a single type 1 copper center. Depending on the organism of origin, its amino acid chain length ranges from 97 to 105 with a molecular mass of approximately 10 kD [81]. The mechanism of electron transport has been comprehensively reviewed in [82]. Plastocyanins are found in photosynthetic bacteria, in algae, and in plant chloroplasts where they are loosely bound to the surface of the inner thylakoid membrane [74]. Plastocyanins are part of the photosynthetic electron-transport chain where they connect the cytochrome $b_6$-*f*-complex and P700 of photosystem I. The electrons are transported up the redox potential gradient [8]. The redox potentials of the plastocyanins are situated at about 350 mV [7] and they are functionally equivalent to cytochrome *c 553* (cytochrome $c_6$) [83–85]. Cytochrome $c_6$ resembles the electron transport proteins of the first photosynthetic structures. When copper became available following oxygenation of the primordial atmosphere, the plastocyanins increasingly replaced cytochrome $c_6$. But even today there are organisms which can only utilize cytochrome $c_6$, while others only use plastocyanin or both electron carriers [8, 10, 15].

**Pseudoazurin**

Until now, pseudoazurin has only been found in bacteria, e.g., in the denitrifying bacteria *Alcaligenes faecalis* and *Achromobacter cycloclastes*. It is the electron donor of the green copper-protein nitrite reductase which catalyses the reduction of nitrite ($NO_2^-$) to nitrogen monoxide (NO) [86–89]. The physiological electron donor of pseudoazurin is as yet unknown [70]. Pseudoazurin has a molecular mass of approximately 13.5 kD and a chain length of about 123 amino acid residues [88]. The additional amino acids, as compared with plastocyanin, form the C-terminal end of the protein (Fig. 14). The pseudoazurins have redox potentials of about 230 mV [90, 91].

**Amicyanin**

Amicyanins function as electron carriers in the respiratory chains of some methylotrophic bacteria, e.g., *Thiobacillus versutus* [92]. They transfer single electrons from methylamine dehydrogenase to a cytochrome *c* [78] which then transfers the electron to cytochrome *c* oxidase. Amicyanin from *Pseudomonas denitrificans* has a molecular mass of 11.6 kD and contains 106 amino acid residues. Amicyanin contains one $\beta$-sheet more than the eight of plastocyanin and pseudoazurin, the result of several additional amino acids at its N-terminus [78] (Fig. 15). Like pseudoazurin, amicyanin is found exclusively in bacteria.

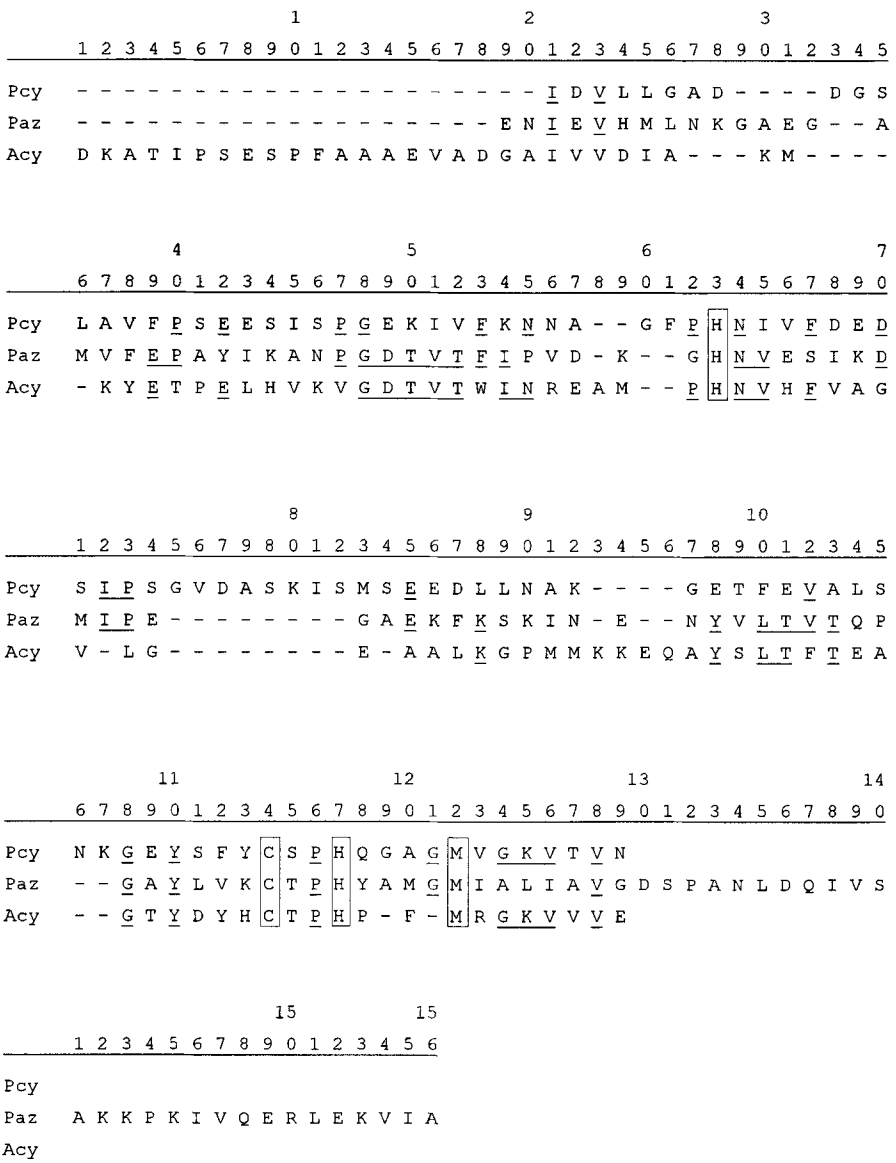


**Fig. 14.** Comparison of the amino acid sequences of plastocyanin (pcy), amicyanin (acy), and pseudoazurin (paz). The copper ligands are *framed*; conserved residues are *underlined*. Based on Guss and Freeman 1983 [22], Ryden and Hunt 1993 [71], and Durley et al. 1994 [78]

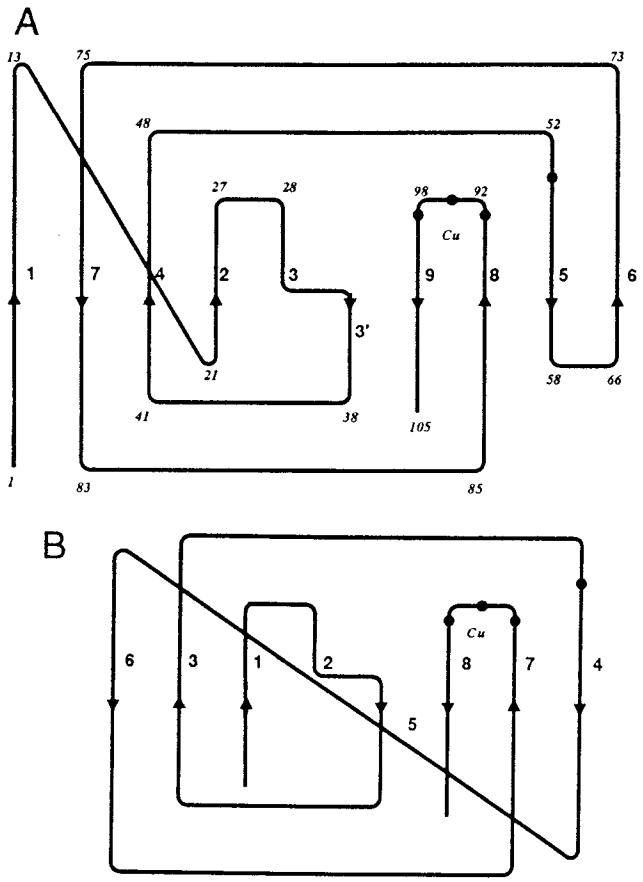


**Fig. 15.** Schematic folding plan and numbering scheme for the $\beta$-sheets of: **A** amicyanin; **B** plastocyanin. From Durley et al. 1993 [78] with permission

## Halocyanin

Halocyanin was recently discovered in *Natronobacterium pharaonis* [74, 75] and is the first small blue protein to be observed in an archaea. It is therefore hardly surprising that there are marked differences between it and the other members of the plastocyanin family. The protein's primary transcript is 163 amino acids long and has a molecular mass of 17.2 kD. Post-translational processing reduces halocyanin's length to 139 amino acids and molecular mass to 15.5 kD. The manner of processing resembles that of bacterial lipoproteins, promising new insights into the mechanisms and origin of archaea processing [74].

Halocyanin does, however, share homologies with plastocyanin, particularly in the three copper ligands located in the C-terminal region, as well as in the fourth N-terminally located ligand. Homologies occur in the four regions which form the $\beta$-meander as well [51]. The N-terminal region of halocyanin is ap-

proximately 45 amino acids longer than that of plastocyanin and is distinctly different. This region is markedly acidic, containing 10 negative residues [74] which do not occur in the other members of the plastocyanin family. This structure is possibly the result of an adaptation to the high salt concentrations of *Natronobacterium*'s natural habitat [93].

The post-translational processing of halocyanin includes a lipid-modification of a cysteine residue which possibly anchors the protein to a membrane. A spacer of seven Asn-Glu-repeats neighbors the modified cysteine, increasing the distance between protein and membrane and thus improves the interactions between halocyanin and electron-donors / electron-acceptors [74].

The main structural feature of halocyanin is, as in plastocyanin, the $\beta$-meander [74] and as a result, the tertiary structures of both proteins are similar. The geometry of halocyanin's type 1 copper center, however, resembles that of azurin [94] – a distorted trigonal bipyramidal structure with the methionine residue most distant from the copper ion. This may be a consequence of the weak coordination of a fifth, axial ligand, a carbonyl O-atom [18] which also occurs in azurin. The positions of halocyanin's copper ligands are Cys 124, His 127, Met 132, and His 86, [74]. Halocyanin's physiological function is also as yet unknown. Its redox potential of +183 mV suggests the function of an electron-donor for a terminal oxidase. This would require halocyanin to be localized on the outer side of the plasma membrane. However, assuming that the lipoprotein-signal peptides are similar between bacteria and archaea, the encoded signal peptide [95] would seem to suggest a cytosolic location for halocyanin [74].

**Comparison of Copper-Binding Centers**

Although the proteins of the plastocyanin family are phylogenetically related, they all possess different redox potentials and partners. Their specificities in redox partners result from the differences in the protein surface surrounding their type 1 copper centers. The differences in redox potentials are achieved by the slight differences in the structures of their type 1 copper centers. As will be discussed in more detail in Sect. 3, the type and conformation of ligands can, to a slight degree, determine the redox potential of a protein by stabilizing one or other oxidation states of the central ion. For, although the ligands and approximate tertiary structure of all three proteins are the same, a closer look at the conformation of the type 1 copper centers reveals small but relevant differences (Table 6).

In all three proteins, the type 1 copper is coordinated in a distorted tetrahedron in which the $Cu^{2+}$ ion is situated 0.35 (Pcy), 0.43 (Paz), and 0.40 Å (Acy) above the plane formed by both histidines and cysteine, towards the methionine residue [20]. In azurin, the distance between the methionine ligand and copper ion is markedly larger than for the members of the plastocyanin family, resulting in a more trigonal pyramidal conformation [20, 21], a ligand stereochemistry which also occurs in halocyanin [18, 94]. Other factors influence the redox potentials as well, e.g., the hydrophobicity of the region surrounding the copper center. However, so little is known about the collaboration between the various factors that it is currently not possible to predict accurately the probable redox potentials of type 1 copper proteins.

**Table 6.** A comparison of copper ligand bond lengths and angles in Pcy, Paz, Acy and Azurin

| distance Pyc/Paz/Acy/Az | Pcy (Å)[a] | Paz (*A. faec.*) (Å)[b] | Acy (*T. vers.*) (Å)[c] | Azurin (Å)[d] |
|---|---|---|---|---|
| Cu–37/40/54$N^{\delta 1}$ | 2.04 | 2.16 | 2.04 | 2.08 |
| Cu–84/78/93$S^{\gamma}$ | 2.13 | 2.17 | 2.13 | 2.14 |
| Cu–87/81/96$N^{\delta 1}$ | 2.10 | 2.29 | 2.13 | 2.00 |
| Cu–92/86/99$S^{\delta}$ | 2.90 | 2.91 | 2.84 | 3.11 |
| Cu–39O | | 3.83 | | |
| angle (°) | | | | |
| 37/40/54$N^{\delta 1}$–Cu–84/78/93 $S^{\gamma}$ | | 140 | 132 | |
| 37/40/54$N^{\delta 1}$–Cu–87/81/96$N^{\delta 1}$ | | 102 | 104 | |
| 37/40/54$N^{\delta 1}$–Cu–92/86/99$S^{\delta}$ | | 85 | 84 | |
| 84/78/93$S^{\gamma}$–Cu–87/81/96$N^{\delta 1}$ | | 108 | 111 | |
| 84/78/93$S^{\gamma}$–Cu–92/86/99$S^{\delta}$ | | 107 | 117 | |
| 87/81/96$N^{\gamma}$–Cu–92/86/99$S^{\delta}$ | | 110 | 101 | |

[a] Guss and Freeman 1983 [22].
[b] Vakoufari et al. 1994 [70].
[c] Romero et al. 1994 [20].
[d] Baker 1988 [21].

### *1.3.1.2 Azurin*

Azurins have, until now, only been found in bacterial organisms. Azurin from *Pseudomonas aeruginosa* is 128 amino acids [80] in length and has a molecular mass of 16 kD [96, 97]. The copper ligands His 46, Cys 112, His 117, and Met 121 form a distorted trigonal pyramid with the axial methionine ligand most distant from the central copper ion [21, 80]. Recent studies have uncovered a fifth, axial copper ligand, a weakly coordinating carbonyl O-atom [21, 23]. The proximity of the O-atom is possibly the basis of the trigonal bipyramidal conformation of azurin as opposed to the distorted tetrahedral conformation of the plastocyanins. This O-atom occurs in the plastocyanins as well but is more distant from the copper ion [22, 23, 36] (Table 7).

Azurin from *Pseudomonas aeruginosa* has a redox potential of 330 mV [80]. Its physiological function may be single-electron transfer to the cytochrome oxidase of bacterial respiration chains [98–100].

**Table 7.** A comparison of the copper ligand bond lenghts in plastocyanin (Pcy) from poplar and azurin (Az) from *Pseudomonas aeruginosa*. Modified from [36]

| Pyc/Aurin | bond length in Pcy (Å) [22] | bond length in AZ (Å) [23] |
|---|---|---|
| Cu–$N^{\delta 1}$His 37/46 | 2.04 | 2.09 |
| Cu–$S^{\gamma}$Cys 84/112 | 2.13 | 2.26 |
| Cu–$N^{\delta 1}$His 87/117 | 2.10 | 2.04 |
| Cu–$S^{\delta}$Met 92/121 | 2.90 | 3.12 |
| Cu–O | 3.82 | 2.95 |

#### *1.3.1.3*
#### *Phytocyanins*

The physiological functions of the phytocyanins are also currently unknown. This family of proteins consists of stellacyanin (20 kD) [97, 101], umecyanin (14 kD), the basic blue protein (from cucumber = plantacyanin) (8 kD), and cusacyanin (molecular masses see [17]).

The type 1 copper center of the phytocyanins differs from that of the other small blue proteins in that the methionine ligand is replaced by a glutamine [24]. The redox potential of stellacyanin from *Rhus vernicifera* is 184 mV [68].

#### *1.3.1.4*
#### *Auracyanin*

Three different auracyanins have been isolated from the green, photosynthetic bacterium *Choroflexus aurantiacus*: auracyanin A [102], B-1, and B-2. The first lacks glycosylation [102] and has a molecular mass of 14 kD. Auracyanin B-1 and B-2 are glycosylated and have molecular masses of 22 and 18 kD [68]. The differences in molecular mass result from differences in their glycosylation. Auracyanin B-2 may, however, be the product of post-translational processing of B-1. All three forms of auracyanin are presumably localized in the periplasm. Their postulated function is the single-electron reduction of cytochrome *c* 554 [68] possibly making them functionally equivalent to cytochrome $c_2$. All three auracyanins have redox potentials of 240 mV, while that of the postulated redox partner, cytochrome *c* 554, is 300 mV [68, 103].

The central copper ion of the auracyanins is probably coordinated by two histidines, one cysteine, and a methionine residue. The auracyanins are unique among the small blue proteins in that they possess a methionine and a glutamine residue (see phytocyanins) which both could act as the fourth ligand coordinating the central copper ion. This copper center is surrounded by a hydrophobic environment similar to that of the other small blue proteins [68]. Amino acid sequence comparisons place auracyanin in a phylogenetic tree at approximately equal distances from azurin and plastocyanin [68, 92].

#### *1.3.1.5*
#### *Rusticyanin*

The chemolithotropic bacterium *Thiobacillus ferrooxidans* is able to oxidize soluble iron(II) aerobically. The energy released is utilized to produce ATP by oxidative phosphorylation [104]. One of the participating electron-carriers is the small blue protein rusticyanin [105, 106]. Neither rusticyanin's position within the electron-transport chain nor its physiological electron-donors or electron-acceptors are known [107].

Rusticyanin has a molecular mass of 16.6 kD [108] and a redox potential of 680 mV [109, 110], by far the highest redox potential known for a small blue protein. Sulfatoiron(II), a possible physiological electron-donor for rusticyanin, has a redox potential of 650 mV [107]. Rusticyanin is extremely acid-stable with

a pH-optimum of pH 1–3 [111]. This is in contrast to the other small blue proteins, whose redox potential and function are extremely pH-dependent.

Rusticyanin's type 1 copper center with its ligands His 85, Cys 138, His 143, and Met 148 resembles those of the other small blue proteins. Although its tertiary structure is a $\beta$-meander, there are distinct differences between the amino acid folding patterns of rusticyanin and the other small blue proteins. Plastocyanin contains 8 [22, 71], amicyanin 9 [20, 78], and rusticyanin 13 $\beta$-strands, respectively [112] (Fig. 16).

The central copper ion is surrounded by 36 amino acids. These 36 residues include the 4 copper ligands, 7 glycins, as well as 20 hydrophobic residues. The remaining five residues are ambivalent: two serines, one threonine, one glutamic acid, and one aspartic acid, both of which are protonated at these low pH values. Thus, the type 1 copper center is protected from the solvent by a hydrophobic micro-environment, thereby achieving acid stability and a high redox potential [112].

### 1.3.2
### *Type 2 Copper Proteins*

As shown in Sect. 3, the structure of type 2 copper centers is less uniform than in types 1 and 3. Type 2 copper proteins can, furthermore, neither be phylogenetically grouped by comparison of amino acid sequences nor by a common tertiary structure. The class of type 2 copper proteins contains oxidases, mono- and di-oxygenases, as well as enzymes, which participate in metabolizing reactive species.

The proteins treated in this section will only contain type 2 copper centers. Additional type 2 copper centers may be found in blue oxidases, in which they form trinuclear centers with type 3 copper ions, and in nitrite reductase. In nitrite reductase, the type 2 copper center is coupled to a type 1 copper center via a cysteine residue.

#### *1.3.2.1*
#### *Non-Blue Oxidases*

Non-blue oxidases are members of the enzyme class of oxidases, which oxidize their substrates by subtracting electrons without the transferal of oxygen. Two electrons are transferred from the substrate to oxygen, which is reduced to hydrogen peroxide. In contrast to the blue oxidases, non-blue oxidases contain neither type 1 copper centers, which are responsible for the former's color, nor type 3.

**Amine Oxidase**

Although there are flavin-dependent as well as copper-dependent amine oxidases, this section will only deal with the copper enzymes. Amine oxidase (EC 1.4.3.6) catalyzes the oxidative reaction of amines to aldehydes and ammonia. The two-step process generates two electrons which are utilized to reduce oxygen to hydrogen peroxide ($H_2O_2$) [28, 113]:

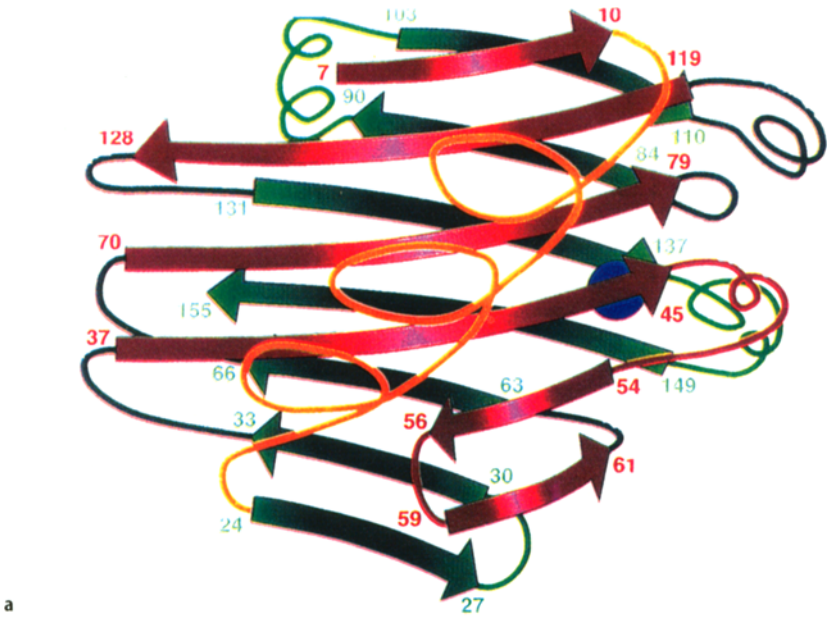


a

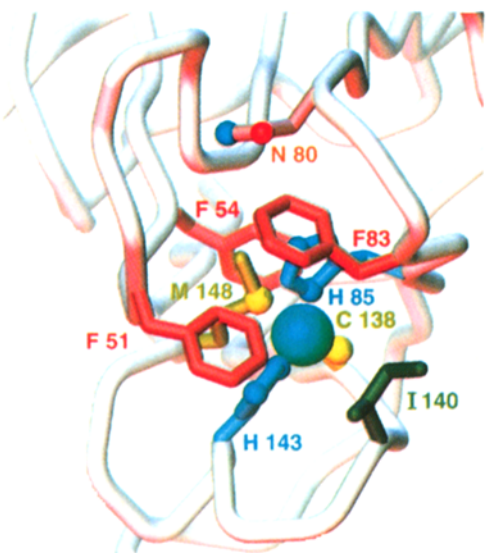


b

**Fig. 16a, b.** Folding pattern of the small blue protein rusticyanin. The protein consists of thirteen $\beta$-strands: **a** ribbon model – the copper ion is represented by the *blue circle* [112]; **b** disposition of ligands and spatially close side-chains in the copper site of one of the solution structures of Cu(I) rusticyanin. [112a] with permission

$EC{=}O + RCH_2NH_2 \rightarrow ECHNH_2 + RCHO$
$ECHNH_2 + O_2 \rightarrow EC{=}O + NH_3 + H_2O_2$
$EC{=}O$ : the enzyme and cofactor
$RCH_2NH_2$ : the substrate

Amine oxidase occurs in all types of organisms, from prokaryotes to animals and plants. While its catalytic function is understood, its physiological function remains unknown. Various functions have been suggested [114]:

- removal of biogenic amines from blood plasma [115];
- cross-linkage of structural proteins such as collagen and elastin [116];
- regulation of the intracellular polyamine concentration [117];
- participation in tumor suppression [118].

**Structure.** Amine oxidase from lentil seeds is a dimeric enzyme with a molecular mass of 140 kD [119]. Each subunit has a length of 569 amino acids and carries two carbohydrate side-chains [119, 120] attached to Asn-234 and Asn-364 [120].

The crystal structure of amine oxidase from *Escherichia coli* reveals that the C-terminal domain (440 amino acids) primarily has a $\beta$-sandwich structure. This domain contains the active site with a type 2 copper center, the cofactor, and the dimerization contact site. Furthermore, there are three domains of approximately 100 amino acids length which have an $\alpha$- and a $\beta$-structure. The second and third of these smaller domains show marked sequence homology and are conserved in the amine oxidases of various organisms. The first of these smaller domains may, however, be lacking in some amine oxidases [28]. The structure of an eukariotic aminoxidase from pea seedling is seen in [121].

**Structure of the active center.** The active centers of this dimeric enzyme are so well embedded into its protein structure that they are inaccessible to the solvent. The two centers are situated approximately 30 Å apart from each other but connected by $\beta$-strands. The active center consists of a type 2 copper center and a cofactor. Sequence comparisons have established that the residues His 8, His 246, and His 357 coordinate the copper ions in both yeast and plants (e.g., lentil seeds) [120,122]. The participating cofactor is typical for amine oxidases, diamine oxidases, and lysyl oxidases but has not yet been found in any other protein – 2,4,5-trihydroxy-phenylalanine quinone [123, 124] (also known as TOPA-quinone, TPQ or 6-hydroxy-DOPA quinone), an internal cofactor which is created by post-translational modification of the tyrosine in position 387 [120]. The consensus sequence of the amino acids neighboring the TOPA cofactor are conserved in all known amine oxidases – Asn-TOPA-Asp/Glu [113, 120, 123, 125–127]. The positions of the histidine ligands relative to TOPA quinone are conserved in all known amine oxidases as well. The chain lengths of the amine oxidase monomers vary according to the organism of origin: 692 residues in yeast [128], 762 in bovine serum amine oxidase [128, 129] and 569 in the enzyme from lentil seeds [120, 130].

The production of TOPA must be strictly regulated as the free compound is extremely neuro- and cytotoxic [131]. It appears improbable that the reaction of

tyrosine to TOPA is catalyzed by one or more additional enzymes which recognize the TOPA consensus sequence, as this sequence, Asn-Tyr-Asp/Glu, also occurs in its non-modified form [113]. The expression of amine oxidase in an organism which has lost its endogenous gene results in a correctly modified cofactor [113]. Consequently, the ability to synthesize TOPA is probably encoded in the amine oxidase itself. One possibility of TOPA synthesis could be catalysis by the neighboring type 2 copper center [127]. This "self-processing" would occur by hydroxylation of the tyrosine ring via a copper-hydroperoxide. The resulting DOPA hydroquinone is then oxidized to the quinone form via a two-electron reduction of oxygen to hydrogen peroxide. Following a 180° rotation of the ring, the residual copper hydroxide would conduct a nucleophilic attack on the C2-atom of DOPA quinone, resulting in the cofactor-factor TOPA quinone [127, 132] (Fig. 17)

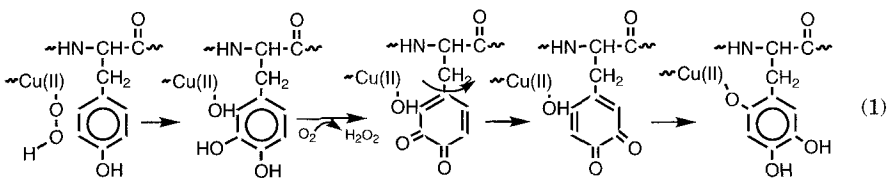


**Fig. 17.** Synthesis of the TOPA quinone cofactor in amine oxidases. From Cai and Klinman 1994 [113] with permission

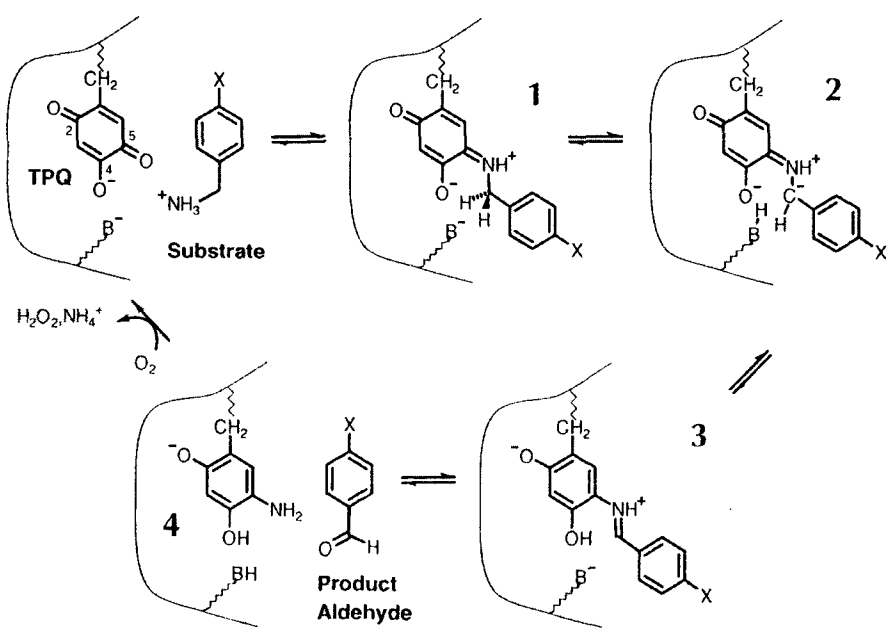


**Fig. 18.** Catalytic cycle of the amine oxidases. Only TOPA quinone is required for catalysis; copper functions solely as a cofactor in its synthesis. From [28] with permission

The postulated catalytic mechanism of amine oxidases starts from the quinone form of the cofactor (Fig. 17). The distal oxygen atom is replaced by an amino group in a transamination reaction. The amine is then re-oxidized by molecular oxygen to the original quinone. The copper ion is not involved directly in catalysis but is only a cofactor in the synthesis of TOPA quinone (Fig. 18).

Amine oxidase crystallizes in two different forms, an active and an inactive form. In the inactive form, the type 2 copper center is coordinated in a distorted tetrahedral conformation by the three histidines and the TOPA cofactor. The conformation of the active type 2 copper center, however, is a distorted planar square. A water molecule and three histidines coordinate the copper ion equatorially, while a second water molecule forms an apical ligand. TOPA is not a direct copper ligand in the active enzyme form, but occupies a position near aspartate 383. This residue is conserved in amine oxidases and possibly functions as a base during catalysis (Figs 19 and 20) [28, 28a].

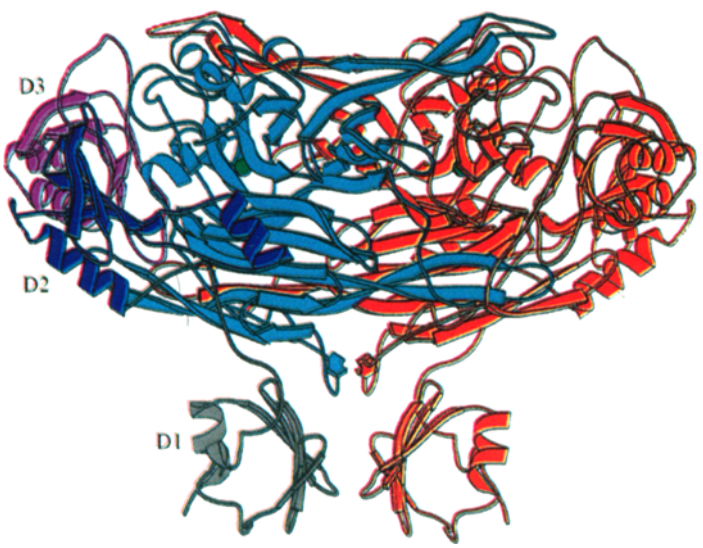


**Fig. 19.** **a** The molecular structure of the *E. coli* amine oxidase dimer. In this view the dyad axis relating the two subunits is vertical in the plane of the page. One 80 kD subunit is colored *red* and the other is colored to identify domain structure. In this subunit domain D1 (residues 1–99) is *grey*, D2 (residues 100–185) is *blue*, D3 (residues 186–285) is *magenta* and the remainder of the subunit, comprising the $\beta$-sandwich domain, is *cyan*. The locations of the active site coppers are indicated by *green* spheres. From [28] with permission

## Diamine Oxidase

Diamine oxidase is a member of the amine oxidases and catalyses the oxidative desamination of putrescine and histamine to amino aldehydes, hydrogen peroxide, and ammonia [133]:

$$RCH_2NH_2 + O_2 + H_2O \rightarrow RCHO + NH_3 + H_2O_2$$


**Fig. 19. b** Three-dimensional structure of pea seedling amine oxidase (PSAO): (a) PSAO dimer viewed perpendicular to the molecular dyad axis. The two subunits are in *orange* and *white*, respectively. The two $\beta$-strand arms which extend from the orange subunit along the surface of the white subunit are seen clearly; (b) PSAO molecule viewed along the molecular dyad axis. The large $\beta$-sandwich domain D4 is in *orange* for one subunit and *white* for the other, as in (a). Domains D2 and D3 of both subunits are shown in *red* and *green*, respectively. An additional N-terminal domain found in E.coli amine oxidase is not coded in the PSAO gene. From each D4 domain, a $\beta$-strand arm (*yellow*) extends along the surface of the molecule towards the D3 domain of the other subunit.With permission from [121]

Diamine oxidase occurs, like amine oxidase, in bacteria, animals, and plants [133]. The comparison of amino acid sequences of the amiloride-binding protein from human kidney, rat colon, diamine oxidase from human placenta, pig kidney, and amine oxidase from *Hansenula polymorpha* and lentil seeds has shown that the amiloride-binding protein and diamine oxidase are identical proteins[29]. The amiloride-binding protein was previously postulated to function as an epithelial sodium-transporter. While its physiological function is still

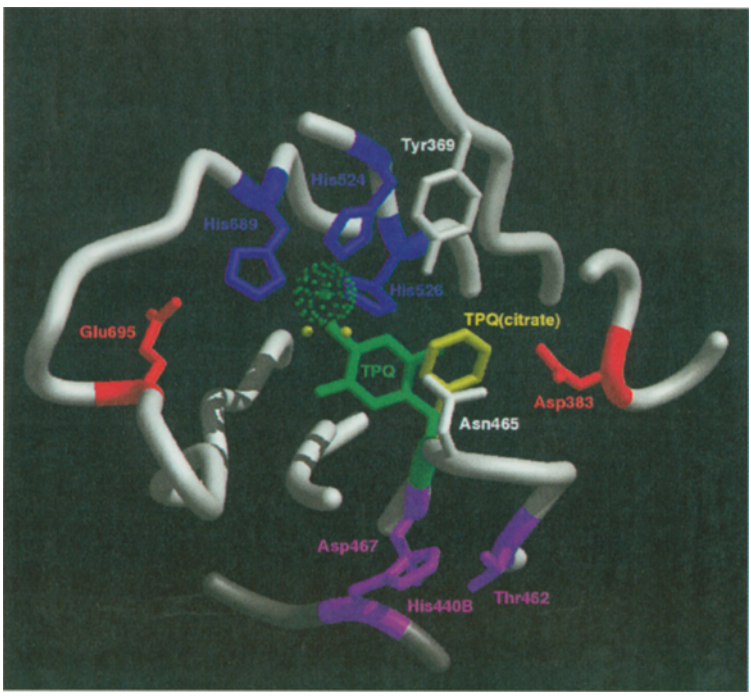


**Fig. 20.** **a** Active site of *E. coli* amine oxidase. The polypeptide backbone is shown as a continuous coil, colored *white* for subunit A and *grey* for subunit B. Conserved residues are shown in all-atom representation, and the copper is shown as a *green* van der Waals dot surface. The position of TPQ in crystal form I is illustrated in *green*, coordinated to the copper. The precise location and orientation of the TPQ ring are not completely determined at the resolution of the current studies of crystal form II, and its general location is indicated by a *yellow* phenyl ring, close to the putative catalytic base Asp 383 (*red*). In crystal form II, TPQ is not a copper ligand, and the copper coordination is completed by two water molecules, shown in yellow (with permission from [28])

not completely known, these data make a function as sodium-transporter improbable [29, 134]. Other functions are still being discussed, for example, the regulation of the activity of exogenous or endogenous histamine in smooth muscle or other target cells [135], the regulation of cell growth by decreasing intracellular concentrations of the growth promoter putrescein [136–138], or even, the regulation of cell mass via the hydrogen peroxide produced by diamine oxidase [139–141].

**Structure.** Diamine oxidases are homo-dimeric enzymes. The subunits weigh between 60 and 105 kD depending upon the organism of origin [114]. Human diamine oxidase from kidneys is composed of 752 amino acid residues, and the corresponding enzyme from rat colon has 747 residues [29]. Diamine oxidases share the TOPA-chinon cofactor with amine oxidases. The ligands of the type 2 copper center in diamine oxidase are possibly the conserved residues Cys 391, Cys 417, and His 510 [29].

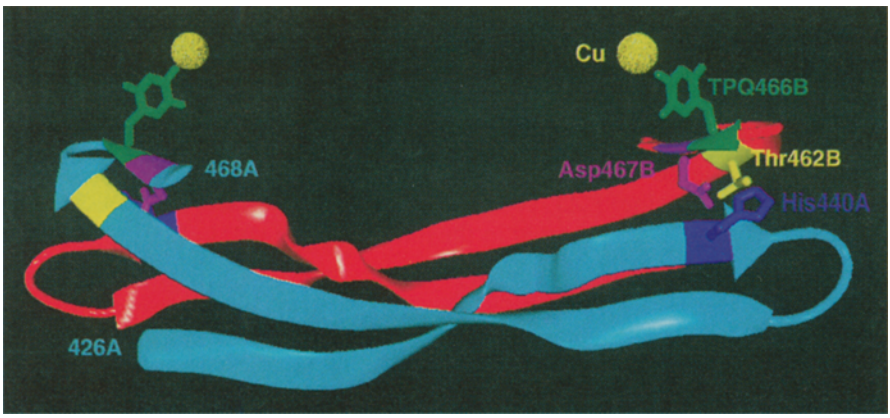


b

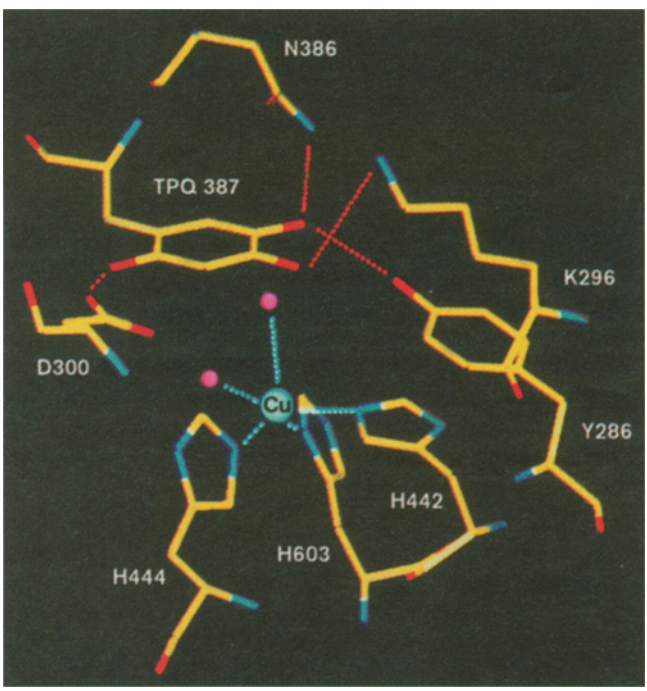


c

**Fig. 20.** b Symmetry-related $\beta$-hairpins linking the active sites of the *E. coli* amine oxidase monomers. $\beta$-strands are shown as flat arrows colored *red* in subunit A and *cyan* in B. The active-site coppers are shown with van der Waals dot surfaces in *green*, and the side chains of a number of conserved residues are in all-atom representation. Asp467A (*red*) and Thr462A (*yellow*) on either side of TPQ466A (*green*) both interact with His440B (*blue*) at the active site of subunit A, and equivalent symmetry-related interactions occur at the other end of the $\beta$-hairpins in the active site of subunit B (with permission from [28]). c Active site of pea seedling amine oxidase, showing the Cu atom (*blue* sphere), the two coordinated water molecules (*magenta* spheres), the Cu-binding residues (His442, His444 and His603), the cofactor (TPQ387), and other active site residues. Hydrogen bonds are shown as *dashed red lines*. (With permission from [121])

**Lysyl oxidase**

Although lysyl oxidase (EC 1.4.3.13) is also a member of the amine oxidases, it possesses little homology in structure or amino acid sequence with the other non-blue oxidases. The native enzyme is a monomer of 32 kD [142]. Its physiological function is the cross-linkage of the structural proteins collagen and elastin. This is achieved by the oxidation of a peptidyl-lysine to an amino-adipate semi-aldehyde (allysine) [143, 144]: the substrate is oxidized, reducing the enzyme. The enzyme is regenerated in the following step [145]:

$$RCH_2NH_2 + Enz_{ox} \rightarrow RCHO + Enz_{red}\text{-}NH_2$$
$$Enz_{red}\text{-}NH_2 + O_2 + H_2O \rightarrow Enz_{ox} + NH_3 + H_2O_2$$

Removal of the coordinated copper catalytically inactivates lysyl oxidase. Nutritional copper deficiencies, consequently, lead to a reduction in the cross-linkage of collagen and elastin, resulting in damaged connective tissues [146–148]. An additional function of lysyl oxidase has been suggested, the participation in the suppression of tumors [149]. As in the other amine oxidases, TOPA is utilized as a cofactor. The catalytic cycle may function as described earlier. Lysyl oxidase is synthesized as a 47 kD precursor (rat). Post-translational processing leads to the removal of a signal peptide of 21 amino acid residues, followed by the tripeptide in position 62–64 and, finally, the dipeptide in position 134–135 [150]. This last dipeptide contains the only conserved amino acid which is glycosylated (Asp 91 in rats and Asp 97 in humans) [151]. The glycosylation may play a role in the post-translational processing and transport of the protein from the Golgi apparatus to the extracellular matrix [151].

The region between residues 284 and 301 of lysyl oxidase is conserved in humans, rats, and mice [151]. It contains four histidine residues (289, 292, 294, and 296), of which at least three participate in the coordination of the copper ion, forming a tetragonally distorted octahedron [151,142] (Fig. 21).

**Galactose Oxidase**

Galactose oxidase (EC 1.1.3.9) differs significantly from the other non-blue oxidases. The enzyme (from the fungus *Dactylium dendroides*) consists of a single peptide chain of 639 amino acids [152] and has a molecular mass of 68 kD [30]. The active center contains a single type 2 copper center. It has neither additional, dissociable prosthetic groups nor TOPA quinone, the typical cofactor of the other non-blue oxidases [153].

**Function.** Galactose oxidase catalyses the oxidation of primary alcohols to aldehydes, reducing oxygen to hydrogen peroxide in a two-electron reduction [30]:

$$RCH_2OH + O_2 \rightarrow RCHO + H_2O_2$$

Its substrate specificity is very low, catalyzing the turnover of a wide range of compounds from small molecules such as propane-1,2-diol to polysaccharides. The best studied substrate is dihydroxyacetone which is oxidized with triple the speed of D-galactose [154]. Although galactose oxidase has a very low substrate specificity, its stereospecificity is absolute: D-glucose and L-galactose are not oxidized [30]. The enzyme's specificity for electron-acceptors is low as well. In

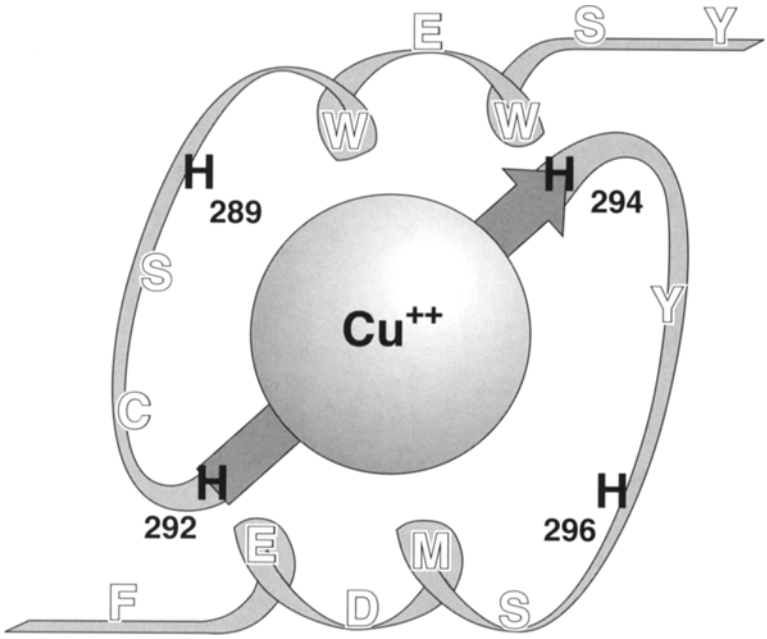


**Fig. 21.** Type 2 copper center of lysyl oxidase. The four histidine residues probably coordinate the copper ion. From Krebs and Krawetz 1993 [151] with permission

the absence of oxygen, it will utilize electron-acceptor compounds such as $K_3Fe(CN)_6$ as well [155].

### Structure

The three-dimensional structure of galactose oxidase consists almost entirely of $\beta$-strands; only a single, short $\alpha$-helix (residues 328–331) occurs. The enzyme can be divided into three domains: domain 1 (residues 1–155), domain 2 (residues 156–532), and domain 3 (residues 533–639) (Fig. 22) [30].

Domain 1 contains the first 8 $\beta$-strands as well as a binding site for a sodium ion and for D-galactose. It is yet unknown whether the sodium ion is of importance for the enzyme's function. Domain 1 is of some distance from the copper center and its function is not clearly defined. It is possibly a "chaperone" for the correct folding of the enzyme, in which domain 1 is utilized as a blueprint for the complicated folding of domain 2. The D-galactose binding site of domain 1 may possibly be needed to attach the enzyme to the cell walls of trees, the natural habitat of *Dactylium dendroides* [30].

Domain 2 is the largest of the three domains, containing 28 $\beta$-strands and the short $\alpha$-helix. It also contains three of the four internal protein ligands, the residues important for the enzyme's catalytic activity and three external ligands: the copper ion as well as two acetate ions. The 28 $\beta$-strands are arranged in a pseudo-sevenfold geometry, known from the neuraminidase of the influenza

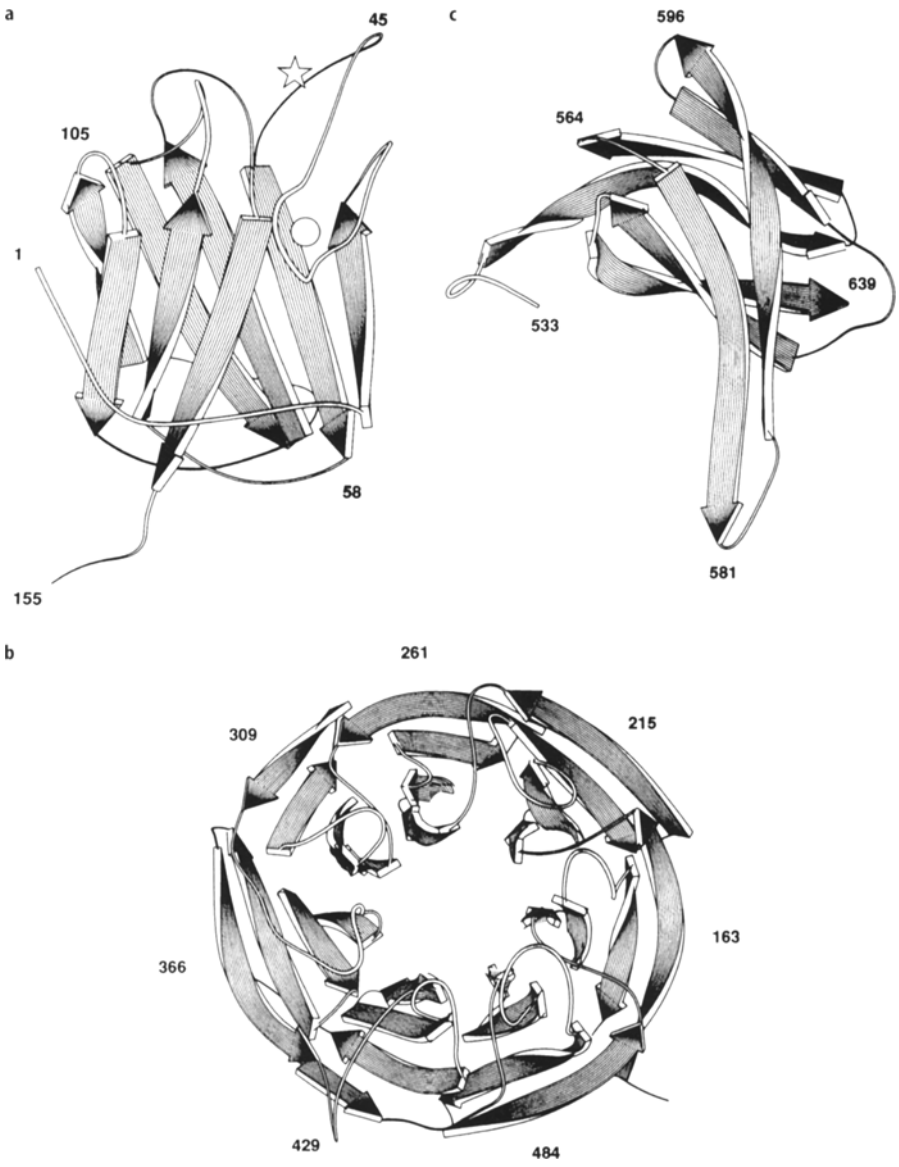


**Fig. 22a–c.** Ribbon model of the three domains of galactose oxidase: **a** domain 1; **b** domain 2; **c** domain 3 of galactose oxidase. From Ito et al. 1994 [30] with permission

virus [156] and from the methylamine dehydrogenase from *Thiobacillus versutus* [157]. However, the amino acid sequences of these enzymes lack homology [30], i.e., these structures are probably the result of a convergent evolution. Domain 2 has a large cavity in its middle which accommodates two $\beta$-strands of domain 3 [30].

Domain 3 is situated to a side of domain 2, opposite the copper center. It consists of seven $\beta$-strands of which two extend into the cavity of domain 2. When beheld from C- to N-terminus, domain 3's topology is very similar to that of the $F_{ab}$ fragment's $C_L$-domain in immunoglobulins. Domain 3's primary function is most probably structural stabilization. The fourth, internal copper ligand (His 581) is situated on the tip of the two $\beta$-strands which extend into domain 2's cavity [30].

**The copper center.** Galactose oxidase is capable of catalyzing a two-electron reduction, although it only contains a single type 2 copper center. This assumption is, however, incorrect. Recent studies show that the copper ion occurs in its divalent state, $Cu^{2+}$, which is antiferromagnetically coupled to a tyrosyl radical (Tyr272) and is, therefore, ESR-inactive [158].

The copper center is situated on the surface of domain 2, close to its sevenfold axis. It is surrounded by a multitude of aromatic side-chains, many of which probably participate in the generation or stabilization of the free radical [30]. The copper ion is coordinated by four internal and a single external ligands: the $O^{\eta}$ from Tyr 272, $N^{\varepsilon 2}$ from His 496, His 581 and an acetate ion almost form a square around the copper ion (Table 8). The $O^{\eta}$ from Tyr 495 is the fifth, axial ligand and is located furthest from the central ion (Fig. 23), indicating a relatively weak coordination of this ligand [159].

The tyrosyl radical is bound to Cys 228 via a thioether. It is as yet unclear how this bond is formed; it may possibly arise during the first catalytic cycle of the enzyme. It is improbable that the bond is formed by another enzyme as the thioether is concealed beneath tryptophane 290 and is, therefore, inaccessible to

**Table 8.** Bond lengths and angles of the galactose oxidase ligands at pH 4.5 and 7.0 (values in parentheses). Water replaces the acetate ion at neutral pH values. According to Ito et al. 1994 [30]

| ligand | bond length (Å) | | ligands | bond angle (°) | |
|---|---|---|---|---|---|
| Cu–$O^{\eta}$ (Tyr 272) | 1.9 | (1.9) | $O^{\eta}$ (Tyr 495)–Cu–$N^{\varepsilon 2}$ (His 581) | 99 | (100) |
| Cu–$N^{\varepsilon 2}$ (His 496) | 2.1 | (2.2) | $N^{\varepsilon 2}$ (His 496)–Cu–$N^{\varepsilon 2}$ (His 581) | 89 | (91) |
| Cu–$N^{\varepsilon 2}$ (His 581) | 2.2 | (2.2) | $N^{\varepsilon 2}$ (His 496)–Cu–O (acetate) | 90 | (–) |
| Cu–$O^{\eta}$ (Tyr 495) | 2.7 | (2.6) | N (His 496)–Cu–O (water) | – | (93) |
| Cu–O (acetate) | 2.3 | (–) | $O^{\eta}$ (Tyr 495)–Cu–$N^{\varepsilon 2}$ (His 581) | 97 | (104) |
| Cu–O (water) | – | (2.8) | $O^{\eta}$ (Tyr 495)–Cu–$N^{\varepsilon 2}$ (His 496) | 106 | (103) |
| | | | $O^{\eta}$ (Tyr 495)–Cu–$O^{\eta}$ (Tyr 272) | 75 | (79) |
| | | | $O^{\eta}$ (Tyr 272)–Cu–O (acetate) | 83 | (–) |
| | | | $O^{\eta}$ (Tyr 272)–Cu–O (water) | – | (76) |
| | | | $O^{\eta}$ (Tyr 495)–Cu–O (acetate) | 91 | (–) |
| | | | $O^{\eta}$ (Tyr 495)–Cu–O (water) | – | (89) |

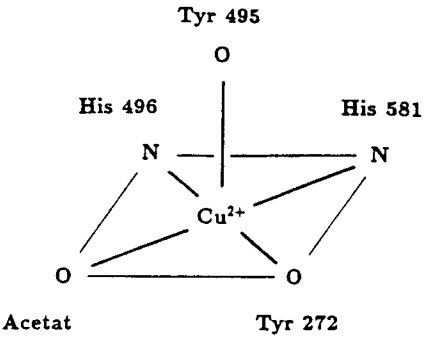


**Fig. 23.** Model of the type 2 copper center of galactose oxidase after Ito et al. 1991 [30]

the solvent. This tryptophane residue not only conceals the thioether bond but probably participates in either stabilizing the free radical or in a different step of the catalytic mechanism as well [30].

**The Tyr–Cys–Trp complex.** This complex participates in the generation or stabilization of the free radical. This radical exhibits an extremely low redox potential (0.41 V [160] in contrast to 0.94 V for free tyrosine [161]), which is probably the result of the thioether bond. The role played by copper in the generation of the radical has not yet been clarified [30]. It may be required for the generation of the radical in its first catalytic cycle (see above), which could then form the thioether bond, reducing its redox potential. This reduction enables future radical formation without assistance from the copper ion [30].

**Substrate binding.** The copper center contains a pocket [30,162] which, in the enzyme's native state, is occupied by an acetate ion and water. This pocket is structurally complementary to D-galactose in its chair conformation. The O6-atom of D-galactose can, after displacing the acetate ion and water molecule, coordinate directly with the copper ion. Steric effects hinder L-galactose in binding to the active center [30].

Galactose oxidase, as well as the other non-blue oxidases, avoids the necessity of an external cofactor by creating an internal cofactor via modification of a residue of its own peptide chain. The amino acid residue which is modified in all cases is a tyrosine. While the amine oxidases produce TOPA quinone, galactose oxidase forms a thioether bond between the tyrosine and a cysteine residue. This modified tyrosine is the site which carries the free radical.

### *1.3.2.2*
### *Monooxygenases*

#### Dopamine β-Hydroxylase

Dopamine β-hydroxylase (EC 1.14.17.1) is a glycoprotein which hydroxylates dopamine to norepinephrine during the biosynthesis of catecholamines. The enzyme occurs in the synaptic vesicles of noradrenergic and adrenergic brain

nerves and sympathetic ganglions, as well as in the storage granules of chromaffinic cells of the adrenal medulla [163].

The holoenzyme is a tetramer of 290 kD molecular mass, consisting of two, reversibly associated, disulfide-linked dimers[164–166]. Dopamine β-hydroxylase occurs in a soluble and a membrane-associated form [167, 168], which are both encoded by the same mRNA [163]. Dissociation of the enzyme results in monomers of either approximately 72–73 kD or 75–77 kD molecular mass. While the lighter monomers may occur in either form, the heavier monomers only occur in the membrane-associated enzyme [169, 171].

This membrane-associated form is possibly the precursor of the soluble enzyme [170]. Its release would occur by the removal of the membrane anchor and the loss of a non-covalently bound phospholipid which possibly collaborates in keeping the enzyme membrane-bound [167, 170]. These differences in weight of soluble and membrane-bound enzyme may, however, be based on differences in their degree of glycosylation and not on the lengths of their peptide chains [163, 172], an explanation supported by the fact that the 72–73 kD monomers occur in both forms [163, 169, 171]. This, however, would require that the peptide anchor, if it even exists, is not the only structure for affixing the enzyme to the membrane, a role which might be assumed by the non-covalently bound phospholipid.

**Structure of the copper center.** Each of the enzyme's subunits accommodates an active center containing two copper atoms, which have different ligands and form two mononuclear centers [168, 173, 174]. This is in contrast to other proteins with two copper ions per active center (hemocyanin and tyrosinase) [175–177] possessing binuclear centers in which the copper ions are not isolated from each other [37]. Were dopamine β-hydroxylase to possess a binuclear center, both $Cu^{2+}$ ions would be antiferromagnetically coupled and, thus, ESR-inactive. This, however, is not the case [178, 179]. A structure has been proposed, based on various spectroscopic studies, in which the first copper atom (CuA)

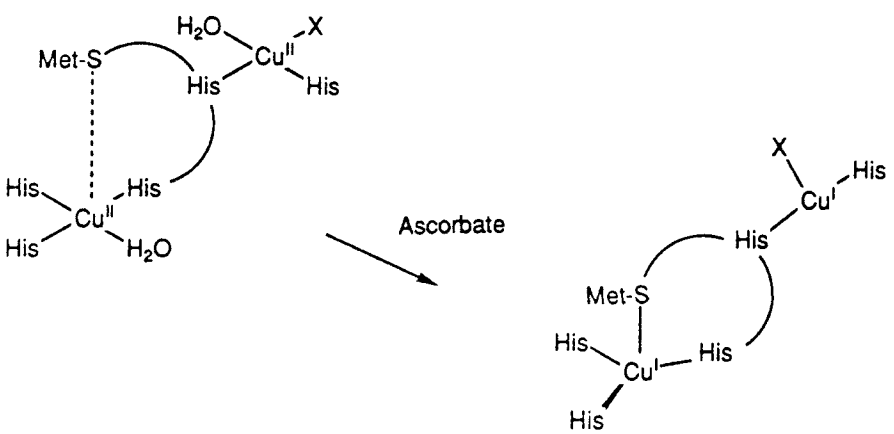


**Fig. 24.** Oxidized and reduced state of the dopamine β-hydroxylase copper center. The reducing agent is ascorbate. From Pettingill et al. 1991 [31] with permission

possesses three and the second copper atom (CuB) two histidine ligands [31] (Fig. 24). The reduced CuA center is coordinated by a fourth ligand, a methionine, which is replaced by a water molecule upon oxidation. The CuA center has four ligands in both oxidation states. The third ligand of CuB, which is not exchanged upon oxidation, has not yet been identified. The fourth coordinative position of the oxidized CuB center is occupied by a water molecule, and is, upon reduction, used to bind an oxygen molecule [31]. The oxidized form is reduced by ascorbate.

A structural motive, which also occurs in other copper enzymes, was discovered, while searching for potential copper ligands in dopamine β-hydroxylase. This motive, HXH* (H* = His or Met), normally participates in copper-binding. In nitrite reductase, it couples the type 1 and type 2 copper centers: the two exterior amino acid residues (both His) coordinate the type 2 copper ion, and the central residue (Cys) the type 1 center [31, 51]. In dopamine β-hydroxylase, this motive couples the two type 2 copper centers. The conserved region in the dopamine β-hydroxylases is V(248)HHM. His 249 and Met 251 are CuA ligands, whereas His 250 belongs to the ligands of CuB. While separating the two copper atoms, this type of ligand arrangement on the peptide chain enables electrons to be transferred between the copper centers [31].

**Mechanism.** Dopamine β-hydroxylase operates via a ping-pong mechanism, in which the oxidized form of the enzyme is reduced by ascorbate (ping). In the second step, dopamine and oxygen bind to the enzyme in a defined sequence creating a tertiary complex. The products are then released following the oxidation of dopamine (pong) [180, 181].

**Phenylalanine Hydroxylase**

Two phylogenetically related forms of phenylalanine hydroxylase exist. One contains iron in its active center, while the other contains copper. Whereas the iron enzyme has been found in a wide variety of organisms, from bacteria to mammalians, the copper enzyme has only been reported for *Chromobakterium violaceum* [182]. The following pertains solely to the copper form.

Phenylalanine hydroxylase (EC 1.14.16.1) is a member of the tetrahydrobiopterin-dependent aromatic-amino acid hydroxylases, which also include tryptophane and tyrosine hydroxylase [183–186]. Phenylalanine hydroxylase from *Chromobakterium violaceum* is a monomeric enzyme of approximately 35 kD molecular mass and 296 amino acid residues. It contains a single copper ion ($Cu^{2+}$) in its active center [187].

Phenylalanine hydroxylase catalyzes the hydroxylation of phenylalanine to tyrosine, in which one oxygen atom of the oxygen molecule is transferred to the substrate, while the other oxygen atom is reduced to water. Two of the four required electrons are subtracted from the C–H bond of the substrate, and the other two are taken from the cofactor tetrahydrobiopterin [188]. The role played by copper is unknown, although it must be reduced to $Cu^{+}$ before the catalytic cycle can begin [188–191]. Recent studies suggest that copper is not a required prosthetic group, but is, as $Cu^{2+}$, an inhibitor of the enzyme [192]. The apoenzyme is catalytically completely active, whereas the binding of copper, zinc, iron, or cobalt results in inhibition. The histidine residues His 138 and His

143, which are extremely conserved in pterin-dependent monooxygenases, are probably of great importance to the catalytic activity of phenylalanine hydroxylase. Being bound by divalent copper prevents them from fulfilling their catalytic function [182]. These studies suggest that phenylalanine hydroxylase from *Chromobakterium violaceum* did not simply exchange the metal ion of its prosthetic group for another, but made itself completely independent of metal of any type. As the amino acid residues, which are responsible for metal binding, have remained essential for the enzyme's function, the danger of enzyme inactivation by metal binding persists.

**Methane Monooxygenase**

Methane monooxygenase is the first enzyme in the methane oxidation of methanotrophic bacteria, catalyzing the oxygen-dependent oxidation of methane to methanol [193]. Two methane monooxygenases exist, a soluble, cytosolic and a membrane-bound form [193, 194]. Although both enzymes catalyze the same reaction, analysis of their genes has shown them to be non-related [195–198]. The soluble methane monooxygenase consists of three components: a hydroxylase, a reductase, and a small, regulatory protein [199]. The hydroxylase contains two binuclear iron-clusters and is capable of oxidizing methane to methanol [199–202]. This methane monooxygenase has, until now, only been found in a few, methanotrophic bacteria, e.g., *Methylococcus capsulatus* (Bath), *Methylosinus trichosporium*, *Methylosinus sporium*, *Methylocystis* sp. M and *Methylomonas methanica* 68-1 strains [196, 197, 203, 204]. Depending on the copper content of the growth medium, they produce either the soluble or membrane-bound form of methane monooxygenase. The presence of copper suppresses synthesis of the soluble iron-enzyme [205]. Even among the methanotrophic bacteria there are strains reminiscent of the primordial bacteria which, following the oxygenation of the atmosphere, had already learned to utilize copper and had not yet lost the ability to synthesize iron-enzymes.

In contrast to the soluble form of methane monooxygenase, the membrane-bound form probably occurs in all methanotrophic bacteria [195]. Characterization of this enzyme is difficult, as its enzyme activity is hard to maintain in vitro [206]. A reproducible purification of this enzyme has not yet been achieved and, therefore, enzyme studies have had to be conducted with whole cells [195]. Consequently, it is currently probable that the membrane-bound monooxygenase is a copper enzyme, but this is not yet proven. This view is supported by the fact that methane monooxygenase activity increases with increasing copper concentrations in the growth medium and that, following expression of methane monooxygenase, its enzyme activity can be increased by adding copper [205]. The membrane-bound methane monooxygenase has a high substrate specificity and is susceptible to oxygen analogs and metal, especially copper, chelators [194, 206, 207].

**Function.** An obvious function of methane monooxygenase is the oxidation of methane to methanol. The membrane-bound form could fulfill this function within an electron-transport chain. A further, possible function could be derived from the observation that, in methanotrophic bacteria grown in copper-enriched medium, the main mass of membrane-bound proteins is methane

monooxygenase. The mass of the cytosolic membrane is markedly increased as well under these conditions. Studies of these methane-monooxygenase enriched membranes have revealed that these membranes can accept extremely large amounts of copper. The second, possible function of methane monooxygenases is that of copper storage, in which copper is stored as $Cu^{+}$ and $Cu^{2+}$. It is, however, improbable that this is its physiological function as the copper structures show redox activity which would be unusual for a simple storage protein [195].

**The role of copper.** The largest amount of membrane-bound copper occurs in trinuclear clusters. Spectroscopic studies have assigned these clusters to type 2 copper centers. $Cu^{+}$ and $Cu^{2+}$ occur in these clusters, of which, $Cu^{+}$ has the higher affinity to oxygen. Both copper species occur in different surroundings, making their participation in the redox processes probable. On the other hand, this large number of copper ions could be utilized as carriers, shuttling electrons between a different redox-active cofactor and the substrate. The trinuclear clusters are reminiscent of blue oxidases which contain type 2/type 3 trinuclear centers. These copper structures are the active centers of blue oxidases [208, 209]. The structural similarities of the trinuclear centers suggest that they are the active centers of the methane monooxygenases as well [195]. If these copper structures participate in catalysis, they can only exhibit catalytic activity if and when all three copper ions are bound. The methane monooxygenase molecule is already inactivated by the lack of a single copper ion, an explanation for the increase of membrane-bound enzyme activity when copper is added to the growth medium. This increase can only be observed while the copper structures are not yet saturated with copper. It has not been proven that copper participates in catalysis, although evidence suggests that the methane monooxygenases are type 2 copper monooxygenases [195].

#### *1.3.2.3*
#### *Dioxygenases*

Dioxygenases function by disrupting cyclic organic substrates, such as tryptophane and catechols [210]. The copper-dependent dioxygenase quercetinase from *Aspergillus flavus* [211] disrupts quercetin by transferal of both oxygen atoms of a dioxygen molecule to the heterocyclic ring [210] (Fig. 25). During the reaction, the 3-hydroxy and 4-carbonyl groups of quercetin appear to chelate the $Cu^{2+}$ ion of the enzyme's active center [212–214]. The products of the disruption are carbon monoxide and the phenolic ester 2-protocatechoyl phloroglucinol carbonic acid [211]. Little is known of the amino acid sequence, the exact structure, or the active center of the enzyme.

#### *1.3.2.4*
#### *Superoxide Dismutases*

*Cu,Zn-Superoxide Dismutase.* Although Cu,Zn-superoxide dismutase (Cu,Zn-SOD) only occurs in eukaryotes, it may be found in almost all types of eu-

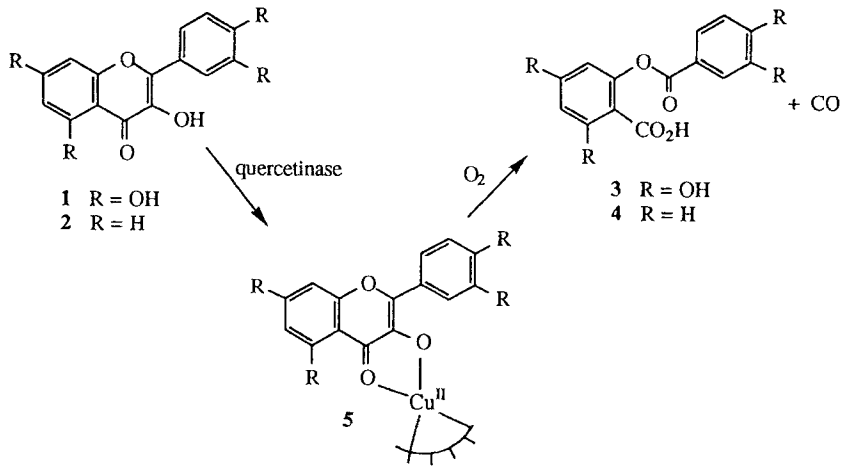


**Fig. 25.** The reaction of quercetinase. From Speier 1993 [210] with permission

karyotic tissues [215]. The intracellular form of Cu,Zn-SOD is a homodimeric enzyme with subunits of 16 kD molecular mass and a length of 151 amino acids each (bovine) [32, 216]. Each subunit has an active center which contains a $Cu^{2+}$ and a $Zn^{2+}$ ion [33, 217]. While the amino acid sequence of extracellular, tetrameric Cu,Zn-SOD is partially homologous to that of the intracellular form [218], both enzymes are encoded by different genes. In addition to the dimeric and tetrameric form, a monomeric Cu,Zn-SOD exists as well. The dimeric Cu,Zn-SOD is more stable and possesses a sevenfold higher activity than the monomeric form [219]. Intracellular Cu,Zn-SOD is the only copper enzyme to appear in the cytosol [220]. All other copper proteins and enzymes occur extracellularly, i.e., in the extracellular space, periplasm, organelles, or vesicles.

The postulated physiological function of Cu,Zn-SOD is the disproportionation of superoxide radicals ($\bullet O_2^-$) to oxygen ($O_2$) and peroxide ($O_2^{2-}$) [221–227]. The redox potential of Cu,Zn-SOD lies between those of both half-reactions, so it can alternately shuttle between electron-transfer to, or electron-subtraction from, a superoxide radical [228]:

$$O_2 + e^- \rightarrow O_2^- \qquad E^\circ = -0.16\ V$$
$$SODCu^{2+} + e^- \rightarrow SODCu^+ \quad E^\circ = +0.36\ V \text{ (human)}; +0.32\ V \text{ (bovine)}$$
$$O_2^- + e^- + 2H^+ \rightarrow H_2O_2 \qquad E^\circ = +0.89\ V$$

Consequently, there are two single reactions in the disproportionation of a superoxide radical:

$$\text{I. } SODCu^{2+} + \bullet O_2^- \rightarrow SODCu^+ + O_2$$
$$\text{II. } SODCu^+ + \bullet O_2^- + 2H^+ \rightarrow SODCu^{2+} + H_2O_2$$

**Structure of the active center.** The active center of Cu,Zn-SOD is situated at the end of a channel whose walls consist of conserved, charged residues [229]. The superoxide radical does not reach the active center by diffusion, it is directed

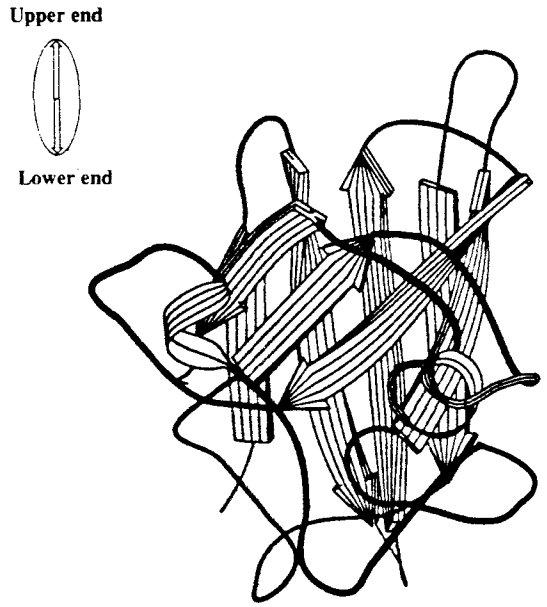


**Fig. 26.** $\beta$-Strand structure of Cu,Zn-superoxide dismutase. From Bordo et al. 1994 [220] with permission

there by these conserved residues [220, 229]. The enzyme's active center is embedded in a shallow $\beta$-barrel motive, consisting of eight antiparallel $\beta$-strands and three external loops [220] (Fig. 26).

The active center of Cu,Zn-SOD is unique among copper enzymes in that it contains not only a type 2 copper ion ($Cu^{2+}$) but a further metal ion ($Zn^{2+}$) as well (Fig. 6). The $Cu^{2+}$ ion is coordinated in a distorted, square planar confor-

**Table 9.** Bond angles of the Cu- and Zn-ligands of Cu,Zn-superoxide dismutase. Taken from Banci et al. 1994 [235]. The shifted amino acid renumbering of [229] by 2 residues each should be noticed.

| bond | bond angle (°) |
|---|---|
| $N^{\varepsilon 2}$ (His 120)–Cu–$N^{\varepsilon 2}$ (His 48) | 106.4 |
| $N^{\varepsilon 2}$ (His 120)–Cu–$N^{\delta 1}$ (His 46) | 93.7 |
| $N^{\varepsilon 2}$ (His 63)–Cu–$N^{\delta 1}$ (His 46) | 74.7 |
| $N^{\varepsilon 2}$ (His 48)–Cu–$N^{\varepsilon 2}$ (His 63) | 89.1 |
| $N^{\varepsilon 2}$ (His 120)–Cu–$N^{\varepsilon 2}$ (His 63) | 164.5 |
| $N^{\varepsilon 2}$ (His 48)–Cu–$N^{\delta 1}$ (His 46) | 130.2 |
| $N^{\delta 1}$ (His 65)–Zn–$N^{\delta 1}$ (His 71) | 111.1 |
| $N^{\delta 1}$ (His 65)–Zn–$O^{\delta 1}$ (Asp 83) | 100.0 |
| $N^{\delta 1}$ (His 80)–Zn–$O^{\delta 1}$ (Asp 83) | 124.1 |
| $N^{\delta 1}$ (His 80)–Zn–$N^{\delta 1}$ (His 71) | 130.0 |
| $N^{\delta 1}$ (His 71)–Zn–$O^{\delta 1}$ (Asp 83) | 78.7 |
| $N^{\delta 1}$ (His 63)–Zn–$N^{\delta 1}$ (His 80) | 107.5 |

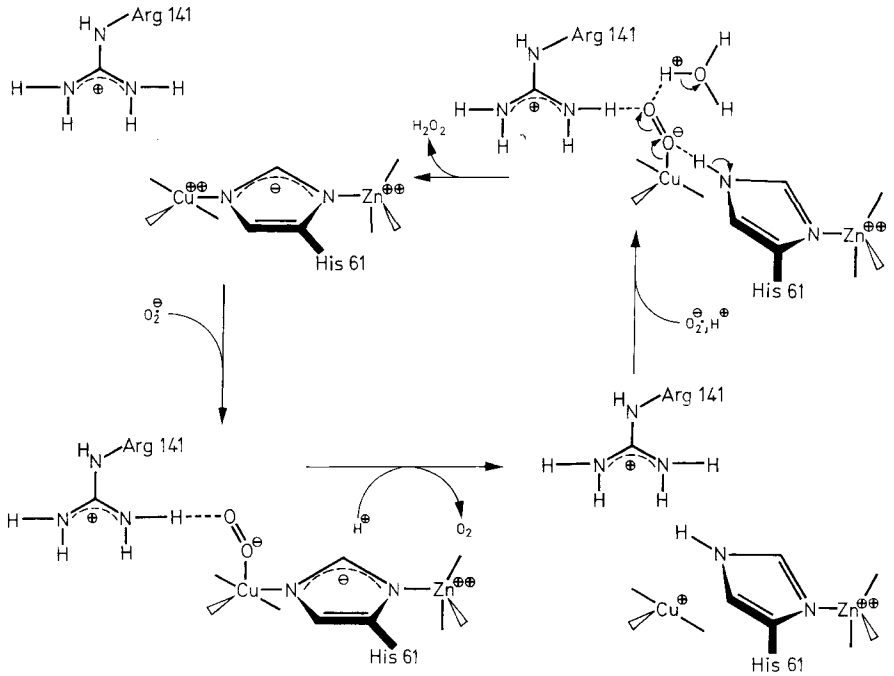


**Fig. 27.** The catalytic mechanism of Cu, Zn-superoxide dismutase: $\cdot O_2^-$ displaces the axial water molecule of $Cu^{2+}$ reducing it to $Cu^+$. Protonation of the $CuO_2$ complex liberates $O_2$ and dissolves the ligand bond between His61 and copper. A second $\cdot O_2^-$ binds to copper, oxidizing it to $Cu^{2+}$. Protonation produces $H_2O_2$, whereas deprotonation of His61 reestablishes the Cu-His61 bond, releasing $H_2O_2$. From Getzoff et al. 1983 [229] with permission

mation by His46 ($N^{\delta 1}$), His48 ($N^{\varepsilon 2}$), His63 ($N^{\varepsilon 2}$), and His120 ($N^{\varepsilon 2}$) [220]. The conformation surrounding the $Zn^{2+}$ ion is a distorted tetrahedron created by three histidines and an aspartate residue: His63 ($N^{\varepsilon 1}$), His71 ($N^{\delta 1}$), His80 ($N^{\delta 1}$), and Asp83 [220] ($O^{\delta 1}$) (Table 9). The bridging ligand His63 lies in a straight line between $Cu^{2+}$ and $Zn^{2+}$, which are separated by 6 Å [217, 233–235]. During catalysis, copper is the redox partner of the superoxide radical, whereas the oxidative state of $Zn^{2+}$ does not change during disproportionation. The $Zn^{2+}$ ion does not appear to be directly involved in catalysis (Fig. 27).

### 1.3.3
### *Type 3 Copper Proteins*

#### *1.3.3.1*
#### *Hemocyanin*

The hemocyanins are the oxygen-transport proteins of the three largest classes of mollusks (e.g., snails and squids), and of arthropods (e.g., spiders and scorpions). Mollusk and arthropod hemocyanin resemble each other in function

and structure of their oxygen-binding sites. However, their protein structures and amino acid sequences are very different [34].

**Arthropod Hemocyanins**

Arthropod hemocyanins (A-Hc) are proteins with molecular masses of up to 450 kD. They may be dissociated into six functional subunits of 75 kD mass, each of which contains a binuclear type 3 copper center responsible for oxygen binding. These proteins are, consequently, hexamers or multiple units thereof, which occur as native aggregates of $1\times6$, $2\times6$, $4\times6$, and $8\times6$ subunits. The latter have molecular masses of 3600 kD. The spider *Eurypelma californicum* possesses a hemocyanin structure of $4\times6$ [34]. These 24 subunits may be classified into 7 different types: a,b,c,d,e,f, and g, of which subunits a,d,e,f, and g occur 4 times, and the subunits b and c twice [236]. Each subunit has a specific position within the structure of the protein. Each protein subunit, i.e., the oxygen-binding unit, consists of three domains. Domains 1 (175 amino acids) and 2 (230 amino acids) have a pronounced $\alpha$-helical structure, whereas domain 3 (250 amino acids) consist almost completely of $\beta$-strands, which are arranged in a $\beta$-barrel structure similar to that of Cu,Zn-SOD [34].

The function of domain 1 has not yet been completely elucidated, although it may function as a medium of cooperative oxygen binding [37]. Domain 3 screens the copper center of domain 2 [237] from solvent. This copper center in domain 2 [34] is coordinated by six histidines from the helices 2.1 (2 His), 2.5 (2 His), 2.2 (1 His), and 2.6 (1 His). The histidine residue of helix 2.1 occurs in the sequence His-His-Trp-His-Trp-His, which is conserved in many arthropod hemocyanins. The histidines in helix 2.5 occur in the structure His-X-X-X-His. The coordination of two copper atoms with six ligands leaves two coordination sites free: these two sites are utilized to bind oxygen [34].

A similar situation is found in the hemocyanin of the horseshoe crab *Limulus polyphemus*. It consists of eight immunologically different subunits I, II, IIA, IIIA, IIIB, IV, V, and VI, which associate to hexamers [238] (the Roman numerals are qualitatively equivalent to the a–f classification of *Eurypelma* hemocyanin). Each of these subunits has a specific function [239, 240] and location [241] within the 48-mer protein. Oxygen binding is cooperative and is regulated allosterically. The protein's affinity to oxygen is lowered by chloride ions and increased by protons [242–245]. These properties as well as the cooperative oxygen binding are observed in isolated subunit II-hexamers, in which each monomer contacts four other monomers [37] (Fig. 28).

The hemocyanin subunits from *Limulus polyphemus* are also subdivided into three domains, which consist of the amino acids 1–154 (domain 1), 155–380 (domain 2), and 381–628 (domain 3) (Fig. 29). Domains 1 and 2 are primarily $\alpha$-helical, whereas domain 3 consists mainly of $\beta$-strands. Domain 2 is situated between the other two domains and contains the copper center. Each copper is coordinated by three histidine residues, which come from two helices. Subunit 2 is primarily responsible for the contact between the hexamer subunits. The chloride-binding site is situated between domains 1 and 2, and the calcium-binding site is located in domain 3, which has a seven-ribbon $\beta$-meander structure [37].

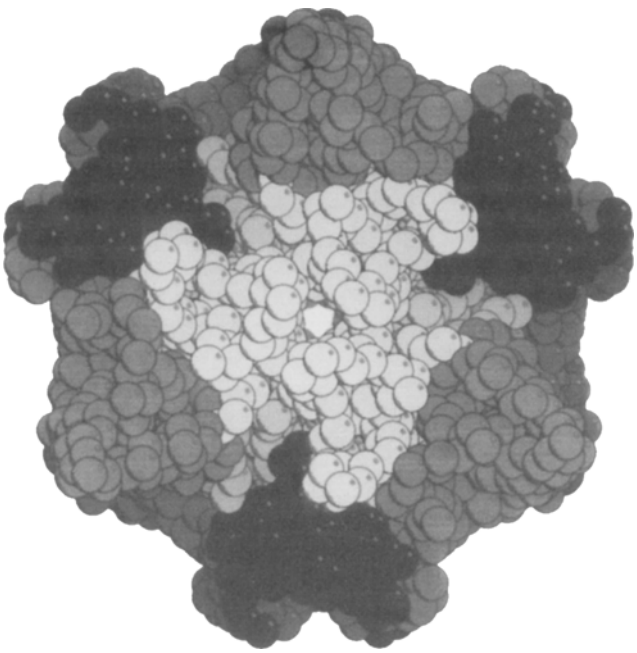

**Fig. 28.** Model of a subunit II-hexamer of *Limulus polyphemus* hemocyanin. The domains 1, 2, and 3 of each subunit are represented in *black, light gray* and *dark gray* respectively. From Hazes et al. 1993 [37] with permission

**Regulation of oxygen binding.** Three allosteric regulators are known for hemocyanin from *Limulus polyphemus* – $Cl^-$, $Ca^{2+}$, and $H^+$ [242–245]. Chloride ions do not affect all hemocyanins in the same manner. Only the subunits II, IIA, IIIA, and IIIB are affected in *Limulus polyphemus* hemocyanin. Chloride lowers the oxygen-affinity of hemocyanin by binding more strongly to the T-form (tense) than to the R-form (relaxed). Calcium ions stabilize the hexameric structure of hemocyanin. They also reduce oxygen-affinity, but increase the cooperativity of the multihexameric complex. An increase in $H^+$ concentration increases the oxygen-affinity of *Limulus polyphemus* hemocyanin as well – a "reversed" Bohr-effect [37, 239, 240, 243].

### Mollusk Hemocyanins

Mollusk hemocyanins are very large, cylindrical molecules which are assembled from up to 160 functional units, each of which, similar to arthropod hemocyanin, contains a binuclear type 3 copper center for oxygen binding. One functional unit weighs 50–55 kD, resulting, consequently, in a total molecular mass of 8000–9000 kD [34, 35]. Each polypeptide chain contains eight of these functional units and weighs 400 kD [34]. Arthropod and mollusk hemocyanins share practically no structural similarities. An exception is the His-X-X-X-His structure, which contains 2 of the 6 copper ligands and is situated within a con-

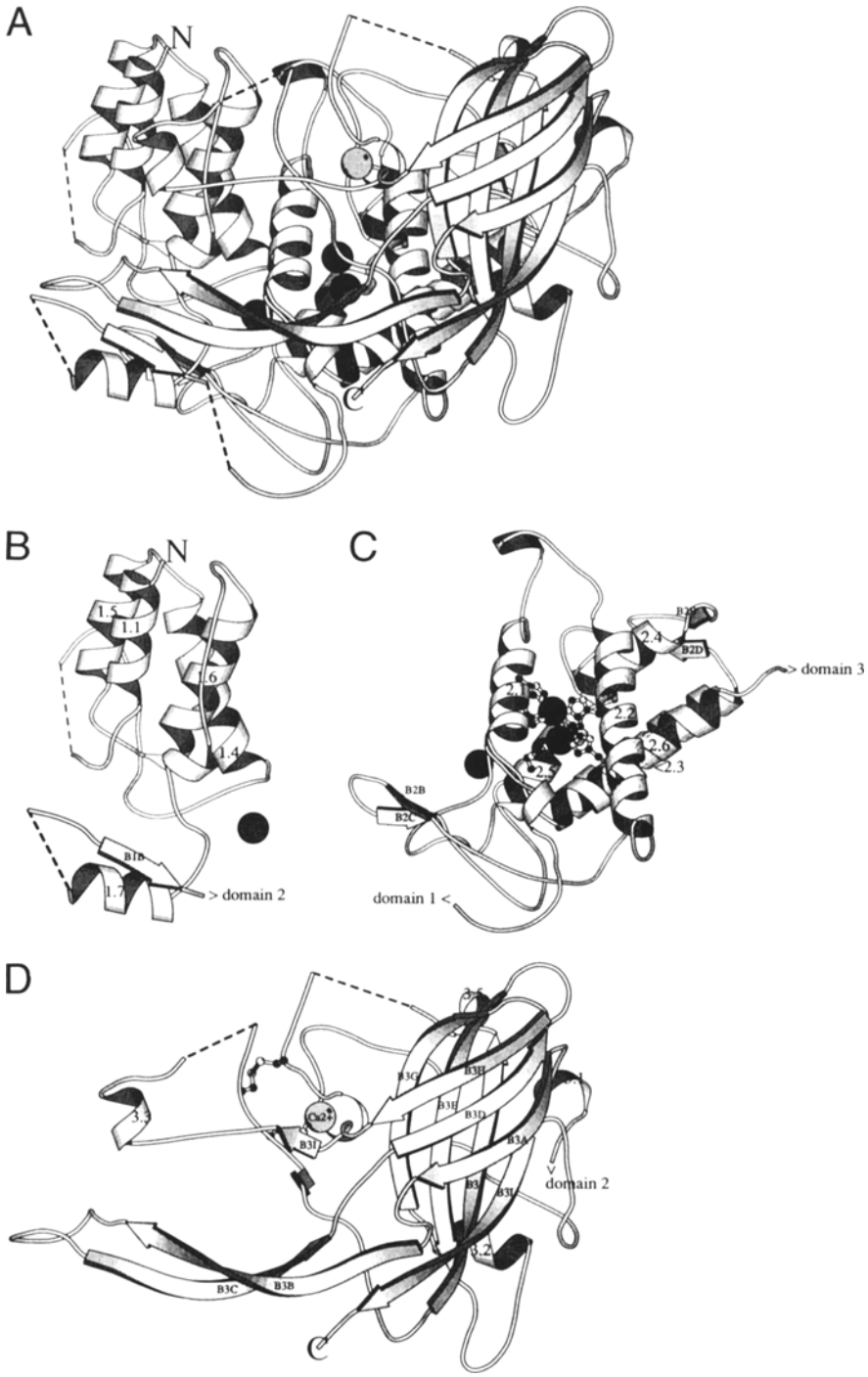


**Fig. 29a–d.** Ribbon model of the three domains of hemocyanin subunit II from *Limulus polyphemus*: **A** whole subunit; **B** domain 1; **C** domain 2; **D** domain 3. From Hazes et al. 1993 [37] with permission. Secondary structure nomenclature according to [246]

served stretch of 42 amino acids [247]. It not only occurs in arthropod and mollusk hemocyanin, but in tyrosinases as well [34, 247].

### 1.3.3.2
### *Type 3 Copper Centers of Hemocyanins and Tyrosinases*

Depending on the organism of origin, the two $Cu^+$ ions in the binuclear type 3 copper centers are situated between 3.4 Å [248, 249] and 4.6 Å [37] apart from each other. Both coppers are coordinated by three histidines each, and form an almost coplanar structure (Fig. 30a), i.e., the coordination of $Cu_A$ and $Cu_B$ is a distorted, trigonal plane. The $Cu_A$- and $Cu_B$-ligands (Table 10) are arranged in an almost antiprismatic orientation (Fig. 30b). This conformation differs from that of the type 3 copper center of ascorbate oxidase (a type 2/type 3 copper protein), in which the ligands are arranged prismatically [36]. There is no bridging ligand between these two copper ions [37].

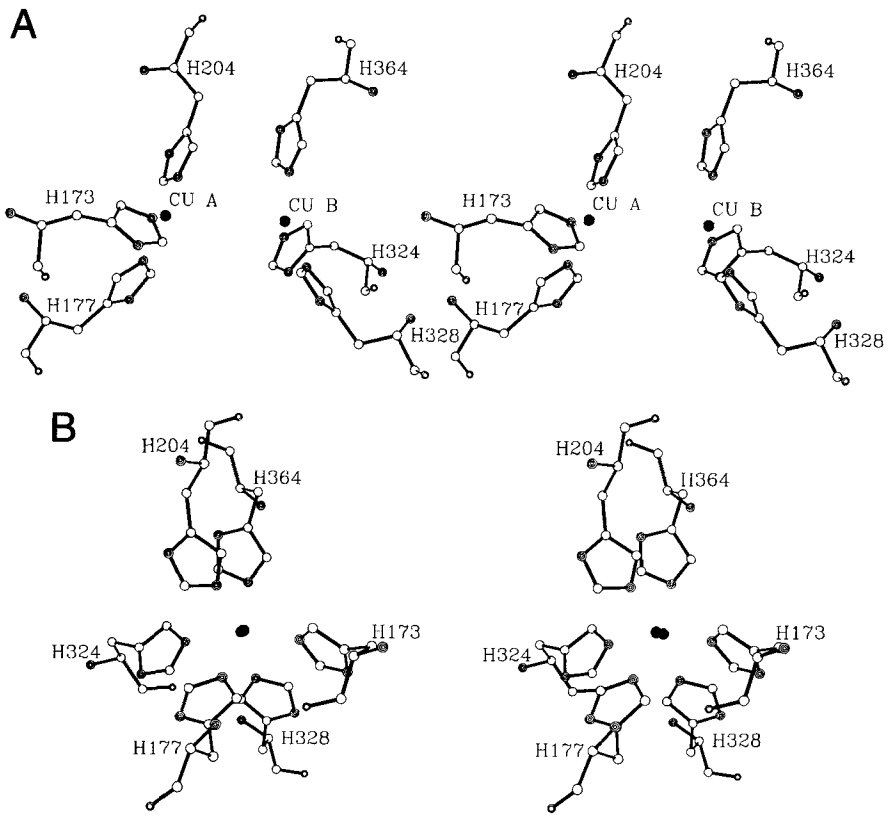


**Fig. 30a, b.** Structure of the binuclear copper center of hemocyanin from *Limulus polyphemus:* A view, vertical to the CuCu axis; B view along the CuCu axis. From Hazes et al. 1993 [37] with permission

**Table 10.** Bond lengths and angles of the subunit II copper center of *Limulus polyphemus* hemocyanin. According to Hazes et al. 1993 [37]

| CuA | | CuB | |
|---|---|---|---|
| bond | bond length (Å) | bond | bond length (Å) |
| CuA–CuB | 4.61 | | |
| CuA–N$^{\varepsilon}$173 | 2.10 | CuB–N$^{\varepsilon}$324 | 2.16 |
| CuA–N$^{\varepsilon}$177 | 2.01 | CuB–N$^{\varepsilon}$328 | 2.08 |
| CuA–N$^{\varepsilon}$204 | 1.04 | CuB–N$^{\varepsilon}$364 | 1.92 |
| bond | bond angle (°) | bond | bond angle (°) |
| N$^{\varepsilon}$173–CuA–N$^{\varepsilon}$177 | 99 | N$^{\varepsilon}$324–CuB–N$^{\varepsilon}$328 | 97 |
| N$^{\varepsilon}$173–CuA–N$^{\varepsilon}$204 | 131 | N$^{\varepsilon}$324–CuB–N$^{\varepsilon}$364 | 108 |
| N$^{\varepsilon}$177–CuA–N$^{\varepsilon}$204 | 126 | N$^{\varepsilon}$328–CuB–N$^{\varepsilon}$364 | 142 |

**Oxygen binding.** Oxygen arrives at the oxygen-binding site via a small channel. This channel is bordered by two glutamate residues, which are conserved in many of the studied hemocyanins. The glutamate's negative charge appears to be of essential importance in protecting the active center against substrates other than oxygen [37]. Oxygen is bound in hemocyanins, as in tyrosinase, as a side-on $\mu$-$\eta^2$:$\eta^2$ dimer [250].

Upon oxygen binding, the $Cu^+$ ions are oxidized to $Cu^{2+}$ [34]; oxygen is bound as a peroxide. This is accompanied by a change in the enzyme's color from colorless to blue [34]. Hemocyanins release bound dioxygen molecules in oxygen-depleted areas, reducing both copper centers back to $Cu^+$. Tyrosinases, on the other hand, transfer one oxygen atom to a substrate, reducing the second one to water.

#### *1.3.3.3*
#### *Tyrosinase*

While hemocyanins can only be found in two phyla, tyrosinases (EC 1.14.18.1) may be found in almost all types of organisms – from bacteria to mammals [251]. Tyrosinase, a monooxygenase, is responsible for the production of melanin and related pigments. It catalyses the *o*-hydroxylation of monophenols to *o*-diphenols (monophenolase activity), as well as the two-electron oxidation of *o*-diphenols to *o*-quinones (catecholase activity) [252, 253].

The active centers of tyrosinase and hemocyanins are very similar [254], although they fulfill very different functions. In both proteins, a binuclear center is coordinated by six histidines, leaving two coordination sites free to bind oxygen [237]. The main difference in the active centers of the proteins is their position within the protein. In arthropod hemocyanin, the copper center is located in domain 2 of every subunit. Domain 3 folds over the copper center, rendering it inaccessible to substrates larger than oxygen [237]. In tyrosinase, a C-terminal peptide of 200 amino acid residues is removed by post-translational

processing. This peptide is equivalent to domain 3 of arthropod hemocyanin [237]. Following its removal, the oxygen-binding site of tyrosinase is freely accessible for solvent and substrates enabling their conversion [255, 256]. Mollusk hemocyanins also possess a C-terminal peptide, equivalent to domain 3 of arthropod hemocyanin, although shorter [237]. The shortening of this protective structure appears to make the oxygen-binding site of these hemocyanins accessible to substrates. Mollusk hemocyanins actually show tyrosinase activity, although 50–100 times less than tyrosinase itself. This activity may be increased, however, by treating mollusk hemocyanin with compounds which disturb protein structures [237, 257–259].

### 1.3.4
### *Blue Oxidases*

The functional unit of blue oxidases contains one or more type 1 copper centers and a trinuclear center which, formally, consists of a type 2 and two type 3 copper atoms [25, 208]. The former probably serves as an electron-carrier, while the latter functions as the active center [260–263]. Blue oxidases are, in addition to cytochrome oxidases, the only known enzymes which catalyze the four-electron reduction of oxygen to water [71].

#### *1.3.4.1*
#### *Laccase*

Laccase (EC 1.10.3.2) is the simplest blue oxidase [263]. Its native form is monomeric with a chain length of approximately 540 amino acids [71] and a molecular mass of 65 kD [264, 265]. The monomer can be divided into three domains which show marked sequence homology with each other [71, 208, 266]. Laccases occur in a wide range of higher plants and fungi [264] where they catalyze the oxidation of numerous aromatic phenols, amino phenols and diamines via complete reduction of di-oxygen to water [265]. Laccase's physiological function is probably lignin degradation [71].

Laccase contains four copper atoms, one of which occurs in the type 1 copper center located in domain 3 [36]. The other three are located in a trinuclear center consisting, formally, of a type 2 copper center and a binuclear type 3 copper center with antiferromagnetically coupled copper ions [262, 263, 265]. This trinuclear center is the active center of the enzyme [262, 263, 265]. The type 1 center of *Polyphorus versicolor* laccase has a redox potential of +785 mV [19].

#### *1.3.4.2*
#### *Ascorbate Oxidase*

Ascorbate oxidase (EC 1.10.3.3) occurs exclusively in higher plants [267]. Its physiological function is as yet unknown, although it may play a role in ripening [36, 268], growth control, or disease control [269]. Ascorbate is probably the enzyme's physiological electron-donor.

Ascorbate oxidase is a dimeric enzyme (140 kD) whose subunits weigh 70 kD and have a chain length of 552 amino acids (zucchini). As in laccase, the subunits consist of three domains and contain four copper ions. The type 1 copper center is located in domain 3, and the trinuclear copper center is situated between domains 1 and 3. The subunits are glycosylated on their asparagine 92 residues [36].

The binding site for the reductant is on the surface of the enzyme, near the type 1 copper center. The oxygen-binding site, i. e., the trinuclear copper center, is embedded inside the enzyme and accessible by two channels of different sizes [36].

**Structure.** The main structural characteristic of ascorbate oxidase is the $\beta$-strand (Fig. 31). Domain 1 is shaped by two four-stranded $\beta$-meanders forming a $\beta$-sandwich structure. Domain 2 contains a six- and a five-stranded $\beta$-meander, whereas domain 3 is shaped by two five-stranded $\beta$-meanders, forming a $\beta$-barrel, and a four-stranded $\beta$-meander. In contrast to its 33 $\beta$-strands, ascorbate oxidase only contains 7 $\alpha$-helices. One occurs in domain 2, another connects domains 2 and 3, and the last five $\alpha$-helices are situated in domain 3 [36].

**Structure of the copper centers.** The mononuclear type 1 copper center (CU1) is located in domain 3 and is coordinated by His 445 ($N^1$), His 512 ($N^1$), Cys 507 (S), and Met 517 (S). These ligands form a distorted trigonal pyramid, similar to the type 1 copper center of plastocyanins (Table 11). In the latter, as in the

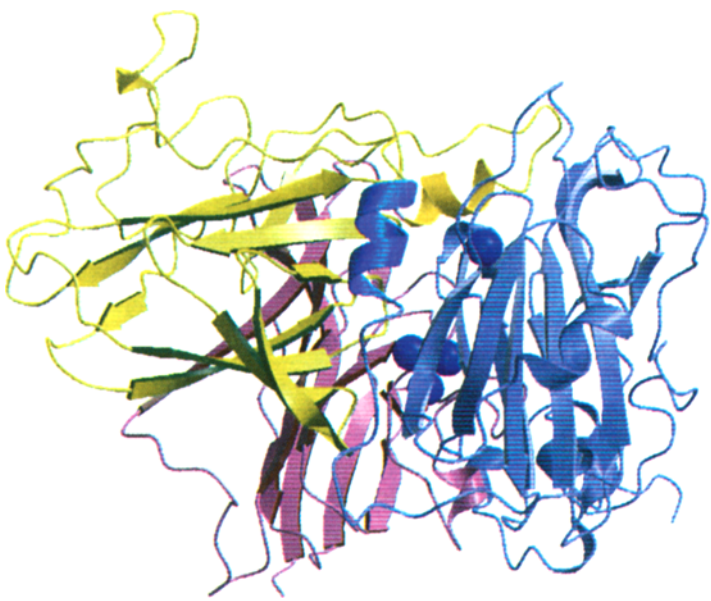

**Fig. 31.** Representation of the monomeric structure of ascorbate oxidase. From Messerschmidt et al. 1992 [36] with permission

former, methionine is the axial ligand which is furthest removed from the copper center [36].

The trinuclear copper center consists, formally, of a type 2 and type 3 copper center. Its coordination requires eight histidines, one $OH^-$ (or $O^{2-}$), and a second $OH^-$ (or $H_2O$). Six histidine ligands coordinate both copper ions of the type 3 copper center in a trigonal prismatic structure; the ligands of copper ion CU2 are His 102 ($N^2$), His 450 ($N^2$), and His 506 ($N^2$), and those of CU3 are His 62 ($N^1$), His 104 ($N^2$), and His 508 ($N^2$). Both copper ions are additionally linked by a $OH^-$ (or $O^{2-}$) bridge, giving rise to their strong antiferromagnetic coupling. The type 2 copper ion (CU4) is coordinated by two histidine residues, His 60 ($N^2$) and His 448 ($N^2$), and a OH (or $H_2O$) [36].

**Substrate binding centers.** The reducing substrate, ascorbate, is bound near the type 1 copper center. Following electron-abstraction, the resulting semihydroascorbate disproportionates [270]. Models of ascorbate binding suggest that His 512, whose $N^{\varepsilon 2}$ atom is directed to the solvent, as well as Trp 362 and Trp 163, participate in ascorbate-binding and electron-transfer. Oxygen is bound at the trinuclear copper center, which is connected to the solvent by two channels. The

**Table 11.** Copper-copper and copper-ligand distances between and within the copper centers. According to Messerschmidt et al. 1992 [36]

| Cu-Cu or Cu-ligand | distance (Å) |
|---|---|
| distance of the type 1 copper center to the trinuclear center | |
| CU1–CU2 | 12.2 |
| CU1–CU3 | 12.69 |
| CU1–CU4 | 14.87 |
| type 1 copper center | |
| CU1–$N^{\delta 1}$His 445 | 2.11 |
| CU1–$S^{\gamma}$Cys 507 | 2.08 |
| CU1–$N^{\delta 1}$His 512 | 2.08 |
| CU1–$S^{\delta}$Met 517 | 2.87 |
| CU1–O 444 | 4.81 |
| trinuclear copper center | |
| CU2–CU3 | 3.71 |
| CU2–CU4 | 3.86 |
| CU3–CU4 | 3.68 |
| CU2–$N^{\varepsilon 2}$His 106 | 2.17 |
| CU2–$N^{\varepsilon 2}$His 450 | 2.08 |
| CU2–$N^{\varepsilon 2}$His 506 | 2.08 |
| CU3–$N^{\varepsilon 2}$His 62 | 2.08 |
| CU3–$N^{\varepsilon 2}$His 104 | 2.17 |
| CU3–$N^{\varepsilon 2}$His 508 | 2.11 |
| CU4–$N^{\varepsilon 2}$His 60 | 2.01 |
| CU4–$N^{\varepsilon 2}$His 448 | 2.07 |
| CU4–OH1 | 2.00 |
| CU3–OH1 | 2.03 |
| CU4–OH3 | 2.03 |

wider of the two leads to the type 3 and the smaller channel to the type 2 copper center. It is, however, as yet unknown through which of the two channels oxygen reaches its binding site [36].

**Mechanism.** The enzyme must be fully reduced to bind oxygen. The completely oxidized form, in which all copper ions occur as $Cu^{2+}$, is inactive. Reactivation is achieved by four single-electron reductions of the type 1 copper center with ascorbate; three of these single electrons are transferred to the trinuclear center. All copper ions in this regenerated ascorbate oxidase occur as $Cu^{+}$. Oxygen binding at the reduced trinuclear center oxidizes both type 3 and the single type 1 copper centers, resulting in an $O_2^{3-}$ radical. Two protons split this radical into an $H_2O$ and an $O^{-}$, which abstracts an electron from the type 2 copper center. The resulting $O^{2-}$ unites with two additional protons to form a second water

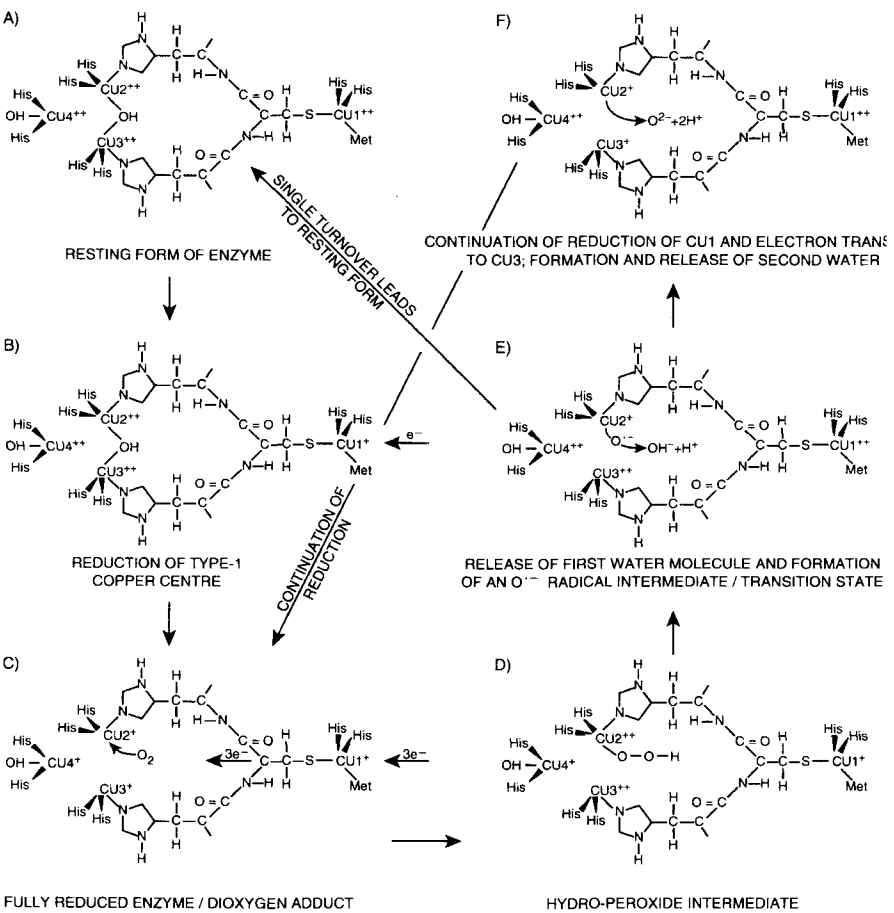


**Fig. 32.** Postulated mechanism of the ascorbate oxidase. From Messerschmidt et al. 1992 [36] with permission

molecule. The enzyme is now in its fully-oxidized, non-resting form. The difference between this fully-oxidized active and the inactive (or resting) form is that the type 2 copper ion of the inactive form is coordinated, in addition to the two histidines, by a hydroxide ion, which is missing in the active form [36] (Fig. 32).

#### *1.3.4.3*
#### *Ceruloplasmin*

Laccase occurs in plants and fungi [264] while ascorbate oxidase is abundant in higher plants [267] and ceruloplasmin (EC 1.16.3.1) is found in vertebrates. The latter copper protein is a monomer with a chain length of 1046 amino acid residues (human) and a molecular mass of 132 kD. Glycosylation accounts for 7–8% of its mass. Ceruloplasmin's physiological function is not yet entirely understood. The following functions have been suggested: copper transport, ferro oxidase amine oxidase, and anti-oxidant, of which the ferro oxidase function appears the likeliest [25]. The schematic structure of ceruloplasmin's copper-binding center is depicted in Fig. 8.

### 1.3.5
### *Type 1 and 2 Copper Proteins*

#### *1.3.5.1*
#### *Nitrite Reductase*

Nitrite reductase (EC 1.7.99.3) is one of the two copper enzymes in the dissimilatory pathway of denitrifying bacteria (for example *Achromobacer, Pseudomonas, Rhodobacter*):

$$NO_3^- \rightarrow NO_2^- \rightarrow NO \rightarrow N_2O \rightarrow N_2 \qquad [271].$$

It catalyses the single-electron reduction of nitrite ($NO_2^-$) to nitrogen monoxide (NO) and water:

$$E\text{-}Cu^{2+} + e^- + NO_2^- \rightarrow E\text{-}Cu^{+}\text{-}NO_2^-$$
$$E\text{-}Cu^{+}\text{-}NO_2^- + 2H^+ \rightarrow E\text{-}Cu^{2+} + NO + H_2O$$

Although there is another nitrite reductase (EC 1.9.3.2), which contains iron and utilizes the redox-active cytochromes *c* and $d_1$, the following will only treat the copper enzyme [90].

Nitrite reductase is a homotrimer in its native state [272]. Depending on the origin the chain lengths of the respective subunits vary between 340 and 379 amino acid residues. The trimer contains three type 1 and three type 2 copper centers. The type 1 copper centers are localized within the subunits, whereas the type 2 copper centers are coordinated by residues from two different subunits [272, 273] (Fig. 33).

The physiological electron-donor of nitrite reductase is the type 1 copper protein pseudoazurin, which transfers a single electron to the type 1 copper center of nitrite reductase, from where it is transferred to the type 2 copper

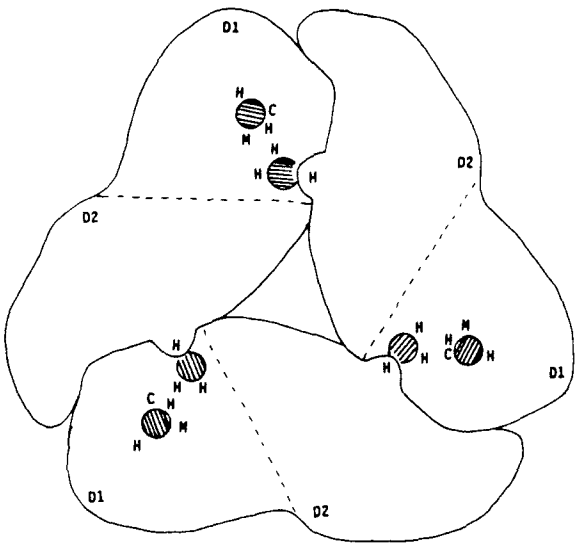


**Fig. 33.** Type 1 and 2 copper centers of the trimer nitrite reductase. From Fenderson et al. 1991 [273] with permission

center. The type 2 copper center is the binding-site for nitrite and where it is reduced to nitrogen monoxide [26].

**Structure** (of nitrite reductase from *Alcaligenes faecalis*). The subunits of nitrite reductase contain two domains. Each domain consists of a $\beta$-barrel structure, similar to that in the small blue proteins [272]. The type 1 copper center is embedded in one of these $\beta$-barrels and is coordinated by the ligands His 95 (domain 1), Cys 136, His 145, and Met 150 (domain 2) [26]. The type 2 copper center is coordinated by a water molecule and three histidine ligands: His 100 and His 135 (subunit x) as well as His 306 (subunit y). It is situated at the interface of two subunits [272]. The water molecule is displaced from the type 2 copper ion upon nitrite binding (Fig. 34). Although both copper ions are coordinated by neighboring residues, they are located approximately 12.5 Å apart, which prevents a direct electron transfer [272].

Most proteins with type 1 copper centers are blue, although the nitrite reductases from *Achromobacter cycloclastes, Alcaligenes faecalis,* and *Pseudomonas aureofaciens,* are green [26, 27]. This is probably caused by a distortion of the type 1 copper center, although the interrelation of distortion and absorption properties of the copper centers have not yet been clarified [27].

**Mechanism.** The electron-transport pathway of nitrite reductase begins with the type 1 copper center of pseudoazurin, continues to the type 1 copper center of nitrite reductase, and from there to its type 2 copper center. This last electron transfer is not conducted directly from copper to copper, but via an intramolecular Cys136-His135 bridge, similar to the one proposed for ascorbate oxidase [26, 208] (Fig. 35).

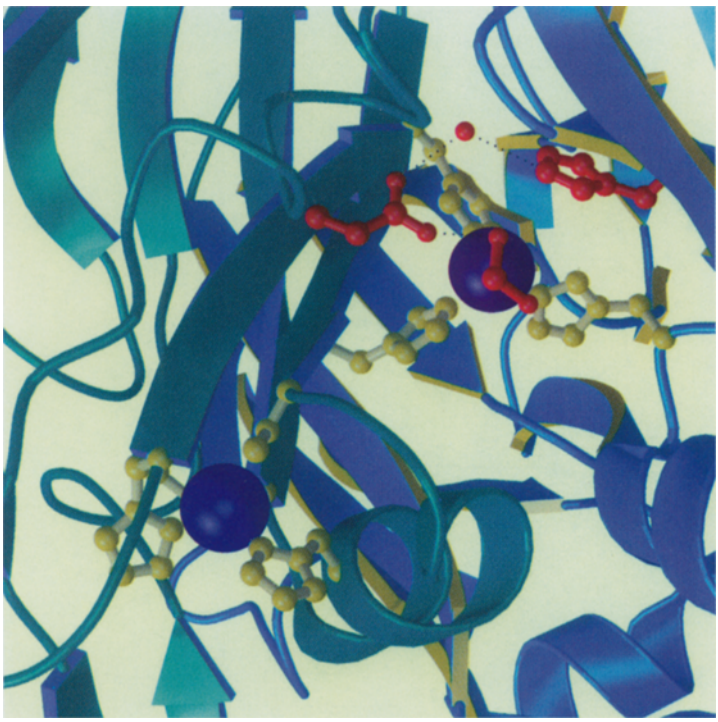

**Fig. 34.** The surrounding structure of the type 1 and type 2 copper-binding centers of nitrite reductase from *Alcaligenes faecalis*. The structure is equivalent to that of *Achromobacter*. From Averill 1996 [26] with permission

### 1.3.6
### *$Cu_A$-/$Cu_B$-Proteins*

$Cu_A$-/$Cu_B$-enzymes are the terminal enzymes in the respiratory chains of a multitude of organisms. In the last step of aerobic respiratory chains, cytochrome oxidases reduce oxygen to water. Dinitrogenoxide reductase reduces $N_2O$ to $N_2$ in the last step of denitrification. The cytochrome oxidases may be subdivided into cytochrome *c* oxidases [274] and ubiquinone oxidases [275–278]. Whereas all cytochrome oxidases possess $Cu_B$-centers, $Cu_A$-centers only occur in cytochrome *c* oxidases [279]. In contrast, all known dinitrogen oxide reductases possess $Cu_A$- [278, 280] but no $Cu_B$-centers.

#### *1.3.6.1*
#### *Cytochrome Oxidases*

Cytochrome oxidases occur in all three kingdoms of life [281, 282]. They are the terminal oxidases of aerobic respiratory chains and, as such, catalyze the four-electron oxidation of oxygen to water, a feat only they and the blue oxidases are capable of.

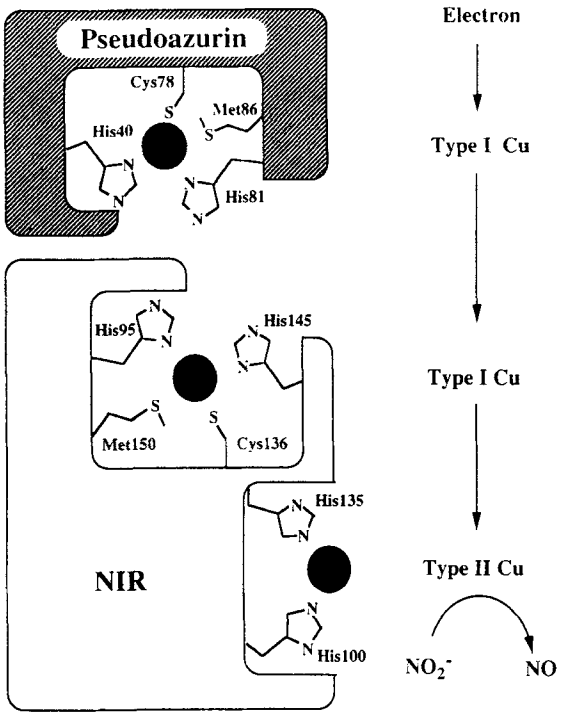


**Fig. 35.** Electron-transfer pathway from the electron-donor pseudoazurin via the type 1 to the type 2 copper center, followed by the reduction of nitrite to nitrogen monoxide. From Kukimoto et al. 1994 [26a] with permission

Cytochrome oxidases are transmembrane protein complexes, which are localized at the inner mitochondrial membrane in eukaryotes or at the plasma membrane in bacteria. In addition to the reduction of oxygen, all cytochrome oxidases studied so far function as proton pumps as well, maintaining the proton gradient for the production of ATP [283–286]. While all cytochrome oxidases oxidize oxygen, they vary in their electron donors. Those receiving electrons from cytochrome *c* are called cytochrome *c* oxidases and those from ubiquinone ubiquinone oxidases [287].

### Cytochrome c Oxidase

Cytochrome *c* oxidases (EC 1.9.3.1) are a heterogenous class of enzymes, which, depending upon the organism of origin, consist of 3 (in prokaryotes [288] including *Paracoccus denitrificans* [279]) to 13 (mammalian) [49] different subunits. In mammalians, subunits IV to XIII are encoded autosomally, whereas subunits I, II, and III are encoded by mitochondrial DNA [26, 283, 288]. This distribution of genes suggests, in accordance with the endosymbiont theory, a bacterial origin of these three subunits I, II, and III. In fact, all studied cytochrome *c* oxidases [288] show homologies in these three subunits. As in ubiquinone oxidase, the functional unit is formed by subunits I and II [279, 285]. The various

**Table 12.** Various types of cytochrome *c* oxidase. The index *3* indicates a heme which transfers electrons directly to oxygen. A hyphen indicates the lack of the corresponding group. According to van der Oost et al. 1994 [279]

| type | heme/copper | | species |
|---|---|---|---|
| | subunit I | subunit II | |
| $cbb_3$ | $bb_3/Cu_B$ | *c*/– | *P. denitrificans* |
| $aa_3$ | $aa_3/Cu_B$ | –/$Cu_A$ | *P. denitrificans* |
| $caa_3$ | $aa_3/Cu_B$ | *c*/$Cu_A$ | *B. subtilis* |
| $ba_3$ | $ba_3/Cu_B$ | –/$Cu_A$ | *T. thermophilus* |

cytochrome *c* oxidases possess three or four redox-active groups, which are arranged in sequence, to transfer the four electrons from cytochrome *c* to oxygen. These redox-active groups are cytochromes (*a, b,* or *c*) and copper centers ($Cu_A$, $Cu_B$) and are all located in the subunits I and II. Cytochrome c oxidases are typified according to the heme group utilized [279] (Table 12).

Heme *a* and $Cu_A$ are single-electron centers, while the antiferromagnetically coupled $a_3Cu_B$ pair is a two-electron center. In the $aa_3$-type cytochrome *c* oxidase from *Paracoccus denitrificans*, which is homologous to the mitochondrially encoded mammalian cytochrome *c* oxidases [279], the electrons from cytochrome *c* are initially transferred to the $Cu_A$-center [279]. They are then transferred via a heme *a* to the binuclear heme $a_3Cu_B$ center [279], from where they are finally conveyed to oxygen [286, 289]. The $cbb_3$-type cytochrome *c* oxidase has no $Cu_A$-center at all. It abstracts electrons from cytochrome *c* by a heme *c*, which transfers them via a heme *b* to the binuclear heme $b_3Cu_B$ center [290, 292]. This cytochrome c oxidase has a very high affinity for oxygen and is expressed under anaerobic or microaerobic conditions [290–293]. This may be a sign that it is closely related to an early form of cytochrome *c* oxidase created for conditions which had prevailed shortly after the advent of photosynthesis. It appears that cytochrome *c* oxidases also have keepsakes of the iron-to-copper evolution driven by the increasing oxygen concentration of the atmosphere.

### Ubiquinone Oxidase

Ubiquinone oxidases (EC 1.10.2.2) are also terminal oxidases of aerobic respiratory chains and, as the name implies, receive their electrons from ubiquinone instead of cytochrome *c*. Consequently, the electron-acceptor site is different in ubiquinone reductases compared to that in cytochrome *c* oxidases. The most marked features are the lack of the $Cu_A$-center and of heme *a* in subunit II [278, 294, 295]. Ubiquinone oxidases are also typified according to the redox centers of subunit I [279] (Table 13).

Although ubiquinone oxidase does not possess a $Cu_A$-center, both types of cytochrome oxidase are so homologous in their subunit II that site-directed mutagenesis can restore ubiquinone oxidase's $Cu_A$-structure [278a].

The heme *a*- and heme *b*-$Cu_B$ clusters of the ubiquinone oxidases resemble the heme $aCu_B$ clusters of the cytochrome *c* oxidases [279, 294]. No ligand

**Table 13.** Various types of ubiquinone oxidases. A hyphen indicates the lack of the corresponding group. From van der Oost et al. 1994 [279]

| type | heme/copper | | species |
|---|---|---|---|
| | subunit I | subunit II | |
| $aa_3$ | $aa_3/Cu_B$ | -/- | *B. subtilis* |
| $bb_3$ | $bb_3/Cu_B$ | -/- | *P. denitrificans* |
| $bo_3$ | $bo_3/Cu_B$ | -/- | *E. coli* |
| $ba_3$ | $ba_3/Cu_B$ | -/- | *A. aceti* |

bridges the $Cu_B$ and Fe sites [43]. In *E. coli,* the $Cu_B$-center is coordinated by two or three histidine ligands: His 333, His 334, and – when coordinated by three histidines – His 284 [279, 294]. This structure, in which two neighboring histidines (His 333 and 334) coordinate the same copper ion, is unique among copper proteins [279].

#### *1.3.6.2*
#### *Dinitrogenoxide Reductase*

Dinitrogenoxide reductase ($N_2O$-reductase) catalyses the last step in the dissimilatory pathway of denitrifying bacteria (for example *Pseudomonas stutzeri*) [296, 297], which is the two-electron reduction of $N_2O$ to $N_2$ and water [298]. The enzyme consists of two identical subunits which weigh 70 kD [280] and contain four copper ions each [299].

Two copper ions form the $Cu_A$-center, which is identical to that in the cytochrome oxidases [41, 300, 301]. The other two copper ions also form a binuclear structure [42].

### 1.3.7
### *Metallothioneins*

Metallothioneins occur in animals, plants, fungi, and eukaryotes as well as in some prokaryotes [56, 57, 302–305]. They are a heterogenous group of small proteins (6–7 kD), which are characterized by their high cysteine content [54]. Monomers have been described as well as dimers and tetramers [306]. Thioneins preferably bind transition metals such as cadmium, zinc, and copper in varying stoichiometries [54, 55]. Metallothioneins participate in metal homeostasis, i.e., the storage and transportation of the essential metals zinc and copper [307, 308]. An additional function is the binding of potentially toxic doses of copper, which could occur during the degradation of copper proteins [56, 309, 310]. Metallothioneins probably co-regulate the expression of genes whose transcription is regulated by zinc-finger proteins [311, 312]. An increase in metallothionein synthesis decreases intracellular zinc concentrations, resulting in its reduced availability for zinc-finger proteins and, consequently, suppresses their binding to DNA. Thus, metallothioneins play a role in transcriptional re-

gulation of proteins [311, 312]. Copper-thioneins possess, in addition to this non-catalytic function, superoxide dismutase activity [313]. A reaction mechanism was proposed for the disproportionation of superoxide radicals ($O_2^-$) by copper-thionein from yeast, in which a thiyl radical occurs transiently. The copper ions do not alter their oxidation state during the reaction [314]:

$$Cu(I)^-SR + {}^\bullet O_2^- \rightarrow Cu(I)^\bullet SR + O_2^{2-}$$
$$Cu(I)^\bullet SR + {}^\bullet O_2^- \rightarrow Cu(I)^-SR + O_2$$

In contrast to Cu,Zn-SOD, the copper ions remain in the oxidation state Cu(I) throughout the reaction cycle, the thiolate group being the redox-active site. This reaction mechanism is supported by the observation that none of the typical Cu(II)-signals occur in the ESR spectrum. The function of Cu(I) may simply be the stabilization of the thiolate group [314].

A reaction product of superoxide radicals is the reactive hydroxyl radical, which reacts with copper-thioneins as well [313]. However, the reaction of superoxide radicals with copper-thioneins can also create hydroxyl radicals: it cannot be excluded that the oxidation of copper-thioneins by superoxide radicals or by other oxidants leads to the release of reactive Cu(II) ions [313]. These reactive Cu(II) ions could then, in an uncontrolled manner, convert more superoxide radicals to hydroxyl radicals, a process which possibly plays a role in inflammations.

The expression of the yeast gene for copper-thionein (CUP1), is inducible by copper ions [315]. The induction occurs by the copper-binding protein ACE1, a transcription activator, which binds to the CUP1 promoter in the presence of copper. ACE1 also induces the expression of the gene for Cu,Zn-SOD (SOD1), although induction is weaker than in CUP1. This is possibly explained by the fact that CUP1's promoter possesses four binding sites for ACE1, while the promoter for SOD1 has only one. However, the distance between the promoter and the structural gene, as well as the synergistic interactions of several transcription factors, may be a factor in the varying efficacies of ACE1 binding [315].

Most metallothioneins occur in various isoforms which are encoded by different genes, whose transcription are induced by different metal ions (Cd, Zn, Cu). This suggests that the various isoforms have different functions in the metal management of organisms [56]. Functional differences may also be observed between the various metallothionein classes. For example, the American lobster *Homarus americanus* produces two isoforms of class I and a single form of class II metallothionein. The latter is capable of transferring copper to hemocyanin. The class I metallothioneins, on the other hand, probably capture the copper ions, which are liberated by hemocyanin degradation [56, 309, 310]. The metallothioneins are divided into three classes according to their amino acid sequence. Class I metallothioneins are those polypeptides whose amino acid sequence is homologous to that of equine kidney metallothionein (Fig. 36).

In mammalians these metallothioneins normally possess chain lengths of 61 amino acids, of which 20 are invariant cysteines residues [58, 316]. These 20 residues participate in the binding of the up to twelve metal ions. Class II metallothioneins show little or no phylogenetic homology to the metallothioneins of class I, for instance, in sea urchins [317] and yeast [318]. Class III metallothio-

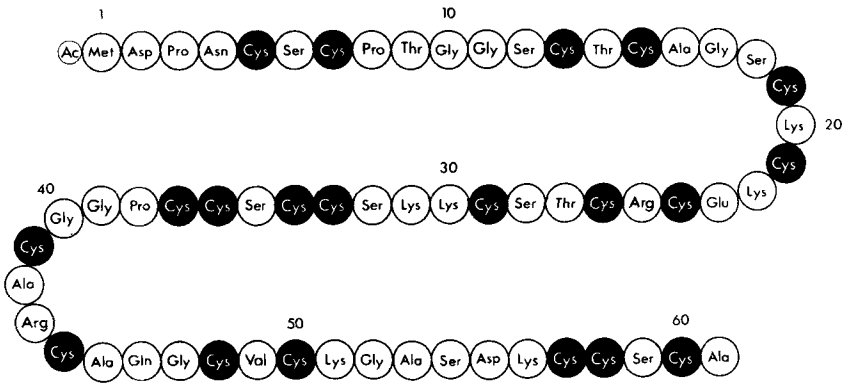


**Fig. 36.** Amino acid sequence of equine class I metallothioneins. From Kojima and Kägi 1979 [316] with permission

neins include the γ-glutamyl-cysteinyl-oligopeptides of plants [319, 320] and the yeast *Schizosaccharomyces piombe* [321].

## 2 Evolution of Copper Proteins

The distribution of copper proteins throughout the three kingdoms of life (archaea, bacteria, and eukarya) reflects their phylogenetic relationship. This section will not only classify individual proteins phylogenetically but discuss the mechanisms of copper protein evolution derived from these relationships as well.

### 2.1 Type 1 Copper Proteins

Small blue proteins were probably the first copper proteins to develop during the oxygenation of the atmosphere. As can be inferred by their occurrence in all three kingdoms of life, their common ancestor must have existed before the divergence of archaea, bacteria, and eukarya. Consequently, this precursor has remained almost completely unchanged not only during its distribution throughout the three kingdoms but also over a time range of more than 1.5 billion years (the time between the divergence and the oxygenation of the atmosphere). The insertion of copper into a preexisting protein must have taken place in an independent but similar manner in all three kingdoms. How is it possible for a protein to remain so well conserved over so much time and throughout so many species? Prior to the oxygenation of the atmosphere, evolution occurred in very small steps, a factor which possibly supported conservation of protein structures. It is, however, also possible that the precursor of the small blue proteins fulfilled an essential function which would also prevent its rapid change. An exclusive development of small blue proteins in the bacte-

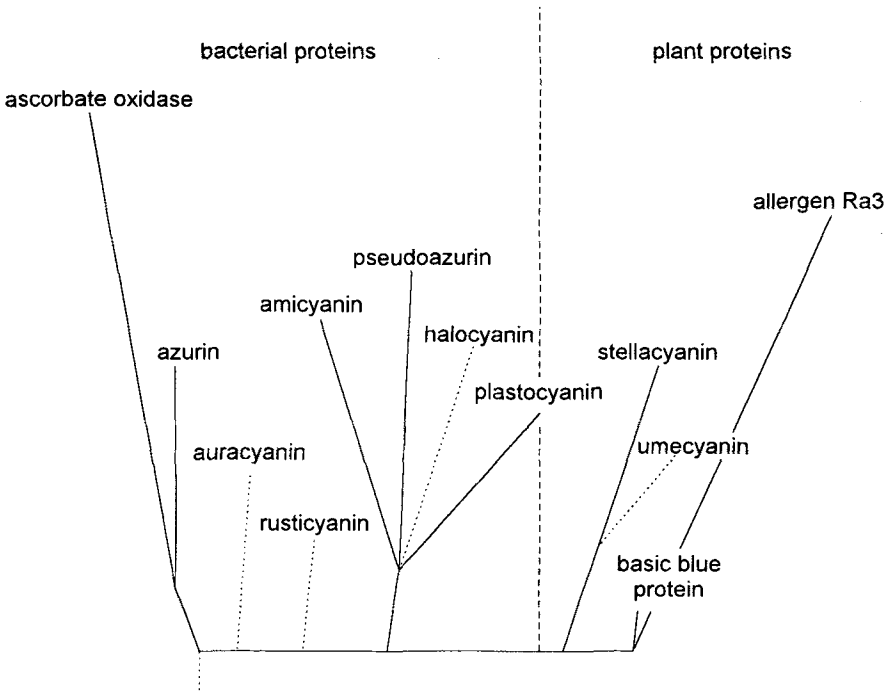


**Fig. 37.** Phylogenetic family tree of the four small blue protein families. The roots as well as the branching points to auracyanin, rusticyanin, halocyanin, and umecyanin are currently not known. Plastocyanin occurs in bacteria as well as in eukaryotes. Ascorbate oxidase was used as reference protein in creating the diagram. The plant allergen Ra3 is a non-copper protein. *Halocyanin is currently the only known archaeate copper protein. Adapted from Rydén and Hunt 1993 [71]

rial kingdom is improbable. While explaining the abundance of bacterial proteins in chloroplasts, it does not explain the development of phytocyanins or the recently discovered occurrence of small blue proteins in archaea.

Independent of how they evolved, the distribution of the small blue proteins throughout the various types of organisms mirrors their phylogenetic relationship and their occurrence in the various families: azurin family, auracyanin, rusticyanin, plastocyanin family, and phytocyanins [71] (Fig. 37).

Comparison of amino acid sequences shows that small blue proteins and blue oxidases have developed from a common precursor [71]. Whereas the former are found in all three kingdoms, blue oxidases are only found in fungi, plants, and animals. In contrast to the small blue proteins, which have chain lengths of approximately 100 amino acid residues, blue oxidases have chain lengths of ca. 540 (laccase, ascorbate oxidase) and 1046 amino acid residues (ceruloplasmin) [71]. The following mechanisms were applied to increase the size of these proteins [71]:

- duplication of domains – chain length growth from 100 to ca. 200 amino acid residues;

- domain expansion – chain length growth from ca. 170 to ca. 1000 amino acid residues;
- glycosylation – increase in molecular mass; this may double the weight of the naked peptide chain.

These principles not only resulted in an increase in size but in new copper centers as well, which display, in addition to electron transport, an almost unique catalytic activity. The transition from protein to enzyme may be seen in the development of blue oxidases.

Phylogenetically, the coagulation factors CF5 and CF8 [71] belong to the blue oxidases. While showing significant sequence homology to ceruloplasmin, they have lost their copper-binding centers and, consequently, all enzymatic activity during evolution. The distribution of blue oxidases and coagulation factors in the plant and animal kingdom reflects their phylogenetic relationship. A comparison of the C-terminal regions of the blue oxidases and coagulation factors (the most highly conserved region based on the common precursor of the small blue proteins and blue oxidases) shows that ceruloplasmin is phylogenetically much more closely related to the coagulation factors than to the blue oxidases of plants [71] (Fig. 38).

Laccase and ascorbate oxidase consist of three, ceruloplasmin of six, homologous domains containing approximately 170 amino acids each. Sequence comparisons were conducted for the individual domains of blue oxidases to clarify the development of the domain structure. The phylogenetic relationship of the individual domains of laccase and ascorbate oxidase on the one hand,

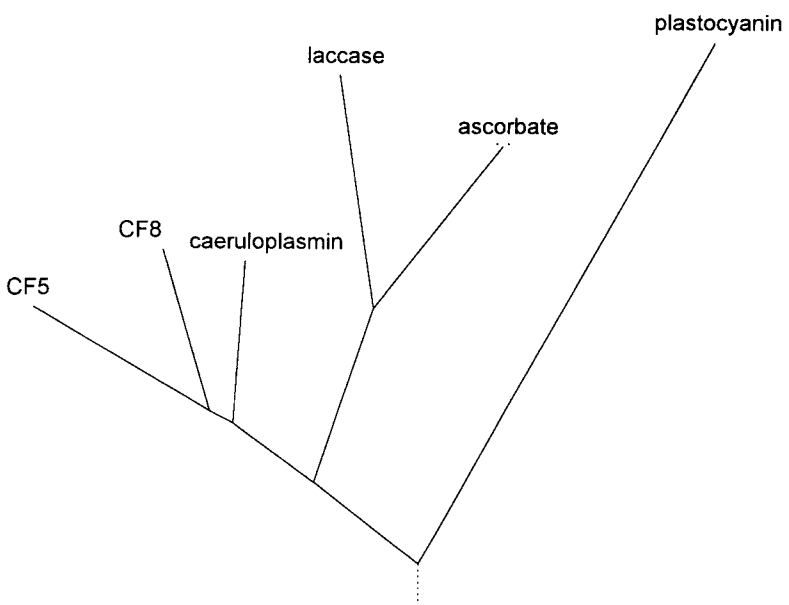


**Fig. 38.** Comparison of the C-terminal regions of blue oxidases and the coagulation factors CF5 and CF8 (reference protein: plastocyanin). According to Rydén and Hunt 1993 [71]

and ceruloplasmin on the other, proves that the development of the three domain structure had occurred in plant oxidases prior to the separation of ascorbate oxidase and laccase. The phylogenetic relationship between the six domains of ceruloplasmin shows that they occurred by two duplications of a double domain and not by the duplication of a triple domain [71] (Fig. 39).

The C-terminal domains of laccase/ascorbate oxidase and the even-numbered domains of ceruloplasmin are most closely related to the small blue pro-

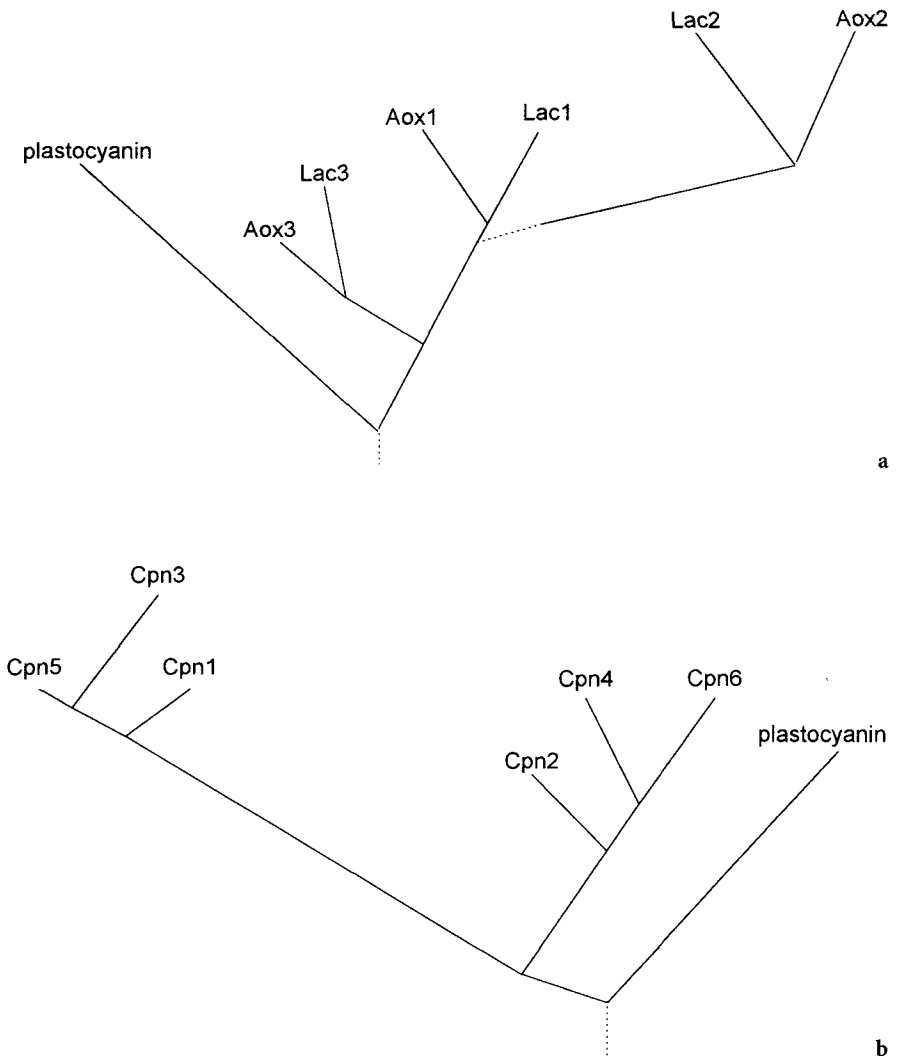


**Fig. 39a, b.** Phylogenetic trees of the structural domains of: a laccase and ascorbate oxidase; b ceruloplasmin. Plastocyanin is the reference protein in both cases. Lac/Aox 1-3 N- to C-terminal domains of laccase/ascorbate oxidase. Cpn 1-6 N- to C-terminal domains of ceruloplasmin. According to Rydén and Hunt 1993 [71]

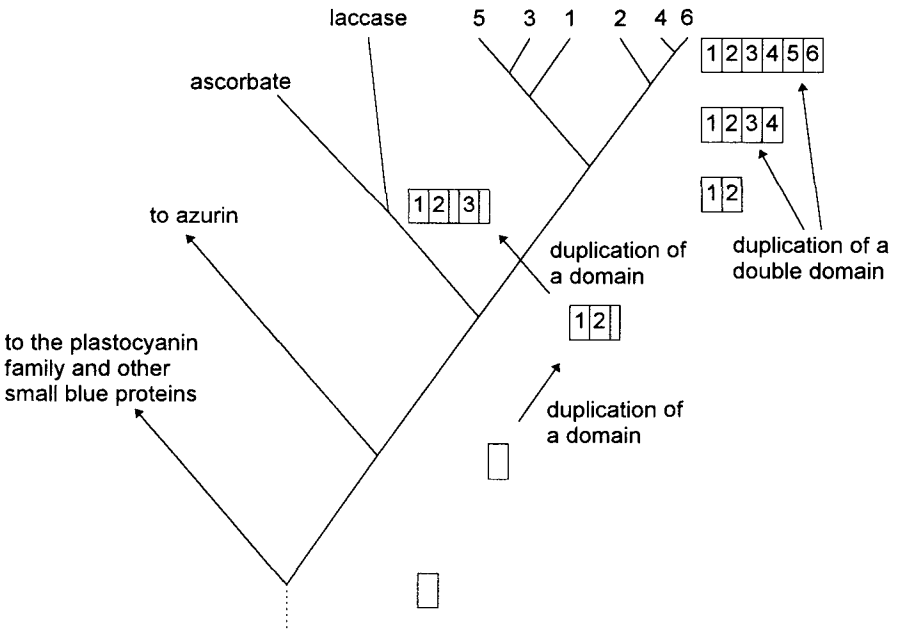


**Fig. 40.** Development of type 1 copper proteins. Modified from Rydén and Hunt 1993 [71]

teins. How did these proteins develop from the precursor of the small blue proteins and thus from the C-terminal region of the blue oxidases (Fig. 40)?

Due to the similarity in size and structure of the small blue proteins, it may be concluded that their variety occurred by point mutations or small insertions and deletions. The original size of the precursor remained more or less unchanged. Laccase and ascorbate oxidase were generated by two duplications of the precursor's single domain. The fact that the equivalent domains of laccase and ascorbate oxidase are more similar to each other than the individual domains within an oxidase themselves (see Fig. 39 a) proves that the triplication of the original domain must have occurred before differentiation to laccase and ascorbate oxidase. In the case of ceruloplasmin, however, the original domain was duplicated and the resulting double domain duplicated twice. This mechanism explains why the odd- or even-numbered domains are more similar to each other than the neighboring domains [71].

Over which time span did the type 1 copper centers and their related copper proteins evolve? The origin of the small blue proteins is unknown, but their distribution among the various organisms can be put into a phylogenetic framework. The eukaryotic cyanobacteria developed approximately 3 billion years ago [71]. Plastocyanin occurs solely in this group, while azurin also occurs in other bacteria. Consequently, the separation of the plastocyanin and azurin families must have occurred at roughly the same time as the development of cyanobacteria. The phylogenetic separation of chloroplasts and cyanobacteria occurred 2.1 billion years ago [71], thus conveying plastocyanin from bacteria to plants.

The phylogenetic paths of plants and animals diverged approximately 1.4 billion years ago, leading to laccase and ascorbate oxidase in the former group, and ceruloplasmin in the latter. Then, 500–800 million years ago, the coagulation factors CF5 and CF8 were created from the precursor of present day ceruloplasmin. This included the loss of the copper centers and, consequently, their catalytic activity [71].

### 2.1.1
### *Nitrite Reductase*

Nitrite reductase catalyses the reduction of $NO_2^-$ to NO. The enzyme's native state is that of a homotrimer. The monomers have two domains (domain 1 and 2) which show clear sequence homology to type 1 copper proteins [272]. Thus, a phylogenetic relationship can be assumed for not only type 1 copper proteins but also for the domains themselves. Domain 1 of nitrite reductase contains type 1 copper, whereas a change in the copper-binding center of domain 2 resulted in its switch from a type 1 to a type 2 copper center. A similar switch from a type 1 to a type 2 copper center may be observed in the development of blue oxidases.

All of the currently known copper proteins which contain type 1 copper centers are derived from a common ancestor. The various characteristics of the small blue proteins, and the development from copper proteins to copper enzymes and from there to non-catalytic, non-copper proteins are the results of a solely divergent evolution.

## 2.2
## Type 2 Copper Proteins

A survey of the functions of type 2 copper proteins reveals that all are directly involved in oxygen metabolism (oxidases, oxygenases, superoxide dismutases). Many of these functions are only relevant for multicellular organisms (synthesis of connective tissue, hormone synthesis). It can therefore be assumed that type 2 proteins occurred after the oxygenation of the atmosphere or with the development of multicellular organisms. There is no phylogenetic relationship between type 1 and type 2 copper proteins.

Sequence homologies are low within type 2 copper proteins. While similarities exist in protein folding or in the structure of the copper centers, they are not based on phylogenetic homologies in amino acid sequence. These similarities are solely the result of separate proteins evolving and adapting to similar functions. In contrast to type 1 copper centers, type 2 copper proteins developed primarily by convergent evolution.

### 2.2.1
### *Cu,Zn-Superoxide Dismutase*

Comparisons of amino acid sequences have revealed that some type 2 copper proteins are phylogenetically related to non-copper proteins of similar func-

tion: Cu,Zn-superoxide dismutase shows similarities to Fe- and Mn-superoxide dismutases [220]. As a result of the earlier biological availability of iron and manganese, the Fe- and Mn-superoxide dismutases are the more primordial forms of these enzymes. They are also more closely related to each other than to Cu,Zn-superoxide dismutase [322, 323]. The occurrence (or non-occurrence) of the three superoxide dismutases in an organism appears to be characteristic for the organism's place on the evolutionary ladder [220]. The iron enzyme occurs primarily in anaerobic bacteria and some prokaryotes [324]. The manganese enzyme may be found in prokaryotes and in the mitochondria of eukaryotes [220], whereas Cu,Zn-superoxide dismutase is found in bacteria and eukaryotes [325, 326].

### 2.2.2
### *Galactose Oxidase*

Galactose oxidase has a unique tertiary structure for a copper protein, comparable with that of the non-copper protein methylamine dehydrogenase. Comparisons of the amino acid sequences [157] show, however, that the enzymes are not phylogenetically related. The tertiary structures developed separately [30].

### 2.2.3
### *Amine Oxidases*

A phylogenetic relationship may be assumed for amine oxidase and diamine oxidase which shows distinct sequence homologies in their C-terminal regions [128]. Lysyl oxidase is not related to the other amine oxidases as it does not share any homology in structure or amino acid sequence [128] with the other amine oxidases. Non-copper enzymes with similar structures or sequences have not yet been found for any of the three enzymes.

### 2.2.4
### *Phenylalanine Hydroxylase*

Two phenylalanine hydroxylases have been described, one containing iron and one containing copper. Both are phylogenetically related to the group of enzymes which hydroxylate aromatic amino acids, including tryptophane and tyrosine hydroxylase [187]. No phylogenetic relationship could be constructed to other proteins [183–186, 327].

### 2.2.5
### *Other Type 2 Copper Proteins*

Amino acid sequence comparisons of the other type 2 copper proteins with various copper and non-copper proteins did not detect any significant phylogenetic relationship.

## 2.3 Type 3 Copper Proteins

The hemocyanins of mollusks and arthropods (M-Hc and A-Hc) vary fundamentally in form, structure, and amino acid sequence. The sole similarity is their identical function suggesting convergent evolution. The two hemocyanins differ in the following ways [34].

- The subunits of A-Hc have a molecular mass of 75 kD, those of M-Hc 50 kD.
- A-Hc is dissociable in individual $O_2$-binding subunits of 75 kD. The smallest M-Hc unit which still binds oxygen weights 350–450 kD and consists of eight functional units.
- The quaternary structure of A-Hc consists of single to multiple units of hexamers, while M-Hc is a hollow, cylindrical particle with a diameter of approximately 30 nm. It contains 10–20 subunits of 400 kD weight, resulting in up to 160 oxygen binding centers of 50 kD weight.
- Ninety percent of the amino acid sequence of M-Hc is non-homologous to that of A-Hc.
- The binuclear copper-binding center in M-Hc is closer to the surface of the protein than in A-Hc.
- M-Hc displays tyrosinase activity, in contrast to A-Hc.

Although 90% of the amino acid sequences of M-Hc and A-Hc are non-homologous, there is a small region of 42 amino acids which is conserved in both proteins [247]. This section encodes the $Cu_B$-binding site of the binuclear copper center [247]. Sequence analysis of the copper-binding site in tyrosinases reveals the same conserved copper-binding sequence. The discovery of a conserved

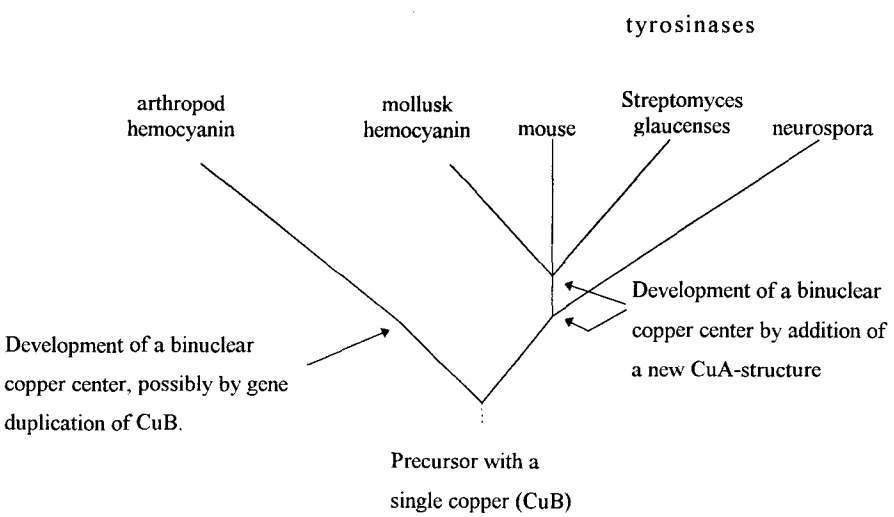


**Fig. 41.** Phylogenetic tree of type 3 copper proteins. According to Drexel et al. 1987 [247]

structure in various proteins suggests divergent evolution and would refute the theory of convergent evolution mentioned above. It is possible, however, that both evolutionary mechanisms were applied in the development of type 3 copper enzymes. The question remains, though, of how.

The sequence homologies of the $Cu_B$-binding sites suggest that they arose from a common precursor. The differences in the $Cu_A$-binding sites, however, lead to the assumption that the type 3 copper centers were generated by different means (Fig. 41).

The origin of the phylogenetic tree is a mononuclear copper protein whose copper-binding site possibly became the $Cu_B$-binding site. This precursor of the type 3 copper proteins evolved into the hemocyanins and tyrosinases. However, the co-evolution of the binuclear center in these proteins occurred differently. The left branch consists of A-Hc, for which it is assumed that the $Cu_A$ binding site developed by gene duplication of $Cu_B$. Not only are the histidine ligands of both copper atoms embedded in the sequence H-X-X-X-H-ca.30X-H, but the N-terminal border of the third histidine consists of a hydrophobic, special aromatic rest as well. However, this is not an unquestionable homology [247].

Sequence comparisons show that the $Cu_A$-binding sites of M-Hc and the tyrosinases did not develop by gene duplication of $Cu_B$, but by the addition of a new copper-binding structure, possibly of a totally new copper protein. In this, M-Hc and most tyrosinases differ from the tyrosinase of Neurospora [34, 247].

A comparison of type 3 copper proteins with other copper proteins, for example, cupredoxins, SOD, or the blue oxidases, could not detect any sequence homologies. Consequently, the $Cu_A$-binding site of M-Hc and the tyrosinases was recruited from a protein which has either not yet been discovered or which has been lost and only survives in the form of $Cu_A$-binding sites. Again, it has possibly only lost its copper-binding ability. A sequence search of non-copper-binding proteins may yet uncover a relative of the protein which was recruited as the $Cu_A$-binding site.

While the $Cu_B$-binding sites of hemocyanin and tyrosinases are clearly the products of divergent evolution, the binuclear type 3 copper centers and protein structures are the results of convergence. However, once they had been established, the active centers of mollusk hemocyanin and the tyrosinases switched to divergent paths.

## 2.4
## $Cu_A$-/$Cu_B$-Proteins

The copper enzymes cytochrome *c* oxidase, ubichinone oxidase, and $N_2O$-reductase contain several redox-active groups: a heme-$Cu_B$- or a binuclear $Cu_A$-center, as well as additional heme-groups. The metal-binding structures of these proteins are conserved [279]. A comparison of the protein structures and amino acid sequences of $cbb_3$-type-cytochrome *c* oxidase and the non-copper enzyme NO-reductase (a *bc*-heme type enzyme which reduces NO to $N_2O$) reveals the close relationship of these enzymes and, thus, a common ancestor. The $cbb_3$-type-cytochrome *c* oxidase also shows a high affinity to oxygen guaranteeing its proper function even in regions of low oxygen content [279]. It is most

**Table 14.** Various types of cytochrome *c* and ubichinone oxidases. According to van der Oost et al. 1994 [279]

| | type | heme/copper | | species |
|---|---|---|---|---|
| | | subunit I | subunit II | |
| cytochrome oxidases | $cbb_3$ | $bb_3/Cu_B$ | c/no $Cu_A$ | *P. denitrificans* |
| | $aa_3$ | $aa_3/Cu_B$ | no heme/$Cu_A$ | *P. denitrificans* |
| | $caa_3$ | $aa_3/Cu_B$ | c/$Cu_A$ | *B. subtilis* |
| ubichinone oxidase | $bo_3$ | $bo_3/Cu_B$ | no heme/no $Cu_A$ | *E. coli* |

likely that the first terminal oxidase which developed during the oxygenation of the atmosphere was a variant of this type of cytochrome *c* oxidase which, as well as all other cytochrome oxidases, evolved from a common ancestor.

Ubichinone oxidases do not contain $Cu_A$-dimers, although they may be restored by site-directed mutagenesis of a few amino acids [278a]. This suggests that the $Cu_A$-binding site which, in cytochrome *c* oxidases, accepts electrons from cytochrome *c*, was lost. The "docking"-function for cytochrome *c* was no longer required as ubichinone is the physiological electron-donor.

$N_2O$-reductase shows no marked sequence homology to the cytochrome oxidases [328]. They only share the $Cu_A$-dimer structure [280]. This could be the result of a translocation of the gene sequence encoding the binding site of the binuclear center, thus leading to the same sequence in two totally unrelated groups of proteins.

The various types of cytochrome oxidases contain different redox-active groups which are responsible for electron-transport from an external donor (cytochrome *c* or ubichinone) to oxygen [279] (Table 14). NO-reductase contains *b*- and *c*-type cytochromes but no $Cu_A$- or $Cu_B$-sites.

A feasible phylogenetic tree can be compiled from a comparison of the amino acid sequences of various cytochrome oxidases and NO reductase [279] (Fig. 42).

Although it is unknown whether the common ancestor of the two enzyme classes was a NO-reductase or a cytochrome oxidase [279], it can be assumed that it had a catalytic function. In all probability, however, copper did not become biologically available until after the two genetic paths had separated. The first copper center inserted into the precursor of the cytochrome oxidases was a $Cu_B$-heme group. This precursor protein was the starting point for several different evolutionary paths, giving rise, for example, to the earliest cytochrome *c* oxidase, the $ccb_3$-type cytochrome *c* oxidase. On a different evolutionary branch, a $Cu_A$-dimer, which probably came from an enzyme similar to $N_2O$ reductase, was inserted in the protein. However, it is possible that the $Cu_A$-dimer was transferred to the cytochrome oxidases and $N_2O$ reductase from yet another enzyme. This new copper center was conserved in the $aa_3$- and $caa_3$-type cytochrome *c*- but lost in the development of the ubichinone oxidases.

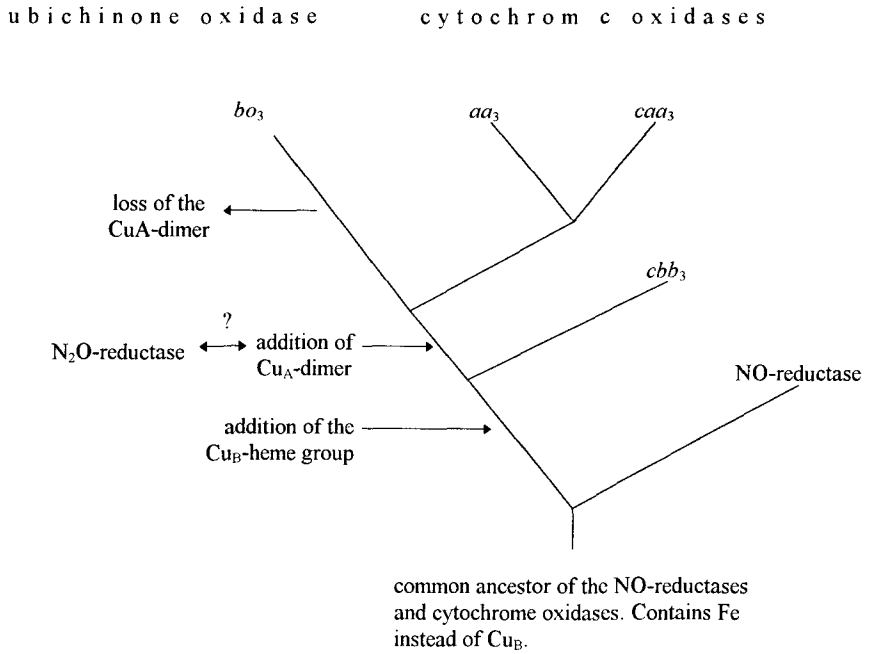


**Fig. 42.** Possible phylogenetic tree of $bo_3/aa_3/caa_3/cbb_3$-type cytochrome oxidases and related enzymes. The distance between branching points is not related to the temporal course of development but simply shows its possible sequence

Accordingly, the cytochrome oxidases are the product of a divergent evolution from the common precursor of the cytochrome oxidases and $N_2O$ reductase. The only convergent evolution found in cytochrome oxidases is the common structure shared with $N_2O$ reductase concerning the independent insertion of a copper center in these dissimilar enzymes.

## 2.5 Metallothioneins

With few exceptions, metallothioneins consist of relatively simple amino acids, aromatic amino acids and histidine only being found in a small number of species [329]. This amino acid composition suggests that metallothioneins evolved early in the evolution of life, probably even before the oxygenation of the atmosphere. A further clue is one of their functions. As metal-transport and storage proteins, thioneins are capable of binding metal ions but release them relatively easily as well. Metallothioneins can therefore be considered a transition from non-metal to metalloproteins. It is improbable, however, that the known copper proteins evolved from copper metallothioneins as there are no homologies between them and other copper proteins or enzymes.

The remarkable structural feature of metallothioneins is the sevenfold repetition of the sequence Cys-X-Cys in class I metallothioneins [58]. These two cy-

**Table 15.** Distribution of copper proteins throughout the various kingdoms of life and their relationship to non-copper proteins

| protein class | known relationship to non-copper proteins | occurrence |
|---|---|---|
| small blue proteins | (+) | archaea, bacteria, eukarya |
| blue oxidases[a] | – | eukarya |
| non-blue oxidases | + | single-celled organismus, eukarya |
| oxygenases | + | single-celled organismus, eukarya |
| Cu,Zn-SOD | + | single-celled organismus, eukarya |
| hemocyanins[a] | – | eukarya |
| cytochrome oxidases | + | single-celled organismus, eukarya |
| nitrite reductase | – | single-celled organismus |
| $N_2O$ reductase | – | single-celled organismus |
| copper thionein | + | single-celled organismus, eukarya |

[a] These enzymes only occur in higher eukarya.

steine residues create a metal binding site of trigonal coordinative geometry with a third, more distant, cysteine [54, 58]. Metallothioneins contain varying amounts of transition metals depending on the tissue from which they are isolated. Sequence data show, however, that this is not based on differing primary structures but on the different distribution of metals among the tissues [58]. Metallothioneins seem especially suited for the binding of copper as the Cu(I)-GSH complex, which is possibly the physiological copper donor for metallothioneins, can displace Zn(II) and Cd(II) from metallothioneins [54].

All of the copper proteins described here, which are phylogenetically or functionally related to non-copper proteins, are important for single-celled organisms (Table 15). No statement can be made concerning the relevance of those non-copper proteins, for which knowledge of a functional relationship with copper proteins is missing, as ignorance is not equivalent to non-existence. Nevertheless, many copper proteins which lack a direct phylogenetic relationship or functional equivalence to phylogenetically older non-copper proteins are of no importance to simple organisms as they are directly related to the multicellularity of organisms. Examples of typical copper proteins of multicellular organisms are enzymes containing trinuclear centers (blue oxidases) and hemocyanins. There are, naturally, also copper proteins which are typical for single-celled organisms and which are of no importance to multicellular organisms – small blue proteins (with the exception of the chloroplasts of plants) and denitrification enzymes.

## 3 The Evolution of Copper-Binding Centers

The evolution of copper-binding centers is closely linked to that of copper proteins and several non-copper proteins. For, not only did the individual proteins and enzymes evolve, but so did the various copper-binding centers. In the following, an attempt will be made to assign copper-binding centers to develop-

mental principles and discuss the relevance of evolutionary mechanisms and the occurrence of certain proteins in certain phylogenetic kingdoms.

Some copper-binding centers evolved by mutations within non-metal proteins, while others evolved by changes to existing metal-binding sites. The following will also differentiate between copper-binding sites which emerged from the binding sites of other metals and those which evolved by recombination and alteration of existing copper-binding sites. The evolution of certain copper-binding sites was only made possible by modifications in proteins, creating totally new catalytic properties. The fine regulation of these properties was achieved by alterations in the copper-binding center itself or its immediate surroundings.

### 3.1
### Type 1 Copper Centers

The earliest types of copper proteins were probably the small blue proteins, which occur only in single-celled organisms and the chloroplasts of plants. As they are at the beginning of various copper-proteins, it is not possible to decide whether they evolved from a metal-binding or a non-metal binding precursor. Nevertheless, it can be assumed that this precursor was already an essential protein. As discussed in Sect. 2, the precursor of small blue proteins probably existed prior to the separation of the three kingdoms of life (bacteria, archaea, and eukarya). It is improbable that it would have remained more or less unchanged throughout the large time span between the separation of the kingdoms and the first bio-availability of copper had it not had an essential function.

In some organisms, small blue proteins (plastocyanin, azurin) and cytochromes ($c_6/c_2$) fulfill the same function. The evolution of these copper proteins occurred separately from that of the cytochromes. The distribution of the two types of electron-carriers throughout the various organisms shows an iron to copper trend which parallels the evolutionary stage of an organism. That the trend went from iron to copper is supported by the observation that organisms which are facultatively capable of producing both proteins only produce the cytochrome carrier during conditions of copper-deficiency, in conditions similar to those which prevailed prior to the oxygenation of the atmosphere. The availability of copper results in a corresponding reduction of cytochrome synthesis.

These iron and copper electron-carriers are not only functionally equivalent – they are also equivalent in the manner of their electron-transfer. Consequently, the utilization of different, but equivalent, electron-carriers for the same purpose is best explained by the bio-availability of the respective metals at the time of protein development.

### 3.2
### Type 2 Copper Centers

The phylogenetic origin of several type 2 copper proteins has not yet been clarified as no other proteins of similar amino acid sequence have been found. The

evolution of other metal-binding centers to copper-binding centers can, however, easily be followed in the type 2 copper enzymes Cu,Zn-superoxide dismutase and phenylalanine hydroxylase. The copper-binding center of Cu,Zn-superoxide dismutase evolved after the phylogenetically older forms Fe- and Mn-superoxide dismutase were widely spread. Although the superoxide dismutases are clearly related, no phylogenetic homologies have yet been found with other enzymes. Phenylalanine hydroxylase also exists in phylogenetically related forms, which utilize different metal-binding centers – a copper- and an iron-dependent form. Additionally, phylogenetically related enzymes are the non-copper proteins tryptophane- and tyrosine hydroxylase. Of all these enzymes, the copper-dependent phenylalanine hydroxylase shows the least homology to the other members of this family. As all three hydroxylases were certainly already necessary and widely spread before copper became biologically available, it may be assumed that the copper enzymes evolved from iron-dependent precursors. Consequently, the occurrence of copper-dependent enzymes support the assumption of an iron to copper evolution.

### 3.3
### Type 3 Copper Centers

No proteins or enzymes have yet been found which possess any significant homology to the hemocyanins or tyrosinases. The development of these proteins, as shown in Sect. 2, suggests that the binuclear centers resulted from the combination of two mononuclear centers.

### 3.4
### Trinuclear Copper Centers

Trinuclear copper centers have only been found in blue oxidases. As shown in Sect. 2, the domains of the blue oxidases are the result of multiple duplications of a single domain, which is phylogenetically closely related to the small blue proteins. These duplications arranged the type 1 copper-binding centers in such a manner that enabled the formation of a totally new type of copper center. Therefore, the copper-binding centers of the blue oxidases are products of alterations and recombinations of previously existing, fully functional copper centers.

#### 3.4.1
#### *Ascorbate Oxidase*

The three-domain structure of ascorbate oxidase is the result of two duplications of the original domain, which was most similar to the small blue proteins and the C-terminal domain (domain 3) of the blue oxidases [71]. These duplications did not, however, lead to a protein with three type 1 copper centers arranged in a row. The original type 1 copper center has only been retained in domain 3, where it has still kept its function of transferring electrons to the active center [36]. The extensive alterations in the amino acid sequence of domain 2

**Table 16.** Ligand distribution in the type 1 and trinuclear copper centers of ascorbate oxidase. CU1: type 1 copper center; CU2, 3, and 4 form the trinuclear center. The domains in which the ligand are located are listed in parentheses behind their position. From Messerschmidt et al. 1992 [36]

| copper ligands of the mono- and trinuclear centers | | | |
|---|---|---|---|
| CU1 | CU2 | CU3 | CU4 |
| His 445 (3) | His 106 (1) | His 62 (1) | His 60 (1) |
| Cys 507[a] (3) | His 450 (3) | His 104 (1) | His 448 (3) |
| His 512 (3) | His 506[a] (3) | His 508[a] (3) | |
| Met 517 (3) | | | |

[a] The type 1 copper center is coupled to the trinuclear center via the amino acid bridge His 506Cys 507His 508.

led to the loss of its metal-binding center. Even domain 1 is no longer able to bind copper by itself. It does, however, contribute three of the eight histidine ligands coordinating the trinuclear copper center of ascorbate oxidase (Table 16) [36]. The trinuclear center is coupled to the type 1 copper center via the peptide bridge His 506-Cys507-His508. The trinuclear center is frequently described as the combination of a type 2 and a type 3 copper center. This formal classification is unfortunate and even misleading as the so-called type 2 and type 3 copper centers are phylogenetically unrelated to other type 2 or 3 centers. The catalytic properties and the relative distribution of the ligands of the trinuclear center differ from those of type 2 or 3 centers as well. Consequently, these trinuclear copper centers should be recognized as a separate type of copper-binding center, for example as a type 4 copper center.

### 3.4.2
### *Ceruloplasmin*

Three type 1 copper centers were maintained in the development of the six domains of ceruloplasmin and are situated in the C-terminal regions of the double-domains [71] (Fig. 43). As in ascorbate oxidase, only the C- and N-terminal domains contribute ligands for the coordination of the trinuclear center. The sequence and positions of the histidine ligands of the trinuclear centers of ascorbate oxidase (CU2, 3 and 4) and ceruloplasmin (CU10, 20 and 30) are homologous [25] (Tables 16 and 17).

The distribution of the copper centers of ascorbate oxidase and ceruloplasmin are remarkably similar:

- the type 1 copper centers are located in the C-terminal region of the double-domains (see Sect. 3.1);
- the coordinating histidine ligands of the trinuclear centers are contributed exclusively by the N- and C-terminal domains;
- the histidine ligands of the trinuclear centers of ascorbate oxidase and ceruloplasmin are homologous.

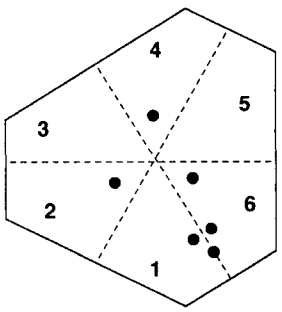


**Fig. 43.** Distribution of ceruloplasmin's copper centers within the six domains. Adapted from [25]

The trinuclear center of ceruloplasmin is formed by ligands from domains 1 and 6. The intermediate domains 2–5 possibly function as 'spacers', constituting the three-dimensional framework which allows the trinuclear center to be formed. Domain 2 of ascorbate oxidase could possibly play an equivalent role to that of ceruloplasmin's domains 2–5. The possible physiological function of the regions between the N- and C-terminal domains would, therefore, be to connect these two domains in such a flexible manner that the histidines ligands are positioned according to the geometric requirements of the trinuclear center, something that would not be achieved without these "spacers".

The extensive homology between the structures of the trinuclear binding sites of the two enzymes suggests that the organization of the copper-binding ligands, and thus the copper-binding site, of the first double-domain, has hardly changed since it was formed by duplication of the precursor of the small blue proteins and the blue oxidases. Only domain 2 of ascorbate oxidase and domains 3 and 5 of ceruloplasmin could afford significant changes in their primary structure without the enzymes suffering the loss of their essential copper-binding sites.

**Table 17.** Ligand distribution in the type 1 and trinuclear copper centers of ceruloplasmin. CU2, 4, and 6 are the type 1 copper centers of domains 2, 4, and 6; CU10 is the so-called "type 2 component", CU20 and CU30 are the "type 3 components" of the trinuclear copper center. The domains in which the ligand are located are listed in parentheses behind their position. From [25] (see also Fig. 8)

| copper ligands of the mono- and trinuclear centers | | | | | |
|---|---|---|---|---|---|
| CU2 | CU4 | CU6 | CU10 | CU20 | CU30 |
| His 276 | His 637 | His 975 | His 101 (1) | His 103 (1) | His 163 (1) |
| Cys 319 | Cys 680 | Cys 1021 | His 978 (6) | His 161 (1) | His 980 (6) |
| His 324 | His 685 | His 1026 | | His 1022 (6) | His 1020 (6) |
| no Met | Met 690 | Met 1031 | | | |

The evolution of blue oxidases from the small blue proteins clearly shows the transition from protein to enzyme, a result of the development of new and the recombination of existing copper centers. That these copper centers are essential for the enzymes' function is demonstrated by the fact that related proteins which have lost their copper centers no longer show enzymatic properties. Only the surface structures of these proteins, i.e., the coagulation factors CF5 and CF8 as well as the pollen antigen Ra3, are required for their function. The evolution of this class of proteins (small blue proteins, pollen antigens, blue oxidases, and coagulation factors) is clearly a result of the evolution of their copper-binding centers.

### 3.5
### Cytochrome Oxidases

The evolution of iron- to copper-dependent redox-active centers can also be observed in the development of cytochrome oxidases. Although the redox centers of the common precursor of NO-reductase and the cytochrome oxidases were solely iron cytochromes, the $Cu_B$-center was introduced during the development of the *cbb*$_3$-type cytochrome oxidase (see also Sect. 2.4). This center reveals the convergent evolution of blue oxidases and the cytochrome oxidases, which separately developed structures capable of reducing oxygen to water by the transfer of four electrons. The origin of the $Cu_B$-center has not yet been solved. The second copper center of the cytochrome oxidases, the $Cu_A$-dimer, also occurs in $N_2O$-reductase. Another similarity to the blue oxidases may be observed in the evolution of ubiquinone oxidases from cytochrome oxidases. In both instances a copper-binding center was lost, which in the latter case, however, did not result in a loss of the catalytic activity of the enzyme. This catalytic activity was maintained as the copper-binding site was not the active centre but only a redox-active center, which transferred electrons to the active center.

Amino acid sequence and structure comparisons of the region surrounding the $Cu_A$-dimer with the small blue proteins reveal marked homologies. The copper ion ligands are one histidine, two cysteines, and a methionine, which may be replaced by a glutamate residue. Both cysteines coordinate both copper ions [43, 44]. These ligands are very reminiscent of the type 1 copper-binding centers of plastocyanin and stellacyanin. The $Cu_A$-dimer could, therefore, have resulted from the connection of two different type 1 copper centers, or from a type 1 structure which was supplemented by additional ligands so that two copper ions could be coordinated by six ligands.

Structural analogies may be seen when comparing the enzymes of the denitrification pathway with cytochrome oxidases. The question arises, in which manner the evolution of the NO-reductases and that of the cytochrome oxidases are chronologically and correlatively linked. Both enzyme classes may have evolved from a common precursor, although it has still not been resolved, whether this precursor was a NO-reductase or a terminal oxidase [279]. If the precursor was a terminal oxidase, what was its substrate? Probably not oxygen, for if it had been oxygen, the precursor would have had to be capable of a four-electron reduction. This would require, though, that the $Cu_B$-center had com-

pletely supplanted a functionally equivalent structure. The cases of the small blue proteins and some type 2 copper enzymes demonstrate, however, that functionally equivalent proteins evolve but are never completely able to supplant their functionally equivalent structures. No life-form has yet been described possessing a terminal oxidase which is capable of reducing oxygen, which is phylogenetically related to the cytochrome oxidases, but does not have a $Cu_B$-center. However, if the substrate of the potential terminal oxidase was not oxygen, why did this enzyme simple disappear from all life-forms following the introduction of the $Cu_B$-structure?

Provided the precursor of the NO-reductases and the cytochrome oxidases was a NO-reductase, it is possible that other enzymes of the denitrification pathway existed. Were this the case, however, it would be possible that the cytochrome oxidases are the product of a combination of various enzymes of this metabolic pathway. The basic structure of the cytochrome oxidases would then have originated from an earlier NO-reductase, in which the $Cu_B$-structure of unknown origin had been added. The $Cu_A$-dimer could have been added to the cytochrome oxidases later by translocation of a gene. The origin of this gene would probably be that of $N_2O$-reductase. If these assumption are correct, aerobic respiration evolved in organisms which were already capable of denitrification.

## 4 Copper Proteins and Ozone

The first pure oxygen compound which confronted organisms following oxygenation of the atmosphere was dioxygen. Its extremely high oxidative properties were, then, fatal for most of the anaerobic organisms. The high redox potential was a large but dormant source of energy, which required appropriate proteins and enzymes for its utilization. The redox potential of the reaction

$$O_2 + 4e^- + 4H^+ \rightarrow 2H_2O$$

is +815 mV. Copper proteins and enzymes were and are unrivaled in coping with these high redox potentials as their own redox potentials are high enough to catalyze a controlled reaction of oxygen, controlled reactions which are necessary to harness the oxidative energy of oxygen into useful energy. Thus, the use of the appropriate enzymes not only detoxicated the initially toxic compound but guided its energy into useful channels.

The occurrence of ozone in the lower atmosphere has brought land-bound organisms into contact with an oxygen compound whose oxidative potential exceeds that of dioxygen by far. The standard reduction potential of the reaction

$$O_3 + 2H^+ (10^{-7}\ \text{mol/l}) + 2e^- \rightarrow O_2 + 2H_2O$$

is +1.65 V [330]. In the search for proteins capable of coping with such a high reduction potential, copper proteins appear to be the best candidates. This section will treat the question whether ozone-metabolizing enzymes are practical or even possible.

## 4.1
## Generation and Decomposition of Ozone

Ozone is produced by the reaction of short-waved, high-energy solar radiation with dioxygen. Light quanta with wavelengths < 242 nm split $O_2$-molecules into two oxygen atoms which react with further oxygen molecules to produce ozone [4]:

$$O_2 + h\nu \rightarrow O: + :O \ (\lambda < 242 \text{ nm})$$
$$O: + O_2 + M \rightarrow O_3 + M^*$$

M is an inert impact partner which, by acquiring some of the kinetic energy, slows the oxygen atom and, thus, enables the generation of ozone. The whole reaction is accordingly the photochemical reaction of three dioxygen molecules to two molecules of ozone:

$$3O_2 + h\nu \rightarrow 2O_3.$$

Ozone decomposes following the absorption of ultraviolet radiation with wavelengths between 220 and 320 nm [4].

$$O_3 + h\nu \rightarrow O: + O_2 \ (220 \leq \lambda \leq 320 \text{ nm})$$

This leads to an equilibrium between generation and decomposition of ozone in the stratosphere, preventing the harsh solar radiation from reaching the earth's surface. Nitrogen oxides and halogenated hydrocarbons catalyze the decomposition of ozone, thus, shifting this equilibrium [4]:

$$NO + O_3 \rightarrow NO_2 + O_2$$
$$NO_2 + :O \rightarrow NO + O_2$$
$$\bullet Cl + O_3 \rightarrow \bullet ClO + O_2$$
$$\bullet ClO + :O \rightarrow \bullet Cl + O_2$$

## 4.2
## Physical and Chemical Properties of Ozone

Ozone is a pale blue gas with a boiling point of −111 °C and a melting point of −193 °C. It consists of three oxygen atoms which are aligned in a binding angle of 117°. The distances between the inner and the outer atoms is 128 pm, which suggests a delocalized $\pi$-bond [331].

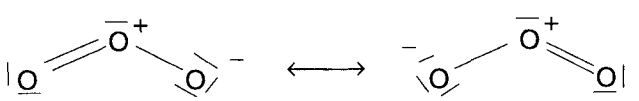

The ozone molecule is paramagnetic as it lacks unpaired electrons. Its oxidative potential is almost as high as that of atomic oxygen and is only exceeded by few other compounds such as $F_2$, $S_2O_8^{2-}$, $H_4XeO_6$, and $KrF_2$ [331]. This is reflected in the standard reduction potential, E° +1.65 V for the reduction of ozone [330]:

$$O_3 + 2H^+ (10^{-7} \text{ mol/e}) + 2e^- \rightarrow O_2 + 2H_2O$$

which is much higher than that of the four-electron reduction of oxygen to water ($E^\circ = 0.815$ V). Ozone is also an extremely unstable and short-lived compound, which decomposes through physical as well as chemical processes.

## 4.3 Ozone's Effect on Organisms

As explained in Sect. 1, the high oxygen concentration in the atmosphere and stratosphere, as well as the high-energy solar radiation, favor the production of ozone. The resulting ozone layer protects the earth's surface very effectively from the harmful effects of the sun's short-wave radiation. Due to the artificial reduction in the volume of the ozone layer, ultraviolet light can penetrate almost unobstructed to the earth's surface. This, in addition to the immediately damaging effects, increases the concentration of ozone in the atmosphere. Ozone is as harmful to organisms in direct exposure as it is advantageous in the stratosphere. The effects of ozone on various regions of the respiratory tract are of special interest. Ozone is less soluble in water than the irritants HCl, $NH_3$, $Cl_2$, and $SO_2$, and is, consequently, not absorbed in the upper section of the respiratory tract. It penetrates deeply into the lungs where it reacts with the double bonds of unsaturated fatty acids [332–339] and with proteins [340–348]. The reaction products of fatty acids are aldehydes, carbonic acids, and $H_2O_2$ [349], as well as secondary ozonides [338], whose decomposition results in radicals [338]. The reaction products of the proteins are the various oxidation products of the amino acids [339, 350]. The reaction of ozone with tertiary amines, sulfides, sulfoxides, phosphites, sterically hindered olefins, certain ethers, and aldehydes [351–354] may even liberate singlet oxygen [350]. In aqueous solutions, ozone even produces hydroxyl radicals and superoxide anions via radical chain reactions [355–357].

The most important antioxidants in coping with ozone stress are vitamin E [358], ascorbate, and uric acid [359]. These antioxidants are, however, only suitable for scavenging the products arising from ozone but is not useful against ozone itself. Circumventing protective measures, these products can, consequently, exhibit their cytotoxic effects between the site of their production and that of their detoxification by the antioxidants, resulting in inflammations, impairments in immunological and respiratory status [360, 361] and even cancer [362, 363].

## 4.4 Structural and Functional Criteria for Ozone-Metabolizing Enzymes

Although equipped with several antioxidants, land-bound organisms have practically no protection against ground-level ozone, as the antioxidant do not protect against ozone itself but only its degradation products. A specific antiozonant is as yet unknown. In any case, it has not yet been necessary, as the organisms' antioxidants were able to cope with the prior ozone concentrations.

Current ozone concentrations have changed to such a degree that ozone-metabolizing enzymes would be a distinct selective advantage.

Which properties would such an enzyme require? The copper proteins and enzymes discussed so far cover a potential range of +0.17 to +0.785 V, switching between copper's Cu(I) and Cu(II) oxidation states. The redox potential of the two-electron reduction of ozone to oxygen and water is, however, 1.65 V. A direct reaction of ozone with one of these copper enzymes would probably lead to irreversible oxidation and damage of the enzyme. The redox potential of Cu(III)/Cu(II)-couples with various copper-glycine complexes, utilizing the N-atom of the peptide bond as a ligand for the central ion, are in the range of 0.5 to 1.0 V [364]. Coordination of copper by even "harder" ligands would, according to the HSAB concept, increase the redox potentials. As ligands, the amino acid tyrosine, as well as "hard" hydroxyl ions, phosphate groups (for example from ATP, ADP, or AMP), sulfate groups (3′-phosphoadenosine-5′-phosphosulfate), and even ethers, anhydrides, siliciumdioxide, or silicates ($SiO_4^{4-}$) would appear suitable. The utilization of a copper center which alternates between the oxidation states Cu(II) and Cu(III) seems most appropriate for the direct metabolism of ozone. The geometric arrangement of the ligands should support the alternation between the two redox states. As $Cu^{3+}$ is isoelectronic to $Ni^{2+}$, it accordingly prefers the same ligand geometry [365, 366]. While $Cu^{2+}$ prefers a square planar geometry with four ligands, $Ni^{2+}$ [17], and thus $Cu^{3+}$, accept square planar as well as tetrahedral geometries. Consequently, copper ligands in an ozone-metabolizing enzyme should be arranged in a geometry which is situated between tetrahedral and square planar. The occurrence of the oxidation state Cu(I), which is promoted by a tetrahedral geometry, would be prevented by the "hard" ligands (tyrosine, hydroxyl ions). The binding site of an ozone-metabolizing enzyme should, independent of its copper ion, possess the following properties:

- 'hard' ligands such as tyrosine and hydroxyl ions;
- tetrahedral geometry of the coordinating ligands; and
- a free binding site for ozone.

Various reaction pathways are conceivable for the conversion of ozone into less reactive oxygen species. Ozone could be reduced by two electrons to water (or a hydroxyl ion) and oxygen, by four electrons to hydrogen peroxide and water, or by six electrons to three equivalents of water:

a) $O_3 + 2e^- + 2H^+ \rightarrow O_2 + H_2O \quad E° = +1.65\ V$ [330]
b) $O_3 + H_2O + 2e^- \rightarrow O_2 + 2OH^- \quad E° = +1.24\ V$ [330]
c) $O_3 + 4e^- + 4H^+ \rightarrow H_2O_2 + H_2O$
d) $O_3 + 6e^- + 6H^+ \rightarrow 3H_2O$

If the oxidation states of copper during its reaction with ozone are limited to Cu(II) and Cu(III), there are various ways in which ozone can bind to mono- or oligonuclear copper centers (Fig. 44). These structures are based on the assumption that copper is, initially, present in its Cu(II) oxidation state and is oxidized to Cu(III) following the binding of ozone. Ozone itself is reduced with one or two electrons, facilitating its further reaction to water and oxygen.

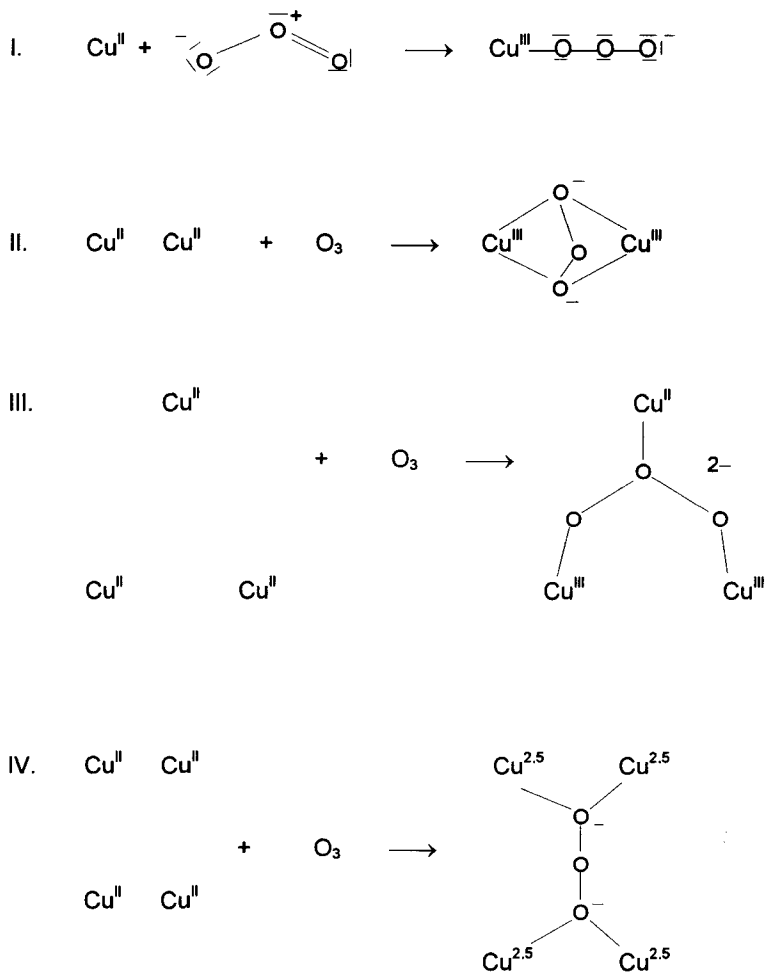


**Fig. 44.** Hypothetical models for the binding of ozone to Cu(II)/Cu(III)-centers appropriate for the two-electron reduction of ozone to water and oxygen. See the text for a description

In example I (Fig. 44), the enzyme only transfers one electron to the bound ozone, necessitating the transfer of a second electron in the reduction of ozone to water and oxygen. The binding type resembles that of the copper-binding center of Cu,Zn-superoxide dismutase. In example II, ozone is bound in a manner reminiscent of hemocyanins or tyrosinases. The third oxygen atom elongates ozone so much that its binding would require a reduction of the angle formed by its three oxygen atoms. The reduction would increase ozone's intramolecular tension, assisting the decomposition of ozone to water and oxygen. Example III represents a binding type, which did not occur in the proteins treated here. The copper ions display differing oxidation states after ozone binding,

which would require different ligands and environments for the individual copper ions. The manner of electron distribution in example IV is modeled on that of the $Cu_A$-center in cytochrome *c* oxidases, in which electrons are delocalized over two copper ions. This would require that the ligand environments are appropriately similar to each other. Examples II-IV allow the direct reaction of the, formally, double negatively charged ozone with two protons. The protons would be taken from, e.g., closely situated histidine residues or from the solvent itself. External or internal electron-donors, such as histidine residues, could then reduce the Cu(III) ions back to Cu(II). A mechanism similar to that of Cu,Zn-superoxide dismutase is not very probable for an ozone-metabolizing enzyme. Ozone could be reduced to water and oxygen in the first step, but in the second step a different ozone molecule would be required to donate two electrons. The redox potential of this step would be prohibitively high, as well as producing additional reactive oxygen species.

## 5 Conclusion

A great number of active centers in proteins and enzymes contain one or more transition metals. Each metal imposes specific catalytic properties on the protein, which could not be achieved when employing a different metal. The special role and characteristic reactivity of coordinated copper is illustrated by looking at the evolutionary aspects of copper proteins.

The evolution of copper-binding centers in biology occurred in three distinct manners. The copper-binding centers of metallothioneins and type 1 copper centers developed in non-metal proteins. The transformation of the metal-binding centers of iron or manganese proteins led to the development of the type 2 copper centers. The trinuclear copper-binding centers of the blue oxidases were formed by alterations and recombinations of type 1 copper centers. Simple, although as yet unknown, mononuclear copper centers gave rise to the type 3 copper-binding sites of hemocyanins and tyrosinases, as well as to the $Cu_A$- and $Cu_B$-centers of the cytochrome oxidases and $N_2O$-reductase. According to this assignment, copper proteins containing either type 1 copper, type 3 copper, $Cu_A$-centers, or $Cu_B$-centers share a common ancestor. They developed at least in part by divergent evolution. Type 2 copper proteins are the product of convergent evolution and, consequently, show little or no phylogenetic homology.

All copper proteins which are known to be phylogenetically related to non-copper proteins – i.e., the small blue proteins, metallothioneins and some type 2 copper proteins – are found in single-celled organisms. Hemocyanins, blue oxidases, and those type 2 copper proteins whose functions are essential for multicellular life-forms are not phylogenetically related to non-copper proteins and do not occur in single-celled organisms.

For an enzyme to be suitable for the metabolism of ozone, its copper-binding site would have to catalyze redox reactions at very high redox potentials. The redox couple Cu(II)/Cu(III) seems to be suitable for this purpose. The stabilization of Cu(III) requires hard ligands, such as tyrosines, hydroxyl anions, phos-

phate- and sulphate-groups, ethers, anhydrides, silicon dioxide, or silicates. To avoid preference of the Cu(II) oxidation state, which would be accompanied by a reduction of the redox potential, the copper ligands should be arranged in a tetrahedral or distorted tetrahedral geometry. These guidelines allow the formulation of both mono- and oligonuclear copper-binding centers.

**Acknowledgements.** The stimulating assistance in both scientific discussions and technical performance given by Irmgard Hähnlein, Yoka Kaup and Dr. Hans-Jürgen Hartmann is highly appreciated. Thanks go to Drs. E. Adman, B. Averill, H.J. Dyson, P. Knowles and A. Messerschmidt for providing original colored illustrations to improve the printing quality. Some experimental sections were supported in part by DFG grants awarded to UW.

## 6 References

1. Brock TD, Madigan MT, Martinko JM, Parker J (1994) Biology of microorganisms, 7th edn. Prentice Hall
2. Press F, Siever R (1974) Earth. WH Freeman
2a. Miller SL (1953) Science 117:528
3. Weisz PB, Keogh RN (1982) The science of biology, 5th edn. McGraw-Hill
4. Huheey JE (1988) Anorganische Chemie, Prinzipien von Strukturen und Reaktivität. Walter de Gruyter, Berlin
5. Wehner R, Gehring W (1990) Zoologie, 22nd edn. Georg Thieme, Stuttgart New York
6. Lippard SJ, Berg JM (1995) Bioanorganische Chemie, Spektrum. Akademischer, Heidelberg
7. Williams RJP (1993) In: Welch AJ, Chapman K (eds) Chemistry of the copper and zinc triads. Royal Society of Chemistry, Cambridge, p 1
7a. da Silva Fraústo JJR, Williams RJP (1994) The biological chemistry of elements, the inorganic chemistry of life. Clarendon Press, Oxford
7b. Williams RJP, da Silva Fraústo JJR(1996) The natural selection of the chemical elements. Oxford University Press
8. Katoh S (1977) Plastocyanin. In: Trebst A, Avron M (eds) Encyclopedia of plant physiology: photosynthesis I, New Series 5. Springer, Berlin Heidelberg New York, p 247
9. Sandmann G, Reck H, Kessler E, Böger P (1983) Arch Microbiol 134:23
10. Bohner H, Böger P (1978) FEBS Lett 85:337
11. Wood PM (1978) Eur J Biochem 87:9
12. Lightbody JJ, Krogmann DW (1967) Biochim Biophys Acta 131:508
13. Biggins J (1967) Plant Physiol 42:1447
14. Sandmann G, Böger P (1980) Plant Sci Lett 17:417
15. Steward AC, Blendall DS (1980) Biochem J 188:351
16. Sandmann G (1986) Arch Microbiol 145:76.
16a. Pearson RG (1963) J Am Chem Soc 85:3533
17. Hughes MN (1990) The inorganic chemistry of biological processes, 2nd edn. John Wiley
18. Brischwein M, Scharf B, Engelhard M, Mäntele W (1993) Biochemistry 32:13710
19. Reinhammar BR (1972) Biochim Biophys Acta 275:245
20. Romero A, Nar H, Huber R, Messerschmidt A, Kalverda AP, Canters GW, Durley R, Mathews FS (1994) J Mol Biol 236:1196
21. Baker EN (1988) J Mol Biol 203:1071
22. Guss JM, Freeman HC (1983) J Mol Biol 169:521
23. Nar H, Messerschmidt A, Huber R, van de Kamp M, Canters GW (1991) J Mol Biol 221:765
24. Nersissian AM, Hart PJ, Mehrabian ZB, Nalbandyan RM, Peisach J, Herrmann RG, Eisenberg D, Valentine JS (1996) J Inorg Biochem 64:93

25. Zaitseva I, Zaitsev A, Card G,Moshkov K, Bax B, Ralph A, Lindley P (1996) J Biol Inorg Chem 1:15
26. Averill BA (1996) Chem Revs 96:2951
26a. Kukimoto M, Nishiyama M, Murphey MEP, Turley S, Adman ET, Horinouchi S, Beppu T (1994) Biochemistry 33:5247
27. Han J, Loehr TM, Valentine JS, Averill BA, Sanders-Loehr J (1993) J Am Chem Soc 115:4256
28. Parsons MR, Convery MA, Wilmot CM, Yadav KDS, Blakeley V, Corner AS, Phillips SEV, McPherson MJ, Knowles PF (1995) Structure 3:1171
29. Novotny WF, Chassande O, Baker M, Lazdunski M, Barbry P (1994) J Biol Chem 269:9921
30. Ito N, Phillips SEV, Yadav KDS, Knowles PF (1994) J Mol Biol 238:794
31. Pettingill TM, Strange RW, Blackburn NJ (1991) J Biol Chem 266:16996
32. Gärtner A, Weser U (1986) Topics in Current Chemistry 132:1
33. Tainer JA, Getzoff ED, Richardson JS, Richardson DC (1983) Nature 306:284
34. Linzen B (1989) Naturwissenschaften 76:206
35. Volbeda A, Hol WGJ (1989) J Mol Biol 209:249
36. Messerschmidt A, Ladenstein R, Huber R, Bolognesi M, Avigliano L, Petruzzelli R, Rossi A, Finazzi-Agró A (1992) J Mol Biol 224:179
37. Hazes B, Magnus KA, Bonaventura C, Bonaventura J, Dauter Z, Kalk KH, Hol WGJ (1993) Prot Sci 2:597
38. Lesk AM, Hardmann KD (1985) Methods Enzymol 115:381
39. Cole JL, Clark PA, Solomon EI (1990) J Am Chem Soc 112:9534
40. Malmström BG, Aasa R (1993) FEBS Lett 325:49
41. Kroneck PHM, Antholine WA, Riester J, Zumft WG (1988) FEBS Lett 242:70
42. Farrar JA, Thomson AJ, Cheesman MR, Dooley DM, Zumft WG (1991) FEBS Lett 294:11
43. Iwata S, Ostermeier C, Ludwig B, Michel H (1995) Nature 376: 660
44. Tsukihara T, Aoyama H, Yamashita E, Tomizaki T, Yamaguchi H, Shinzawa-Itoh K, Nakashima R, Yaono R, Yoshikawa S (1995) Science 269:1069
45. Kelly M, Lappalainen P, Talbo G, Haltia T, van der Oost J, Saraste M (1993) J Biol Chem 268:16/781
46. Tsukihara T, Fukuyama K, Nakamura M, Katsube Y, Tanaka M, Kakudo M, Wada K, Hase T, Matsubara H (1981) J Biochem 90:1763
47. Steffens GCM, Soulimane T, Wolff G, Buse G (1993) Eur J Biochem 213:1149
48. Antholine WE, Kastrau DHW, Steffens GC, Buse G, Zumft WG, Kroneck PMH (1992) Eur J Biochem 209:875
49. Blackburn NJ, Barr ME, Woodruff WH, van der Oost J, de Vries S (1994) Biochemistry 33:10401
50. Saraste MQ (1990) Rev Biophys 23:331
51. Adman ET (1991) Adv Protein Chem 42:145
52. Steffens GJ, Buse G (1979) Hoppe Seyler's Z Physiol Chem 360:613
53. Hosler JP (1993) J Bioenerg Biomembr 25:121
54. Da Costa Ferreira AM, Ciriolo MR, Marcocci L, Rotilio G (1993) Biochem J 292:673
55. Kägi JHR, Schäffer A (1988) Biochemistry 27:8509
56. Brouwer M, Winge DR, Gray WR (1989) J Inorg Biochem 35:289
57. Kägi JHR, Kojima Y (1987) Experintia Suppl 52:35
58. Kägi JHR, Kojima Y, Berger C, Kissling MM, Lerch K, Vašák M (1979) Metallothionein: structure and evolution. In: Weser U (ed) Metalloproteins. Georg Thieme, Stuttgart New York, p 194
59. Li YJ, Weser U (1992) Inorg Chem 31:5526
60. Nielson KB, Winge DR (1985) J Biol Chem 260:8698
61. Nielson KB, Atkin CL, Winge DR (1985) J Biol Chem 260:5342
62. Hartmann HJ, Rupp H, Weser U (1979) Oxidation of copper and sulfur in Cu-thionein. In: Metalloproteins, Weser U (ed), Georg Thieme, Stuttgart New York, p 207
63. Rupp H, Cammak R, Hartmann H-J, Weser U (1979) Biochim Biophys Acta 578:426

64. Rupp H, Weser U (1978) Biochim Biophys Acta 533:209
65. Weser U, Hartmann H-J, Fretzdorff A, Strobel G-J (1977) Biochim Biophys Acta 493:465
66. Hartmann HJ, Li YJ, Weser U (1992) Bio Metals 5:187
67. Weser U, Hartmann H-J (1988) Biochim Biophys Acta 953:1
68. McManus JD, Brune DC, Han J, Sanders-Loehr J, Meyer TE, Cusanovich MA, Tollin G, Blankenship RE (1992) J Biol Chem 267:6531
69. Norris GE, Anderson BF, Baker EN (1986) J Am Chem Soc 108:2784
70. Vakoufari E, Wilson KS, Petratos K (1994) FEBS Lett 347:203
71. Rydén LG, Hunt LT (1993) J Mol Evol 36:41
72. Bergmann C, Gandvik E-K, Nyman PO, Strid L (1977) Biochem Biophys Res Commun 77:1052
73. Bergmann C (1980) PhD thesis (Department of Biochemistry and Biophysics), University of Göteborg, Sweden
74. Mattar S, Scharf B, Kent SBH, Rodewald K, Oesterhelt D, Engelhard M (1994) J Biol Chem 269:14939
75. Scharf B, Engelhard M (1993) Biochemistry 32:12894
76. Petratos K, Dauter Z, Wilson KS (1988) Acta Crystallogr Sect B 44:628
77. Adman ET, Turley S, Bramson R, Petratos K, Banner D, Tsernoglou D, Beppu T, Watanabe H (1989) J Biol Chem 264:87
78. Durley R, Chen L, Lim LW, Mathews FS, Davidson VL (1993) Prot Sci 2:739
79. Kraulis PJ (1991) J Appl Crystallogr 24:946
80. Chothia C, Lesk AM (1982) J Mol Biol 160:309
81. Boulter D, Haslett BG, Peacock D, Ramshaw JAM, Scawen MD (1977) In: Northcote DH (ed) International review of biochemistry, plant biochemistry II, 13. University Park Press, Baltimore, p 1
82. Williams RJP (1995) Eur J Biochem 234:363
83. Krogmann DW (1977) Blue green algae. In: Trebst A, Avron M (eds) Encyclopedia of plant physiology: photosynthesis I, New Series 5. Springer, Berlin Heidelberg New York, p 625
84. Binder A (1982) J Bioenerg Biomembr 14:271
85. Sandmann G, Scherer S, Böger P (1984) General aspects of location and interaction of respiratory and photosynthetic electron transport in blue-green algae. In: Wiessner W, Robinson D, Starr RC (eds) Compartments in algal cells and their interaction. Springer, Berlin Heidelberg New York, p 207
86. Kakutani T, Beppu T, Arima K (1981) Agric Biol Chem 45:23
87. Kakutani T, Watanabe H, Arima K, Beppu T (1981) J Biochem 89:453
88. Kakutani T, Watanabe H, Arima K, Beppu T (1981) J Biochem 89:463
89. Hormel S, Adman ET, Walsh K, Beppu T, Titani K (1986) FEBS Lett 197:301
90. Moir JWB, Baratta D, Richardson DJ, Ferguson SJ (1993) Eur J Biochem 212:377
91. Frew JE, Hill HAO (1988) Eur J Biochem 172:261
92. van Beeumen J, van Bun S, Canters GW, Lommen A, Chothis C (1991) J Biol Chem 266:4869
93. Lanyi JK (1974) Bacteriol Rev 38:272
94. Hildebrandt P, Matysik J, Schrader B, Scharf B, Engelhard M (1994) Biochemistry 33:11426
95. Bouvier J, Pugsley AP, Stragier P (1991) J Bacteriol 173:5523
96. Tang SPW, Coleman JE, Myer YP (1968) J Biol Chem 243:4286
97. Silvestrini MC, Brunori M, Tegoni M, Garvais M, Labeyrie F (1986) Eur J Biochem 161:465
98. Tordi GM, Silvestrini MC, Colosimo A, Tuttobello L, Brunori M (1985) Biochem J 230:797
99. Horio T, Higashi T, Sasagawa M, Kusai K, Nakai M, Okunuki K (1960) Biochem J 77:194
100. Horio T, Higashi T, Yamanaka T, Matsubara M, Okunuki K (1961) J Biol Chem 236:944
101. Omura T (1961) J Biochem (Tokyo) 50:394

102. Trost JT, McManus JD, Freeman JC, Ramakrishna BL, Blankenship RE (1988) Biochemistry 27:7858
103. Meyer TE, Tollin G, Cusanovich MA, Freeman JC, Blankenship RE (1989) Arch Biochem Biophys 272:254
104. Ingledew WJ (1982) Biochim Biophys Acta 683:89
105. Cobley JC, Haddock BA (1975) FEBS Lett 60:29
106. Cox JC, Boxer DH (1978) Biochem J 174:497
107. Blake II RC, Shute EA (1994) Biochemistry 33:9220
108. Ronk M, Shively JM, Shute EA, Blake RC II (1991) Biochemistry 30:9435
109. Ingledew WJ , Cobley JG (1980) Biochim Biophys Acta 590:141
110. Blake RC II, White KJ, Shute EA (1991) Biochemistry 30:9443
111. Lappin AG, Lewis CA, Ingledew WJ (1985) Inorg Chem 24:1446
112. Hunt AH, Toy-Palmer A, Assa-Munt N, Cavanagh J, Blake II RC, Dyson HJ (1994) J Mol Biol 244:370
112a. Botuyan MV, Toy-Palmer A, Chung J, Blake II RC, Bevoza I, Case DA, Dyson HJ (1996) J Mol Biol 263:752
113. Cai D, Klinman JP (1994) Biochemistry 33:7647
114. Janes SM, Palcic MM, Scaman CH, Smith AJ, Brown DE, Dooley DM, Mure M, Klinman JP (1992) Biochemistry 31:12147
115. Buffoni F (1966) Pharmacol Rev 18:1163
116. Knowles PF, Yadav KDS (1984) In: Lontie R (ed) Copper proteins and copper enzymes. CRC Press, Boca Raton, FL, p 103
117. Mondovi B, Riccio P, Agostinelli E (1988) In: Zappia V, Pagg AE (eds) Advances in experimental medicine and biology, progress in polyamine research, novel biochemical, pharmacological and clinical aspects 250. Plenum Press, New York, p 147
118. Perrin A, Sessa A, Desiderio MA (1985) In: Mondovi B (ed) Diamine oxidases in regenerating and hypertrophic tissues. Structure and functions of amine oxidases. CRC Press, Boca Raton, FL, p 179
119. Floris G, Giartosio A, Rinaldi A (1983) Phytochemistry 22:1871
120. Rossi A, Petruzzelli R, Agró AF (1992) FEBS Lett 301:253
121. Kumar V, Dooley DM, Freeman HC, Guss MJ, Harvey I, McGuirl MA, Wilce MCJ, Zubak VM (1996) Structure 4:943
122. Scott RA, Dooley DM (1985) J Am Chem Soc 107:4348
123. Janes SM, Mu D, Wemmer D, Smith AJ, Kaur S, Maltby D, Burlingame AL, Klinman JP (1990) Science 248:981
124. Pedersen JZ, El-Sherbini S, Finazzi Agró A, Rotilio G (1992) Biochemistry 31:8
125. Janes SM (1990) Ph.D. Thesis, University of California, Berkeley, USA
126. Brown DE, McGuirl MA, Dooley DM, Janes SM, Mu D, Klinman JP (1991) J Biol Chem 266:4049
127. Mu D, Janes SM, Smith AJ, Brown DE, Dooley DM, Klinman JP (1992) J Biol Chem 267:7979
128. Mu D, Medzihradszky KF, Adams GW, Mayer P, Hines WM, Burlingame AL, Smith AJ, Cai D, Klinman JP (1994) J Biol Chem 269:9926
129. Janes SM, Klinman JP (1991) Biochemistry 30:4599
130. Bruinenberg PG, Evers M, Waterham HR, Kuipers J, Arnberg AC, Ab G (1989) Biochim Biophys Acta 1008:157
131. Graham DG, Tiffany SM, Bell WR, Gutknecht WF (1978) Mol Pharmacol 14:644
132. Cai D, Klinman JP (1994) J Biol Chem 269:32039
133. Buffoni F (1986) Pharmacol Rev 18:1163
134. Goldstein O, Asher C, Barbry P, Cragoe E Jr, Clauss W, Garty H (1993) J Biol Chem 268:7856
135. Sattler J, Lorenz W (1990) J Neural Transm 32:291
136. Bachrach U, Ash I, Rahamin E (1987) Tissue & Cell 19:39
137. Bachrach U, Ash I, Abu-Elheiga L, Hershkovitz M, Loyter A (1987) J Cell Biol 131: 92
138. Dowling RH (1990) Digestion 46:331

139. Pierce GB, Parchment RE, Lewellyn AL (1991) Differentiation 46:181
140. Parchment RE, Pierce GB (1989) Cancer Res 49:6680
141. Pierce GB, Lewellyn AL, Parchment RE (1989) Proc Nat Acad Sci USA 86:3654
142. Gacheru SN, Trackman PC, Shah MA, O'Gara CY, Spacciapoli P, Greenaway FT, Kagan HM (1990) J Biol Chem 265:19022
143. Siegel RC (1979) Int Rev Connect Tissue Res 8:73
144. Kagan, HM. (1986) In: Mecham RP (ed) Biology of extracellular matrix 1. Academic Press, Orlando, FL. p 321
145. Williamson PR, Kagan HM (1986) J Biol Chem 261:9477
146. Chou WS, Savage JE, O'Dell BL (1969) J Biol Chem 244:5785
147. Buckingham K, Heng-Khoo DS, Dubick MJ, Lefevre M, Cross C, Julian L, Rucker R (1981) Proc Soc Exp Biol Med 166:310
148. Miller EJ, Martin GR, Mecca CE, Piez KA (1965) J Biol Chem 240:3623
149. Kenyon K, Contente S, Trackman PC, Tang J, Kagan HM, Friedman RM (1991) Science 253:802
150. Trackman PC, Bedell-Hogen D, Tang J, Kagan HM (1992) J Biol Chem 267:8666
151. Krebs CJ, Krawetz SA (1993) Biochim Biophys Acta 1202:7
152. McPherson MJ, Ogel ZB, Stevens C, Yadav KDS, Keen J, Knowles PF (1992) J Biol Chem 267:8146
153. Kosman DJ, Ettinger MJ, Weiner RE, Massaro EJ (1974) Arch Biochem Biophys 165:456
154. Kosman DJ (1984) In: Lontine R (ed) Copper proteins and copper enzymes 1. CRC Press, Boca Raton Publishers, Boca Raton, FL. p 1
155. Kwiatkowski LD, Adelman M, Pennelly R, Kosman DJ (1981) J Inorg Biochem 14:209
156. Varghese JN, Laver WG, Colman PM (1983) Nature 303: 35
157. Vellieux FMD, Huitema F, Groendijk H, Kalk KH, Frank J Jr, Jongejan JA, Duine JA, Patratos K, Drenth J, Hol WGJ (1989) EMBO J 8:2171
158. Whittaker MM, DeVito VL, Asher SA, Whittaker JW (1989) J Biol Chem 264:7104
159. Ito N, Phillips SEV, Stevens C, Ogel ZB, McPherson MJ, Keen JN, Yadav KDS, Knowles PF (1991) Nature 350:87
160. Hamilton GA, Adolf PK, de Jersey J, DuBois GC, Dyrkacz GR, Libby RD (1978) J Am Chem Soc 100:1899
161. DeFelippis MR, Murthy CP, Faraggi M, Klapper MH (1989) Biochemistry 28:4847
162. Connolly MJ (1983) J Appl Crystallogr 16:548
163. Lewis EJ, Asnani LP (1992) J Biol Chem 267:494
164. Wallace EF, Krantz MJ, Lovenberg W (1983) Proc Nat Acad Sci USA 70:2253
165. Rosenberg RC, Loverberg W (1977) Mol Pharmacol 13:652
166. Saxena A, Hensley P, Osborne JC Jr, Fleming PJ (1985) J Biol Chem 260:3386
167. Winkler H, Apps DK, Fischer-Colbrie R (1986) Neuroscience 18:261
168. Stewart LC, Klinman JP (1988) Annu Rev Biochem 57:551
169. Saxena A, Fleming PJ (1983) J Biol Chem 258:4147
170. Sabban EL, Greene LA, Goldstein M (1983) J Biol Chem 258:7812
171. McHugh EM, McGee R Jr, Fleming PJ (1985) J Biol Chem 260:4409
172. Oyarce AM, Fleming PJ (1989) J Mol Neurosci 1:171
173. Ash DE, Papadopoulos NJ, Colombo G, Villafranca JJ (1984) J Biol Chem 259:3395
174. Klinman JP, Krueger M, Brenner M, Edmondson DE (1984) J Biol Chem 259:3399
175. Blackburn NJ, Pettingill TM, Seagraves KS, Shigeta RT (1990) J Biol Chem 265:15383
176. Stewart LC, Klinman JP (1987) Biochemistry 26:5302
177. Brenner MC, Klinman JP (1989) Biochemistry 28:4664
178. Blackburn NJ, Collison D, Sutton J, Mabbs FE (1984) Biochem J 220:447
179. Blackburn NJ, Concannon M, Khosrow Shahiyan S, Mabbs FE, Collison D (1988) Biochemistry 27:6001
180. Fitzpatrick PF, Harpel MR, Villafranca JJ (1986) Arch Biochem Biopys 249:70
181. Ahn N, Klinman JP (1983) Biochemistry 22:3096
182. Balasubramanian S, Carr RT, Bender CJ, Peisach J, Benkovic SJ (1994) Biochemistry 33:8532

183. Kaufmann S, Fisher DB (1974) In: Hayaishi O (ed) Molecular mechanism of oxygen activation. Academic Press, New York, p 295
184. Kaufmann S (1985) Biochem Soc Trans 13:433
185. Ledley FD, DiLella AG, Kwok SCM, Woo SLC (1985) Biochemistry 24:3389
186. Ledley FD, Grenett HE, Woo SLC (1985) Am J Hum Genet 37:A235
187. Onishi A, Liotta LJ, Benkovic SJ (1991) J Biol Chem 266:18454
188. Blackburn NJ, Strange RW, Carr RT, Benkovic SJ (1992) Biochemistry 31:5298
189. Wallick DE, Bloom LM, Gaffny BJ, Benkovic SJ (1984) Biochemistry 23:1295
190. Marota JJA, Shinman R (1984) Biochemistry 23:1303
191. Pember SO, Villafranca JJ, Benkovic SJ (1986) Biochemistry 25:6611
192. Carr RT, Benkovic SJ (1993) Biochemistry 32:14132
193. Shiemke AK, DiSpirito AA, Lidstrom ME, Chan SI (1985) J Gen Microbiol 131:155
194. Bedard C, Knowles R (1989) Microbiol Rev 53:68
195. Nguyen HHT, Shiemke AK, Jacobs SJ, Hales BJ, Lidstrom ME, Chan SI (1994) J Biol Chem 269:14995
196. Stainthorpe AC, Lees V, Salmond GPC, Dalton H, Murrell JC (1990) Gene (Amst) 91:27
197. Stainthorpe AC, Salmond GPC, Dalton H, Murrell JC (1991) FEMS Microbiol Lett 70:211
198. Murrell JC (1993) In: Murrell JC, Kelly DP (eds) Microbial growth on C1 compounds. Intercept, Andover, UK, p 109
199. Fox BG, Froland WA, Jollie DR, Lipscomb JD (1990) Methods Enzymol 188:191
200. Froland WA, Andersson KK, Lee S-K, Liu Y, Lipscomb JD (1992) J Biol Chem 267:17588
201. Dewitt JG, Bentsen JG, Rosenzweig AC, Hedman B, Green J, Pilkington S, Papaefhymiou GC, Dalton H, Hodgson KO, Lippard SJ (1991) J Am Chem Soc 113:9219
202. Rosenzweig AC, Frederick CA, Lippard SJ, Nordlund P (1993) Nature 366:537
203. Nakajima T, Uchiyama H, Yagi O, Nakahara T (1992) Biosci Biotech Biochem 56:736
204. Koh S-C, Baumeen JP, Sayler GS (1993) Appl Environ Microbiol 59:960
205. Prior SD, Dalton H (1985) J Gen Microbiol 131:155
206. Burrows KJ, Cornish A, Scott D, Higgins IJ (1984) J Gen Microbiol 130:3327
207. Cornish A, MacDonald J, Burrows KJ, King TS, Scott D, Higgins IJ (1985) Biotechnol Lett 5:319
208. Messerschmidt A, Rossi A, Ladenstein R, Huber R, Bolognesi M, Gatti G, Marchesini A, Petruzzelli R, Finazzi-Agro A (1989) J Mol Biol 206:513
209. Allendorf MD, Spira DJ, Solomon EI (1985) Proc Natl Acad Sci USA 82:3063
210. Speier G (1993) Copper dioxygenation chemistry relevant to quercetin dioxygenase. In: Karlin KD, Tyeklár Z (eds) Bioinorganic chemistry of copper. Chapman & Hall, London
211. Oka T, Simpson FJ (1971) Biochem Biophys Res Commun 43:1
212. Makasheva E, Golovhina NT (1973) Zh Obschch Khim 43:1640
213. Thomson M, Williams CR (1976) Anal Chim Acta 85:375
214. Takamura K, Ito M (1977) Chem Parm Bull 25:3218
215. Hartz JW, Funakoshi S, Deutsch HF (1973) Clin Chim Acta 46:125
216. Steinmann HM, Naik VR, Abernethy JL, Hill RL (1974) J Biol Chem 249:7326
217. Tainer JA, Getzoff ED, Beem KM, Richardson JS, Richardson DC (1982) J Mol Biol 160:181
218. Tibell L, Aasa R, Marklund SL (1993) Arch Biochem Biophys 304:429
219. Lin CT, Lin MT, Chen YT, Shaw JF (1995) Plant Mol Biol 28:303
220. Bordo D, Djinovic K, Bolognesi M (1994) J Mol Biol 238:366
221. Fridovich I (1974) Adv Enzymol 41:35
222. Fridovich I (1986) Adv Enzymol Relat Areas Mol Biol 58:61
223. Valentine JS, Pantoliano MW (1981) In: Spiro TG (ed) Copper proteins. Wiley, New York, p 291
224. McCord JM, Fridowich I (1969) J Biol Chem 244:6049
225. Sawyer DT, Valentine JS (1981) Acc Chem Res 14:393
226. Fee JA, Bull C (1986) J Biol Chem 261:13000
227. Natvig DO, Imlay K, Touati D, Hallewell RA (1987) J Biol Chem 262:14697

228. Azab HA, Banci L, Borsari M, Luchinat C, Sola M, Viezzoli MS (1992) Inorg Chem 31:4649
229. Getzoff ED, Tainer JA, Weiner PK, Kollmann PA, Richardson JS, Richardson DC (1983) Nature 306:287
230. Jones TA (1978) J Appl Crystallogr 11:268
231. Vriend G (1990) J Mol Graph 8:52
232. Priestly JP (1988) J Appl Crystallogr 21:572
233. Kitagawa Y, Tanaka N, Hata Y, Kusonoki M, Lee G, Katsube Y, Asada K, Aibara S, Morita Y (1991) J Biochem 109:447
234. Djinovic K, Gatti G, Coda A, Antolini L, Pelosi G, Desideri A, Falconi M, Marmocchi F, Rotilio G, Bolognesi M (1992) J Mol Biol 225:791
235. Banci L, Carloni P, Orioli PL (1994) Proteins: Struct Funct Genet 18:216
236. Markl J, Savel A, Linzen B (1981) Hoppe-Seyler's Z Physiol Chem 362:1255
237. Beltramini M, Salvato B, Santamaria M, Lerch K (1990) Biochim Biophys Acta 1040:365
238. Brenowitz M, Bonaventura C, Bonaventura J, Gianazza E (1981) Arch Biochem Biophys 210:748
239. Sullivan B, Bonaventura C, Bonaventura J (1974) Proc Natl Acad Sci USA 71:2558
240. Brenowitz M, Bonaventura C, Bonaventura J (1984) Arch Biochem Biophys 230:238
241. Lamy J, Lamy J, Sizaret P-Y, Billiald P, Jollés P, Jollés J, Feldmann RJ, Bonaventura J (1983) Biochemistry 22:5573
242. Brouwer M, Bonaventura C, Bonaventura J (1977) Biochemistry 16:3897
243. Brouwer M, Bonaventura C, Bonaventura J (1982) Chloride and pH dependence of co-operative interactions in *Limulus polyphemus* hemocyanin. In: Bonaventura J, Bonaventura C, Tesh S (eds) Physiology and biology of horseshoe crabs: studies on normal and environmentally stressed animals. Alan R Liss, New York, p 231
244. Brouwer M, Bonaventura C, Bonaventura J (1983) Biochemistry 22:4713
245. Brouwer M, Serigstad B (1989) Biochemistry 28:8819
246. Gaykema WPJ, Hol WGJ, Vereijken JM, Soeter NM, Bak HJ, Beintema JJ (1984) Nature, 309:23
247. Drexel R, Siegmund S, Schneider HJ, Linzen B, Gielens C, Préaux G, Lontie R, Kellermann J, Lottspeich F (1987) Biol Chem Hoppe-Seyler 368:617
248. Brown JM, Powers L, Kincaid B, Larrabee JA, Spiro TG (1980) J Am Chem Soc 102:4210
249. Woolery GL, Powers L, Winkler M, Solomon EI, Spiro TG (1984) J Am Chem Soc 106:86
250. Baldwin MJ, Root DE, Pate JE, Fujisawa K, Kitajiama N, Solomon EI (1992) J Am Chem Soc 114:10421
251. Lerch K (1981) Met Ions Biol Syst 13:143
252. Mason HS (1965) Annu Rev Biochem 34:594
253. Lerch K (1988) In: Bagnara JT (ed) Advances in pigment cell research. Alan R Liss, New York, p 85
254. Himmelwright RS, Eickman NC, LuBien CD, Lerch K, Solomon EI (1980) J Am Chem Soc 102:7339
255. Lerch K, Germann UA (1988) In: Oxidases and related redox systems. Alan R Liss, New York, p 331
256. Kupper U, Niedermann DM, Travaglini G, Lerch K (1989) J Biol Chem 264:17250
257. Ghiretti F (1956) Arch Biochem Biophys 63:165
258. Salvato B, Jori G, Piazzesi A, Ghiretti F, Beltramini M, Lerch K (1983) Life Chem Rep Sup 1:313
259. Nakahara A, Suzuki S, Kino J (1983) Life Chem Rep Sup 1:319
260. Andréasson L-E, Reinhammar B (1976) Biochim Biophys Acta 445:579
261. Andréasson L-E, Reinhammar B (1979) Biochim Biophys Acta 568:145
262. Cole JL, Ballou DP, Solomon EI (1991) Am Chem Soc 113:8544
263. Cole JL, Tan GO, Yang EK, Hodgson KO, Solomon EI (1990) J Am Chem Soc 112:2243
264. Reinhammar B (1984) In: Lontine R (ed) Copper proteins and copper enzymes, 3. CRC Press, Boca Raton, FL, p 1
265. Ricchelli F, Beltramini M, Bubacco L, Salvato B, Filippi B (1992) Inorg Chim Acta 193:237

266. Messerschmidt A, Huber R (1990) Eur J Biochem 187:341
267. Chichiricco G, Geru MP, D"Alessandro A, Oratore A, Avigliano L (1989) Plant Sci 64:61
268. Marchesini A, Cappalletti P, Canonica L, Danieli B, Tollari S (1977) Biochim Biophys Acta 484:290
269. Butt VS (1980) Direct oxidases and related enzymes. In: Davies R (ed) The biochemistry of plants. A comprehensive treatise. Metabolism and respiration 2. Academic Press, New York, p 85
270. Yamazaki I, Piette LH (1961) Biochim Biophys Acta 50:62
271. Payne W (1985) In: Golterman HL (ed) Denitrification in the nitrogen cycle. Plenum Publishing, New York, p 47
272. Godden JW, Turley S, Teller DC, Adman ET, Liu MY, Payne WJ, LeGall J (1991) Science 253:438
273. Fenderson FF, Kumar S, Adman ET, Liu MY, Payne WJ, LeGall J (1991) Biochemistry, 30:7180
274. Ludwig B (1987) FEMS Microbiol Rev 46:41
275. Chepuri V, Lemieux L, Au DC-T, Gennis RB (1990) J Biol Chem 265:11185
276. Lübben M, Kolmerer B, Saraste M (1992) EMBO J 11:805
277. Santana M, Kunst F, Hullo MF, Rapoport G, Danchin A, Glaser P (1992) J Biol Chem 267: 10225
278. van der Oost J, Lappalainen P, Musacchio A, Warne A, Lemieux L, Rumbley J, Gennis RB, Aasa R, Pascher T, Malmström BG, Saraste M (1992) EMBO J. 11:3209
278a. Wilmanns M, Lappalainen P, Kelly M, Sauer-Eriksson E, Saraste M (1995) Proc Natl Acad Sci USA 92:11955
279. van der Oost J, de Boer APN, de Gier JWL, Zumft WG, Stouthamer AH, van Spanning RJM (1994) FEMS Microbiol Lett 121:1
280. Viebrock A, Zumft WG (1988) J Bacteriol 170:4658
281. Woese CR, Fox GE (1977) Proc Natl Acad Sci USA 74:5088
282. Woese CR, Kandler O, Wheelis ML (1990) Proc Natl Acad Sci USA 87:4576
283. Capaldi RA (1990) Annu Rev Biochem 59:569
284. Chan SI, Li PM (1990) Biochemistry 29:1
285. Saraste M (1990) Q Rev Biophys 23:331
286. Babcock GT, Wilkström M (1992) Nature 356:301
287. Castresana J, Lübben M, Saraste M, Higgins DG (1994) EMBO J 13:2516
288. Meunier B, Colson A-M (1993) FEBS 335:338
289. Malmström BG (1990) Chem Rev 90:1247
290. Bosma G (1989) PhD Thesis, Vrije Universiteit, Amsterdam
291. Garcia-Horsman A, Shapleigh J, Gennis RB (1994) Biochemistry 33:3113
292. Preisig O, Antamatten D, Hennecke H (1993) Proc Natl Acad Sci USA 90:3309
293. Keefe RG, Maier RJ (1993) Biochim Biophys Acta 1183:91
294. Hosler JP, Ferguson-Miller S, Calhoun MW, Thomas JW, Hill J, Lemieux LJ, Ma J, Greorgiou C, Fetter J, Shaphleigh J, Tecklenburg MMJ, Babcock GT, Gennis RB (1992) J Bioenerg Biomembr 25:121
295. Puustinen A, Finel M, Haltia T, Gennis RB, Wikström M (1991) Biochemistry 30:3936
296. Zumft WG, Kroneck PMH (1991) FEMS Symp Ser 56:37
297. Knowles R (1982) Microbiol Rev 46:43
298. Zumft WG, Kroneck PMH (1995) Adv Inorg Biochem 11:193
299. Coyle CL, Zumft WG, Kroneck PMH, Körner H, Jakob W (1985) Eur J Biochem 153:459
300. Lowry OH, Rosebrugh NJ, Farr AL, Randall RJ (1951) J Biol Chem 193:265
301. Aasa R, Vanngard T (1975) J Mag Res 19:308
302. Hamer DH (1986) Ann Rev Biochem 55:913
303. Nordberg M, Kojima Y (1979) Report from the first international meeting on metallothionein and other low molecular mass metal-binding proteins. In: Kägi JHR, Nordberg M (eds) Metallothionein, Birkhäuser, Basel p 41
304. Lerch K (1979) In: Kägi JHR, Nordberg M (eds) Metallothionein, Birkhäuser, Basel p 173
305. Prinz R, Weser U (1975) Hoppe-Seyler's Z Physiol Chem 356:767

306. Palumaa P, Vasak M (1992) Eur J Biochem 205:1131
307. Li TY, Kraker AJ, Shaw III CF, Petering DH (1980) Proc Natl Acad Sci USA 77:6334
308. Hartmann H-J, Morpurgo L, Schechinger T, Desideri A, Rotilio G, Weser U (1987) Life Chem Rep 5:305
309. Sadhu C, Gedamu L (1988) J Biol Chem 263:2679
310. Schmidt CJ, Hamer DH (1986) Proc Natl Acad Sci USA 83:3346
311. Zeng J, Heuchel R, Schaffner W, Kägi JH (1991) FEBS Lett 279:310
312. Zeng J, Vallee BL, Kägi JH (1991) Proc Natl Acad Sci USA 88:9984
313. Felix K, Lengfelder E, Hartmann HJ, Weser U (1993) Biochim Biophys Acta 1203:104
314. Deters D, Hartmann HJ, Weser U (1994) Biochim Biophys Acta 1208:344
315. Gralla EB, Thiele DJ, Silar P, Valentine JS (1991) Proc Natl Acad Sci USA 88:8558
316. Kojima Y, Kägi JHR (1978) Trends Biochem Sci 3:90
317. Nemer M, Wilkinson DG, Travaglini EC, Sternberg EJ, Butt TR (1985) Proc Natl Acad Sci USA 82:4992
318. Winge DR, Nielson KB, Gray WR, Hamer DH (1985) J Biol Chem 260:14464
319. Grill E, Winnacker EL, Zenk MH (1987) Proc Natl Acad Sci USA 84:439
320. Jackson PJ, Unkefer CJ, Doolen JA, Watt K, Robinson NJ (1987) Proc Natl Acad Sci USA 84:6619
321. Reese RN, Mehra RK, Tarbet EB, Winge DR (1988) J Biol Chem 263:4186
322. Stallings WC, Pattridge KA, Strong RK, Ludwig ML (1984) J Biol Chem 259:10695
323. Brogstahl GEO, Parge HE, Hickey MJ, Beyer WF Jr, Hallewell RA, Tainer JA (1992) Cell 71,107
324. Ludwig ML, Metzger AL, Pattridge KA, Stallings WC (1991) J Mol Biol 219:335
325. Stallings WC, Pattridge KA, Strong RK, Ludwig ML, Yakamura F, Isobe T, Steinmann HM (1987) Active site homology in iron and manganese superoxide dismutase. In: Glusker JP, Patterson BK, Rossi M (eds) Patterson and Pattersons, Oxford, p 505
326. Parker MW, Blake CCF (1988) J Mol Biol 199:649
327. Grenett HE, Ledley FD, Read LL, Woo SLC (1987) Proc Natl Acad Sci USA 84:5530
328. Zumft W, Braun C, Cuypers H (1994) Eur J Biochem 219:481
329. Mehra RK, Garey JR, Butt TR, Gray WR, Winge DR (1989) J. Biol. Chem. 264:19747
330. Cotton FA, Wilkinson G (1988) Advanced Inorganic Chemistry 5th edn. Wiley, New York
331. Riedel E (1994) Anorganische Chemie 3. Aufl Walter de Gruyter, Berlin
332. Rabinowitz JL, Bassett DJP (1988) Exp Lung Res 14:477
333. Freeman BA, Sharman MC, Mudd JB (1979) Arch Biochem Biophys 197:264
334. Roehm JN, Hadley JG, Menzel DB (1971) Arch Environ Health 23:142
335. Srisankar EV, Patterson LK (1979) Arch Environ Health 34:346
336. Giamalva DH, Church DF, Pryor WA (1988) Chem Res Toxicol 1:144
337. Pryor WA, Das B, Church DF (1991) Chem Res Toxicol 4:341
336. Lai CC, Finlayson-Pitts BJ, Willis WV (1990) Chem Res Toxicol 3:517
339. Santrock J, Gorski RA, O'Gara JF (1992) Chem Res Toxicol 5:134
340. Dooley MM, Mudd JB (1982) Arch Biochem Biophys 218:459
341. Mudd JB, Leavitt R, Ongun A, McManus TT (1969) Atmos Environ 3:669
342. Goldstein BD, McDonagh EM (1975) Environ Res 9:179
343. Chan PC, Kindya RJ, Kesner L (1977) J Biol Chem 252:8537
344. Giese AC, Leighton HL, Bailey R (1952) Arch Biochem Biophys 40:71
345. Previero A, Coletti-Previero M-A, Jollés P (1967) J Mol Biol 24:261
346. Kuroda M, Sakiyama F, Narita K (1975) J Biochem 78:641
347. Todd GW (1958) Physiol Plant 11:457
348. Uppu RM, Pryor WA (1994) Chem Res Toxicol 7:47
349. Teige B, McManus TT, Mudd JB (1974) Chem Phys Lipids 12:153
350. Kanofsky J, Sima P (1991) J Biol Chem 226:9039
351. Eisenberg WC, Taylor K, Murray RW (1985) J Am Chem Soc 107:8299
352. Murray RW, Kaplan ML (1968) J Am Chem Soc 90:537
353. Murray RW, Lin JW-P, Kaplan ML (1970) Ann NY Acad Sci 171:121
354. Stray FE, Emge DE, Murray RW (1976) J Am Chem Soc 98:1880

355. Weiss J (1935) Trans Faraday Soc 31:668
356. Hoigne J, Bader H (1976) Water Res 10:377
357. Forni L, Bahnemann D, Hart EJ (1982) J Phys Chem 86:255
358. Menzel DB (1992) Ann NY Acad Sci 669:141
359. Cross CE, Motchnik PA, Bruener BA, Jones DA, Kaur H, Ames BN, Halliwell B (1992) FEBS 298:269
360. Wright ES, Dziedic D, Wheeler CS (1990) Toxicol Lett 51:153
361. Hazucha MJ (1987) J Appl Physiol 62:1671
362. Hasset C, Mustafa MG, Coulson WF, Elashoff RM (1985) J Natl Cancer Inst 75:771
363. Menzel DB (1984) J Toxicol Environ Health 13:183
364. Margerum DW, Wong LF, Bossu FP, Chellappa KL, Czarnecki JJ, Kirksey ST jr, Neubecker TA (1977) Copper(II)- and copper(III)-peptide complexes. In: Gould RF (ed) Advances in chemistry series. American Chemical Society, p 281
365. Brown DG, Weser U (1979) Inorg Chem 19:264
366. Brown DG, Weser U (1979) Naturforsch 34:989